

# **Electrochemical screening of biological membrane active compounds**

**Shahrzad Mohamadi**

*Submitted in Accordance with the Requirements for the Degree of  
Doctor of Philosophy*

The University of Leeds  
School of Chemistry

October, 2014

*The candidate confirms that the work submitted is her own and that appropriate  
credit has been given where reference has been made to the work of others.*

*This copy has been supplied on the understanding that it is copyright material and  
that no quotation from the thesis may be published without proper acknowledgement*

The candidate confirms that the work submitted is her own, except where work which has formed part of jointly authored publications has been included. The contribution of the candidate and the other authors to this work has been explicitly indicated below. The candidate confirms that appropriate credit has been given within the thesis where reference has been made to the work of others.

The work in Chapter 5 of the thesis has appeared in publication as follows:

Interaction of Imidazolium-Based Room-Temperature Ionic Liquids with DOPC Phospholipid Monolayers: Electrochemical Study. Published in Langmuir, 2013, Galluzzi M, Zhang S, Mohamadi S, Vakurov A, Nelson A.

This copy has been supplied on the understanding that it is copyright material and that no quotation from the thesis may be published without proper acknowledgement

© 2014 The University of Leeds and Shahrzad Mohamadi

The right of Shahrzad Mohamadi to be identified as Author of this work has been asserted by her in accordance with the Copyright, Designs and Patents Act 1988.

# ACKNOWLEDGEMENTS

I would like to begin my list of appreciation by expressing my thanks to my supervisor, Professor Andrew Nelson. From day one all the way through the four years, you have been extremely supportive and inspiring. You gave me the freedom to express my ideas, to be innovative as well as develop new skills. This has been an enjoyable time and I have been amazed and enthralled by all the research we have achieved in the group. Thank you for giving me the opportunity to be part of it!

From here, I wish to make special thanks to my lab colleagues with special mention of Dr Alexander Vakurov

No Acknowledgment can be complete without special thanks to my family; I wish to express fond gratitude to my sister, Sophia who kept me smiling and entertained especially towards the end of my PhD course and to my mother Shahnaz from whom I must have received my fondness for chemistry and qualities such as perseverance and diligence which certainly helped to complete this thesis!

Of course this was all also made possible by all the funding bodies and University of Leeds; thank you for the opportunity.

Lastly, I wish to make a very special mention of my partner Chris. It has been difficult to put my appreciation into words, for really I have no words to express my heartfelt gratitude for all the support you have given me. Thank you for your patience, support and encouragement over the years. These years will be in my fondest memories; absolutely amazing. To many more!

# ABSTRACT

Interactions of biomembrane-active compounds with phospholipid monolayers on microfabricated Pt/Hg electrodes in an *on-line* high throughput flow system are demonstrated by recording capacitance current peak changes in rapid cyclic voltammograms (RCV). Detection limits of the compounds' effects on the layer have been estimated from the data. Compounds studied include steroids, polycyclic aromatic hydrocarbons, tricyclic antidepressants, tricyclic phenothiazines pyridinium compounds, spiperone and spiperone analogues and a range of serotonin and dopamine receptor ligands. The results show that the extent and type of interaction depends on the: - (a) presence and number of aromatic rings and substituents, (b) presence and composition of side chains and, (c) molecular shape. Interaction is only indirectly related to compound hydrophobicity. For a selection of tricyclic antidepressants and tricyclic phenothiazines the detection limit in water is related to their therapeutic normal threshold. The sensing assay has been tested in the presence of humic acid as a potential interferent and in a tap water matrix. It was subsequently tested in a natural water matrix. The system can be applied to the screening of putative hazardous substances allowing for early detection thereof in the water supply. The measurements are made in real time which means that potentially toxic compounds are detected rapidly in <10 minutes per assay. This technology will contribute greatly to environment safety and health.

# CONTENTS

ACKNOWLEDGEMENTS.....	iii
ABSTRACT.....	iv
CONTENTS.....	v
FIGURES.....	xiv
TABLES.....	xxviii
ABBREVIATIONS.....	xxx
COMMONLY USED SYMBOLS.....	xxxiii
CHAPTER 1 INTRODUCTION .....	1
1.1 INTRODUCTION.....	1
1.1.1 MONOLAYER CAPACITANCE – THE RELATIONSHIP BETWEEN CHARGE, CURRENT AND CAPACITANCE .....	5
1.1.2 ADSORPTION .....	9
1.1.3 RC CIRCUIT .....	12
1.2 THE ELECTRIC DOUBLE LAYER .....	13
1.3 MEMBRANE MODELS.....	18
1.4 INNOVATIVE TOOLS.....	19
1.5 SUMMARY .....	21

REFERENCES.....	22
CHAPTER 2 ANALYTICAL TECHNIQUES - MATERIALS AND METHODS.....	23
2.1 INTRODUCING ANALYTICAL TECHNIQUES.....	23
2.1.1 POTENTIOMETRY .....	24
2.1.2 VOLTAMMETRY .....	25
2.1.3 CYCLIC VOLTAMMETRY.....	27
2.2 MEMBRANE-BASED SUPPORT SYSTEMS.....	30
2.2.1 LANGMUIR TROUGH.....	30
2.2.2 HANGING MERCURY (Hg) DROP ELECTRODE (HMDE) .....	32
2.2.3 MICROFABRICATED PLATINUM ELECTRODE (MFE).....	34
2.3 USING MFE MEMBRANE SUPPORT SYSTEM .....	36
2.3.1 Hg ELECTRODEPOSITION .....	36
2.3.2 RAPID CYCLIC VOLTAMMETRY .....	37
2.3.3 METHODS .....	38
2.4 LIMIT OF DETECTION.....	42
2.5 MATERIALS .....	44
2.5.1 PHOSPHATE BUFFERED SOLUTION (PBS) .....	44
2.5.2 PIRANHA SOLUTION.....	44
2.6 SUMMARY .....	45

REFERENCES.....	46
CHAPTER 3 MFE SYSTEM CHARACTERISATION AND OPTIMISATION.....	47
3.1 INTRODUCTION.....	47
3.2 INSTRUMENT LIMITATIONS .....	48
3.2.1 REFERENCE ELECTRODE.....	48
3.2.2 NOISE .....	50
3.2.3 FLOW RATE .....	51
3.2.4 LEAKS.....	51
3.3 NEW FLOW CELL.....	52
3.3.1 STABLE MONOLAYER .....	53
3.4 CONTAMINATION AND CARRYOVER .....	54
3.4.1 ELECTROCHEMICAL CLEANING .....	56
3.4.2 CHEMICAL CLEANING .....	57
3.4.3 MANUAL CLEANING.....	58
3.5 ANALYSING PARAMETERS .....	59
3.6 COMPARING TO OTHER SYSTEMS.....	60
3.7 SUMMARY .....	61
REFERENCES.....	64
CHAPTER 4 PHOSPHOLIPID MONOLAYERS ON ELECTRODE SURFACES .....	65

4.1 INTRODUCTION.....	65
4.1.1 LIPIDS IN NATURE .....	65
4.1.2 BEHAVIOUR OF PHOSPHOLIPIDS .....	68
4.2 MATERIALS AND METHODS.....	73
4.3 RESULTS AND DISCUSION.....	74
4.3.1 EFFECT OF VARYING pH ON DOPC .....	74
4.3.2 INCORPORATING STEROLS WITH DOPC .....	78
4.3.3 CAPACITANCE PROFILES OF VARIOUS LIPIDS.....	82
4.3.5 DOPE .....	84
4.3.6 DOPG.....	85
4.3.7 DOPS .....	88
4.4 SUMMARY .....	90
REFERENCES.....	92
 CHAPTER 5 THE MODES OF ACTION OF LONG CHAIN ALKYL COMPOUNDS	93
5.1 INTRODUCTION.....	93
5.1.2 N-ALKYL SPIPERONE DERIVATIVES .....	95
5.1.3 BIS PYRIDINIUM COMPOUNDS .....	96
5.1.4 IONIC LIQUIDS.....	97
5.2 MATERIALS AND METHODS.....	98



5.3 RESULTS AND DISCUSSION .....	99
5.3.1 SPIPERONE .....	99
5.3.3 IONIC LIQUIDS .....	108
5.4 SUMMARY .....	112
REFERENCE .....	113
<b>CHAPTER 6 INTERACTION STUDIES I .....</b>	<b>114</b>
6.1 INTRODUCTION .....	114
6.2 MATERIALS AND METHODS .....	117
6.3 RESULTS AND DISCUSSION .....	118
6.4 SUMMARY .....	125
REFERENCES .....	126
<b>CHAPTER 7 INTERACTION STUDIES II .....</b>	<b>127</b>
7.1 INTRODUCTION .....	127
7.1.1 TRICRESYL PHOSPHATE .....	129
7.1.2 CHLORAMPHENICOL .....	129
7.1.3 SPIPERONE AND ANALOGUES .....	130
7.1.4 METHYLYXANTHINES .....	131
7.2 MATERIALS AND METHODS .....	132
7.3 RESULTS AND DISCUSSIONS .....	133

7.3.1 TRICRESYL PHOSPHATE.....	133
7.3.2 CHLORAMPHENICOL.....	134
7.3.3 METHYLYXANTHINES.....	135
7.3.4 SPIPERONE AND ANALOGUES.....	136
7.4 NEGATIVE CONTROL.....	139
7.5 SUMMARY.....	140
REFERENCES.....	141
CHAPTER 8 POLYCYCLIC AROMATIC HYDROCARBONS.....	142
8.1 INTRODUCTION.....	142
8.2 MATERIALS AND METHODS.....	146
8.3 RESULTS.....	146
8.4 DISCUSSION.....	151
8.5 SUMMARY.....	153
REFERENCES.....	154
CHAPTER 9 STEROIDS.....	156
9.1 INTRODUCTION.....	156
9.2 MATERIALS AND METHODS.....	160
9.3 RESULTS AND DISCUSSION.....	162
9.3.1 STEROID – DOPC INTERACTION STUDY.....	162

9.3.2 POTENTIAL SHIFT VS. CONCENTRATION .....	165
9.3.3 DIPOLE MOMENT .....	166
9.4 SUMMARY .....	169
REFERENCES.....	171
 CHAPTER 10 TRICYCLIC ANTIDEPRESSANTS AND PHENOTHIAZINES .....	 173
10.1 INTRODUCTION.....	173
10.1.1 NEUROTRANSMITTERS: BRIEF INTRODUCTION TO 5-HT AND DOPAMINE .....	174
10.1.1.1 SEROTONIN (5-HT) AND 5-HT RECEPTOR.....	174
10.1.1.2 DOPAMINE AND DOPAMINE RECEPTOR.....	175
10.1.2 TRICYCLIC ANTIDEPRESSANTS AND PHENOTHIAZINES.....	176
10.1.3 FLUORESCENCE SPECTROSCOPY .....	179
10.2 MATERIALS AND METHODS.....	180
10.2.1 ASSAY EXPERIMENT .....	180
10.2.2 FLUORESCENCE SPECTROSCOPY .....	181
10.3 RESULTS AND DISCUSSION .....	183
10.3.1 RCV SCANS .....	183
10.3.2 EFFECTS OF VARYING pH.....	185
10.3.3 BINDING AFFINITY TO RECEPTORS.....	187
10.3.4 FLUORESCENCE SPECTROSCOPY .....	192

10.4 SUMMARY .....	195
CHAPTER 11 APPLICATION OF FLOW CELL SYSTEM AS BIOSENSOR .....	199
11.1 INTRODUCTION.....	199
11.1.1 FINGERPRINT SCREENING .....	202
11.1.2 MATRIX EFFECT AND FRESHWATER/CAVE WATER SAMPLING .....	203
11.1.3 MIXTURES.....	203
11.2 MATERIALS AND METHODS.....	204
11.2.1 MATRIX EFFECTS AND CAVE WATER SAMPLING .....	204
11.3 RESULTS AND DISCUSSIONS.....	206
11.3.1 FINGERPRINT DATABASE .....	206
11.3.2 MATRIX EFFECTS .....	208
11.3.3 NATURAL WATER .....	210
11.3.4 COMPOUND MIXTURES .....	211
11.3.4.1 PYRENE AND PROCHLORPERAZINE .....	212
11.3.4.2 DDT AND PYRENE .....	216
11.3.4.3 ANTHRACENE AND PROCHLORPERAZINE .....	217
11.3.4.4 MB779 AND PYRENE .....	218
11.5 SUMMARY .....	220
REFERENCES.....	222

CHAPTER 12 CONCLUDING REMARKS .....	224
APPENDIX A           MFE FLOW CELL: PARAMETERS FOR ASSAY .....	230

# FIGURES

Figure 1.1: Equivalent resistance-capacitance (RC) circuit for a membrane model..	7
Figure 1.2: Diagram of the interfacial region separating phases $\alpha$ and $\beta$ [6].	10
Figure 1.3: Models of the electric double layer at a negatively charged surface representing a) the Helmholtz model, b) the Gouy–Chapman model, and c) the Stern model; S being the Stern layer. OHP is the outer Helmholtz plane. $\Phi_s$ and $\Phi_m$ is the potential difference in solution and on the metal respectively.	16
Figure 2.1: Representation of redox reaction at electrode surface.	25
Figure 2.2: Concentration gradient from electrode surface, where D is diffusion layer, C is concentration gradient.	27
Figure 2.3: Example of a cyclic voltammogram [4].	28
Figure 2.4: Schematic representation of the Langmuir trough [9].	31
Figure 2.5: Diagram of HMDE during Hg filling [12].	33
Figure 2.6: Microfabricated electrode with deposited DOPC monolayer a) schematic representation of the order of phospholipids on Hg coated electrode support. b) a working microfabricated electrode chip [13].	34
Figure 2.7: The flow cell designed to hold the Hg/Pt electrodes [14].	35
Figure 2.8: a) RCV recorded at $40 \text{ Vs}^{-1}$ of an uncoated and clean Hg electrode in PBS at pH 7.4 with potential excursions from -0.4V to -1.8V. b) RCV recorded at $40 \text{ Vs}^{-1}$ of	

a DOPC coated Pt/Hg electrode in PBS at pH 7.4 with potential excursions from -0.4V to -1.2V.....	38
Figure 2.9: a) RCV recorded at 40 Vs <sup>-1</sup> with potential excursions of -0.4 V to -3.00 V. This process is used for electrochemical in-situ cleaning and phospholipid deposition.	
b) RCV recorded at 40 Vs <sup>-1</sup> with potential excursions of -0.4 V to -3.00 V after introduction of 50µl of 0.2 mg cm <sup>-3</sup> DOPC dispersion in PBS at pH 7.4. c) RCVs recorded at 40 Vs <sup>-1</sup> of a DOPC coated Pt/Hg electrode in PBS at pH 7.4 with potential excursions of -0.4 V to -1.2 V following the DOPC deposition procedure. ....	41
Figure 2.10: The control system of the flow cell based sensing device. Pathways are represented by black arrows. ....	
42	
Figure 3.1: RCVs recorded at 40 Vs <sup>-1</sup> of a DOPC coated Pt/Hg electrode in PBS at pH 7.4 using a) an internal Pt <i>pseudo</i> reference electrode (black line) and capacitance current peaks post anthracene testing (red line) and b) comparison of capacitance current peak shifts using internal Pt <i>pseudo</i> reference electrode (red line) and when using 3.5 mol dm <sup>-3</sup> KCl Ag/AgCl standard reference electrode (black line). ....	
49	
Figure 3.2: RCVs recorded at 40 Vs <sup>-1</sup> of a DOPC coated Pt/Hg electrode in PBS at pH 7.4 with switching potential of -1.8V a) affected by electrical noise interference and b) in standard conditions. ....	
50	
Figure 3.3: RCVs recorded at 40 Vs <sup>-1</sup> of a DOPC coated Pt/Hg electrode (black line) and removal of lipids from Pt/Hg electrode when flow rates exceed 20 cm <sup>3</sup> min <sup>-1</sup> (red line). ....	
51	
Figure 3.4: The particulate ingress damaging the soft PTFE valve seal. ....	
52	
Figure 3.5: RCVs recorded at 40 Vs <sup>-1</sup> of a DOPC coated Pt/Hg electrode at a) 0 minutes and b) 20 minutes. ....	
54	

Figure 3.6: RCVs recorded at  $40 \text{ Vs}^{-1}$  of a) DOPC coated Pt/Hg electrode (black line) being affected by contamination (red line) and b) an uncoated Pt/Hg electrode (black line) being affected by contamination (red line) in PBS at pH 7.4. ....55

Figure 3.7: RCVs recorded at  $40 \text{ Vs}^{-1}$  of a Pt/Hg electrode in PBS at pH 7.4 showing chemical cleaning using a) 0.4M NaOH, b) peroxide solution in a ratio of 2:100 by volume of hydrogen peroxide, c) dilute piranha solution (piranha solution is made using  $\text{H}_2\text{SO}_4$  and 30%  $\text{H}_2\text{O}_2$  in a mixture with ratio of 3:1 respectively) in a ratio of 1:100 by volume of piranha, d)  $3 \text{ mg dm}^{-3}$  humic acid in PBS at pH 7.4. ....56

Figure 3.8: RCV at a scan rate of  $100 \text{ Vs}^{-1}$  of a Pt/Hg electrode with potential excursion from  $-0.4 \text{ V}$  to  $-3.00 \text{ V}$ . The peak appearing at approximately  $-0.8\text{V}$  indicates a contaminant on the Hg surface. After electrochemical cleaning, the peak at  $-0.8\text{V}$  disappears indicating that the contaminant has been removed as shown on bold line. ....57

Figure 3.9: RCV at  $40 \text{ Vs}^{-1}$  of a Pt/Hg electrode (dotted line) and showing faradaic reaction (black line) in PBS at pH 7.4. ....58

Figure 3.10: RCVs recorded at  $40 \text{ Vs}^{-1}$  of a DOPC coated Pt/Hg electrode (black line) in the presence of  $0.0005 \text{ } \mu\text{mol dm}^{-3}$  (blue line) and  $0.002 \text{ } \mu\text{mol dm}^{-3}$  (red line) pyrene in PBS at pH 7.4. ....59

Figure 4.1: molecular structures of a) 1, 2-dioleoyl-*sn*-glycero-3-phosphocholine (DOPC), b) 1-palmitoyl-2-oleoyl-*sn*-glycero-3-phosphocholine (POPC) c) 1,2-di-(9Z-octadecenoyl)-*sn*-glycero-3-phosphoethanolamine (DOPE), d) 1,2-di-(9Z-octadecenoyl)-*sn*-glycero-3-phospho-(1'-*rac*-glycerol) (DOPG), e) 1,2-dioleoyl-*sn*-glycero-3-phospho-L-serine (DOPS), f) cholesterol, g) ergosterol, h) stigmasterol. .67



Figure 4.2: Data from RCV of a DOPC coated Pt/Hg electrode in PBS at pH 7.4 measured at $40\text{V}\cdot\text{s}^{-1}$ with potential excursions from -0.4V to -1.2V.....	69
Figure 4.3: a) Data from RCV of a Pt/Hg electrode (black line) and coated with DOPC (red line) measured at $40\text{V}\cdot\text{s}^{-1}$ with potential excursions from -0.4V to -1.8V in PBS at pH 7.4. b) Illustration of the possible phase transitions occurring upon varying the applied potential.....	70
Figure 4.4: Illustration of lipid organisation of various phospholipids PC,PG,PS and PE. ....	75
Figure 4.5: RCVs recorded at $40\text{Vs}^{-1}$ of a DOPC coated Pt/Hg electrode in PBS at pH 7.4 (black line) in the presence of a) pH 2 (red line), b) pH 13.5 (red line) and c) calcium chloride $0.1\ \mu\text{mol dm}^{-3}$ (red line). d) Graph representing the first capacitance current peak of DOPC coated Pt/Hg electrode vs. solution pH. e) Graph representing headgroup surface charge vs. solution pH [19]. ....	77
Figure 4.6: RCVs recorded at $40\text{Vs}^{-1}$ of a DOPC coated Pt/Hg electrode in PBS at pH 7.4 (black line) with a switching potential of -1.8V in the presence of 0, 0.092, 0.184, 0.230, 0.276, 0.656 and 0.920 $x_c$ of CHOL:DOPC in PBS at pH 7.4. The $x_c$ values shown in legend inset and colour coded. ....	79
Figure 4.7: Plot of the mean of the first and second capacitance current peak heights ( $\mu\text{F cm}^{-2}$ ) vs. mole fraction ( $x_c$ ) of CHOL:DOPC coated Pt/Hg electrode in PBS at pH 7.4. ....	80
Figure 4.8: RCVs recorded at $40\text{Vs}^{-1}$ with potential excursions from -0.4V to -1.8V of a DOPC coated Pt/Hg electrode in PBS at pH 7.4 (black line), a 0.2 mole fraction of DOPC/cholesterol coated Pt/Hg electrode in PBS at pH 7.4 (orange line), a 0.16 mole fraction of DOPC/ergosterol coated Pt/Hg electrode in PBS at pH 7.4 (red line) and a	

0.16 mole fraction of DOPC:stigmasterol coated Pt/Hg electrode in PBS at pH 7.4 (blue line).....81

Figure 4.9: RCV recorded at  $40 \text{ Vs}^{-1}$  of a  $0.2 \text{ mg cm}^{-3}$  DOPC coated Pt/Hg electrode with potential excursions from  $-0.4\text{V}$  to  $-1.8\text{V}$  (red line) and a  $0.2 \text{ mg cm}^{-3}$  POPC coated Pt/Hg electrode with potential excursions from  $-0.4\text{V}$  to  $-1.5\text{V}$  (black line). All experiments conducted in PBS at pH 7.4.....82

Figure 4.10: RCVs recorded at  $40 \text{ Vs}^{-1}$  in PBS at pH 7.4 of a) a DOPC coated Pt/Hg electrode; switching potential  $-1.2\text{V}$ , b) a DOPE coated Pt/Hg electrode with switching potential  $-1.4\text{V}$ , c) a DOPG coated Pt/Hg electrode with switching potential of  $-1.3\text{V}$  and d) a DOPS coated Pt/Hg electrode with switching potential of  $-1.4\text{V}$ . The switching potentials are chosen due to their individual stability profiles. ....83

Figure 4.11: RCVs recorded at  $40 \text{ Vs}^{-1}$  of a DOPE coated Pt/Hg electrode in PBS at pH 7.4 (black line) in the presence of a) pH 2 (red line) and b) pH 10 (red line). ....84

Figure 4.12: RCV recorded at  $40 \text{ Vs}^{-1}$  of DOPE coated Pt/Hg electrode in PBS at pH 7.4 a) showing unstable capacitance current peaks at switching potential of  $-1.4\text{V}$  and b) at switching potential of  $-1.8\text{V}$ . ....85

Figure 4.13: RCVs recorded at  $40 \text{ Vs}^{-1}$  of a DOPG coated Pt/Hg electrode with switching potential of  $-1.4\text{V}$  in the following conditions: a) a continuous PBS flow at pH 7.4, b) a continuous PBS flow at pH 2 (black line) and after 10 seconds (red line), c) a static cell containing PBS at pH 2 and d) a static cell containing PBS at pH 2 at switching potential of  $-1.5\text{V}$ . ....87

Figure 4.14: RCVs recorded at  $40 \text{ Vs}^{-1}$  of a DOPS coated Pt/Hg electrode in PBS at pH 7.4 with switching potential of  $-1.4\text{V}$  (black line) representing a) attempts to

produce similar reproducible capacitance current peaks and b) introducing varying pH which are colour coded and listed on the legend inset. ....89

Figure 4.15: RCVs recorded at  $40 \text{ Vs}^{-1}$  of a) DOPC coated Pt/Hg electrode (black line) in the presence of  $1 \mu\text{mol dm}^{-3}$  imipramine (red line) and b) DOPS coated Pt/Hg electrode (black line) in the presence of  $1 \mu\text{mol dm}^{-3}$  imipramine (red line). ....90

Figure 5.1: Molecular structures of a) spiperone, b) bis(pyridinium) and c) bis(4-tert-butylpyridinium), d) 1-butyl-3-methylimidazolium bis(trifluoromethylsulfonyl)imide ..94

Figure 5.2: RCVs recorded at  $40 \text{ Vs}^{-1}$  of a DOPC coated Pt/Hg electrode in PBS at pH 7.4 (black line) in the presence of  $0.25 \text{ mmol dm}^{-3}$  spiperone with the following alkyl chain lengths (a)  $\text{C}_0$ , (b)  $\text{C}_2$ , (c)  $\text{C}_3$ , (d)  $\text{C}_4$  and (e)  $\text{C}_6$ . (f) Current capacitance peaks recovering after testing with  $0.25 \text{ mmol dm}^{-3}$   $\text{C}_0$  spiperone (blue line) and after testing with  $0.25 \text{ mmol dm}^{-3}$   $\text{C}_6$  spiperone (red line). ....100

Figure 5.3: Graph showing the effect of increasing alkyl chain length of spiperone on the first capacitance current peak height (red line) and extent of recovery of the capacitance current peak height (blue line). The value of R is -0.9835 showing a strong negative correlation. The values are presented in Table 5.1. ....101

Figure 5.4: Exposure time (30 seconds) on the effect of spiperones with varying alkyl chain on DOPC monolayer first capacitance current peaks. ....102

Figure 5.5: RCVs recorded at  $40 \text{ Vs}^{-1}$  of a DOPC coated Pt/Hg electrode in PBS at pH 7.4 (black line) in the presence of  $20 \mu\text{mol dm}^{-3}$  bis(4-tert-butylpyridinium) compounds (red line) a) MB408, b) MB442, c) MB444, d) MB505, e) MB775, f) MB520, g) MB778, h) MB779 and i)  $20 \mu\text{mol dm}^{-3}$  (red line) and  $50 \mu\text{mol dm}^{-3}$  (blue line) MB777. ....104

Figure 5.6: RCVs recorded at 40 Vs<sup>-1</sup> of a DOPC coated Pt/Hg electrode in PBS at pH 7.4 (black line) in the presence of 20 μmol dm<sup>-3</sup> bis(4-tert-butylpyridinium) compounds (red line) a) MB582, b) MB781, c) MB782, d) MB327, e) MB583, f) MB780, g) MB783, h) MB784, i) MB786 and j) 20 μmol dm<sup>-3</sup> (red line) and 50 μmol dm<sup>-3</sup> (blue line) MB785. ....105

Figure 5.7: Graph of capacitance current peak height of Bis 4-tert butyl and Bis pyridinium compounds on DOPC coated Hg electrode in PBS at pH 7.4 vs. n-alkyl chain length. ....106

Figure 5.8: Effect of N1-alkyl chain lengths against anti-malarial toxicity [16]......108

Figure 5.9: RCVs recorded at 40 Vs<sup>-1</sup> of a DOPC coated Pt/Hg electrode in PBS at pH 7.4 (black line) with potential excursions from -0.4V to -1.8V in the presence of 0.1 μmol dm<sup>-3</sup> [CnMIM][NTf2] with n2 (blue dashed line), n4 (red dash-dotted line), n8 (green dotted line), and n12 (pink line). The numbers 1 – 3 represent the DOPC transition phases (Chapter 4). ....109

Figure 5.10: Correlations of a) toxicity values of EC50 for Vibrio fischeri and b) log K<sub>ow</sub> all vs. LoD at DOPC coated Hg electrode in PBS at pH 7.4. ....111

Figure 6.1: Molecular structures of (a) naphthalene, (b) anthracene, (c) pyrene, (d) benzanthracene, (e) imipramine, (f) clomipramine, (g) amitriptyline, (h) 1,1,1-trichloro-2,2-di(4-chlorophenyl)ethane (DDT), (i) ethinyl estradiol, (j) dexamethasone, (k) phenothiazine, (l) chlorpromazine, (m) prochlorperazine, (n) alachlor, (o) theophylline, (p) caffeine and (q) nadolol. ....116

Figure 6.2: RCVs recorded at 40 Vs<sup>-1</sup> of a DOPC coated Pt/Hg electrode (black line) in the presence of (a) 0.0005 μmol dm<sup>-3</sup> (red line) and 0.002 μmol dm<sup>-3</sup> (blue line) pyrene, (b) 3 μmol dm<sup>-3</sup> dexamethasone (red line), (c) 0.3 μmol dm<sup>-3</sup> clomipramine

(red line), (d) 0.3  $\mu\text{mol dm}^{-3}$  DDT (red line), (e) 5  $\mu\text{mol dm}^{-3}$  phenothiazine (red line) and (f) 0.3  $\mu\text{mol dm}^{-3}$  prochlorperazine (red line), in PBS at pH 7.4. ....119

Figure 6.3: Method for LoD determination by estimating concentration corresponding to three times standard deviation (SD) of DOPC control capacitance current peak height on the capacitance current peak height versus concentration curve for, (a) benzantracene, (b) anthracene, (c) pyrene and (d) naphthalene interaction with DOPC coated Hg in PBS at pH 7.4.....120

Figure 6.4: Scatter plot of compounds' LoD at DOPC coated Hg electrode in PBS at pH 7.4 vs their respective log octanol - water partition coefficient ( $\log K_{ow}$ ) for following compounds and classes of compounds: DDT (filled circle), polycyclic aromatic hydrocarbons (open circle), tricyclic phenothiazines (open triangle), tricyclic antidepressants (filled squares), methylxanthines (open squares), alachlor (plus sign) and steroids (diagonal cross signs). Symbols representing compounds belonging to same class are connected by line for clarity.....121

Figure 7.1: Molecular structures a) tricresyl phosphate, b) chloramphenicol c) imidazole, d) caffeine e) theophylline f) fallypride g) flumazenil, h) DASB i) diprenorphine j) raclopride k) rolipram l) WAY m) spiperone n) amiloride o) tryptophan .....128

Figure 7.2: RCVs recorded at 40  $\text{Vs}^{-1}$  of a DOPC coated Pt/Hg electrode in PBS at pH 7.4 (black line) in the presence of a) 0.003  $\mu\text{mol dm}^{-3}$  (red line) and 0.14  $\text{nmol dm}^{-3}$  (blue line) TcP and b) 0.05  $\mu\text{mol dm}^{-3}$  (red line) TcP. d) LoD determination by estimating concentration corresponding to three times SD of DOPC control capacitance current peak height on capacitance current peak height versus concentration curve for TcP interaction with DOPC coated Hg in PBS at pH 7.4 (error bars within the markers).....133

Figure 7.3: RCVs recorded at  $40 \text{ Vs}^{-1}$  of a DOPC coated Pt/Hg electrode in PBS at pH 7.4 (black line) in the presence of a)  $3 \times 10^{-4} \mu\text{mol dm}^{-3}$  chloramphenicol (red line) and b)  $6 \times 10^{-4} \mu\text{mol dm}^{-3}$  chloramphenicol (red line). c) RCV recorded of uncoated Pt/Hg electrode (black line) at  $40 \text{ Vs}^{-1}$  in PBS at pH 7.4 in the presence of  $3 \times 10^{-4} \mu\text{mol dm}^{-3}$  chloramphenicol (red line) and d) RCVs recorded at  $40 \text{ Vs}^{-1}$  in PBS at pH 7.4 of uncoated Pt/Hg electrode (black line) and uncoated Pt/Hg electrode post chloramphenicol studies (red line). ..... 134

Figure 7.4: RCVs recorded at  $40 \text{ Vs}^{-1}$  of a DOPC coated Pt/Hg electrode in PBS at pH 7.4 (black line) in the presence of (a)  $10 \mu\text{mol dm}^{-3}$  imidazole (red line) b)  $10 \mu\text{mol dm}^{-3}$  theophylline (red line) and c)  $10 \mu\text{mol dm}^{-3}$  caffeine (red line). ..... 135

Figure 7.5: RCVs recorded at  $40 \text{ Vs}^{-1}$  of a DOPC coated Pt/Hg electrode in PBS at pH 7.4 (black line) in the presence of  $0.25 \text{ mmol dm}^{-3}$  (red line) a) fallypride, b) flumazenil ,c) DASB, d) diprenorphine, e) raclopride, f) WAY, g) rolipram h) serotonin and i) spiperone ..... 137

Figure 7.6: RCVs recorded at  $40 \text{ Vs}^{-1}$  of a DOPC coated Pt/Hg electrode in PBS at pH 7.4 (black line) in the presence of a) amiloride with increasing concentrations from  $0.005$  to  $5 \mu\text{mol dm}^{-3}$  and b) l-tryptophan with increasing concentrations from  $0.005$  to  $5 \mu\text{mol dm}^{-3}$  ..... 139

Figure 8.1: Molecular structures of compounds (a) benzene, (b) naphthalene, (c) anthracene, (d) pyrene (e) benzanthracene ..... 144

Figure 8.2: RCVs recorded at  $40 \text{ Vs}^{-1}$  of a DOPC coated Pt/Hg electrode in PBS at pH 7.4 (black line) in the presence of a)  $8 \mu\text{mol dm}^{-3}$  benzene (red line), b)  $0.8 \mu\text{mol dm}^{-3}$  (blue line) and  $8 \mu\text{mol dm}^{-3}$  (red line) naphthalene, c)  $0.06 \mu\text{mol dm}^{-3}$  (blue line) and  $0.6 \mu\text{mol dm}^{-3}$  (red line) anthracene, d)  $0.0005 \mu\text{mol dm}^{-3}$  (blue line) and  $0.002$

$\mu\text{mol dm}^{-3}$  (red line) pyrene and e)  $0.8 \mu\text{mol dm}^{-3}$ (blue line) and  $8 \mu\text{mol dm}^{-3}$  (red line) benzanthracene..... 147

Figure 8.3: Plot showing the effect of PAH compounds on the potential (-V) of the second capacitance current peak vs. concentration ( $\mu\text{mol dm}^{-3}$ ). Potential values were obtained from the RCV experiments ( $-0.4\text{V}$  to  $-1.2\text{V}$  at  $40\text{V}\cdot\text{s}^{-1}$  in PBS at pH 7.4). ..... 148

Figure 8.4: LoD determination by estimating concentration corresponding to three times SD of DOPC control capacitance current peak height on capacitance current peak height versus concentration curve for, (a) benzanthracene, (b) anthracene, (c) pyrene and (d) naphthalene interaction with DOPC coated Hg in PBS at pH 7.4. . 149

Figure 8.5: Scatter plot of PAH compounds' log LoD at DOPC coated Pt/Hg in PBS at pH 7.4 for benzene, naphthalene, anthracene, pyrene and benzanthracene vs. their respective log octanol - water partition coefficient ( $\log K_{ow}$ )..... 150

Figure 9.1: Molecular structures of a) cholesterol, b) ergosterol, c) stigmasterol, d) ethinyl estradiol, e) dexamethasone..... 160

Figure 9.2: RCVs recorded at  $40 \text{Vs}^{-1}$  of a DOPC coated Pt/Hg electrode (black line) in the presence of (red lines) a)  $6 \mu\text{mol dm}^{-3}$  cholesterol, b)  $6 \mu\text{mol dm}^{-3}$  stigmasterol, c)  $3 \mu\text{mol dm}^{-3}$  ergosterol, d)  $30 \mu\text{mol dm}^{-3}$  ethinyl estradiol and (e)  $3 \mu\text{mol dm}^{-3}$  dexamethasone. f) shows the recovery of capacitance current peaks post  $3 \mu\text{mol dm}^{-3}$  dexamethasone interaction..... 163

Figure 9.3: LoD determination by estimating concentration corresponding to three times standard deviation (SD) of DOPC control capacitance current peak potential versus concentration curve for a) cholesterol, b) stigmasterol, c) ergosterol d) ethinyl

estradiol and e) dexamethasone interaction with DOPC coated Hg in PBS at pH 7.4. .....	164
Figure 9.4: Plot showing capacitance current potential (-E/V) vs. concentration ( $\mu\text{mol dm}^{-3}$ ) of the steroid compounds cholesterol (red line), stigmasterol (black line), ergosterol (blue line), ethinyl estradiol (green line) and dexamethasone (yellow line). Potential values were obtained from RCV experiments (-0.4V to -1.2V at $40\text{V}\cdot\text{s}^{-1}$ in PBS at pH 7.4).....	165
Figure 9.5: Plot showing the relationship of potential shift (-E/V) and dipole moment ( $\mu$ ) of steroids. The values are listed in Table 9.1.....	167
Figure 9.6: Plot of dipole moment ( $\mu$ ) vs. limit of detection (LoD) at DOPC coated Pt/Hg in PBS at pH 7.4 for steroid compounds. ....	168
Figure 10.1: Molecular structure of plasma membrane with integrated G-coupled protein. ....	178
Figure 10.2: Molecular structures of tricyclic antidepressants and tricyclic phenothiazines. a) phenothiazine, b) imipramine, c) clomipramine, d) amitryptilline, e) chlorpromazine f) prochlorperazine.....	179
Figure 10.3: RCVs recorded at $40\text{Vs}^{-1}$ of a DOPC coated Pt/Hg electrode (black line) in the presence of a) $0.3\ \mu\text{mol dm}^{-3}$ clomipramine, b) $0.3\ \mu\text{mol dm}^{-3}$ imipramine, c) $0.3\ \mu\text{mol dm}^{-3}$ amitryptilline, d) $0.3\ \mu\text{mol dm}^{-3}$ prochlorperazine e) $0.3\ \mu\text{mol dm}^{-3}$ chlorpromazine, and f) $5\ \mu\text{mol dm}^{-3}$ phenothiazine (red line) in PBS at pH 7.4.....	184
Figure 10.4: Plot of therapeutic effective concentrations (TEC) from sources as referenced on diagram vs. limit of detection (LoD) at DOPC coated Pt/Hg in PBS at pH 7.4 for tricyclic phenothiazines and antidepressants. Best fit line for plot and equation therefore shown on diagram.....	185



Figure 10.5: Plot of the first capacitance current peaks ( $\mu\text{F cm}^{-2}$ ) vs. pH for the interaction of a) imipramine with DOPC coated Pt/Hg electrode in PBS with concentrations 0.3, 6 and 15  $\mu\text{mol dm}^{-3}$  as shown in the legend inset and b) clomipramine with DOPC coated Pt/Hg electrode in PBS with concentrations 0.3, 6 and 15  $\mu\text{mol dm}^{-3}$  as shown in the legend inset. ....186

Figure 10.6: Binding affinities ( $K_i$ ) <sup>(i)</sup> for TCAs and tricyclic phenothiazines with dopamine receptors D2 and D3 vs. their LoD at DOPC coated Pt/Hg in PBS at pH 7.4. The values are listed in Table 10.1. ....188

Figure 10.7: Plot of log of the binding affinity,  $K_i$  to the receptor 5-HT vs. LoD at DOPC coated Hg electrode in PBS at pH 7.4 for the compounds listed in Table 10.2.....190

Figure 10.8: Stern–Volmer plots for KI induced fluorescence quenching of TCAs and tricyclic phenothiazines (listed and colour coded in legend inset) with DOPC vesicles in PBS at pH 7.4. ....192

Figure 10.9: Scatter plot to show % of TCA and tricyclic phenothiazines compounds that have penetrated into DOPC vesicles vs. their respective LoD at DOPC coated Pt/Hg. These values are listed in Table 10.4.....193

Figure 11.1: RCVs recorded at 40  $\text{Vs}^{-1}$  of a DOPC coated Pt/Hg electrode in PBS at pH 7.4 (black line) in the presence of compounds a) to n) (red line). The RCV scans can be used a “fingerprint” database for compounds. a) 10  $\mu\text{mol dm}^{-3}$  chlorpromazine, b) 0.25  $\text{mmol dm}^{-3}$  C<sub>2</sub> spiperone, c) 1  $\mu\text{mol dm}^{-3}$  anthracene, d) 20  $\mu\text{mol dm}^{-3}$  MB520, e) 1  $\mu\text{mol dm}^{-3}$  stigmasterol, f) 1  $\mu\text{mol dm}^{-3}$  clomipramine, g) 0.25  $\mu\text{mol dm}^{-3}$  DDT, h) 5  $\mu\text{mol dm}^{-3}$  phenothiazine, i) 10  $\text{mmol dm}^{-3}$  theophylline, j) 0.25  $\text{mmol dm}^{-3}$  diprenorphine, k) 0.25  $\text{mmol dm}^{-3}$  DASB, l) 10  $\mu\text{mol dm}^{-3}$  BMIM Br, m) 10  $\mu\text{mol dm}^{-3}$  ethinyl estradiol and n) 0.003  $\mu\text{mol dm}^{-3}$  TcP. ....208

Figure 11.2: RCV scans at  $40 \text{ Vs}^{-1}$  of DOPC coated Pt/Hg electrode (black line) in the presence of (a)  $3 \text{ mg dm}^{-3}$  solution of humic acid in PBS at pH 7.4, (b)  $3 \text{ mg dm}^{-3}$  solution of humic acid in PBS at pH 7.4 with  $0.002 \text{ } \mu\text{mol dm}^{-3}$  pyrene, (c) tap water, (d) tap water spiked with  $0.002 \text{ } \mu\text{mol dm}^{-3}$  pyrene and (e) PBS at pH 7.4 with  $0.002 \text{ } \mu\text{mol dm}^{-3}$  pyrene.....210

Figure 11.3: RCV scans at  $40 \text{ V s}^{-1}$  of DOPC coated Pt/Hg electrode in PBS at pH 7.4 (black line) in the presence of a) surface running water (red line), b) water sample from cave (red line) and c) surface running water spiked with  $0.002 \text{ } \mu\text{mol dm}^{-3}$  pyrene (red line). .....211

Figure 11.4: RCV scans at  $40 \text{ V s}^{-1}$  of DOPC coated Pt/Hg electrode in PBS at pH 7.4 (black line) in the presence of a)  $0.0025 \text{ } \mu\text{mol dm}^{-3}$  pyrene, b)  $0.26 \text{ } \mu\text{mol dm}^{-3}$  prochlorperazine, c)  $0.0025 \text{ } \mu\text{mol dm}^{-3}$  pyrene and  $1.3 \text{ } \mu\text{mol dm}^{-3}$  prochlorperazine (red line). .....212

Figure 11.5: Plot showing the effect on capacitance current peak heights vs. increasing concentrations of prochlorperazine with a)  $0.2 \text{ mg cm}^{-3}$  dispersion of DOPC coated Pt/Hg electrode in PBS at pH 7.4 (red line) and in a mixture with  $0.025 \text{ } \mu\text{mol dm}^{-3}$  pyrene (yellow line) affecting the first capacitance current peak height, b)  $0.2 \text{ mg cm}^{-3}$  dispersion of DOPC coated Pt/Hg electrode in PBS at pH 7.4 (blue line) and in a mixture with  $0.025 \text{ } \mu\text{mol dm}^{-3}$  pyrene (red line) affecting the second current capacitance peak height. ....213

Figure 11.6: Plot showing the effect on capacitance current peak heights vs. increasing concentration of pyrene with a)  $0.2 \text{ mg cm}^{-3}$  dispersion of DOPC coated Pt/Hg electrode in PBS at pH 7.4 (red line) and in a mixture with  $1.3 \text{ } \mu\text{mol dm}^{-3}$  prochlorperazine (blue line) affecting the first capacitance current peak height and b)  $0.2 \text{ mg cm}^{-3}$  dispersion of DOPC (red line) and in a mixture with  $1.3 \text{ } \mu\text{mol dm}^{-3}$

prochlorperazine (green line) effecting the second capacitance current peak height.  
.....214

Figure 11.7: LoD determination by estimating the concentration corresponding to three times SD of DOPC control capacitance current peak height on capacitance current peak height versus concentration curve for a) prochlorperazine when in a mixture with  $0.025 \mu\text{mol dm}^{-3}$  pyrene in PBS at pH 7.4 and b) pyrene when in a mixture with  $1.3 \mu\text{mol dm}^{-3}$  prochlorperazine PBS at pH 7.4. Error bars confined within the markers. ....215

Figure 11.8: RCV scans at  $40 \text{ V s}^{-1}$  of DOPC coated Pt/Hg electrode in PBS at pH 7.4 (black line) in the presence of a)  $0.3 \mu\text{mol dm}^{-3}$  DDT (red line), b)  $0.0025 \mu\text{mol dm}^{-3}$  pyrene (red line) and c)  $0.00125 \mu\text{mol dm}^{-3}$  pyrene and  $0.002 \mu\text{mol dm}^{-3}$  DDT (red line).....216

Figure 11.9: RCV scans at  $40 \text{ V s}^{-1}$  of DOPC coated Pt/Hg electrode in PBS at pH 7.4 (black line) in the presence of a)  $0.03 \mu\text{mol dm}^{-3}$  anthracene (red line), b)  $0.003 \mu\text{mol dm}^{-3}$  anthracene in a mixture with  $0.26 \mu\text{mol dm}^{-3}$  prochlorperazine (red line) and c)  $0.06 \mu\text{mol dm}^{-3}$  anthracene in a mixture with  $0.26 \mu\text{mol dm}^{-3}$  prochlorperazine (red line). d) LoD determination of DOPC control capacitance current peak height on capacitance current peak height versus concentration curve for anthracene in a mixture with of  $0.3 \mu\text{mol dm}^{-3}$  prochlorperazine in PBS at pH 7.4.....217

Figure 11.10: RCV scans at  $40 \text{ V s}^{-1}$  of DOPC coated Pt/Hg electrode in PBS at pH 7.4 (black line) in the presence of a)  $0.05 \mu\text{mol dm}^{-3}$  pyrene (red line), b)  $20 \mu\text{mol dm}^{-3}$  MB779 (red line) and c)  $20 \mu\text{mol dm}^{-3}$  MB779 and  $0.05 \mu\text{mol dm}^{-3}$  pyrene (red line).  
.....219

Figure 12.1: Illustration of membrane bound target receptors on Pt/Hg for future developments and research.....228



# TABLES

Table 3.1: Typical measuring parameters in biomembrane studies.....	62
Table 3.2: Typical permeability assays to compare with MFE flow cell assay. ....	63
Table 5.1: Alkyl lengths ( <i>n</i> ) of spiperone and their capacitance current peak height ( $\mu\text{F cm}^{-2}$ ).....	101
Table 5.2: Antimalarial toxicity for compounds' alkyl length listed [16].....	108
Table 5.3: Parameters for the ionic liquids used in this study. (a) <i>Ecotoxicol. Environ. Saf.</i> 2004, 58: pp396–40. (b) <i>Green Chem.</i> 2011, 13: pp1507–1516.....	110
Table 6.1: Log $K_{\text{OW}}$ values of compounds and their LoDs using sensing device. (i) Values from PubChem Compound database. ....	124
Table 8.1: Log $K_{\text{OW}}$ values of compounds, their number of aromatic ring and their calculated LoDs. (i) Values from PubChem Compound database.....	149
Table 9.1: Dipole moments ( $\mu$ ) of steroids and average potential shifts (-V) of concentrations ranging from 0.5 to 10 $\mu\text{mol dm}^{-3}$ .....	167
Table 9.2: Dipole moment values of the steroid compounds and their LoDs. ....	168
Table 10.1: Representing listed compounds with their calculated LoD and $K_i$ values <sup>(i)</sup> for dopamine receptors, D2 and D3. (i) These values were verified by comparison with log D (7.4) values from the ChemSpider database ( <a href="http://www.chemspider.com">http://www.chemspider.com</a> ). ....	189

Table 10.2: List of compounds with their calculated LoD using sensing device and  $K_i$  values for 5-HT<sup>(i)</sup>. (i) These values were verified by comparison with log D (7.4) values from the ChemSpider database (<http://www.chemspider.com>).....190

Table 10.3: List of compounds with their respective LoD values (using sensing device) and % of DOPC vesicle penetration (calculated using Stern-Volmer plots).....193

# ABBREVIATIONS

ACV	alternating current voltammetry
at.%	atomic weight percent
AC	alternating current
A0	electrode area
CaCCs	Ca <sup>2+</sup> -activated Cl <sup>-</sup> channels
CAMP	cationic antimicrobial peptides
CF	cystic fibrosis
CFTR	cystic fibrosis transmembrane conductance regulator
C <sub>O</sub>	concentration of oxidant
C <sub>R</sub>	concentration of reductant
C <sub>sp</sub>	specific capacitance (F·m <sup>-2</sup> )
CV	cyclic voltammetry
DC	direct current
DME	dropping mercury electrode
DOPC	1,2-Dioleoyl-sn-glycero-3-phosphocholine
DOPE	1,2-Dioleoyl-sn-glycero-3-phosphoethanolamine

DOPG	1,2-Dioleoyl-sn-glycero-3-[phospho-rac-(1-glycerol)] (sodium salt)
DOPS	1,2-Dioleoyl-sn-glycero-3-[phospho-L-serine] (sodium salt)
EIS	electrochemical impedance spectroscopy
EDL	electric double layer
HMDE	hanging mercury drop electrode
Hg	mercury
HMW	high molecular weight
IL	ionic liquid
LMW	low molecular weight
LoD	limit of detection
M	molecular weight
MA	(log MA) membrane affinity
MFE(s)	micro fabricated electrode(s)
PAH	polynuclear aromatic hydrocarbon
PBS	phosphate buffered saline
ppb	parts per billion
ppm	parts per million
$p_m$	molar density



POPC	1-palmitoyl-2-oleoyl- <i>sn</i> -glycero-3-phosphocholine
Pt	platinum
PTFE	polytetrafluoroethylene
PZC	potential of zero charge
Q	charge
RC	resistor and capacitor in series
RCV	rapid cyclic voltammetry
SAM(s)	self-assembled monolayer(s)
SAR	structure-activity relationship
SD	standard deviation
TCA(s)	tricyclic antidepressant(s)
WE	working electrode

# COMMONLY USED SYMBOLS

$\Delta$	difference
C	capacitance (F)
D	distance (m)
$\epsilon_0$	permittivity of free space ( $8.854188 \times 10^{-12} \text{ F} \cdot \text{m}^{-1}$ )
$e_0$	electron charge ( $-1.60218 \times 10^{-19} \text{ C}$ )
E	electric field ( $\text{V} \cdot \text{cm}^{-1}$ )
$E^\ominus$	standard electrode potential (V)
$E^0$	redox potential
F	Faradays constant ( $9.64853 \times 10^4 \text{ C} \cdot \text{mol}^{-1}$ )
I	electric current (A)
$k_e$	coulomb's constant
$\Omega$	angular frequency (Radians)
$\rho$	density
pa	peak anode
pc	peak cathode
Q	electric charge (C)

R	resistance ( $\Omega$ )
t	time
T	temperature (K)
v	scan rate
V	potential (V)
<b>x<sub>c</sub></b>	mole fraction
X	reactance ( $\Omega$ )
Y	admittance (S)
Z	impedance ( $\Omega$ )

# CHAPTER 1

## INTRODUCTION

### 1.1 INTRODUCTION

Electrochemical studies of lipids on Hg surface are fundamental in the determination of the structure and properties of the monolayer. The studies conducted in the following chapters have been extended to look at the monolayer under potential control in the presence of various compounds. The coated electrodes give characteristic responses in the capacitance/voltage curve in response to various test substances in solution. Microfabricated platinum electrodes with coated mercury (Hg) have been used as the working electrode of choice in the current studies of the membrane model. The microfabricated platinum electrodes will herein be referred to as MFE. Observing the capacitance current peaks obtained during the electrochemical studies, we can detect changes in the peaks when chemical compounds interact with the layers. In this way, detection limits and sensitivities for each chemical compound can be recorded. During preliminary studies, it was found that the phase transitions and hence capacitance current peaks are very sensitive to the monolayer interaction with certain compounds. Any change in the form of the peaks can thus be attributed to compound interaction. The changes in phase

transition can then be assessed and used to identify a potential toxic contaminant in the environment, specifically, as a practical application in toxicity sensing for water companies to assess exposure of hazardous substances to water.

Phospholipids are known to have interesting properties when exposed to applied potentials making electrochemical methods an effective way of investigating their structure and properties. Phospholipids have been studied using lipid coated Hg techniques, one technique being the hanging Hg drop electrode (HMDE) and more recently MFE. Phospholipids contain two fatty acid tails attached to a glycerol head. The third alcohol group of glycerol is attached to a phosphate molecule. The phosphate group is then linked to other functional groups for example choline. The phosphate group and the glycerol group render the head of the phospholipid polar, the fatty acid tail is apolar and therefore phospholipids are amphipathic [1].

One of the most important properties of the phospholipid is its mobility and fluidity. This mobility can change with temperature. The electrochemical response of the phospholipid is reflective of the phase behaviour of the bilayer. At various temperatures, the phospholipid bilayer can exist in either liquid or solid (gel) phase. In the liquid phase, the molecules in the bilayers diffuse freely; a given lipid will rapidly exchange locations with its neighbour millions of times a second and through 'random walk' can migrate over long distances. Also, the physical property of the tail length is significant as it can affect the physical quality and interaction ability of the phospholipid. Longer tailed lipids have more area in which to interact thereby increasing the interaction between individual phospholipids and increasing their solid (gel)/liquid phase transition temperature.

The transition temperature is also affected by the degree of unsaturation of the hydrocarbon chain. A decrease by one carbon in the chain length, causes a decrease in transition temperature by 10°C and when a single double bond is added to the

hydrocarbon chain, the transition temperature decreases by upto 70°C. The double bond of the unsaturated fatty acid introduces “kinks” to the hydrocarbon chain therefore the lipid molecules will not pack together in a regular structure and will remain fluid at low temperatures [2] [3]. Saturated lipid molecules pack well and are solid at low temperatures. An example of this occurrence in everyday life is the difference in butter and vegetable oil. Butter at room temperature is solid having mostly saturated hydrocarbon chains. Vegetable oil being more unsaturated, is liquid at room temperature.

If we looked at nature and the biological cell membrane, we find that, in order to keep the membrane fluid at physiological temperatures, the cell will alter the composition of its phospholipids. There exists the appropriate ratio of saturated and unsaturated fatty acids which maintains lipid fluidity at any temperature conducive to living processes. Furthermore, the existence of cholesterol modifies the packing of the fatty acid tails and moderates the fluidity [4]. Phospholipids in the monolayer configuration have been studied for a long time. These studies involve numerous physical chemical approaches. These include permeability studies, chemical analyses, electrical impedance measurements, electron microscopy, surface tension studies and global electrical measurements. These studies and the devices used contribute to a vast array of knowledge into the properties of phospholipid monolayers including an insight into physical properties such as resistance, capacitance, dielectric constants and dimensions of monolayer and bilayer assemblies.

One of the most important biophysical properties of the phospholipid monolayer is the electric double layer which is present on a phospholipid monolayer surface. The electric double layer is formed where two different phases are in contact. The biological cell surface carries many chemical groups each having different dissociation constants therefore there will be varying electric charges present at physiological pH. It can be concluded that biological membrane surfaces are

chemically heterogeneous. The pH differential that exists across the barrier plays an important role in the energetics of cellular processes. Electrically, a cell membrane functionally forms part of a diffusion cell. If the interior pH differs from the exterior pH, which reflects a difference in proton concentration on both sides then functioning of the cell will be affected, or if there are toxins present which influence the pH, or if the membrane's dielectric properties are altered, then functioning of the cell will be affected. Some measurements on the capacitance of a phospholipid bilayer at various pH levels with and without present of cholesterol were conducted by Ohki and Goldup [5]. It was found that capacitance is dependent on pH. Capacitance also increases when pH is decreased or increased [5]. The effect of pH on lipid monolayers using electrochemical methods is discussed in Chapter 4 and further explored with inclusion of compound interaction in Chapter 10.

Furthermore, ion exchange is constantly taking place between the living cell and the extracellular fluid therefore; there is emergence of electric potential differences between the cell interior and the fluid bulk. This is known as the transmembrane potential [6]. These electrochemical processes can be measured and subsequently help us to understand the physical characteristics of the bilayer and if these can be exploited for use in medicine, toxicology and drug delivery. Information obtained from these studies can be quantified and thus, we could predict the outcome of the lipid bilayer when in certain conditions. Phospholipid monolayers can be deposited on to Hg electrode surfaces to form stable structures whose properties depend on the electrode potential. Using voltammetric techniques, it is possible to investigate their behaviour in the presence of an electric field. The coating technique is simple and stable. The lipid films can also be renewed readily. The binding or interactions of the lipids with various species in an electrolyte can be measured electrochemically via measurements of capacitance/voltage and the changes in the capacitance observed. The capacitance peaks respond selectively to different components and therefore can

be used to assess water quality in tap water and sea water. In this way, lipid coated Hg electrodes can be used as a sensing element in a detector.

### **1.1.1 MONOLAYER CAPACITANCE – THE RELATIONSHIP BETWEEN CHARGE, CURRENT AND CAPACITANCE**

Charge is a fundamental property of matter with units of coulombs, C. An individual electron or proton has a charge of  $1 \times 10^{-19}$  C, the electron is negatively charged  $-1 \times 10^{-19}$  C and the protons positively charged  $+1 \times 10^{-19}$  C. A normal atom has equal number of electrons and protons therefore its total charge is zero. Charge has a role to play in currents. The amount of charge that passes through a point over a given time produces an electric current such that,

$I = Q/t$  where I is the current in amps, Q is the charge in coulombs and t is the time in seconds.

It is possible to store an accumulated amount of charge to be used at a later time. The device for this is a capacitor. A capacitor stores energy in the form of an electric charge. When a capacitor is being charged, the power supply pulls electrons from one plate which becomes positive and the other becomes negative. The charge on the capacitor builds up until it reaches a point where the power supply has insufficient energy to push the electrons onto the plate against the repulsion of the electrons already present. The electrode-solution interface has been shown to behave like a capacitor. The metal electrode carries a certain number of electrons, and the solution is composed of ions. Capacitance of the interface characterizes its ability to store charge in response to perturbation in potential. The distance and surface area play a role in the total capacitance. In parallel plates, one of the plates will acquire a positive charge and the other a negative charge. As the charge builds up then the voltage potential between the plates also build up. The voltage potential across the capacitor



continues to build up until it matches the voltage source. The amount of charge stored in a capacitor can be determined by the equation  $Q=CV$  where  $C$  is the capacitance and  $V$  is the voltage.

We can calculate the electrical energy from charge multiplied by potential difference. As a capacitor discharges, the potential difference across it will fall at the same time. To increase capacitance, we can increase the surface area which spreads the charge out and increases the capacitance of the component. The value of capacitance is thus directly proportional to the area;  $A$ . Therefore, if the area of the capacitor plate doubles, so does the capacitance.

The charge flows into the capacitor in response to the potential difference applied across it. The attractive forces of the positive and negative surfaces play an important role as the attractive forces tend to hold the charge on the plate. The greater the distance,  $(d)$  between the two capacitor surfaces, the smaller the capacitance. Capacitance is therefore directly proportional to  $1/d$ .

The ability of a dielectric to support an electric field is called permittivity. Capacitance is directly proportional to permittivity. However, this is often expressed as relative permittivity to free space where the capacitance is directly proportional to the permittivity of free space multiplied by the relative permittivity of a given dielectric.

Membranes display a variety of electrical properties. If an applied potential is placed across a membrane, then current flows through the membrane which suggests that the membrane has a large resistance capability. The presence of charged groups at the membrane-water interface provides the site for redistribution of charge at the membrane surface when the transmembrane potential changes which is similar to that found in capacitors. The change in applied potential produces a change in net charge on the capacitors. We could describe the resistance-capacitance network of a membrane model by using an RC circuit model and to test the membrane response

to an applied potential [6]. A bathing solution is also added to the circuit which has its own resistance. In Figure 1.1,

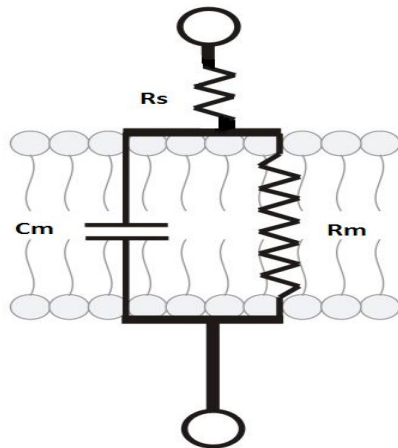


**Figure 1.1: Equivalent resistance-capacitance (RC) circuit for a membrane model.**

$C_m$  and  $R_m$  are membrane capacitance and membrane resistance respectively.  $R_s$  is the total resistance of the bathing solution and electrodes. Consider placing these components in a circuit and applying a potential from  $V = 0$  and increasing  $V$ . The voltage  $V$  gets dissipated through the resistor  $R_s$  and also through the capacitor  $C_m$ . To measure how much  $V$  is dissipated, we measure the potential drop in the two components [7]. In  $R_s$ , the voltage drop is

$$VR = iR_s \quad (1.1)$$

In  $C_m$ , the potential drop is

$$VC_m = q/C_m \quad (1.2)$$

The total potential drop for the circuit is therefore  $V = Vr + Vc$  which is

$$V = iR_s + q/C_m \quad (1.3)$$

The current  $i$  is charge per unit of time  $dq/dt$  therefore

$$V = R_s (dq/dt) + q/C_m \quad (1.4)$$

The equation can be re-arranged to form

$$dq/dt + q/R_s C_m = V/R_m \quad (1.5)$$

Furthermore,  $R_s C_m$  are functions of time and can be replaced by symbol  $\tau$ . To solve the differential equation, each term of the equation can be multiplied by the exponential of the function  $\exp(t/\tau)$  and both sides of the equation integrated with respect to  $dt$ . This becomes:

$$d/dt\{q[\exp(t/\tau)]\}dt = (V/R_s)[\exp(t/\tau)]dt \quad (1.6)$$

Then integrate each side when  $t=0$  and  $t=a$  finite time.

$$\{[q(t)][\exp(t/\tau)] - [q(0)][\exp(0)]\} = (V/R_s) [\exp(t/\tau) - \exp(0)] \quad (1.7)$$

At  $t=0$ , there is no charge on the capacitor. Also, the exponential on the left can be eliminated by multiplying both sides by  $\exp(-t/\tau)$

$$= VC_m [1 - \exp(-t/\tau)] \quad (1.8)$$

This equation is relating to charge with a time dependency. The potential  $V_C$  can now be determined as a function of time. When  $V_C = q(t)/C_m$  then

$$V_C = V[1 - \exp(-t/\tau)] \quad (1.9)$$

Therefore, at time zero, the potential that reaches the capacitor is also zero as charge has not reached the capacitor over zero time. Over time, the potential reaches the capacitor and the capacitor will continue to accumulate charge over time until the

potential reaches the desired final  $V$ . This is where the capacitor voltage is balanced and it will not take any more charge. No further current will flow. The time to reach this level depends on the size of the capacitor and resistor. Charging time can be increased by increasing resistance. The potential across a resistor is also a function of time shown by the equation [6].

$$V_R = V[\exp(-t/\tau)] \quad (1.10)$$

### 1.1.2 ADSORPTION

Adsorption is the accumulation of atoms, ions, biomolecules or molecules of gas, liquids or dissolved solids to a surface. This process creates a film of the adsorbate on the surface of the adsorbent. Adsorption is a consequence of surface energy. In the bulk material all the bonding requirements of the constituent atoms of the material are filled by other atoms in the material. However, atoms on the surface of the adsorbent are not wholly surrounded by other adsorbent atoms and therefore can attract adsorbates. The nature of the bonding depends on the species involved. Generally there are weak van der Waals forces, covalent bonding and electrostatic attractions. Adsorption is usually described through isotherms, that is the amount of adsorbate on the adsorbent as a function of its pressure (if gas) or concentration (if liquid) at constant temperature. The quantity adsorbed is nearly always normalised by the mass of the adsorbent to allow comparison of different materials. Graphically, the adsorption isotherm is a plot of the concentration or the amount of species on a surface as a function of its concentration in the bulk phase.

The properties of the interface are governed by differences in the concentration of the component.

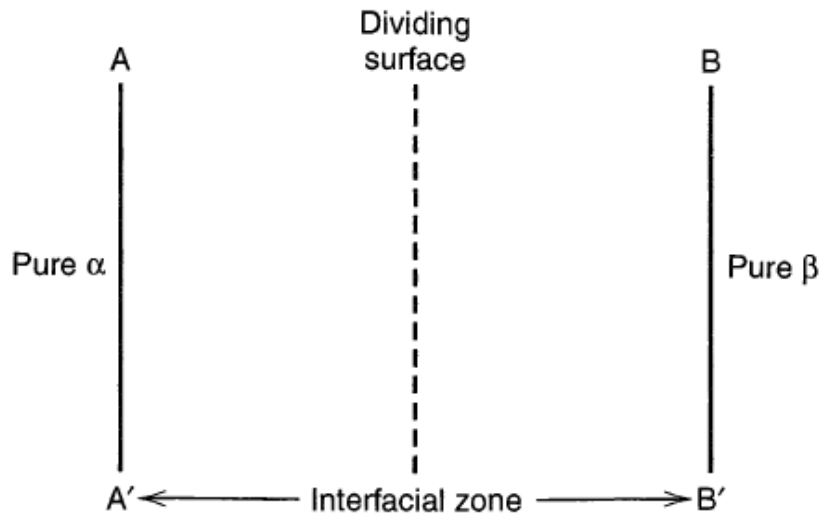


**Figure 1.2: Diagram of the interfacial region separating phases  $\alpha$  and  $\beta$  [6].**

Figure 1.2 shows two phases,  $\alpha$  and  $\beta$ . The surface phase is found in between these two phases. The bulk regions of  $\alpha$  and  $\beta$  remain fairly constant, but the concentration of the components of the interfacial region will gradually vary from bulk concentration of  $\alpha$  to the bulk concentration of  $\beta$  over a distance  $x$ .

The ideal system that Gibbs proposed suggests that distance between the interface takes on a value of zero. However, in reality that is not the case [8]. The reference system in Gibb's ideal system is used to show that the properties of the interface are actually governed by excesses and deficiencies depending on concentrations of various species in the bulk phases in comparison to the reference system. These differences between the reference and the actual system are called the surface excess quantities.

Surface excess is the extra amount of per unit of the solute that is present at or near the surface, when the surface is equilibrated with the phase containing the solute. In an idealised model, the components of  $\alpha$  and  $\beta$  bulk phases remains unchanged except when approaching the dividing surface. The total number of moles of any

component remains constant in the bulk phases but varies in the surface phases for the real system. An equation of surface excess representing the number of moles of any species is

$$n_i = n_i^s - n_i^r \quad (1.11)$$

where  $n$  is the stoichiometric number of electrons involved in an electrode reaction,  $n_i^s$  is the number of moles of any species in the actual system and  $n_i^r$  is the number of moles of any species in the reference system [8].

Another variable that needs to be included in the system is the area,  $A$ . In real systems, the interfacial area can change therefore in Gibb's equation; the free energy depends on area. Other variables include temperature and pressure which are constants [8].

Measurements of surface tension play an important role in the Gibb's Adsorption Isotherm equation [9]. Surface tension is a consequence of surface energy. Surface energy is the work required to increase the surface area of a substance by a unit area and is derived from the unsatisfactory bonding of molecules at the surface. Water molecules being polar, have strong interactions with each other. The molecules near the surface (the air/water interface) have stronger attractions to the water molecules in the bulk than the air molecules. So, the liquid exposed at the surface contracts to the smallest possible area due to unequal intermolecular forces. This gives rise to surface free energy. Molecules at the surface will try to remove free energy by creating bonds with molecules in the adjacent phase. This is the concept of surface tension.

Surface energy is also closely linked to surface hydrophobicity. Because water has a large binding capacity, any material with a high surface energy can interact with water and therefore is hydrophilic. Hydrophilic surfaces of material will have more surface energy than hydrophobic surfaces of materials.

When lipids are poured on to a water surface in a trough, the phospholipids form a single layer on the water with the phosphate head group in the water and the fatty acid tails facing towards the air. They are able to decrease the surface tension through the phosphate group binding with water molecules and also cover a large surface area.

As mentioned earlier, the air/water interphase has free energy. This can be made accessible by measurements of surface tension. The surface tension of water is  $0.072\text{N}\cdot\text{m}^{-1}$  at  $20^\circ\text{C}$  [10], which is a high value compared to other liquids and therefore, renders water a very good substrate for monolayer studies. When a solution of an amphiphile is placed on a water surface, the solution spreads rapidly to cover the available area and a monolayer is formed. However, the available area for the monolayer is large as the distance between the adjacent molecules is large and their interactions are weak. Under these conditions the monolayer has little effect on the surface tension of water. If the available surface area of the monolayer is decreased by a system, the molecules start to exert a repulsive effect on each other. This two-dimensional analogue of a pressure is called surface pressure. This system will be explained further when discussing the Langmuir-Blodgett trough.

### 1.1.3 RC CIRCUIT

Changes in phospholipid potential can be described using electric circuits. The cell membrane can act as a resistance – capacitance (RC) circuit. Similar to a RC circuit, membrane potential can change as an inverse exponential with time [11]. When a current flows through a circuit having a resistor, capacitor and battery, the capacitor begins to charge. At first instance, the voltage (E) of the battery appears across the resistor, the charging current for the capacitor being determined by Ohm's law  $i = E/R$ .

Over time, the capacitor voltage  $V_C$  begins to increase. The voltage that remains on the resistor  $V_R$  begins to decrease therefore the rate at which the capacitor is now charging reduces. This will continue until the capacitor is charged to the voltage (E). The values of R and C will affect the amount of time it takes C to get fully charged. The charging current is constantly changing as the voltage across C increases [12]. We can look at the steadily decreasing rate of charge with the equation.

$$i_c = C \cdot dV_C/dt \quad (1.12)$$

where  $i_c$  is the current flowing through the capacitor, C being the value of the capacitor,  $dV_C$  is the change in the voltage of the capacitor over dt, the change in time. ( $dV_C/dt$  can be explained as the change in capacitor voltage over time). The current that is charging the capacitor is the current that is going through the resistor R. Through this we can apply Ohm's law

$$i_c = i_R = (E - V_C)/R \quad (1.13)$$

## 1.2 THE ELECTRIC DOUBLE LAYER

In this section, the nature of the electrode/electrolyte interface is discussed. At any electrode immersed in an electrolyte solution, a specific interfacial region is formed. This region is called the electric double layer (EDL). The electrical properties of this layer are important, since they affect electrochemical measurements. For electrodes which are under potentiostatic control there will also be the influence of the charge at the electrode as the surface charge can be manipulated on an electrode upon applying potential. Electrostatic interactions between ions in solution and the electrode surface result in the electrode holding a charge density. In order for the



interface to remain neutral, a layer of counter ions is established close to the electrode surface resulting in a double layer capacitance.

There is no general model that can be used in all experimental situations. This is because the EDL structure depends on several parameters including electrode material, type of solvent, type of electrolyte, extent of specific adsorption of ions and molecules and temperature. Helmholtz highlights a model (Figure 1.3a)). The electrode holds a charge which can alter via induced potential. In order for the interface to remain neutral, ions redistribute to come close to the electrode surface. The electrode in Figure 1.3a) is negatively charged therefore attracting positively charged ions. The distance between an ion and the electrode will be dependent on the radius of the ion and the solvation sphere around the individual ion [13]. Two layers of charge are produced, and this is the double layer. The OHP is the "outer Helmholtz plane" which is the potential drop occurring only on this region.  $\Phi_s$  represent the potential difference in solution and  $\Phi_m$  is the potential difference on the metal (Figure 1.3a)). The potential changes linearly with distance from the electrode surface. The Helmholtz model is limited in explaining double layer theory. It does not consider factors such as adsorption on the surface, diffusion in solution or interaction between solvent dipole moment and electrode.

Another model is the Gouy Chapman model (Figure 1.3b)). It disputes the rigidity of the ions at the electrode surface and suggests that the counter ions are not rigidly held, but tend to diffuse into the liquid phase. In this model the potential difference changes exponentially and including over the region called the diffuse layer. However, the Gouy Chapman model creates an overestimation of the EDL capacitance.

The Stern model encompasses both Gouy Chapman model and Helmholtz model [14] (Figure 1.3c)). Ions are still assumed to be able to move in solution and there is a region close to the electrode surface known as the Stern layer (S). At the stern layer,

there are the specifically adsorbed cations but also and non-specifically adsorbed solvated anions.

The capacitance in EDL ( $C_{dl}$ ) is a combination of the capacitances from, the Stern double layer ( $C_H$ ) and the diffusion layer region ( $C_{diff}$ ) [15]. Thus,  $C_{dl}$  can be expressed by the following equation:

$$1/C_{dl} = 1/C_H + 1/C_{diff} \quad (1.18)$$

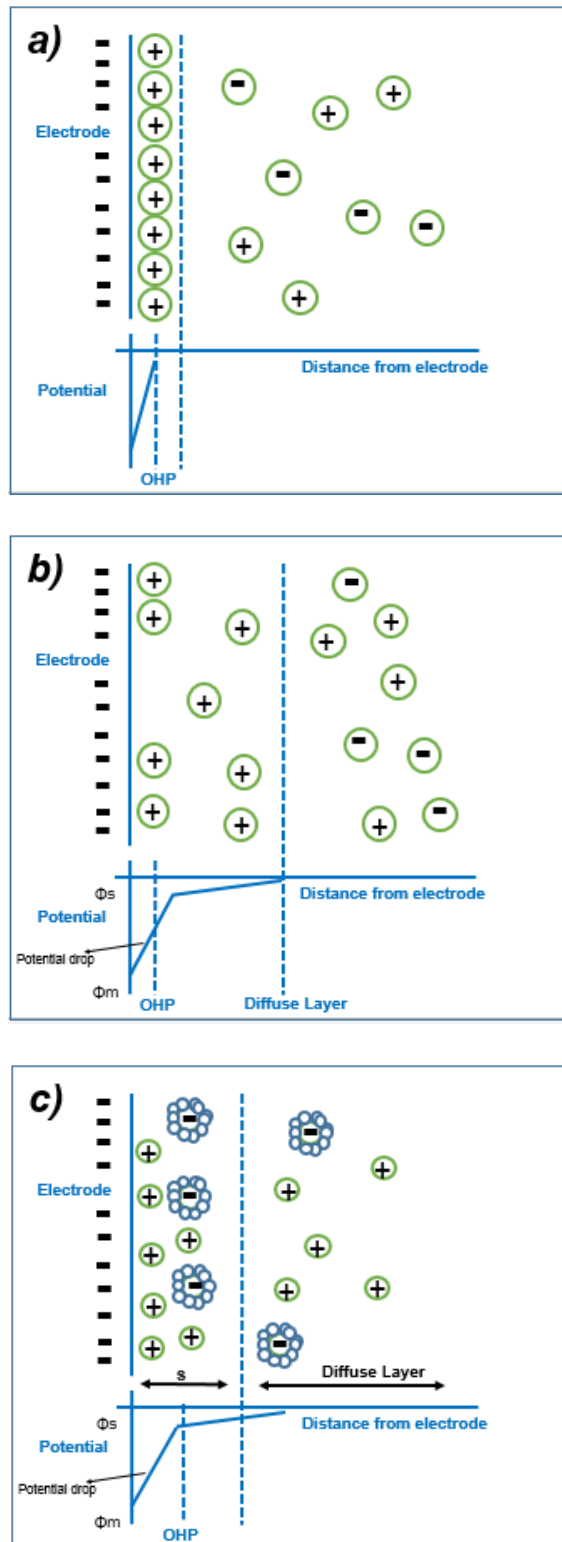


**Figure 1.3: Models of the electric double layer at a negatively charged surface representing a) the Helmholtz model, b) the Gouy–Chapman model, and c) the Stern model;  $s$  being the Stern layer. OHP is the outer Helmholtz plane.  $\Phi_s$  and  $\Phi_m$  is the potential difference in solution and on the metal respectively.**

This is however a simplified definition as EDL behaviour at the surfaces of electrodes are more complex. Under the influence of an applied potential, electrons redistribute themselves, either towards or away from the electrode surface resulting in a surface charge. The behaviour becomes further complicated when considering inclusion of adsorbed species to the model. Amphiphilic species such as phospholipids adsorbed onto the mercury electrode behave as a dielectric thus increasing charge separation and decreasing capacitance [16]. These changes in capacitance can be plotted against the applied potential to produce profiles which is non-linear and dependent on the applied voltage. These are the characteristic phase transition capacitance peaks.

### 1.3 MEMBRANE MODELS

One of the goals of this project is to develop a new method for the determination and screening of pharmaceutical compounds and toxicants. The other is to be able to understand these compounds' modes of activity. The reasons for the development and optimisation of a screening device is highlighted in points below.

- Pharmaceutical compound use has increased over the years. In the U.S. there were nearly 3.4 billion prescriptions dispensed in 2005. This is an increase of nearly 60% since 1995 [17] which means there is a large quantity being exposed to the environment.
- It is still unclear how some pharmaceutical compounds interact or metabolise, and these compounds are being exposed to the environment on a regular basis. It is important to be able to screen them regularly and understand how they interact.
- It is also important to understand how they interact in the environment; bearing in mind, most of the compounds will be in metabolised form upon excretion.
- To be able to identify health risks

This MFE system provides the screening tool needed to detect pharmaceutical compounds; due to their specific "fingerprint", they will be easily identified. Also, the system provides an analytical tool, to help understand how the compounds are interacting at the fundamental level.

Data of surface properties of compounds with DOPC lipid monolayer are reported throughout the thesis.

## 1.4 INNOVATIVE TOOLS

Due to the small complexity and size of lipid bilayer systems, it can be difficult to study certain interaction processes of compounds such as permeation. The MFE system allows for the practical use and theoretical approaches to further understand interactions.

One of the goals of this thesis is to establish an innovative tool for measuring toxicants and pharmaceutical compounds along with any other compound to bridge gaps in the knowledge of these compounds. It is still not known how some medicinal compounds work. This is especially the case for atypical antipsychotics. These antipsychotics can also cause concerning side effects which is why it is important to study their toxicity profiles. Toxicity profile studies such as repeated dose toxicity is used to evaluate chronic toxic effects.

Other goals are to screen a whole host of compounds using high throughput MFE assays. The data produced from these assays can then be used to identify and understand compound induced biological pathways/activity at a molecular level. Compounds in similar class and therefore with similar molecular and chemical features are expected to have the same biological targets. This is an important basis for drug development. Understanding interaction profiles is important for drug development. Filtering through the database can be used to prioritise those compounds with optimal functional groups that can be used for further drug development.

MFE assays like many *in vitro* assays allow the investigation of key events that occur when compounds are exposed to membranes. These events can be easily quantified. The results from MFE assay studies have been compared to EC50 studies [18]. The MFE assays employ an electrochemical technique which is explained in Chapter 2.

As well as developing a “fingerprint” database, the collected database can be used to understand functional groups to predict interaction. It has been found that both hydrophobic compounds as well as those that act on receptors also have characteristic fingerprints that are shared with similar compounds in their class. Chapters 5 to 10 presents the individualistic fingerprint data for class of compound. This has vast implications not just on sensor and environmental technology but also the pharmaceutical industry.

Various attempts have been made to transform the data into an automated quantified form including fast transform. However after consulting mathematical and simulation colleagues, it is concluded that the most valuable data is the initial raw recorded voltammograms.

## 1.5 SUMMARY

This thesis focuses on the optimisation and then applications of electrochemical techniques. Potential applications include the analysis of the interactions that can occur between a drug or a biologically active compound and biomembranes, the screening of environmental toxicants and pharmaceutical compounds and the characterization of new drugs at the earlier stage of their discovery and/or throughout their production.

It is known that electrochemical techniques and consequently, the capacitance data produced can provide a wealth of information with regards to compound interaction. There are a multitude of reactions that can occur on the electrode surface. Kinetic information concerning electron transfer rates is readily available using techniques such as cyclic voltammetry and chronocoulometry. All these are positive attributes in optimizing electrochemical techniques to a broader range of application.

Briefly, the main set up includes a microfabricated platinum electrode (MFE) with Hg layer coating. A phospholipid layer is adsorbed on the Hg layer. All this is contained within a miniaturised flow cell. The techniques will be detailed in Chapter 2. These types of layers adsorbed on the Hg layer mimic a simplified biological membrane and can be used to study biologically active compounds. Such adsorbed layers present many interesting opportunities such as the ability to chemically functionalize electrode surfaces and investigate interactions of molecules with the membrane surface and/or membrane associated molecules. The various applications that resulted from this model membrane setup are discussed throughout the thesis.



## REFERENCES

- [1] Muntean A. *The Langmuir trough Analysis of Lipid Monolayers Idea*: Biophysik Institut, Physik Department, TU München.
- [2] Geoffrey CM. *The Cell, A Molecular Approach*, **2000**, 2nd edition Boston University, Sunderland.
- [3] Silvius DR. *Thermotropic Phase Transitions of Pure Lipids in Model Membranes and Their Modifications by Membrane Proteins*. **1982** John Wiley & Sons, Inc., New York.
- [4] Subcellular biochemistry volume 28 cholesterol: its functions and metabolism in biology and medicine, r bittman. Plenum press new York 1997
- [5] Shinpei O. *Biophysical journal* **1969** 9(10): pp1195-1205.
- [6] Starzak ME. *The physical chemistry of membranes* **1984** Academic Press.
- [7] Geiger B. *Nature Reviews Molecular Cell Biology* **2001** 2: pp793-805.
- [8] Bard AJ, Faulkner LR. *Electrochemical methods*, **2001** pp534-631
- [9] Belton GR, *Metallurgical transactions B*, **1976** 7(1): pp35-42
- [10] [www.physics.usyd.edu.au/teach\\_res/jp/fluids/surface.pdf](http://www.physics.usyd.edu.au/teach_res/jp/fluids/surface.pdf)
- [11] Hemmings HC, Hopkins PM, *Foundations of anesthesia: Basic Sciences for Clinical Practice*, **2000** pp227
- [12] [http://www.electronics-tutorials.ws/rc/rc\\_1.html](http://www.electronics-tutorials.ws/rc/rc_1.html).
- [13] Bard AJ, Faulkner LR. *Electrochemical methods*, **2001**, 2nd Edition pp534.
- [14] Zhang LL, Zhao XS, *Chem. Soc. Rev.* **2009**, 38: pp2520–2531.
- [15] Stern O, *Electrochem*, **1924**, 30: pp508.
- [16] Nelson A, Benton A. *Journal of Electroanalytical Chemistry*, **1986** 202: pp253–270.
- [17] Miller L. *Chain Pharmacy Industry Profile*. 9th ed. Alexandria VA: NACDS Foundation. **2006**, pp8.
- [18] Galluzi M. *Langmuir* **2013** 29: pp6573–6581.

## **CHAPTER 2**

# **ANALYTICAL TECHNIQUES - MATERIALS AND METHODS**

### **2.1 INTRODUCING ANALYTICAL TECHNIQUES**

Electroanalytical techniques are methods by which an analyte is studied by measuring the potential and/or current in an electrochemical cell at electrodes. In this way electroanalytical techniques are suited for the study of reactions that occur at a surface. Reactions that occur at a surface can involve many steps. There are various processes to consider, namely adsorption and desorption steps, interaction of reagents or products, surface catalysis, material transport towards the surface that could come across limitations or barriers or chemical reactions that precede the electrode reactions. However, these extensive reactions are what needs to be understood. It is possible to achieve control over these reactions using electrochemical methods. For the studies mentioned in subsequent chapters, the analytical measurements focus on the measurements of current at an electrode which is manipulated with applied voltage. These reactions are a reflection of the changes

in concentration of analyte over time as a result of electrolysis and other reactions due to the applied potential.

Electroanalytical methods have advantages over other analytical methods. They allow for the determination of different redox states of compounds in a solution and the ability of producing low detection limits due to their sensitivity. This means that a large amount of characterization and kinetics data can be obtained. The other important advantage is that although large volume of samples can be prepared, the electrode surface is small and thus the analytical procedure has short measuring times. This means that repeated measurements can be made within the same bulk solution. This has advantages of low cost and very low wastage due to the small scale apparatus used. The equipment components are also readily available and can be made more portable for environmental analysis.

This chapter focuses on the analytical methodology. The inclusion and possibilities of a microfabricated platinum electrode and flow cell system as a membrane support is briefly introduced and will be highlighted in more detail in Chapter 3.

### **2.1.1 POTENTIOMETRY**

Potentiometry involves measurement of the potential between two electrodes one of which is the reference electrode. The potential of the reference electrode is constant so the measured cell potential can be interpreted involving a species which effects the potential in contact with the working electrode. Data from potentiometric measurements can be used to calculate the analyte concentrations directly from the Nernst equation for a redox reaction.

The Nernst equation takes the form

$$E = E_{O/R}^0 + (2.303 RT/nF) \ln(C_O/C_R) \quad (2.1)$$

Where  $R$  is the gas constant ( $8.314 \text{ VC K}^{-1} \text{ mol}^{-1}$ ),  $T$  is the temperature in  $\text{K}$ ,  $n$  is the stoichiometric number of electrons involved in the process,  $F$  is the faraday constant ( $96500 \text{ C mole}^{-1}$ ).  $E$  is the cell potential and  $E^0$  is the standard redox potential for the couple involving the oxidised (O) and reduced (R) species.  $C_{\text{O}}$  is the concentration of the oxidized species of the couple and  $C_{\text{R}}$  is the concentration of the reduced species.

A potentiostat is a control and measuring device. It measures current flow between the working and counter electrodes. It comprises of electric circuit which controls the current between working and counter electrodes by sensing changes in the voltage between the working and reference electrodes [1].

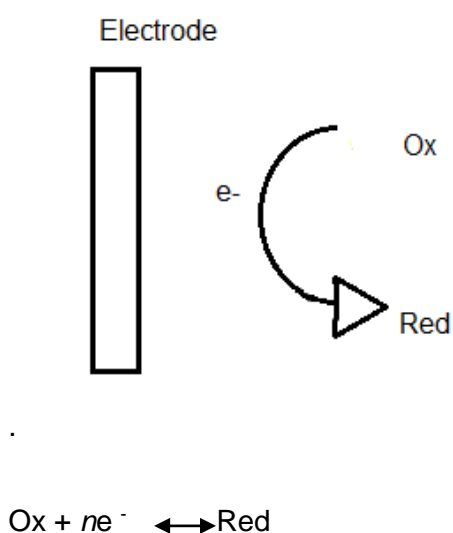


**Figure 2.1: Representation of redox reaction at electrode surface.**

### 2.1.2 VOLTAMMETRY

Voltammetric techniques involve an electrochemical cell which consists of a working electrode, a reference electrode and a counter electrode [2]. The reduction or oxidation of a species at the working electrode with applied potential results in transport of material to the electrode and current generation.

The current ( $I$ ) is measured as a function of changing potential ( $E$ ). The technique employed in voltammetry involves the use of three electrodes. The changing potential is applied to the working electrode to drive a redox reaction. The counter electrodes conduct the electricity between the two electrodes and the reference electrode maintains a constant potential throughout. As a potential is applied, electrolysis of the analyte is initiated, and the current rises until it reaches a certain limiting current. This can be plotted as a voltammogram of  $I$  vs.  $E$ .

All voltammetric techniques involve the application of a potential ( $E$ ) to an electrode and monitoring the resulting current ( $I$ ). The applied potential can be varied and the current can be monitored over a period of time ( $t$ ). The applied potential controls the redox process and this can also be described by the Nernst equation. For a reversible electrochemical reaction which can be described by  $Ox + ne^- \rightleftharpoons Red$ , applying potential ( $E$ ) forces the concentrations of O and R ( $C_O$  and  $C_R$  respectively) at the surface of the electrodes to a ratio in compliance with the Nernst equation as mentioned above [3]. The current is a quantitative measure of the rate at which a species is being reduced or oxidised at the electrode surface.

It is established that the processes being recorded are taking place at the electrode surface. As the reaction proceeds, the analyte on the electrode surface will begin to deplete. This creates a concentration gradient between the electrode surface and the solution bulk where a diffusion layer develops. This is depicted in Figure 2.2. The analyte diffuses from the bulk solution to electrode surface, thus maintaining electrolytic interaction. If the applied potential increases, the current flow increases. This causes the analyte to diffuse between the solution bulk and electrode surface at a faster rate to maintain the current. The diffusion layer can also be affected for example, in the absence of stirring the solution. The thickness of diffusion in the unstirred state will remain mainly towards bulk solution. Putting these explained voltammetric models into practice, it is possible to determine electroactive organic

and inorganic substances using voltammetry as these substances are reduced and oxidised at the electrode surface. They can do this at trace levels which means it is an effective technique for screening toxic compounds. The detection limits for both organic and inorganic species have been recorded to be as low as  $10^{-10}$  to  $10^{-12}$  mol  $\text{dm}^{-3}$ .

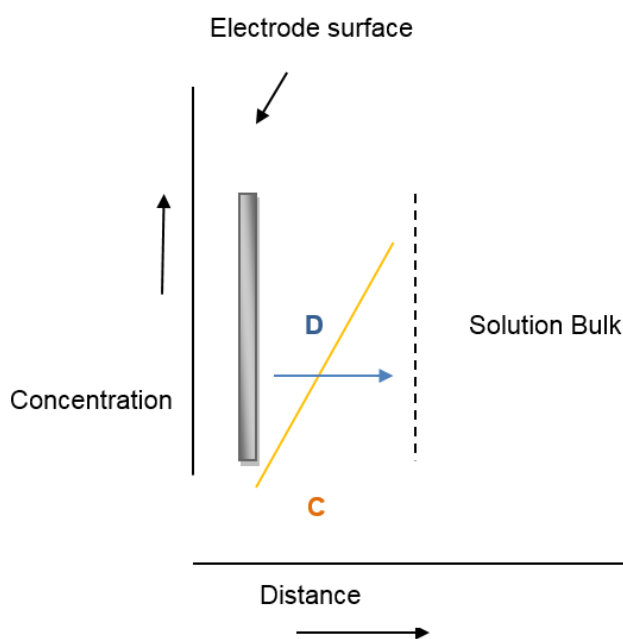


**Figure 2.2: Concentration gradient from electrode surface, where D is diffusion layer, C is concentration gradient.**

Voltammetric techniques are used for a wide range of analytical chemistry including fundamental studies of redox processes, adsorption processes on surfaces, kinetics of electron transfer mechanisms and determination of compounds of pharmaceutical interest.

### 2.1.3 CYCLIC VOLTAMMETRY

In cyclic voltammetry, a triangular potential waveform is applied to the working electrode that produces a resulting current. The potential in this current study is

ramped from a negative to more negative potentials. A switching point potential is chosen at a sufficiently negative applied potential. On the negative going or cathodic scan, a reduction current is observed that occurs at a specified voltage. That voltage is dependent on the properties of the analyte that is being measured. In the reduction process, a current is observed as a result of gain of electrons manifest as a reduction peak. The potential is then reversed to show the oxidation peak. In the oxidation peak, the potential applied is based on the characteristics of the molecule [4].

This technique is widely used for the study of redox potentials. The predominant variables in cyclic voltammetry are the scan rate and the position and size of the voltage excursion.

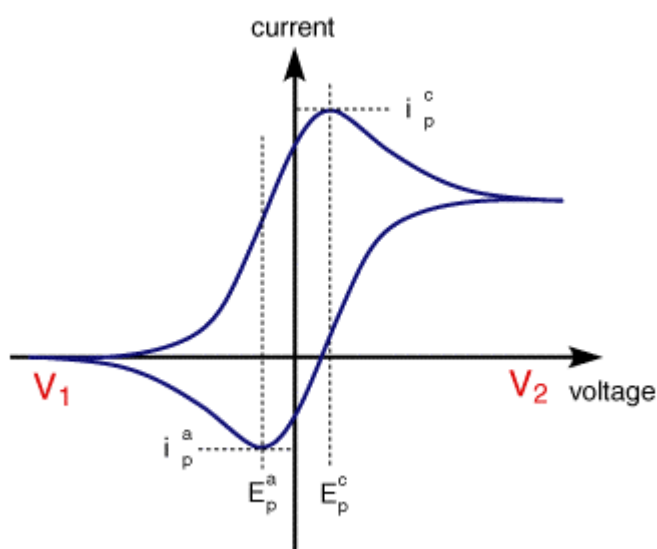


**Figure 2.3: Example of a cyclic voltammogram [4]**

The important parameters in a cyclic voltammogram are shown in Figure 2.3; the peak potentials ( $E_{pc}$ ,  $E_{pa}$ ) and peak currents ( $i_{pc}$ ,  $i_{pa}$ ) of the cathodic and anodic processes respectively. If the electron transfer process is fast compared to the analyte diffusion rate, then the reaction is said to be electrochemically reversible and the peak separation is

$$\Delta E_p = E_{pa} - E_{pc} = 2.303RT / nF \quad (2.2)$$

Therefore,  $\Delta E_p$  at 25°C with  $n$  electrons is  $0.0592/nV$  or equivalent to  $\sim 60mV$  per one electron transfer. There may be a slower electron transfer rate relative to the analyte diffusion rate causing  $\Delta E_p$  to be greater than  $0.0592/nV$ . [5]. Curve shape, peak height, peak width and the position of a voltammogram is affected depending on the compound and the interaction being analysed and hence can be used to describe the (I) vs. (E) behaviour [6].

Inspection of Figure 2.3 shows that there is a reduction current that occurs at a particular voltage on the negative potential going sweep. That voltage is dependent on the properties of the analyte. When there is reduction, a current is observed due to gain of electrons. The current observed is proportional to concentration. Once reduced, the potential is reversed and there is an oxidation peak on the positive potential going sweep. The potential characterizing the oxidation peak is also dependent on the properties of the analyte.



## 2.2 MEMBRANE-BASED SUPPORT SYSTEMS

### 2.2.1 LANGMUIR TROUGH

Phospholipid coverage can be studied using the Langmuir trough; also known as the Langmuir-Blodgett trough. It is an apparatus that compresses the monolayers onto a subphase in order to measure surface phenomena. The Langmuir trough uses the concept of surface pressure in order to determine the characteristics of the monolayers. The Langmuir technique is a very useful device as it allows precise control of monolayer thickness. Surface pressure is an important property of monolayers characterized within the Langmuir trough system [7].

The surface area of the liquid called the sub-phase where the monolayers are spread can be compressed or expanded and the area density then measured. The Langmuir trough can also be used to transform an organised monolayer to multilayers. This can be achieved by controlling the compression that is being used.

Commonly teflon™ is the material used to make up the trough. This is a highly sensitive apparatus and contamination can easily become an issue therefore a lot of care is conducted on the choice of trough material and attention to detail should be exercised during the testing. Teflon is also chemically inert which makes it a favourable material in this case. The trough is filled with an aqueous solution. The solution of lipids with some solvent can then be micro-syringed onto the subphase. The solvent instantly evaporates and the lipid material will begin to spread rapidly over the area. The individual lipid molecules can be spaced out due to repulsive forces between them. A barrier system in place begins to compress the monolayers closer together. Surface pressure can be measured simply by calculating the area of the sub-phase surface available for each molecule. It is important to monitor the level of compression as the space between the lipids can be decreased to a certain amount

before they start to interact with each other [8]. Further monolayer studies with the Langmuir film balance can also be used for transferring highly organised multilayers to solid substrates. This is carried out by passing a solid substrate down through the monolayer while simultaneously keeping the surface pressure constant. Consequently the spread monolayer is transferred to the solid substrate. A second layer can be transferred to the substrate by withdrawing the solid substrate from the sub-phase. In this way multilayer structures of hundreds of layers can be produced. These multilayer structures are commonly called Langmuir-Blodgett (LB) films.

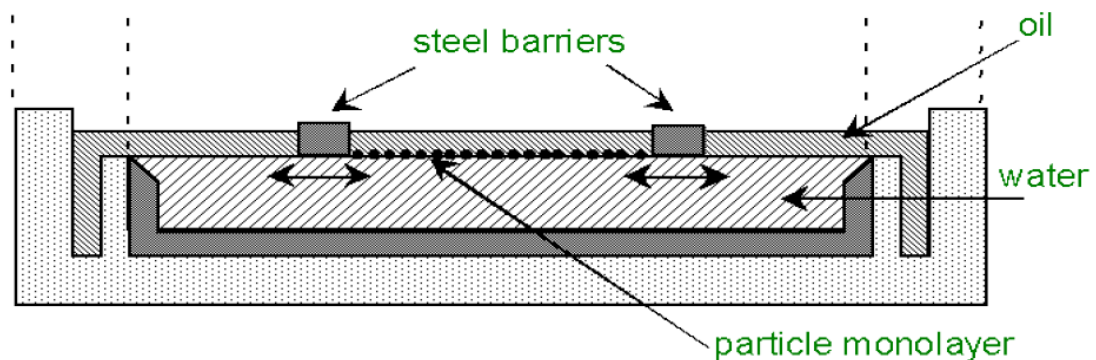


**Figure 2.4: Schematic representation of the Langmuir trough [9].**

The measurements of surface pressure versus sub-phase surface area can be plotted on a graph which can be used to estimate the area of the molecules on the surface. The number of molecules added is known, so this allows the area per molecule and the surface coverage in molecules per area to be determined.

The area per molecule  $A_{\text{mol}}$  is calculated from the total area  $A_{\text{tot}}$  and the total number of molecules,  $N$  on the surface.

$$A_{\text{mol}} = A_{\text{tot}}/N \quad (2.3)$$

The volume per molecule can also be measured by finding the density of the surface material using the equation

$$\rho_m = \rho / M \quad (2.4)$$

where  $\rho_m$  is the molar density,  $\rho$  is the density and  $M$  is the molecular weight. The volume per molecule can then be found by the inverse of  $\rho_m$  which gives volume per mole. This quantity is then divided by Avogadro's number to give volume per molecule [10]. To find the height of the monolayer, the following equation is used

$$h = (\text{volume/molecule}) \cdot (\text{area/molecule}) \quad (2.5)$$

### 2.2.2 HANGING MERCURY (Hg) DROP ELECTRODE (HMDE)

The HMDE is a spherical stationary of mercury (or Hg) electrode. A Hg drop is suspended at the end of a glass capillary and its size can be adjusted with a micrometer screw. The Hg drop can thus be proportioned and this accounts for the reproducibility of its surface area. The device mechanism is based on the controlled flow of Hg through a glass capillary that can be closed with a needle valve.

In order to spread phospholipid on to the Hg surface, the electrode is slowly lowered into the electrochemical cell containing the electrolyte on to which a monolayer phospholipid is spread via a microliter syringe [11].

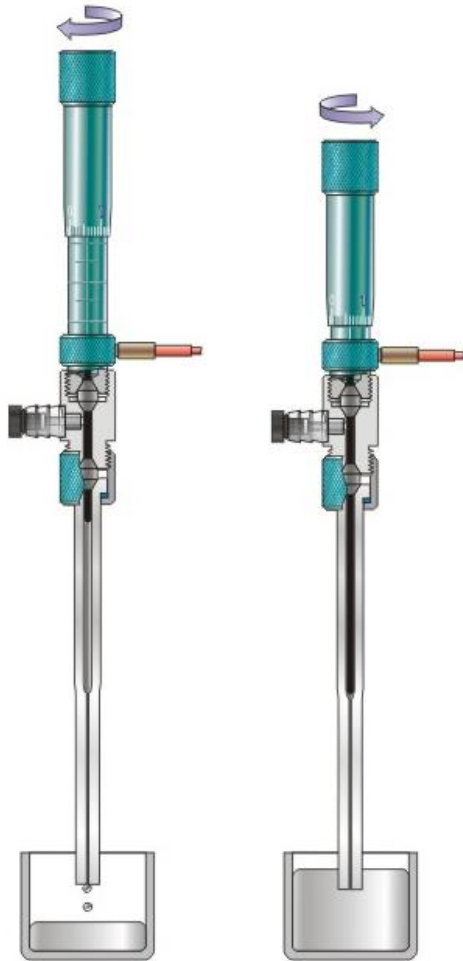
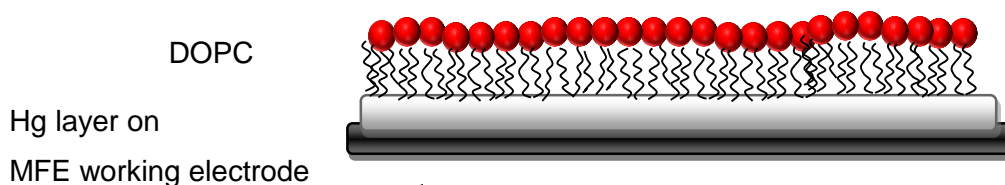


**Figure 2.5: Diagram of HMDE during Hg filling [12].**

### 2.2.3 MICROFABRICATED PLATINUM ELECTRODE (MFE)

a) Lipid monolayer on surface of Hg coated electrode



b) Microfabricated platinum electrode chip

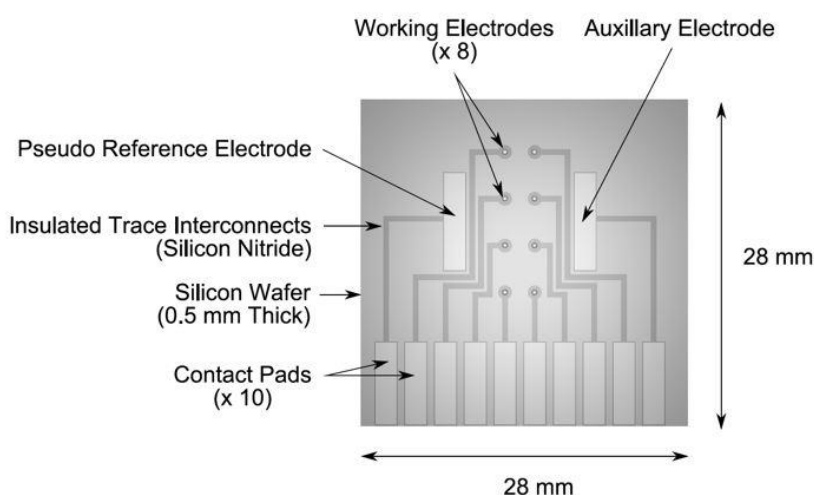


**Figure 2.6: Microfabricated electrode with deposited DOPC monolayer a) schematic representation of the order of phospholipids on Hg coated electrode support. b) a working microfabricated electrode chip [13].**

The Hg electrode is an ideal support for phospholipid monolayers however; it has disadvantages such as being fragile. The disadvantages can be resolved by transferring the electrodes on to a stable platform such as platinum (Pt). Pt is routinely used in fabrication and Hg adheres strongly to its surface making the electrode more robust than the HMDE [14, 15]. The use of fabricated Pt microelectrodes minimises the amount of Hg used alleviating Hg toxicity risks.

The microfabricated platinum electrodes (MFE) used in this work are supplied by The Tyndall National Institute, Ireland. They are composed of Pt discs with a radius of 0.480mm embedded on a silicon wafer substrate, addressed via  $\text{Si}_3\text{N}_4$ -insulated interconnections to 2.54 mm Pt electrical contacts. See Figure 2.6. The Pt electrodes with electrodeposited Hg will be referred to as MFE hereafter. The flow cell holding the electrode is made of perspex.

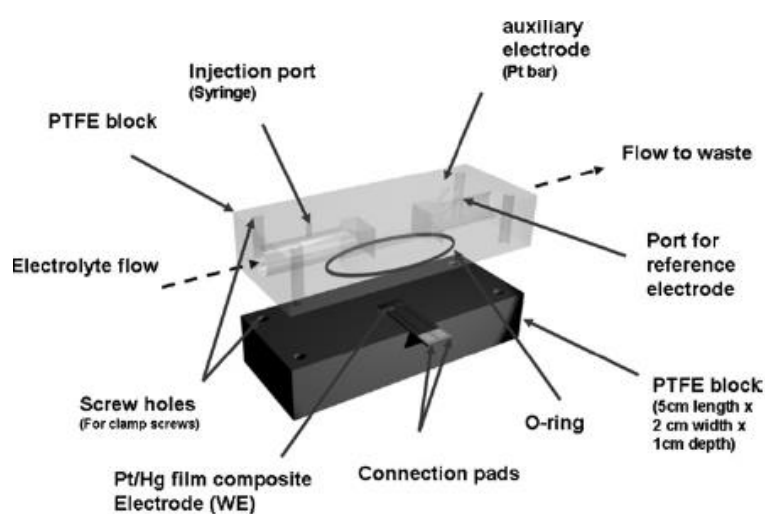


Figure 2.7: The flow cell designed to hold the Hg/Pt electrodes [14].

## 2.3 USING MFE MEMBRANE SUPPORT SYSTEM

The electrodes being used with deposited Hg makes them an ideal monolayer support. Hg is highly polarisable and as such provides easy manipulation and presents an opportunity to study adsorbed ions and organic molecules within the electrical double layer over a wide potential range. Although using Hg is a topic that has come up with scrutiny due to its well known toxicity, its deployment is justified since minute amounts of Hg are used and its fluid surface is highly compatible with the fluid phospholipid. This compatibility is not obtained with other metal supports. The Hg on the electrodes can be readily electrodeposited and the resulting Hg electrodes are reproducible within a well-defined geometry. The Hg film is maintained in a stable configuration on the Pt surface to which it is bound without its composition being undermined. The Pt electrodes with electrodeposited Hg will be referred to as Pt/Hg electrodes throughout the texts.

### 2.3.1 Hg ELECTRODEPOSITION

Hg can be electrodeposited onto Pt disc electrodes using a standard three electrode set up. Prior to electrodeposition, the MFE are cleaned by placing in a solution of  $\text{H}_2\text{SO}_4$  and 30%  $\text{H}_2\text{O}_2$  with a volume ratio of approximately 3:1 respectively. The MFE are then dried under  $\text{N}_2$ . To perform the electrodeposition, the MFE is placed in a three electrode cell that contains a double junction reference electrode (containing  $3.5 \text{ mol dm}^{-3}$  KCl, Ag/AgCl inner filling and  $0.1 \text{ mol dm}^{-3}$  perchloric acid outer filling) and a Pt bar auxiliary electrode (Metrohm). Electrodes are connected to a PGSTAT12 potentiostat (Autolab, Metrohm). Hg was deposited on to the Pt disc at  $-0.4\text{V}$  vs. Ag/AgCl (Sat. KCl) from a solution of  $\text{Hg}(\text{NO}_3)_2$  and was monitored by chronocoulometry. After one coulomb per electrode passed, the MFE was removed immediately to prevent dissolution of Hg, rinsed with Milli-Q water ( $18.2\text{M}\Omega$ ) and dried

under N<sub>2</sub> gas. The MFE has eight electrodes which can be coated with Hg. Normally only one electrode is used for an assay. They are then stored in the designated flow cell at room temperature and have a shelf life of up to 6 months.

### 2.3.2 RAPID CYCLIC VOLTAMMETRY

The Hg microelectrodes can be used to obtain results via rapid cyclic voltammetry (RCV). These cyclic voltammograms employing scan rates in excess of 1 Vs<sup>-1</sup>. In the voltammograms since there is an absence of faradaic reaction at the electrode, the current is proportional to the capacitance and is termed the capacitance current. RCV is used to determine the area of the Hg/electrolyte interface and to monitor adsorption/desorption/interaction events on the electrode surface. In the presence of a redox species or at potentials outside of the hydrogen over potential, RCV scans contain information about both the electrode surface capacitance and redox processes occurring at the electrode. In the absence of faradaic reactions the recorded current (*I*) is directly proportional to the specific capacitance (*C<sub>sp</sub>*) and therefore the area of both the HMDE and Pt/Hg electrodes were determined using equation (2.6) below. The *C<sub>sp</sub>* for Hg in 0.1 mol dm<sup>-3</sup> KCl on the “water hump” maximum is 40 μFcm<sup>-2</sup> as determined by Grahame [15]. This value was used together with values of current from the Pt/Hg electrodes to determine their surface areas. *C<sub>sp</sub>* is calculated from the RCV current (*I*) using equation:

$$C_{sp} = I / (v \times A_0) \quad (2.6)$$

where *A<sub>0</sub>* is the electrode area, and 40Vs<sup>-1</sup> is the RCV scan rate. This scan rate was chosen because the resulting currents as capacitance currents were significant enough to be recorded at a good resolution while maintaining a good signal-to-noise ratio.



For the preliminary studies, the acquisition program Scope™ software (AD Instruments) is set to record a scan every 10 seconds for ease of comparing changes.

Figure 2.8 a) represents the capacitance profile uncoated Pt/Hg electrode using RCV. Figure 2.8 b) represents the changes in capacitance profile when DOPC is coated on the Hg surface. There are clear differences in capacitance profiles observed. This technique can thus be used to produce capacitance profiles of adsorbed phospholipid monolayers on Hg and changes in the capacitance observed on interaction with compounds.

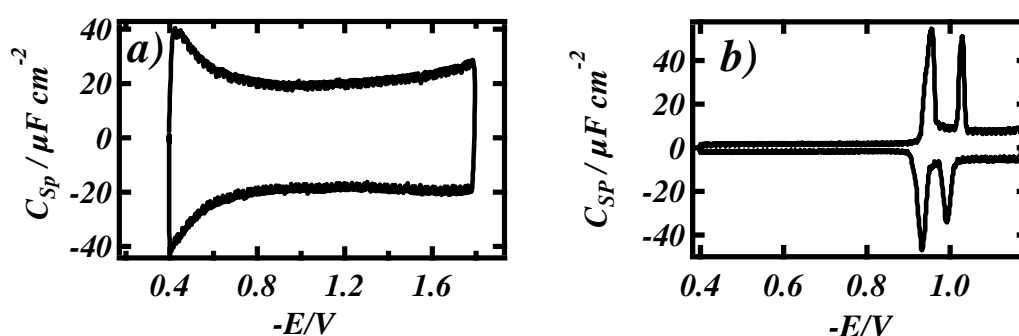


**Figure 2.8:** a) RCV recorded at  $40 \text{ Vs}^{-1}$  of an uncoated and clean Hg electrode in PBS at pH 7.4 with potential excursions from -0.4V to -1.8V. b) RCV recorded at  $40 \text{ Vs}^{-1}$  of a DOPC coated Pt/Hg electrode in PBS at pH 7.4 with potential excursions from -0.4V to -1.2V.

In the absence of contamination in the cell, these scans are reproducible and stable even after repetitive scans. The Hg electrodes can also be washed repeatedly with distilled water and even left in the flow cell without any loss of Hg.

### 2.3.3 METHODS

The electrolyte used throughout the experiments was  $0.1 \text{ mol dm}^{-3}$  KCl, calcined at  $600 \text{ }^{\circ}\text{C}$  for two hours and buffered at pH 7.4 with  $0.01 \text{ mol dm}^{-3}$  phosphate (hereinafter

referred to as phosphate buffered saline or PBS). For the assays, the MFE was contained in a flow cell. When in use as a working electrode only the part of the wafer containing the disc electrodes was in contact with electrolyte while the remaining part was connected to a potentiostat by crocodile clips attached to either contact pad. A constant flow of PBS was passed over the electrode with a flow rate of  $5\text{-}10\text{ cm}^3\text{min}^{-1}$  maintained by a peristaltic pump. A notable feature of the system compared to the one described previous [16] to this work is the facility to introduce three separate solutions into the flow cell as follows: (i) control PBS, (ii) DOPC dispersion in PBS and (iii) sample/standard in PBS. Note also the three way solenoid valve which allows only one of these solutions to be introduced into the flow cell at one time. The exposed MFE in flow cell is connected to the PGSTAT12 potentiostat where the input voltage functions are applied through Scope™ software (AD Instruments). Capacitance current vs potential profiles were monitored with Scope™ software using rapid cyclic voltammetry (RCV) at scan rate  $40\text{Vs}^{-1}$ . In the RCV experiments the fabricated rectangular Pt electrode on the wafer was employed as a counter electrode and a  $3.5\text{ mol dm}^{-3}$  KCl Ag/AgCl inserted into the flow cell was used as reference electrode. All potentials in this paper are quoted versus this reference electrode. The Ag/AgCl reference electrode was preferred to the previously used Pt pseudo-reference electrode [16] since it maintains greater potential stability which is very necessary in precise analytical work and is not affected by contamination from the analyte compounds. 20 minutes prior to and continuously throughout each experiment, a blanket of argon gas (Air Products) is maintained above the control and sample electrolytes and DOPC dispersion to exclude  $\text{O}_2$ .

Prior to DOPC deposition the solenoid valve was switched to allow control PBS to flow through the flow cell. Subsequently, phospholipid deposition on the MFE was carried out as follows. A potential excursion was applied from  $-0.4\text{ V}$  to  $-3.00\text{ V}$  (Figure 2.9a) at a scan rate of  $100\text{ Vs}^{-1}$  at which point  $50\text{-}100\text{ }\mu\text{L}$  DOPC dispersion

was introduced into the flow cell by switching the solenoid valve to allow its entry. After 1 to 2 s, the characteristic voltammetric peaks appear corresponding to the potential enabled phase transitions of the phospholipid (Figure 2.9b)) [14]. At this point, the valve was switched back to allow the control PBS entry to flow cell and the potential excursion was altered to -0.4 to -1.2 V. Subsequently, by repetitive cycling, the characteristic RCV profile of DOPC on Hg with two voltammetric peaks is maintained which confirms the coverage and stability of the monolayer (Figure 2.9 c)). The solenoid valve was again switched to allow introduction of the sample/standard in place of the control PBS into the flow cell. Interactions of compounds with the DOPC monolayer were monitored by RCV while cycling the electrode potential from -0.4 to -1.2 V for 2 minutes during compound exposure and recording the changes that take place in the capacitance-potential profiles.

Following compound assay, the valve was switched to allow introduction of PBS control electrolyte in place of sample/standard electrolyte. The electrode was cleaned *in-situ* by repetitive cycling from -0.4 to -3.00 V. This procedure removes insoluble/soluble adsorbed organic material. Normally a 30s to 60s time period is sufficient to remove contaminants from the electrode surface. However, contamination from previous analyses (*i.e.* memory effects) does sometimes appear. To remove the memory effect from persistent samples, dilute piranha solution of ratio of 1:100 by volume of piranha: water is cautiously passed over the electrode for some seconds while repetitive cycling at -0.4V to -3.00 V. All liquids: DOPC dispersion, control and sample which passed through flow cell go on to waste. Figure 2.10 shows the whole process in a schematic representation.

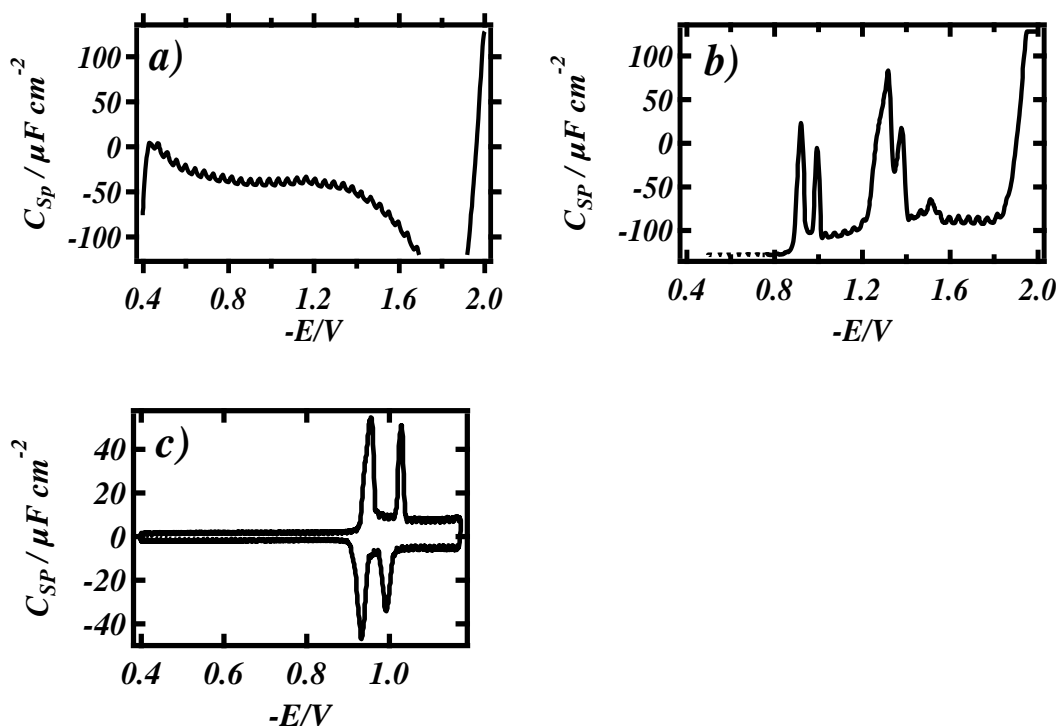
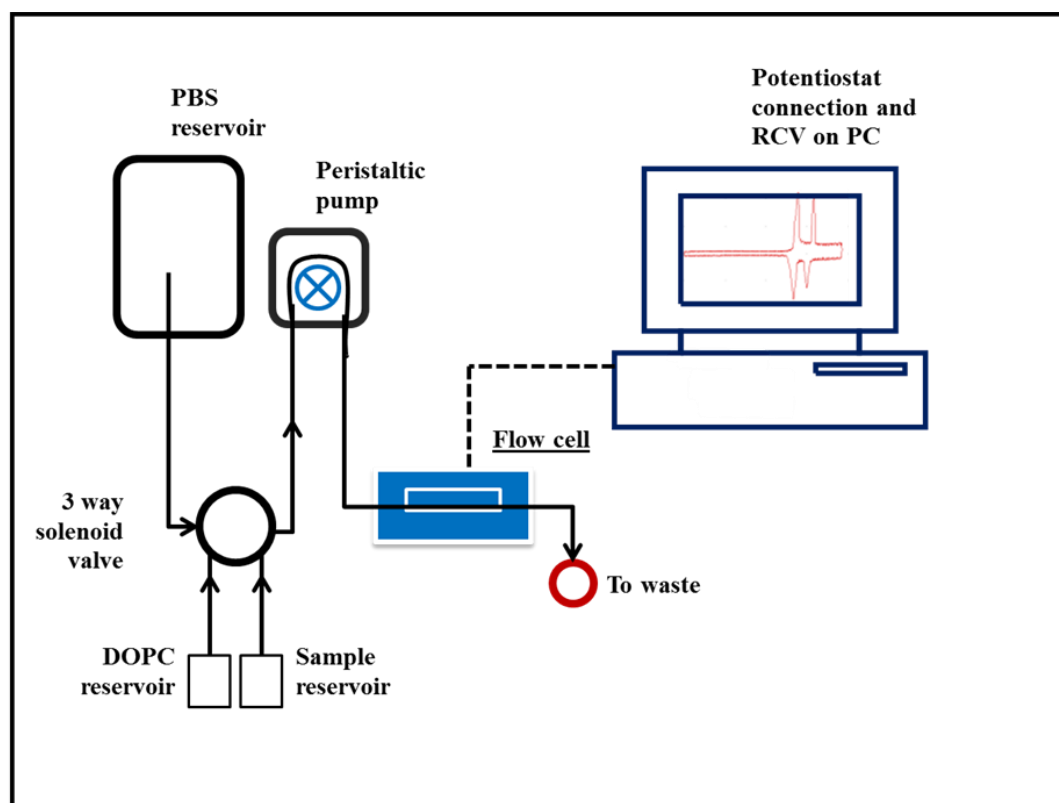


Figure 2.9: a) RCV recorded at  $40 \text{ Vs}^{-1}$  with potential excursions of  $-0.4 \text{ V}$  to  $-3.00 \text{ V}$ . This process is used for electrochemical in-situ cleaning and phospholipid deposition. b) RCV recorded at  $40 \text{ Vs}^{-1}$  with potential excursions of  $-0.4 \text{ V}$  to  $-3.00 \text{ V}$  after introduction of  $50 \mu\text{l}$  of  $0.2 \text{ mg cm}^{-3}$  DOPC dispersion in PBS at pH 7.4. c) RCVs recorded at  $40 \text{ Vs}^{-1}$  of a DOPC coated Pt/Hg electrode in PBS at pH 7.4 with potential excursions of  $-0.4 \text{ V}$  to  $-1.2 \text{ V}$  following the DOPC deposition procedure.



**Figure 2.10: The control system of the flow cell based sensing device. Pathways are represented by black arrows.**

## 2.4 LIMIT OF DETECTION

In order to obtain a more quantitative estimate of the effect of each compound on the DOPC layer, detection limits for each compound in PBS were estimated. This quantity is the minimum concentration of the compound in PBS which has a statistically significant effect on the monolayer's properties. The capacitance current peak on the RCV at more negative potentials was used for the limit of detection (LoD) estimation. The LoD is measured by plotting a calibration graph of capacitance current peak height vs. compound solution concentration following interaction with the respective compound. Subsequently the reproducibility of the capacitance current peak height from the RCVs of the DOPC coated Hg electrode in PBS was estimated by taking ten replicate measurements. The three times standard deviation (SD) of this capacitance

peak height was calculated as a control. Accordingly the concentration of test compound which has an equivalent suppressive effect on the capacitance current peak height relating to three times the SD of the control was read off the calibration curve to estimate the detection limit values. The detection limits are estimated and quoted as the minimum concentration of compound in water to elicit a response and these detection limits are related to compound molecular structure and the known biological effect of each compound.

The work includes the following compound classes: steroids, polycyclic aromatic hydrocarbons (PAH), tricyclic depressants (TCA) and tricyclic phenothiazines, methylxanthines, spiperone, other serotonin and dopamine receptor analogues, tricresyl phosphate, bispiridinium compounds, ionic liquids and other miscellaneous pharmaceutical compounds; some of which are negative controls. Previous work looking at similar groups of compounds was carried out some time ago [16-18]. Those studies used the system of phospholipid layers supported on a Hg drop electrode (HMDE) and selective interactions between classes of compounds and the phospholipid layers were reported. However the fragility of the electrode and the length of time required to carry out the assays precluded the use of the system as a working sensor. The developed present *on-line* high throughput analytical technology offers a significant noteworthy improvement, on the original concept and later developments [16]. The present system enables a large number of compounds to be screened rapidly and efficiently. Employing a suitable configuration of flow systems and electrodes, the system is shown to have the capability to screen in high throughput mode the biomembrane activity of pharmaceuticals and pollutants in water. Another improvement to the previous system is that the relation between the compounds' limit of detection (LoD) as screened in water can be calculated. A more comprehensive profile of the compounds' physical, structural properties and biological activity can be determined that precedes the previous system.

## 2.5 MATERIALS

All the test compounds were of 99% or greater purity and purchased from commercial suppliers, and were used as received. All phospholipids employed for coating electrodes were purchased from (Avanti Polar Lipids Alabaster, AL) and were >99% pure. All other reagents were of analytical grade and purchased from Sigma-Aldrich. There are two highly used reagents that are commented on in detail below.

### 2.5.1 PHOSPHATE BUFFERED SOLUTION (PBS)

0.1 mol dm<sup>-3</sup> solutions of potassium chloride phosphate buffered to pH 7.4 were prepared in bulk volumes (commonly 5 dm<sup>-3</sup>) and dispensed when required. The solutions was prepared with 0.1 mol dm<sup>-3</sup> KCl, calcined at 600 °C for two hours and buffered at pH 7.4 with 0.01 mol dm<sup>-3</sup> phosphate. For all following chapters hereinafter, phosphate buffered saline is referred to as PBS.

### 2.5.2 PIRANHA SOLUTION

Piranha solution is concentrated sulphuric acid (H<sub>2</sub>SO<sub>4</sub>) and hydrogen peroxide (H<sub>2</sub>O<sub>2</sub>). It is used to clean organic residues off substrates by solubilising organic residues and thus useful for cleaning contaminated glassware. Piranha solution was used frequently to clean the glassware used in these studies. The solution was prepared by addition of H<sub>2</sub>O<sub>2</sub> (30%v/v) (Fisher, UK) to sulphuric acid (98%) (Fisher, UK) in a pyrex flask in a ratio of 3:1 (v:v). The solution was prepared and poured into required glassware and left for some minutes all in a fume cupboard. Piranha solution is prepared fresh for every time apparatus need cleaning. After use, the solution is diluted with copious amounts of water and left to settle before disposing down the drain.

## 2.6 SUMMARY

- Electrochemical techniques have been discussed that measure an electrode's capacitance. This data can show changes in structure of the electrical double layer that are either potential induced or caused by the analyte composition or introduced compounds. The changes caused by introduced compounds will be discussed in later chapters. The interactions and systems discussed have applications in sensing, pharmaceutical novel compound screening, and understanding molecular interactions.
- The particular methods used throughout this thesis employ phospholipid coated fabricated Pt/Hg electrodes (MFE) configured within a flow system.
- The MFE set-up (as represented in Figure 2.10) has been successfully configured to screen the type and concentration of organic compounds in water. All the compound testing and interaction studies which have been successfully analysed with the MFE set-up is explained in subsequent chapters.
- The system allows for evaluation of toxicity, biomembrane permeation and damage; including a broad range of kinetic information.



## REFERENCES

- [1] Bard AJ, Faulkner LR. *Electrochemical Methods: Fundamentals and Applications.*, **2000** 2nd Edition
- [2] Samuel P. Kounaves, *Handbook of Instrumental Techniques for Analytical Chemistry*, **2004** 37: pp3219
- [3] Van Benschoten JJ, Lewis JY, Heineman WR. *Chem. Ed.* **1983**, 60: pp772.
- [4] Andrienko D *Cyclic Voltammetry* **1998** 25: pp95-100.
- [5] Monk P, Mortimer R, *Electrochromism and Electrochromic Devices* **2001** Cambridge University Press.
- [6] Milner DJ, Rice JR, Riggan RM. *Anal. Chem.* **1981**, 53: pp2258.
- [7] Moore BG, Rondelez F *J.Phys. Chem.* **1990**, 94: pp4588-4595.
- [8] Chechel OV, Nikolaev EN. *Instruments and Experimental Techniques*, **1991** 34(4): pp750-762.
- [9] Paunov *Compression and Structure of Monolayers of Charged Latex Particles at Air/Water and Oil/Water Interface.* **1999** Presentation at the 73rd ACS Symposium of Colloid & Interfacial Science.
- [10] Starzak ME, *The physical chemistry of membranes* **1984**. Academic Press.
- [11] Chen S, Abruna H D *Langmuir* **1994** 10 (9) 3343-3349.
- [12] [http://ichf.edu.pl/offers/instrum/Hg'2004/Hg\\_pliki/1\\_pliki/q6.htm](http://ichf.edu.pl/offers/instrum/Hg'2004/Hg_pliki/1_pliki/q6.htm)
- [13] Brett OAM, De Battisti A. *Electrochimica Acta* **2009** 54: pp4954–4962
- [14] Coldricka Z, Steenson P, Millnerc P, Davies D, Nelson A *Electrochimica Acta* **2008** 54: pp4954-4962.
- [15] Bizzotto D, Nelson A *Langmuir* **1998** 21: pp6269-6273
- [16] Coldrick Z Penezic A Gasparovic B, Steenson P, Merrifield J, Nelson A. *J Appl Electrochem*, **2011**, 41: pp939–949.
- [17] Nelson A. *Analytica Chimica Acta*, **1987**, 194: pp139–149
- [18] Nelson A, Auffret N, Borlakoglu J. *Biochimica et Biophysica Acta*, **1990**, 1021: pp205–216.

# CHAPTER 3

## MFE SYSTEM CHARACTERISATION AND OPTIMISATION

### 3.1 INTRODUCTION

The development of an electrode capable of replacing the HMDE for membrane studies and as an analytical tool has been achieved. It was now necessary to provide proof of concept and to commence measurements. However, the MFE system was yet to be ideally suited for rapid high-throughput sampling.

The DOPC coated microfabricated Pt/Hg electrode installed within a flow cell has been successfully configured to screen the type and concentration of organic compounds in water. The MFE is contained in a flow cell. A constant flow of pH 7.4 PBS is passed over the electrode by a peristaltic pump. The flow cell is connected to a research potentiostat interfaced to a Powerlab signal generator and controlled by Scope software. Standardised capacitance/voltage plots are produced when various electric potentials are applied. Thus, a profile can be obtained which is non-linear and dependent on the applied voltage. The monolayers undergo phase transitions corresponding to redistribution of charges and growth processes. These are depicted by capacitance current peaks. The data enables detection limits which represent the

lowest concentration of compound in water which statistically interacts with the DOPC layer to be calculated from the data. It is an *on-line* high throughput system. Data analysis and interpretation using the MFE system is conducted in parallel to data acquisition via an *on-line* system. Acquisition of new data is performed in seconds and can be immediately analysed for results without the need to transfer samples to other tools of analysis. No further specialist equipment is required other than a potentiostat to perform CV and a PC for on-screen visualisation of the data output. In summary, data analysis and interpretation is conducted in real-time with the same system used for data acquisition.

In this chapter, we discuss the MFE system optimisation and the developments which led to its enhanced performance so solving its limitations.

## **3.2 INSTRUMENT LIMITATIONS**

### **3.2.1 REFERENCE ELECTRODE**

An impediment to the previous designed MFE system was the constant need to clean the electrodes between testing which would have otherwise caused constant and gradual peak shifts of the standard DOPC and thus affect the overall result. Empirical observations indicated that this was due to heavy contamination from organic material of the internal platinum pseudo reference. Originally, in an attempt to simplify the screening system, platinum was evaporated onto the MFE chip in the same fabrication processing step that produces the working electrodes to be used as an internal reference electrode. The main disadvantage of using this platinum pseudo reference electrode is its uncontrolled reference potential that varies significantly with the electrolyte composition and concentration, memory effects and contamination. These effects was notable during the preliminary PAH tests (Figure 3.1).

After sampling a concentration of anthracene, the system was electrochemically cleaned by applying negative potential (-3.05V) while flushing the system with PBS. This removed the DOPC and any anthracene that was used. However a memory effect persisted. Figure 3.1 a) shows this. The black line is the DOPC monolayer before testing which is stable and at the standard reference potential. The red line is a newly deposited DOPC monolayer post anthracene testing. It can be seen that there is a shift in reference potential and the peaks remain irregular. This was resolved by changing the reference electrode using a double junction reference electrode (containing  $3.5 \text{ mol dm}^{-3}$  KCl, Ag/AgCl inner filling and  $0.1 \text{ mol dm}^{-3}$  perchloric acid outer filling) and a platinum bar auxiliary electrode (Metrohm) which is inserted into the flow cell and referred to as the standard reference electrode. The comparison of external and internal reference electrodes is shown in Figure 3.1 b).

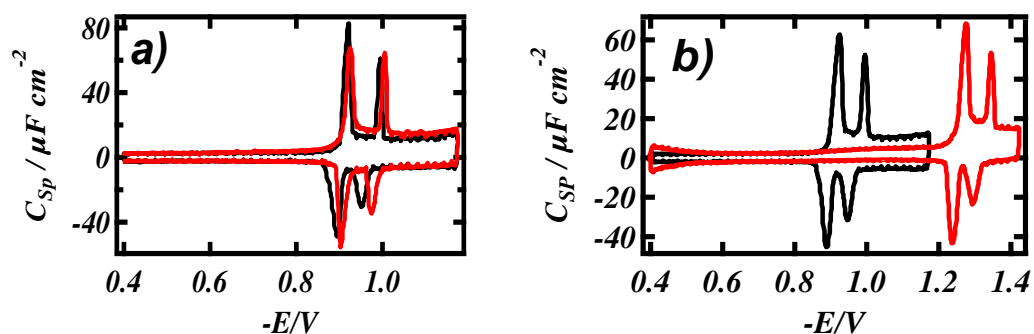


**Figure 3.1: RCVs recorded at  $40 \text{ Vs}^{-1}$  of a DOPC coated Pt/Hg electrode in PBS at pH 7.4 using a) an internal Pt *pseudo* reference electrode (black line) and capacitance current peaks post anthracene testing (red line) and b) comparison of capacitance current peak shifts using internal Pt *pseudo* reference electrode (red line) and when using  $3.5 \text{ mol dm}^{-3}$  KCl Ag/AgCl standard reference electrode (black line).**

### 3.2.2 NOISE

Electrical noise can also be decreased by isolating the device from radio frequency radiation by shielding cabling and equipment that may act as aerials for electrical noise. A faraday cage can be used in extreme cases. Figure 3.2 compares the RCV plots during noise disturbances and standard conditions.

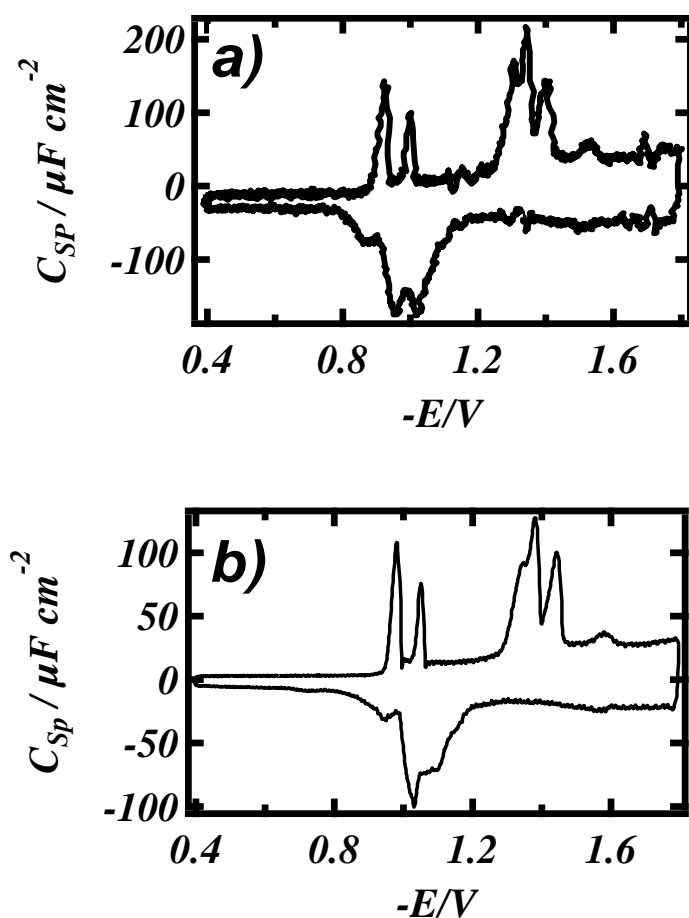


Figure 3.2: RCVs recorded at 40 Vs<sup>-1</sup> of a DOPC coated Pt/Hg electrode in PBS at pH 7.4 with switching potential of -1.8V a) affected by electrical noise interference and b) in standard conditions.

### 3.2.3 FLOW RATE

During experiments, a constant flow of electrolyte passed over the MFE surface at a rate of 5 to 10  $\text{cm}^3\text{min}^{-1}$  maintained by a 520DU peristaltic pump (Watson Marlow, UK). The lipids can withstand a particular flow rate. When the flow rate is particularly high, the lipids are removed from the mercury surface as shown in Figure 3.3.

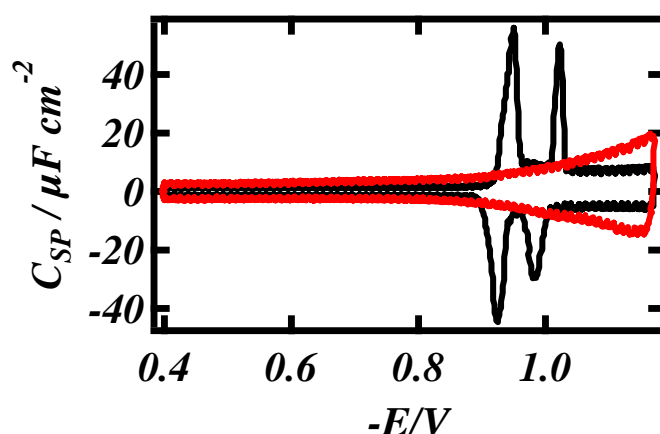


Figure 3.3: RCVs recorded at  $40 \text{ Vs}^{-1}$  of a DOPC coated Pt/Hg electrode (black line) and removal of lipids from Pt/Hg electrode when flow rates exceed  $20 \text{ cm}^3\text{min}^{-1}$  (red line).

### 3.2.4 LEAKS

Electrolyte leaks proved to be a major practical concern with the first flow cell design. Fine gaps between the silicon wafer and the PTFE cell under the main cell O-ring did not form a perfect seal. This allowed a small volume of electrolyte to come into contact with the crocodile clips connecting to the working electrode bond pads. This unintended additional electrochemical junction resulted in electrical interference due to rusting at the contacts.

### 3.3 NEW FLOW CELL

The previous flow cell had various design faults. Many of the leaks and contaminations mentioned were mainly due to the material and design of the flow cell. The previous design was a cylindrical block made of soft PTFE with four clamp screws. Every time the flow cell was unscrewed to gain access to electrode, the seals would erode/wear down. This occurred repeatedly if the valves needed to be unscrewed from the sides for example, to change tubing. This caused the seal to collapse allowing leaks to occur. Over time, the flow cell became a reservoir for containing contamination or particles as over time as sediments or contaminants would settle in any eroded part and thus hinder results. At the extreme, these sediments would eventually block the tubing and effect the pump and PBS flow. Normally PTFE has good physical parameters. It maintains high strength, toughness and self-lubrication at low temperatures down to 5 K (-268.15°C; -450.67 F), and good flexibility with high heat resistance at temperatures above 194 K (-79°C; -110°F) [1]. However it was soft, malleable and not transparent. This prompted the need to make changes to the physical properties and materials of the flow cell.

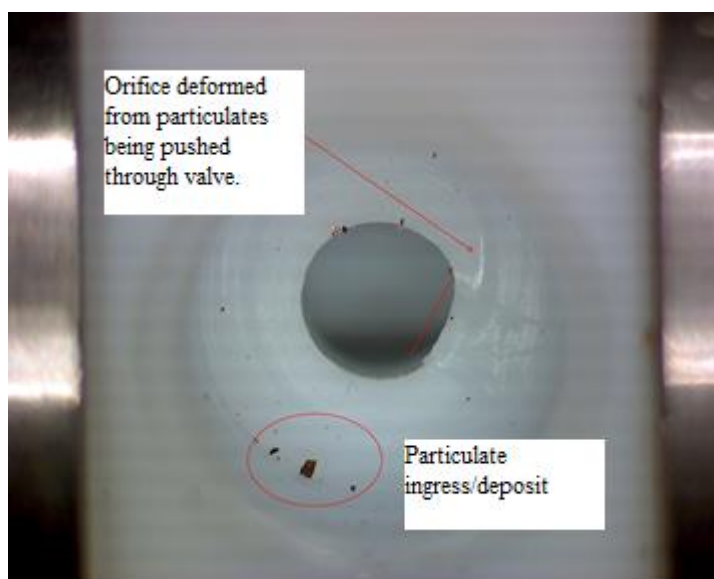


**Figure 3.4: The particulate ingress damaging the soft PTFE valve seal.**

The material of choice for the new flow cell is poly (methyl methacrylate) or Perspex. This has many useful features for use as flow cell, it is transparent so that it is easy to see any defects within the cell or to check on system easily without having to open the cell, it has high thermal withstanding and pressure properties; for example in the use of large aquariums to withstand the water pressure. It also has a good degree of compatibility with human tissue. The flow cell was custom made. The base block contained five nuts cylindrical holes for clamp screws. A groove was cut to accommodate the microfabricated electrode. The cell was formed by clamping the upper block to the lower block by tightening five clamp screws with the device in place. An O-ring is used to form a seal over the electrode. A 2mm diameter electrolyte flow channel was drilled into the upper block that passed into the cylindrical cavity above the face of the electrode. Electrolyte flowed in via this channel and exited the cell through a similar 2mm diameter channel. Tubing was attached to the cell via bespoke connectors sourced from the University of Leeds Physics Workshop.

### **3.3.1 STABLE MONOLAYER**

Once these problems were eradicated, it was possible to produce similar lipid monolayers on the MFE in a stable and reproducible configuration. Figures 3.5 a) and b) display the stability of the lipid monolayer.



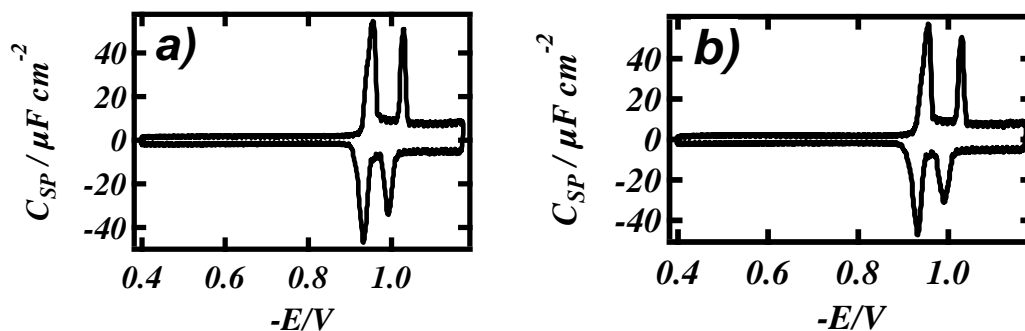


Figure 3.5: RCVs recorded at  $40 \text{ Vs}^{-1}$  of a DOPC coated Pt/Hg electrode at a) 0 minutes and b) 20 minutes.

### 3.4 CONTAMINATION AND CARRYOVER

During studies, the electrodes were subject to contamination from various materials and sources, including the air. There is no single procedure that is applicable to clean all the types of contaminations/substrates. Some contaminants are more persistent than others and require harsher treatments. Carryover is a significant problem that can occur and could impede the reliability of measurement and can cause false positive or negative results. Following the successful redesign of the flow cell, the interactions studied increased, and therefore compound carryover can become a real problem.

Procedures have been tested for the effective and efficient removal of interfering compounds that have originated from the previous analysis in the MFE system. This cleaning procedure should be able to remove strongly bound compounds without having to manually interfere with the system.

In many cases so far, the products and reactants of the electrochemical reaction do not adsorb or preconcentrate on the electrode persistently. Therefore simply, the electrode can be cleaned *in situ*. However, contamination from previous analyses (*i.e.*

memory effects) do sometimes appear and are more pronounced during prolonged accumulation of certain known bioaccumulative compounds on the electrode surface.

An unspecified contaminant from the air was inducing effects on lipid monolayer. The lipid layer was unstable after 10 minutes of exposure to conditions. The contaminant also affected bare Hg capacitance. Figures 3.6 a and b show this occurring.

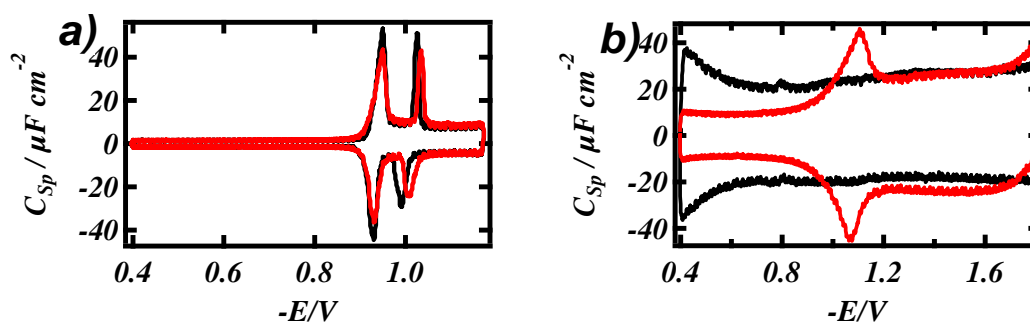


**Figure 3.6: RCVs recorded at  $40 \text{ Vs}^{-1}$  of a) DOPC coated Pt/Hg electrode (black line) being affected by contamination (red line) and b) an uncoated Pt/Hg electrode (black line) being affected by contamination (red line) in PBS at pH 7.4.**

Not only is this evidence of high sensitivity, but also that the contamination meant that the system is sensitive to air contaminants; a potential to develop the sensor. Various cleaning agents were tested and shown in Figure 3.7.

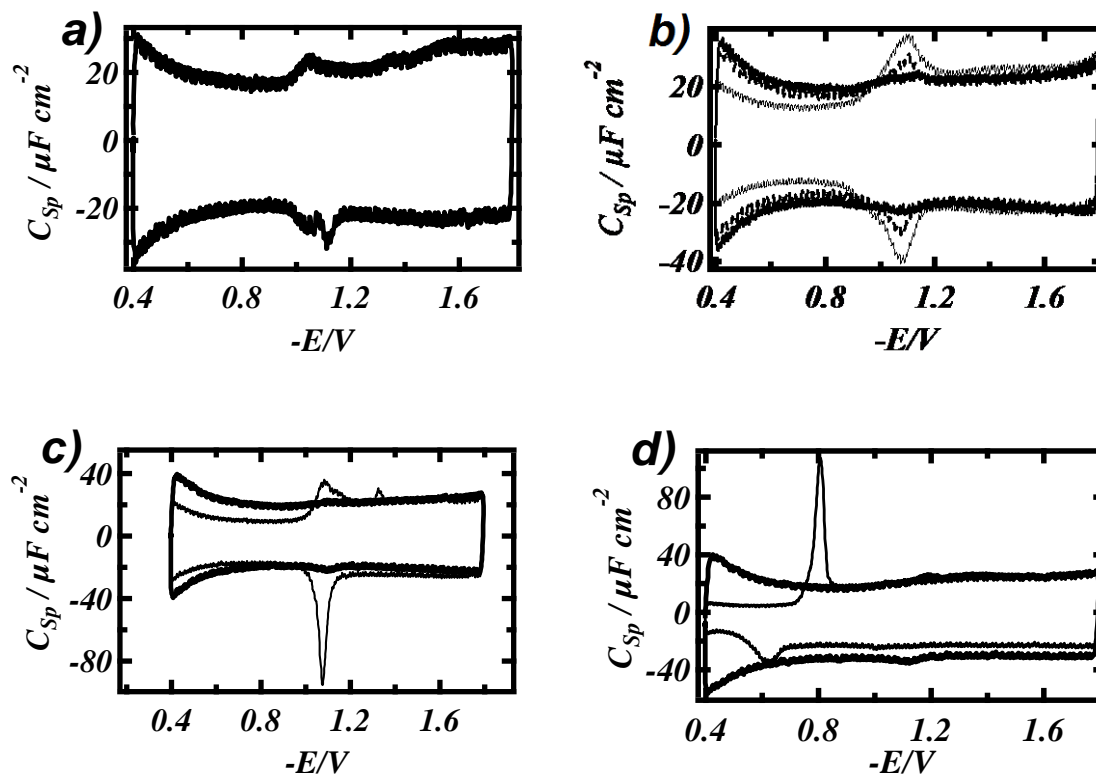
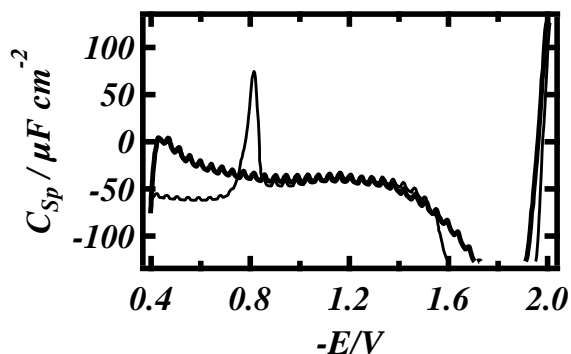


Figure 3.7: RCVs recorded at 40 Vs<sup>-1</sup> of a Pt/Hg electrode in PBS at pH 7.4 showing chemical cleaning using a) 0.4M NaOH, b) peroxide solution in a ratio of 2:100 by volume of hydrogen peroxide, c) dilute piranha solution (piranha solution is made using H<sub>2</sub>SO<sub>4</sub> and 30% H<sub>2</sub>O<sub>2</sub> in a mixture with ratio of 3:1 respectively) in a ratio of 1:100 by volume of piranha, d) 3 mg dm<sup>-3</sup> humic acid in PBS at pH 7.4.

### 3.4.1 ELECTROCHEMICAL CLEANING

The Pt/Hg electrode can be cleaned in situ by repetitive cycling from -0.4V to -3.00V. This procedure removes insoluble/soluble adsorbed organic material. Normally a 30s to 60s time period is sufficient to remove contaminants from the electrode surface.



**Figure 3.8: RCV at a scan rate of  $100 \text{ Vs}^{-1}$  of a Pt/Hg electrode with potential excursion from  $-0.4 \text{ V}$  to  $-3.00 \text{ V}$ . The peak appearing at approximately  $-0.8\text{V}$  indicates a contaminant on the Hg surface. After electrochemical cleaning, the peak at  $-0.8\text{V}$  disappears indicating that the contaminant has been removed as shown on bold line.**

### 3.4.2 CHEMICAL CLEANING

Mechanical scratches of any of the tube connections may cause a significant increase in carryover in a separation system by providing a space for increasing the void volume and enabling sample remains to be “trapped” in them. Persistent samples simply bind and can cause carryover effect. The cleaning protocol is simply explained. Dilute piranha solution; a hot solution of sulfuric acid and 30% hydrogen peroxide at a ratio of 3:1 and dilution ratio of 1:100 is passed over the electrode for a few seconds while repetitive cycling at  $-0.4\text{V}$  to  $-3.00\text{V}$ .

An impediment of using peroxide for cleaning is that if excess is used, it can cause a negative slant on the capacitance plots. This indicates faradaic reduction process taking place. This could also occur due to a defect in electrode but more likely it is a contaminant or in this case, the use of peroxide during cleaning. Figure 3.9 displays mercury in a slanting capacitance against the background of how mercury is normally displayed.

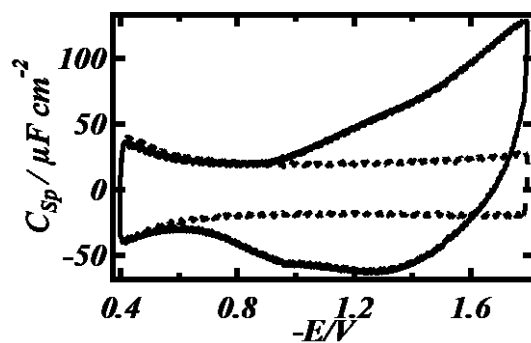


Figure 3.9: RCV at  $40 \text{ Vs}^{-1}$  of a Pt/Hg electrode (dotted line) and showing faradaic reaction (black line) in PBS at pH 7.4.

### 3.4.3 MANUAL CLEANING

Any electrode that is excessively damaged by organics, mishandling or applying inappropriate potentials needs further treatment as electrochemical cleaning methods may not suffice. Removing the MPE from the flow cell, any solid contamination can be removed by carefully rubbing some acetone over the chip while avoiding the mercury. Depending on severity of damage, the MFE may need replacement and re-deposition of the Hg. Platinum electrodes can have their surface damaged through organic contamination, mishandling or use of inappropriate potentials. The mercury or platinum reference electrode could also become damaged or contaminated by certain compounds.

### 3.5 ANALYSING PARAMETERS

Fingerprint profiles from these experiments can determine the effect of various compounds on membrane. Figure 3.10 displays the results of the changes to the RCV plots from the interaction of DOPC with the example compound pyrene in two concentrations. The compounds interact with the DOPC coated electrode can be seen by their effect on the capacitance current peaks in the RCV plot. These capacitance current peaks are representative of the reorientation/adsorption/desorption processes of the DOPC layers in response to potential change.

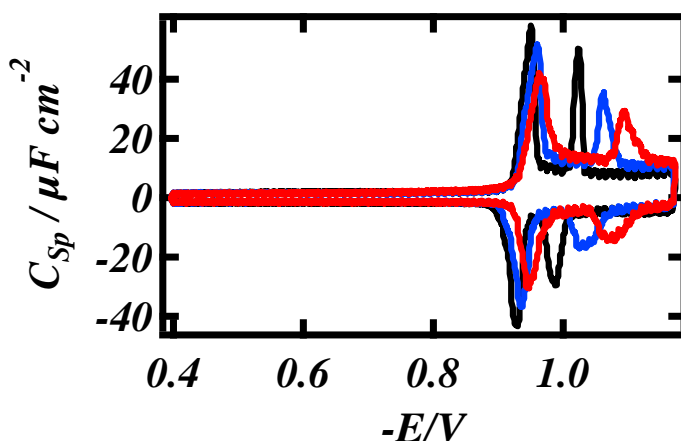


**Figure 3.10:** RCVs recorded at  $40 \text{ Vs}^{-1}$  of a DOPC coated Pt/Hg electrode (black line) in the presence of  $0.0005 \mu mol dm^{-3}$  (blue line) and  $0.002 \mu mol dm^{-3}$  (red line) pyrene in PBS at pH 7.4.

It is observed that each class of compound interaction effects a “fingerprint” visual profile on the RCV plot which manifests itself as an alteration in the shape, height and position of the capacitance current peaks. The extent of damage to the membrane layer would be measured by monitoring of the capacitance peaks produced after the test compound has been flowed over and removed from the flow chamber. By comparing the membrane peaks after contact with the test compound to the original baseline peaks, we can see the extent to which they return to normal baseline levels.

Another calculation that can be made is limit of detection (LOD). Limit of Detection represents the lowest concentration of compound that is detectable, and produces recognisable differences compared to the baseline. The Limit of Detection would be identified through introducing a decreasing concentration of compound through the flow cell across the membrane and identifying at which concentration there is no longer a discernible difference in peak heights compared to the baseline.

### **3.6 COMPARING TO OTHER SYSTEMS**

The MFE system measures membrane permeability of a compound through changes to RCV peak integrity, affected when an interacting compound passes over an artificial DOPC phospholipid membrane. DOPC phospholipids are amphipathic and are a truer representation of lipid bilayers found in nature than hydrocarbon membranes used in PAMPA. Having said this, the system is not capable of making *in vivo* measurements like the Caco-2 assay, which makes use of real lipid membranes in the form of colon cells, and can account for the more complex systems associated with drug permeability. The likeness of Caco-2 assay to the structure of a biological membrane may make it seem more advantageous than MFE system, nevertheless, it is important to understand and use the simplest model first.

The MFE system is less stringent and more flexible than PAMPA assays. The integrity of the lipid membrane is measured within seconds through monitoring of on-screen, real-time voltammogram, as opposed to using a Lucifer yellow label. There is no requirement for a drug-membrane incubation period as with PAMPA as interpretation comes from RCV peak height. It produces label-free, real-time measurements and can be used with less than 10 $\mu$ M of test compound, in fact its sensitivity is as low as nM values. Whereas PAMPA requires 10 $\mu$ M. Because of this the MFE system is a less complex system, requires less setup time, produces less

wastage and produces a larger data output. The MFE system is a potential alternative to PAMPA, and compliments perfectly further downstream assays such as Caco-2.

### **3.7 SUMMARY**

To conclude, Tables 3.1 and 3.2 compares the MFE flow cell to other systems available which are biomimetics or used as part of biomembrane studies.



Parameter	Typical Approach	Range	Quick Summary	Can MFE flow cell measure this
<b>pKa</b>	pH titrations with UV absorbance or pH-metric	-0.5 to 13.0 (3 different methods)	The pK <sub>a</sub> is the pH at which the molecule is 50% protonated.	No test measured yet however this can be easily incorporated by changing the pH of solution that is introduced into flow cell along with the test compound.
<b>Solubility</b>	Thermodynamic solubility assay	N/A	Thermodynamic (or equilibrium) solubility of a compound as a saturated solution in equilibrium.	
<b>Log P(app)</b>	PAMPA avoids the complexities of active transport, allowing test compounds to be ranked based on a simple permeability property alone.[3]	P <sub>app</sub> < 10 x 10 <sup>-6</sup> cm/s and P <sub>app</sub> > 10 x 10 <sup>-6</sup> cm/s	This method provides an <i>in vitro</i> model for passive diffusion.	Samples with MFE are tabulated according to their limits of detection; the lowest concentration at which the compounds interact with the monolayer.
<b>Log D (7.4)</b>	Partition of a compound between an organic solvent (typically octanol) and aqueous buffer – shake flask.[4]	0 to >5	Log D (distribution coefficient) is used as a measure of lipophilicity.	Tests have shown that the log D of a compound is not a reliable indicator of the compound's ability to interact with phospholipid monolayers but is only an approximate guide to the extent of interaction of a series of compounds of related structure.
<b>Membrane Damage</b>				The monolayer is selectively damaged by biomembrane-active compounds in the sample. This damage is detected electrochemically as an alteration in the nanoscale forces of self-assembly within the layer.

Table 3.1: Typical measuring parameters in biomembrane studies.

System	Measurement	Quick summary	Comparing MFE flow cell to system
<b>MDCK Permeability</b>	MDCK cells develop tight junctions and form monolayers of polarised cells (quicker than Caco-2 to prepare) [5]	To study drug efflux, it is also necessary to investigate transport of the compound from the basolateral compartment to the apical compartment and calculate an efflux ratio.	With regards to MDCK, this system results in these assays being too specific and exclusive. The MFE can also be adapted to specific immobilised proteins and/or enzymes that can be adsorbed onto monolayer when specificity is required.
<b>MDR1-MDCK Permeability</b>	Same as above with different cell line	This cell line is ideal for identifying substrates and inhibitors of P-gp, and quantifying the extent of the interaction	As above
<b>P-gp inhibition assay</b>	MDR1-MDCK cells originate from transfection of Madin Darby canine kidney (MDCK) cells with the <i>MDR1</i> gene, the gene encoding for the efflux protein, P-glycoprotein (P-gp) [6]	Inhibition of P-gp has shown to be responsible for several clinical drug-drug interactions. For example, clarithromycin can inhibit the transport of the P-gp substrate digoxin resulting in an elevation of plasma levels and a decrease in renal clearance. [7]	As above
<b>Caco-2 P(app)</b>	The cells are seeded on Millipore Millicell plates and form a confluent monolayer over 20 days. On day 20, the test compound is added to the apical side of the membrane and the transport of the compound across the monolayer is monitored over a 2 hour time period.[8,9]	PAMPA solely provides a measure of passive diffusion whereas the Caco-2 model provides better prediction of the human absorption for compounds which display active uptake or efflux or pass through the membrane via the paracellular route.	Using rapid cyclic voltammetry, a potential excursion is applied from $-0.4$ V to $-3.00$ V at a scan rate of $100$ $\text{Vs}^{-1}$ at which point $0.1$ - $0.2$ $\text{cm}^3$ DOPC dispersion (Avanti Polar Lipids) is introduced via a designated port in the flow cell. A monolayer can thus be deposited onto MFE in flow cell after 1-2 seconds of exposure. Test compounds can be immediately introduced and the monolayer is monitored. Depending on compound and concentration used, the entire test incl. redeposit of new layers take 10 - 20 minutes on average.

Table 3.2: Typical permeability assays to compare with MFE flow cell assay.

## REFERENCES

- [1] Sun, J.Z. et al. *Radiat. Phys. Chem.* **1994** 44 (6): 655–679
- [2] Di L ,Kerns EH, Fan K, McConnell OJ, and Carter GT. *Eur J Med Chem* **2003** 38; 223-232
- [3] Nakabayashi N, Kojima K, Masuhara E *Journal of Biomedical Materials Research*, **1982** 16,265-273
- [4] Xin Li, M A Cooper *Anal. Chem.*, **2012**, 84 (6), pp 2609–2613.
- [5] Wang O et al, *Int J Pharmaceut* **2005** 288; 349-359
- [6] Pastan I et al. *Proc Natl Acad Sci* **1988** 85; 4486-4490
- [7] Wakasugi H et al. *Clin Pharmacol Ther***1998** 64; 123 -128
- [8] Wang Z, Hop C.E., Leung K.H. and Pang J. *J Mass Spectrom* **2000** 35(1); 71-76
- [9] Zhao YH et al. *J Pharmaceut Sci* **2001** 90; 749-784

# CHAPTER 4

## PHOSPHOLIPID MONOLAYERS ON

## ELECTRODE SURFACES

### 4.1 INTRODUCTION

#### 4.1.1 LIPIDS IN NATURE

Biological membranes have widely varying composition. The size of the diversity in composition of biological membranes is reflected in their specific functional roles. Animal species, such as fish or mammals, and their organs, such as brain or liver, are all composed of different lipids. Their contributions to biological events are not limited; they have essential roles, including but not limited to cell recognition, selective ion transfers, adhesion and providing a surface for many catalytic processes. [1] This differentiation shows how important it is to evaluate the interactions within membranes composed of different lipids. There are a large number of lipid species, tailored for a particular organism.

The following phospholipids are studied in this chapter: 1, 2-dioleoyl-*sn*-glycero-3-phosphocholine (DOPC), 1-palmitoyl-2-oleoyl-*sn*-glycero-3-phosphocholine (POPC),

1,2-di-(9Z-octadecenoyl)-*sn*-glycero-3-phosphoethanolamine (DOPE), 1,2-di-(9Z-octadecenoyl)-*sn*-glycero-3-phospho-(1'-*rac*-glycerol) (DOPG) and 1,2-dioleoyl-*sn*-glycero-3-phospho-L-serine (DOPS), along with the following steroids: cholesterol, stigmasterol and ergosterol. Their molecular structures are presented in Figure 4.1.

Generally, membranes have a backbone of a phospholipid bilayer with incorporated membrane bound proteins and/or cholesterol. Phosphatidylcholine (PC) is the most abundant phospholipid in eukaryote cell membranes including human cells. Phosphatidylethanolamine (PE) has some contributions to eukaryotic cell membrane compositions, however it is most prevalent in the cell membranes of higher order plants and fungi and dominant in some bacterial cell membrane strains. Phosphatidylglycerol (PG) is most abundant in prokaryote cell membranes.

PC and PE are the two most abundant phospholipids in many biological membranes. They are not so different to each other however their minor differences play a major role in their physical and curvature characteristics such as melting temperatures, phase transitions and the manner in which they are organised. Since they form the backbone of cell membranes, their composition also affects the way in which ions and other compounds penetrate through or interact with the membranes. For example, dipalmitoylphosphatidylcholine (DPPC) has a transition temperature of 41.3°C and exists as a solid gel type phase at room temperature whereas DOPC has a much lower transition temperature of -16.5°C and therefore is more fluid at room temperature [2].

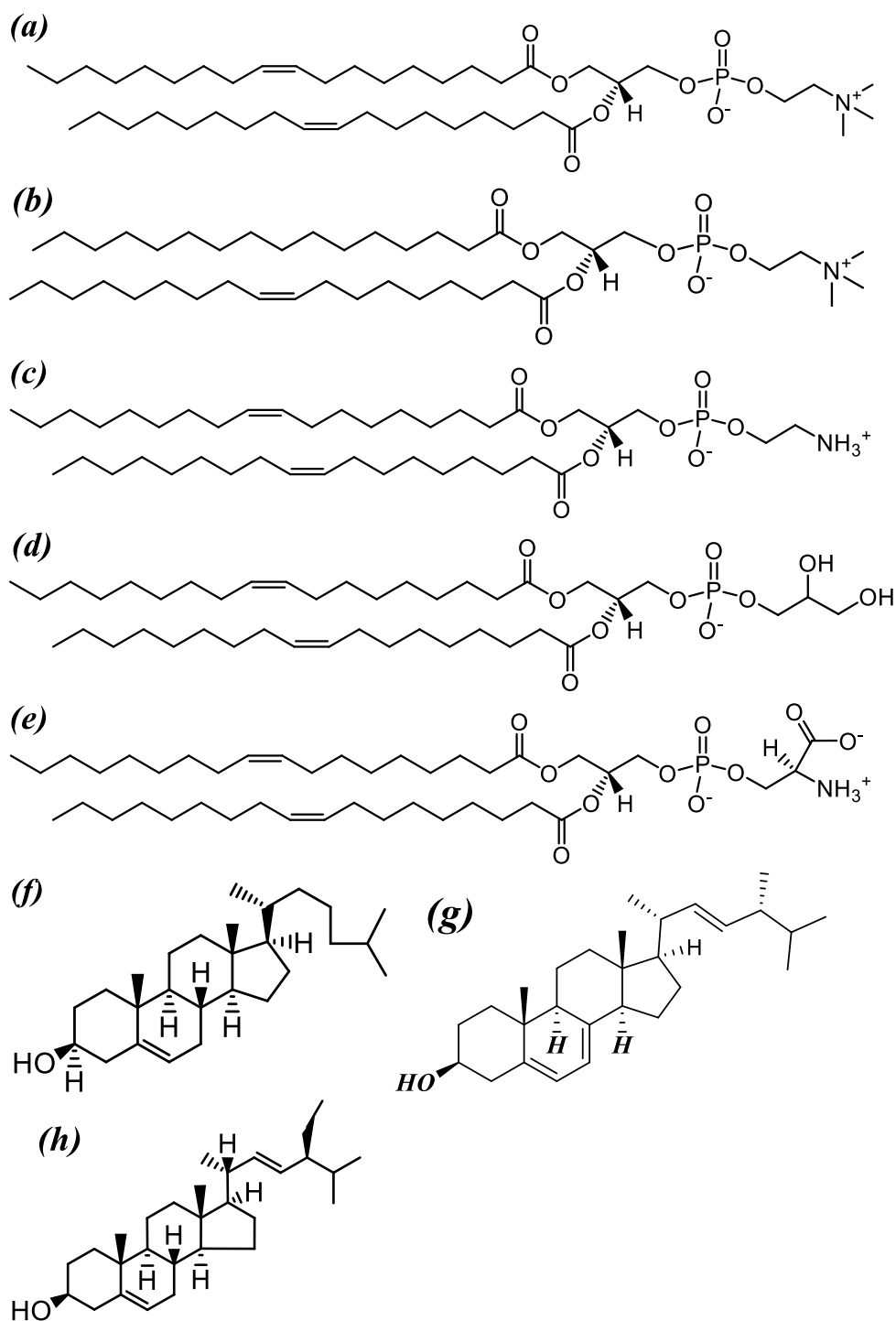


Figure 4.1: molecular structures of a) 1, 2-dioleoyl-*sn*-glycero-3-phosphocholine (DOPC), b) 1-palmitoyl-2-oleoyl-*sn*-glycero-3-phosphocholine (POPC) c) 1,2-di-(9Z-octadecenoyl)-*sn*-glycero-3-phosphoethanolamine (DOPE), d) 1,2-di-(9Z-octadecenoyl)-*sn*-glycero-3-phospho-(1'-*rac*-glycerol) (DOPG), e) 1,2-dioleoyl-*sn*-glycero-3-phospho-L-serine (DOPS), f) cholesterol, g) ergosterol, h) stigmasterol.

Due to the complexity in the nature of lipids, the precise mechanisms of drug-membrane interaction can be difficult to recognise. Therefore it is important to first understand the fundamentals of lipid behaviour. The ability of a molecule to cross the biological membranes (permeability) is a very important biopharmaceutical parameter that governs the pharmacokinetics of a drug [3]. Electrochemical techniques can be used in this case to study the fundamental topographical parameters as well as certain complex interactions such as drug/toxin – biomembrane interactions.

The system of phospholipid layers on Hg is an excellent model of biological membranes. It is known that the phospholipids adsorbed on the Hg surface are sensitive to chemical and physical parameters [4, 5] such that their use in sensing technology is a huge opportunity in fundamental research. The phospholipid sensing element is also convenient, easy to prepare and handle and significant qualitative insights can be extracted from the results. Because of this, phospholipid layers of different composition have been evaluated using the MFE cell system.

In this Chapter, three separate categories of properties of phospholipids are examined.

- The effect of varying pH on the properties of DOPC on Hg
- Phospholipid and sterol-phospholipid association on Hg
- Electrochemical characterisation of four different phospholipids.

#### **4.1.2 BEHAVIOUR OF PHOSPHOLIPIDS**

The behaviour of the phospholipid monolayer on the Hg surface in response to potential changes is of particular interest and as such, quantitative analysis of the properties of the monolayer on the Hg has been studied. The investigation of spread phospholipid monolayers on Hg has continued for over five decades [6]. In that time

the system has been developed and refined considerably. The unique selling point of the technology is the simplistic membrane model allowing for intricate and sensitive interactions to be analysed against a distributed self-assembled phospholipid monolayer.

DOPC as a model phospholipid is used primarily in these experiments. There are numerous advantages to using DOPC over other lipids. RCV scans of the DOPC coated Hg are very reproducible and accord with a defect-free and stable monolayer which remains stable for at least 30 minutes. This has been confirmed by recent AFM measurements of the system [7]. As proven in these studies. It also models the biological membrane accurately and is highly compatible with the MFE flow cell system. The electrochemical technique employed has been previously described in Chapter 2. The capacitance current peaks will be described in more detail here.

To conduct the experiments, RCV measurements are used with potential excursion from  $-0.4\text{V}$  to  $-1.8\text{V}$  at a scan rate of  $40\text{V}\cdot\text{s}^{-1}$ . If the switching potential of excursions is  $-1.2\text{V}$ , the monolayers undergo two pronounced phase transitions characterised by two capacitance current peaks. This is shown in Figure 4.2. The peaks correspond to the redistribution of charges or polar molecules with the monolayer interface [8].

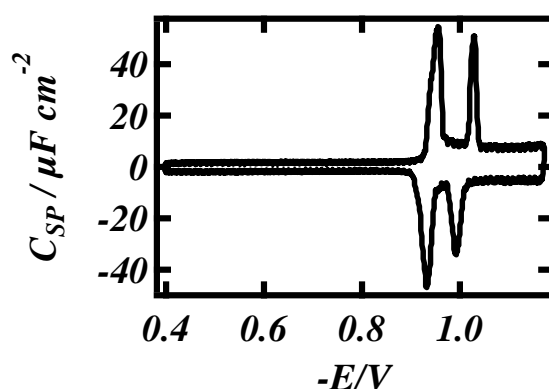


**Figure 4.2:** Data from RCV of a DOPC coated Pt/Hg electrode in PBS at pH 7.4 measured at  $40\text{V}\cdot\text{s}^{-1}$  with potential excursions from  $-0.4\text{V}$  to  $-1.2\text{V}$ .



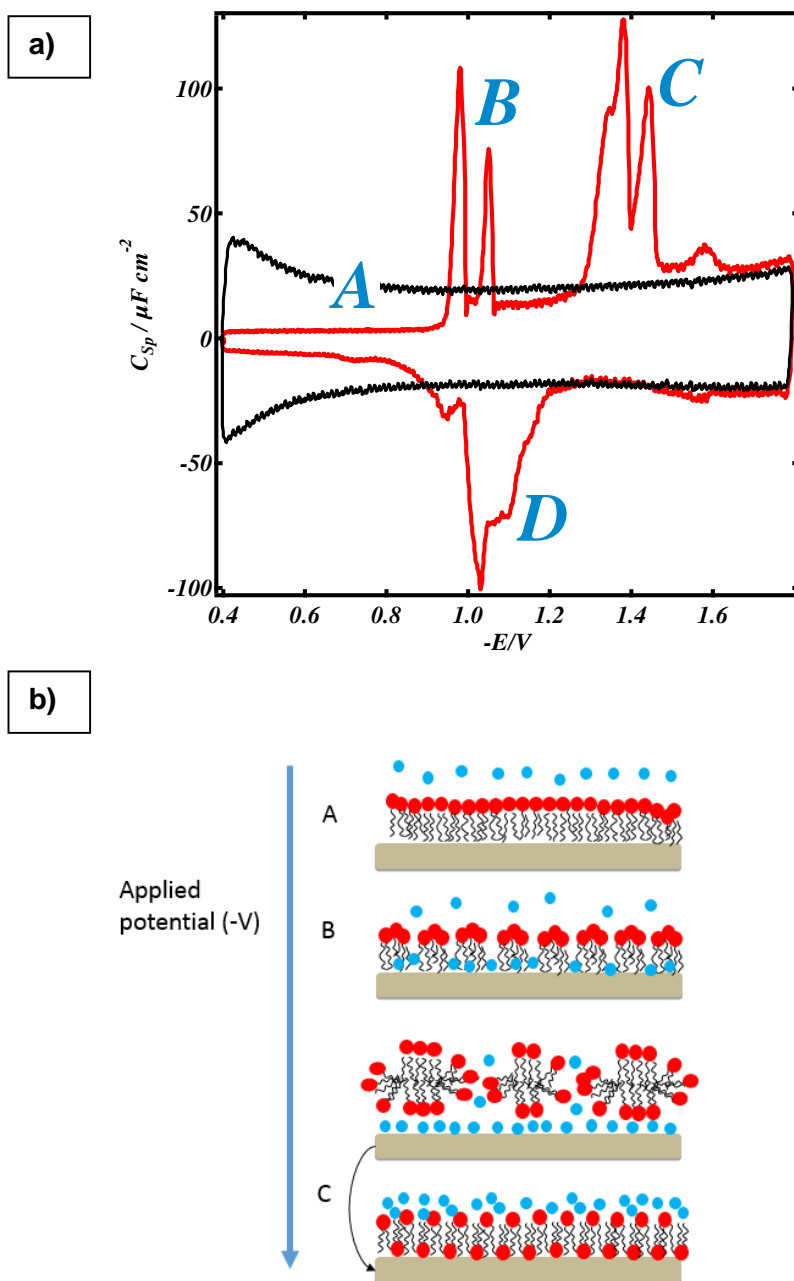


**Figure 4.3: a) Data from RCV of a Pt/Hg electrode (black line) and coated with DOPC (red line) measured at  $40V \cdot s^{-1}$  with potential excursions from  $-0.4V$  to  $-1.8V$  in PBS at pH 7.4. b) Illustration of the possible phase transitions occurring upon varying the applied potential.**

Figure 4.3 represents the same procedures as above except the potential applied has a switching point of  $-1.8V$ . We can see the effect compared to uncoated Hg which is presented by the black line. Capacitance current peaks develop which represent the

sequential phase transitions that occur at different points of negative voltage fields [9, 10].

The area marked A , corresponds to potentials -0.4 V to about -0.95V. -0.4V is close to the PZC of Hg and is the point where monolayers of DOPC on Hg are homogeneous and impermeable to ions [10, 11].

The two peaks B correspond to a structural reorientation of the monolayer as seen in Figure 4.2. The first capacitance current peak corresponds to an increase in membrane permeability to ions, this occurs around -0.95V. The second capacitance current peak represents a phase transition initiated by a nucleation and growth process [8]. This occurs around -1.03V. This peak corresponds to formation of bilayer patches [12]. The nucleation and growth process underlies this process leads to the readsorption of bilayer patches on the electrode surface.

The phase transition peaks proceed from -1.2V to -1.8V and are labelled C collectively. Miller [13] originally indicated that the voltammetric peaks at very negative potentials represented a desorption of the phospholipid from the Hg. The formation of a phospholipid bilayer on Hg in aqueous electrolyte was considered to be unachievable. However, a recent investigation has shown that a near continuous DOPC bilayer is formed on Hg in an applied potential window within -1.0 and -1.4 V [7].

At about -1.4V of applied potential, a partial desorption of a bilayer occurs, leading to semivesicular structures attached to the electrode. At even higher potentials it is found that the bilayer patches subsequently collapse to form a monolayer of uncertain composition.

Figure 4.3 b) illustrates the possible phase transitions occurring in the layered lipid upon varying the applied electric potential.

The positive going peaks, labelled D collectively are a reverse of the processes A to C occurring with a different mechanism.

The capacitance minimum (area marked A) between -0.4 V to -0.8V represents an almost ideal capacitor of a monolayer of phospholipid on Hg. The specific capacitance is represented by the equation:-

$$C_S = C/A = \epsilon\epsilon_0/d \quad (4.1)$$

Where  $C_S$  is the specific capacitance,  $C$  is capacitance,  $\epsilon$  is the relative permittivity for the phospholipids' alkyl tails,  $\epsilon_0$  is the vacuum permittivity which is  $8.85 \times 10^{-12} \text{ F m}^{-1}$  and  $d$  is the thickness of the dielectric.

## 4.2 MATERIALS AND METHODS

The phospholipids employed for coating electrodes were 1, 2-dioleoyl-*sn*-glycero-3-phosphocholine (DOPC), 1,2-di-(9Z-octadecenoyl)-*sn*-glycero-3-phosphoethanolamine (DOPE), 1,2-dioleoyl-*sn*-glycero-3-phospho-L-serine (DOPS), 1,2-di-(9Z-octadecenoyl)-*sn*-glycero-3-phospho-(1'-*rac*-glycerol) (DOPG), 1-palmitoyl-2-oleoyl-*sn*-glycero-3-phosphocholine (POPC) (purchased from Avanti Polar Lipids Alabaster, AL) and were >99% pure. The sterols/steroids were of 99% or greater purity. They were purchased from commercial suppliers and were used as received. All other reagents were of analytical grade and purchased from Sigma-Aldrich. The electrolyte used throughout the experiments was 0.1 mol dm<sup>-3</sup> KCl, calcined at 600°C for two hours and buffered at pH 7.4 with 0.01 mol dm<sup>-3</sup> phosphate (referred to as PBS in the chapters).

### SAMPLE PREPARATION

The phospholipid dispersions for electrode coating was prepared by gently shaking with PBS to give 0.2 mg cm<sup>-3</sup> dispersion. The steroids were dissolved in acetone and concentrations were prepared by adding small aliquots of the working solutions to PBS to provide concentrations for testing. Mole fractions were calculated according to the total quantity of lipids in a given suspension. Binary mixtures of DOPC and sterol were prepared by dissolving DOPC and chosen sterol in a mixture of methanol at concentrations required.

The electrochemical technique for RCV was conducted as previously described in Chapter 2 except for section 4.3.6 (DOPG) where electrochemical technique is performed in static cell. In this condition, there is no continuous buffer flow.

## 4.3 RESULTS AND DISCUSSION

### 4.3.1 EFFECT OF VARYING pH ON DOPC

Although within the human body, temperature and pH are maintained constant by homeostasis, the lipid interactions can also be affected by environmental chemical conditions, such as temperature and pH. Lipids are able to form into multiple associations known as lipid polymorphism. For example, lipids such as PE and PA can arrange into bilayer or non-bilayer phases depending on the solvent conditions [14]. There are structural considerations to lipid polymorphism. Lipids with a small polar head have a molecular shape which resembles a truncated cone and favour organization into inverted micelles (HII phases) such as PS [15]. The hydrophobic tail points towards the outside of tubules and polar head groups are in the centre forming an aqueous channel. Lipids that have similar cross-sectional areas for the polar head and hydrophobic region resemble cylinders. They form lamellar or bilayer phases (Figure 4.4). It has been shown that bacteria are able to maintain their membrane lipid phases between lamellar and HII. For example, *E. coli* maintains a balance between HII formation and bilayer formation lipids by adjusting the composition of the polar head group or the acyl chains [16].

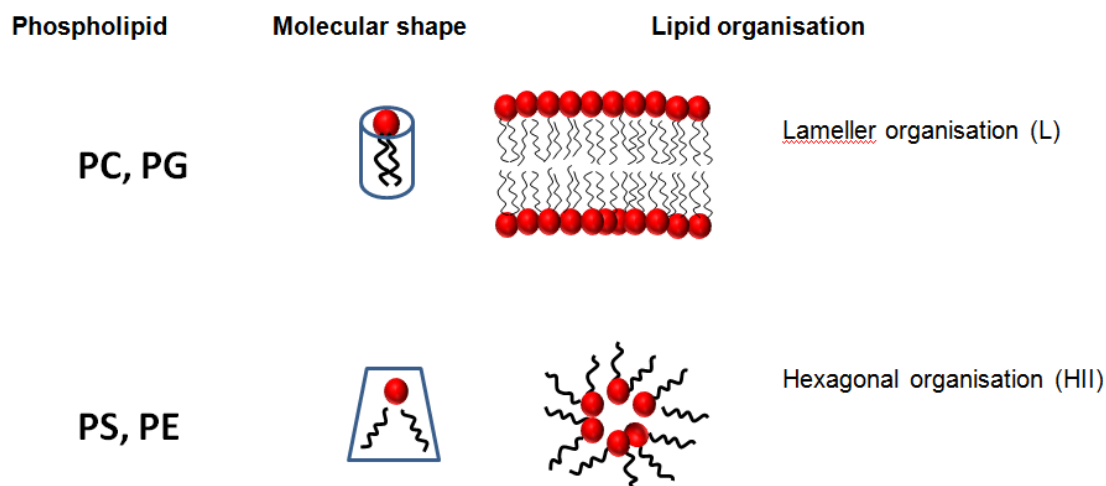


**Figure 4.4: Illustration of lipid organisation of various phospholipids PC,PG,PS and PE.**

The effect of pH on these phase changes has also been established. Lowering the pH induces lamellar to HII formation in charged phospholipid systems for example; diphosphatidylglycerol (DPG) can be induced from lamellar phase to HII upon lowering pH to 2.8 or below [16]. Studies have concluded the effect due to pH changes are attributed to alterations in interfacial region of the membrane in particular membrane surface changes [14] as opposed to inter-membrane regions.

In this study we examined how the distribution of charge brought about by pH changes contributes to DOPC monolayer properties. Phase transition changes brought about by pH will also be discussed for other lipids in the succeeding sections. The RCV results (Figure 4.5) show the effect of solution pH on DOPC capacitance current-voltage peaks.

A solution of pH 2 instigated an alteration in the nature of the capacitance current peaks compared to that observed at solution pH 7.4 (Figure 4.5 a)). The pH solution range from 4 - 12 produced no discernible effect on the capacitance current peaks compared to that observed at pH 7.4. To investigate the effect of higher solution pH

on the phospholipid, borate buffer was used to bring the solution pH to 13.5 (Figure 4.5 b)). Interaction with calcium chloride produced the same phase transitions as pH 2 conditions (Figure 4.5 c)).

The DOPC at neutral pH values is zwitterionic. The phosphate group is negatively charged and the choline group is positively charged and as a result the molecule does not carry a net charge. However the DOPC phosphate group has a pK of ~2 and thus develops a positive charge in solution of pH 2. The effect of protonation of the head groups will cause them to repel each other and this will affect the configuration of the capacitance current peaks. Nonetheless, the state of the phospholipid monolayer is still stable and intact at higher pHs (up to pH 12).

pH can potentially change interfacial electrical properties such as membrane surface charge density and  $\zeta$ -potential. The  $\zeta$ -potential (with unit of mV) relates to the membrane surface charge density and can be calculated from liposome mobility in an applied electric field [17]. The interaction of ions with the membrane can affect membrane mechanics and integrity, and there is experimental evidence that changes in ionic strength affect lipid packing [18].

As solution pH varies, different concentrations of protons/ hydroxide act to neutralise either head groups on PC lipids, thus potentially altering the surface charge. Figure 4.5 e) shows that solution pH has significant effects on the surface charge of PC.

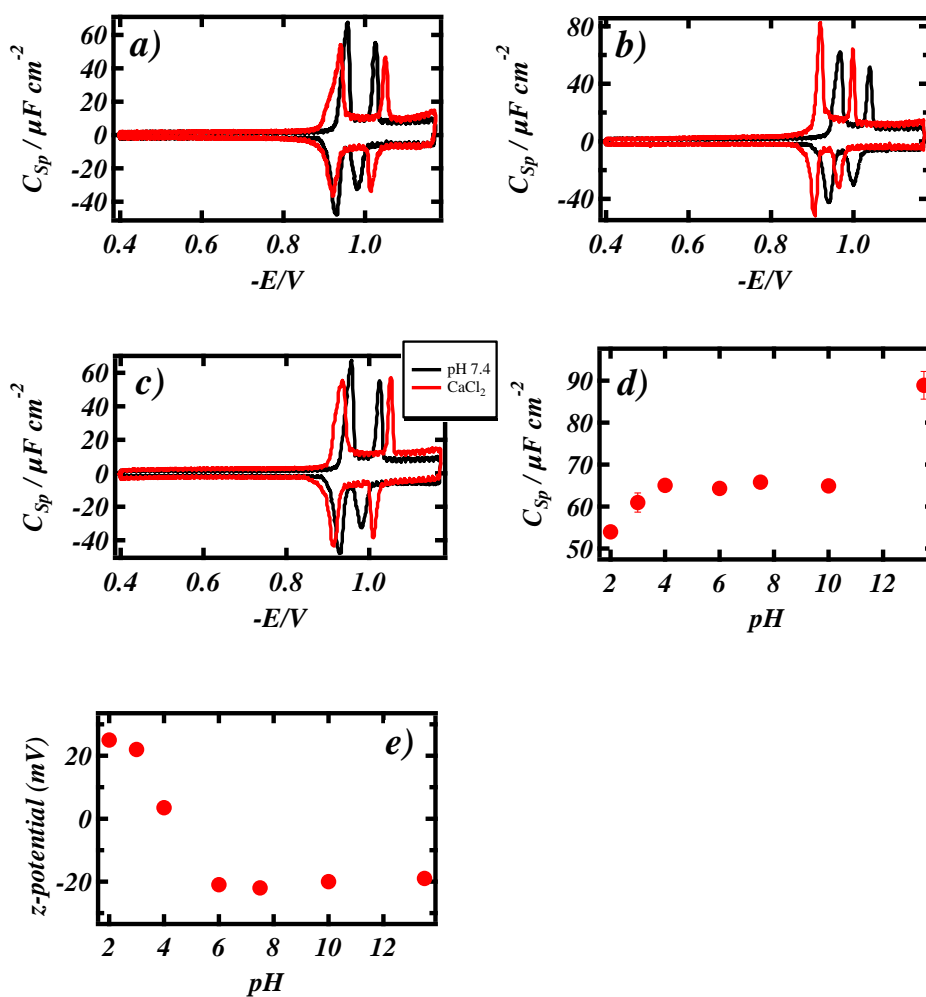


Figure 4.5: RCVs recorded at 40 Vs<sup>-1</sup> of a DOPC coated Pt/Hg electrode in PBS at pH 7.4 (black line) in the presence of a) pH 2 (red line), b) pH 13.5 (red line) and c) calcium chloride 0.1  $\mu mol dm^{-3}$  (red line). d) Graph representing the first capacitance current peak of DOPC coated Pt/Hg electrode vs. solution pH. e) Graph representing headgroup surface charge vs. solution pH [19].



### 4.3.2 INCORPORATING STEROLS WITH DOPC

DOPC has two alkyl chains with a double bond in each chain which lowers its melting point enabling it to be fluid at room temperature. On the other hand, sterols are rigid molecules. It is known that when sterol is incorporated into a lipid layer, it imparts a rigidity to the layer [20]. The sterol molecules intercalate between free spaces in DOPC monolayer, decreasing its flexibility and fluidity. Packing models have been proposed for the molecular interaction between cholesterol and phospholipids. They include van der Waals attraction and hydrogen bonding, which allows the hydrocarbon chains to come in close contact with lipid layer [21].

To elucidate the mechanistic role of sterol molecules on phospholipid membrane properties, the effect of cholesterol on the lipid phase transitions at different concentrations are investigated. The experiments have been conducted with DOPC monolayers to see whether cholesterol/DOPC (CHOL:DOPC) domains can be detected on the MFE in flow cell using RCV. RCV scans for cholesterol with a range of mole fraction ( $x_c$ ) in DOPC bilayers have been conducted. Mole fractions ( $x_c$ ) of 0.16 for ergosterol and stigmasterol were also tested.

At potentials around  $-0.4V$  (position of zero charge (PZC) of mercury), DOPC is oriented with its hydrophobic tails toward the Hg surface and forms a dielectric insulating layer. At more negative potentials, the monolayer begins to be permeable to ions until the first phase transition peaks appear. Any changes to the DOPC fluidity are represented by the appearance of phase transition peaks. DOPC peaks remain in fluid state as evidenced by the sharp phase transition peaks. CHOL:DOPC peaks are broad; not sharp, and the lower fluidity of the layers is represented by the capacitance current peaks being spread over a broader range. The change in shape of the peaks is linearly related to the concentration of cholesterol associated with the monolayer. At sufficiently high concentrations, the presence of cholesterol in the

layers can diminish capacitance current peaks completely. This can be seen in Figure 4.6.

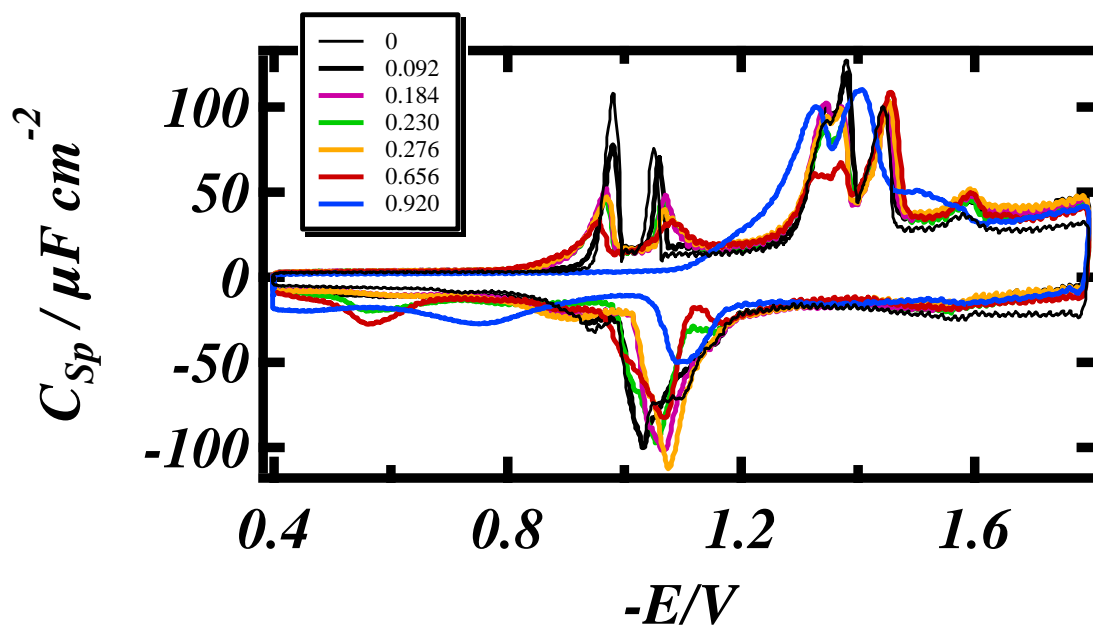
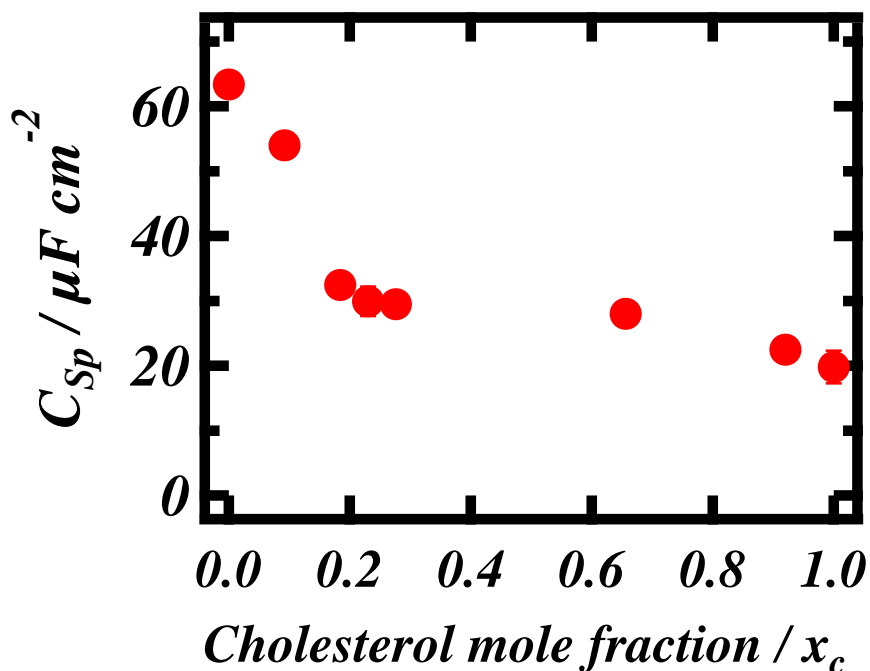


Figure 4.6: RCVs recorded at  $40 \text{ Vs}^{-1}$  of a DOPC coated Pt/Hg electrode in PBS at pH 7.4 (black line) with a switching potential of  $-1.8\text{V}$  in the presence of 0, 0.092, 0.184, 0.230, 0.276, 0.656 and 0.920  $x_C$  of CHOL:DOPC in PBS at pH 7.4.

The  $x_C$  values shown in legend inset and colour coded.



**Figure 4.7:** Plot of the mean of the first and second capacitance current peak heights ( $\mu F cm^{-2}$ ) vs. mole fraction ( $x_c$ ) of CHOL:DOPC coated Pt/Hg electrode in PBS at pH 7.4.

The capacitance minimum of DOPC in the potential range between  $-0.4V$  and  $-0.8V$  has increased indicating that cholesterol has entered the DOPC monolayer structure (Figure 4.6). The inclusion of cholesterol with DOPC layers at various mole fractions elicits a suppression of the capacitance current peaks. At the highest concentration, the capacitance current peaks are no longer present, and the capacitance current value is constant between  $-0.4V$  to  $-1.1V$ . Figure 4.7 shows the effect of increasing mole fraction of CHOL:DOPC on capacitance current peak height of DOPC. The decrease in peak height indicates a change in the permeability of the DOPC layer to ions and water.

It is also interesting to note that ergosterol and stigmasterol produce a greater effect on capacitance current peaks at lower concentrations compared to CHOL:DOPC (Figure 4.8) and the largest effect to current peaks is instigated by stigmasterol. The

decrease in capacitance current peaks is indicative of a change in the permeability of the DOPC layer to ions and water. One reason for these differences between ergosterol and stigmasterol is that ergosterol is a bulky molecule which is unable to interact effectively with phospholipid molecules. The double bonds present in one of the rings and the methylated side chain is thought to be responsible for this limited interaction [22].

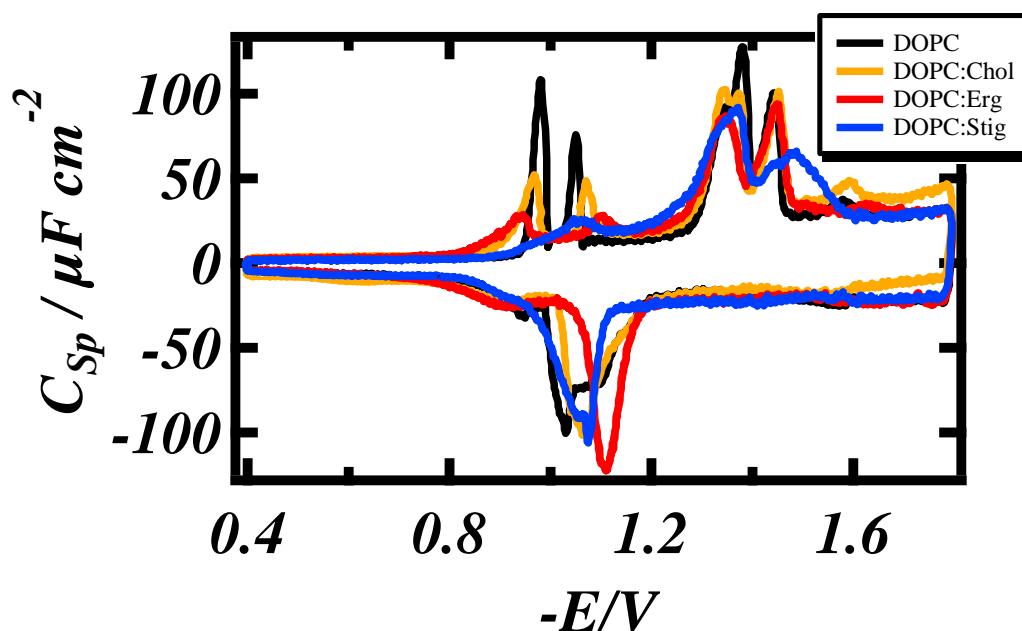


Figure 4.8: RCVs recorded at  $40 \text{ Vs}^{-1}$  with potential excursions from  $-0.4\text{V}$  to  $-1.8\text{V}$  of a DOPC coated Pt/Hg electrode in PBS at pH 7.4 (black line), a 0.2 mole fraction of DOPC/cholesterol coated Pt/Hg electrode in PBS at pH 7.4 (orange line), a 0.16 mole fraction of DOPC/ergosterol coated Pt/Hg electrode in PBS at pH 7.4 (red line) and a 0.16 mole fraction of DOPC:stigmasterol coated Pt/Hg electrode in PBS at pH 7.4 (blue line).

The RCV recorded for POPC coated Pt/Hg electrode required potential excursions between -0.4V to -1.5V. This is because POPC layer on Pt/Hg electrode is less stable at potentials lower than -1.5V. POPC has one double bond compared to DOPC that has two. As a result it is less fluid and has a higher thermotropic phase temperature (-2°C) compared to DOPC (-17°C). POPC is more rigid than DOPC and the effect can be seen with the diminished capacitance current peaks (Figure 4.9).

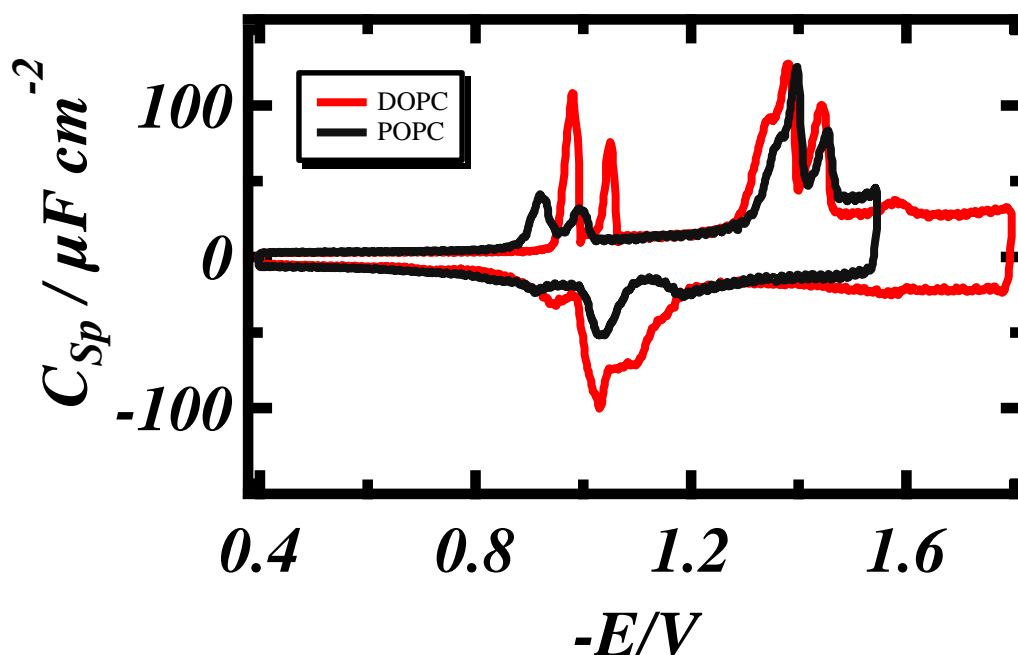
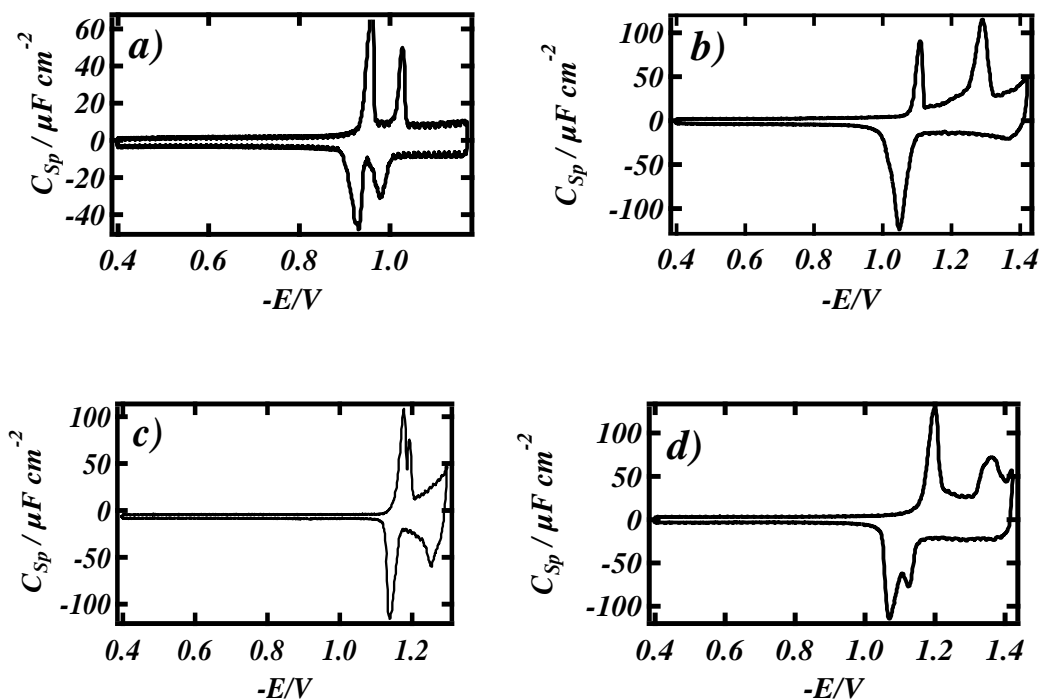


Figure 4.9: RCV recorded at  $40 \text{ Vs}^{-1}$  of a  $0.2 \text{ mg cm}^{-3}$  DOPC coated Pt/Hg electrode with potential excursions from -0.4V to -1.8V (red line) and a  $0.2 \text{ mg cm}^{-3}$  POPC coated Pt/Hg electrode with potential excursions from -0.4V to -1.5V (black line). All experiments conducted in PBS at pH 7.4.

#### 4.3.3 CAPACITANCE PROFILES OF VARIOUS LIPIDS

Capacitance current peaks of four phospholipids, DOPC, DOPE, DOPG and DOPS is investigated here using RCV. The phospholipids each produced a unique fingerprint capacitance current profile consisting of a series of peaks differing in their

magnitudes, spread, the potential at which they occur and the potential at which they are they are stable.



**Figure 4.10: RCVs recorded at  $40 \text{ Vs}^{-1}$  in PBS at pH 7.4 of a) a DOPC coated Pt/Hg electrode; switching potential  $-1.2\text{V}$ , b) a DOPE coated Pt/Hg electrode with switching potential  $-1.4\text{V}$ , c) a DOPG coated Pt/Hg electrode with switching potential of  $-1.3\text{V}$  and d) a DOPS coated Pt/Hg electrode with switching potential of  $-1.4\text{V}$ . The switching potentials are chosen due to their individual stability profiles.**

DOPC and DOPE are stable up to  $-1.8\text{V}$  whereas DOPG and DOPS are stable up to  $-1.4\text{V}$ . The differences in stability of the various monolayers are related to the charge on the different head groups. DOPC and DOPE are zwitterionic in PBS (pH 7.4); they remain stable at more negative potentials. DOPS and DOPG have a negative headgroup, and are less stable at negative potentials.

The next section focuses on the effect of varying pH on the integrity and stability of these different lipids.

### 4.3.5 DOPE

DOPE is a zwitterionic amphiphile that forms reverse hexagonal phases (HII) at physiological pH and is widely believed to promote fusion with cell membranes [23]. Because DOPE is zwitterionic, it can participate in equilibrium reactions with both hydrogen ions and hydroxyl anions and thus become charged at extremes in pH. Unlike DOPC, it is challenging to adsorb DOPE on to mercury and often the control is difficult to reproduce. But once DOPE is established on Hg, it is stable. Also, similar to DOPC, it does have characteristic capacitance current peaks which are stable up to -1.8V. Capacitance current peaks of DOPE with varying pH is investigated here using RCV.

Figures 4.11 a) and b) demonstrate the changes in DOPE capacitance current peaks induced by varying pH. At pH below 4, an additional current peak appears around -1.3V (Figure 4.11 a) shows this effect at pH 2). There are no changes to capacitance current peaks from pH 4 – 8. Figure 4.11 b) shows the effect of pH 10, a peak appears around -1.2V.

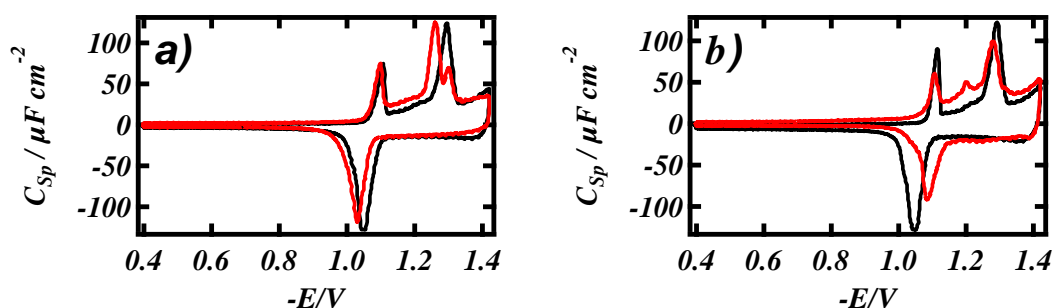
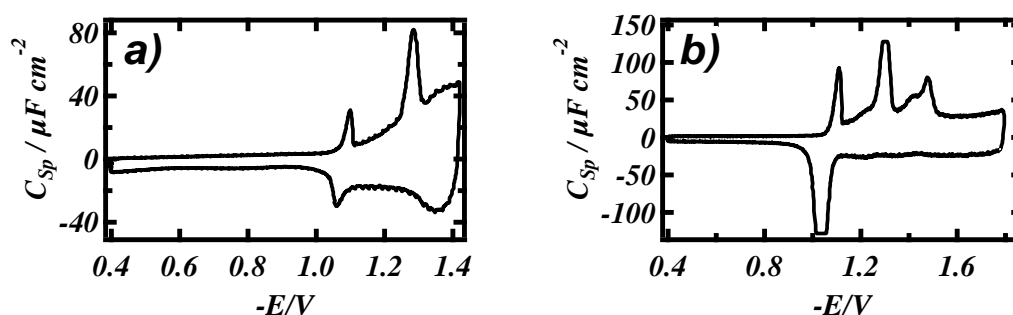


Figure 4.11: RCVs recorded at 40 Vs<sup>-1</sup> of a DOPE coated Pt/Hg electrode in PBS at pH 7.4 (black line) in the presence of a) pH 2 (red line) and b) pH 10 (red line).

At high pH, the amine in the head group becomes deprotonated, and the lipid attains a negative charge. The negative charge induces repulsion between head groups thus encouraging a change in arrangement of lipid structure. Conditions below pH 4 also cause changes to capacitance current peaks. It is known that DOPE arranges in an inverted hexagonal phase (HII) at near neutral or acidic pH [23] which is the energetically favourable arrangement. The change in peaks may be attributed to the change in arrangement of these lipids, thus affecting the capacitance profile.



**Figure 4.12: RCV recorded at  $40 Vs^{-1}$  of DOPE coated Pt/Hg electrode in PBS at pH 7.4 a) showing unstable capacitance current peaks at switching potential of -1.4V and b) at switching potential of -1.8V.**

DOPE as compared with DOPC is shown to be unstable on the Pt/Hg electrode (Figure 4.12 a)). Generally, DOPE produces capacitance current peaks that is not easily reproduced. Figure 4.12 a)) is not as Figure 4.10 b)). Similar to DOPC, DOPE is stable over a larger potential range (Figure 4.12 b)).

#### 4.3.6 DOPG

PG is mostly found in bacterial lipid such as *Synechocystis sp* and *Escherichia coli*, and in the cell membranes of higher plants. They have very particular membrane defence properties. Upon any exposure to stressors such as toxic organic solvents, it is thought that the surface charge density changes and therefore the lipid area



changes. It is thought that this change leads to reduced permeability of the organism to toxins. For instance, certain bacteria add lysine to their membrane incorporated with PG thus converting the net negative charge of PG to a net positive charge in Lysine-PG. By doing this, the bacteria is able to defend itself against cationic antimicrobial peptides (CAMPs) secreted by other microbes or produced by the immune system of a host organism [24].

Another property of PG is that the glycerol in the head group is able to mimic the solvation properties of water; it has hydrogen bonding capabilities and thus increasing its bonding properties.

Capacitance current peaks of DOPG with varying pH are investigated here using RCV using either static cell or continuous buffer flowing through the cell.

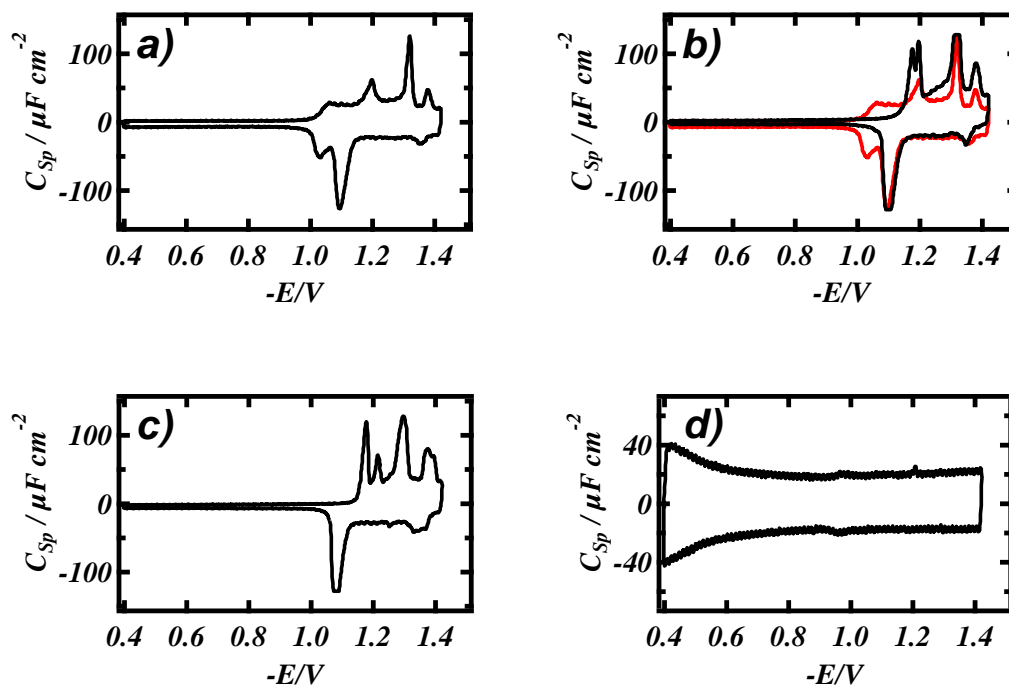


**Figure 4.13: RCVs recorded at  $40 \text{ Vs}^{-1}$  of a DOPG coated Pt/Hg electrode with switching potential of  $-1.4\text{V}$  in the following conditions: a) a continuous PBS flow at pH 7.4, b) a continuous PBS flow at pH 2 (black line) and after 10 seconds (red line), c) a static cell containing PBS at pH 2 and d) a static cell containing PBS at pH 2 at switching potential of  $-1.5\text{V}$ .**

Looking back to Figure 4.10 c), the stability of DOPG at pH 7.4 can only be monitored up to  $-1.3\text{V}$ . At pH 7.4, with applied potential of  $-1.3\text{V}$ , the capacitance current peaks remain stable.

Decreasing the potential applied to  $-1.4\text{V}$  causes the peaks to destabilise and desorb within a second as shown in Figure 4.13 a).

Upon reducing the pH to 2, the capacitance current peaks are stable for longer at  $-1.4\text{V}$ , but only remain stable for around 10 seconds (Figure 4.13 b)).

When static cell conditions are introduced, rather than a continuous buffer flow, and keeping the pH at 2, the capacitance current peaks remained stable at -1.4V (Figure 4.13 c)).

Lowering the potential applied to -1.5V caused the capacitance current peaks to rapidly diminish until settling on a trace similar to uncoated Hg which is indicative of lipid desorption. (Figure 4.13 d)).

### **4.3.7 DOPS**

Capacitance current peaks of DOPS with varying pH are investigated here using RCV. The PS head group is protonated. Decreasing the pH causes neutralisation of the PS head groups, thus reducing head-head repulsion. In theory, this eventually leads to HII phase curvature [25]. In neutral pH, the head group is charged, allowing head-head repulsion, thus a more lamellar monolayer structure exists.

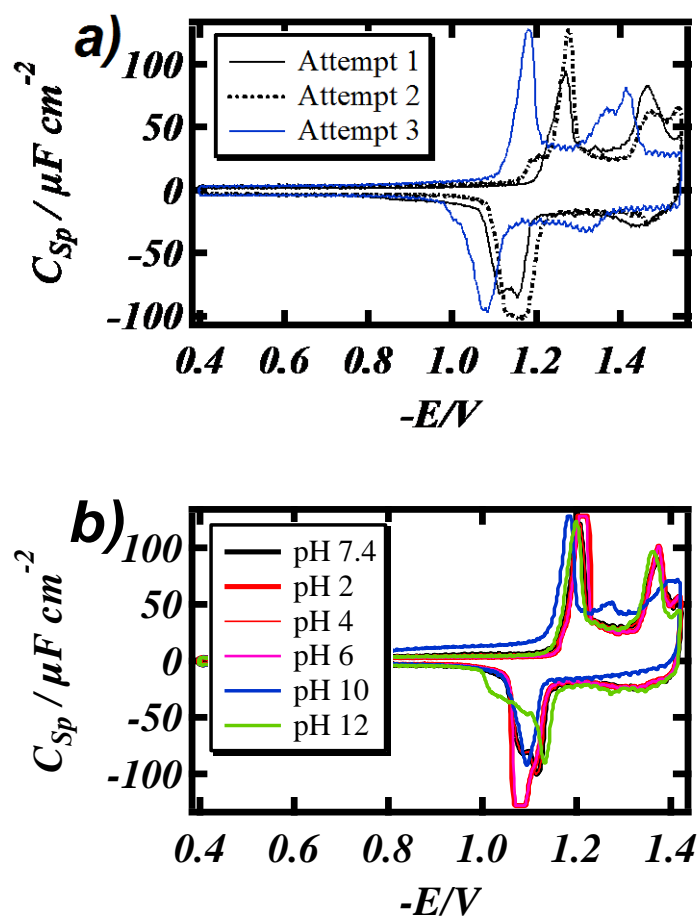
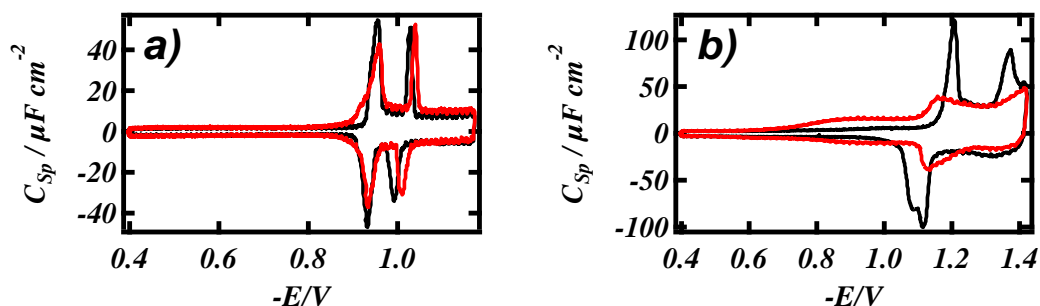


Figure 4.14: RCVs recorded at 40 Vs<sup>-1</sup> of a DOPS coated Pt/Hg electrode in PBS at pH 7.4 with switching potential of -1.4V (black line) representing a) attempts to produce similar reproducible capacitance current peaks and b) introducing varying pH which are colour coded and listed on the legend inset.

DOPS represented the most unstable lipid as compared with the other lipids. The layers on Pt/Hg were difficult to reproduce (Figure 4.14 a)) and often not stable.

A preliminary compound interaction was conducted with DOPS. Imipramine was chosen as it is well known to interact with biomembranes (Figures 4.15 a) and b)). Compared to DOPC, imipramine's effect on DOPS is much more significant.



**Figure 4.15:** RCVs recorded at  $40 \text{ Vs}^{-1}$  of a) DOPC coated Pt/Hg electrode (black line) in the presence of  $1 \mu\text{mol dm}^{-3}$  imipramine (red line) and b) DOPS coated Pt/Hg electrode (black line) in the presence of  $1 \mu\text{mol dm}^{-3}$  imipramine (red line).

#### 4.4 SUMMARY

In this Chapter, an array of experiments has been conducted with lipid layers and several conclusions can be made from these.

DOPC as compared with other fluid phospholipids is shown to be the most stable and reproducible sensing element layer on a Pt/Hg electrode.

All the lipids used in this Chapter are able to self-assemble and organise in their unique way due to a balance of attractive and repulsion forces. These differences could be observed on the RCV scans as capacitance current peaks.

The effects of pH on the integrity and stability of lipids, DOPE, DOPG and DOPS were investigated. The experiments were conducted using RCVs recorded at  $40 \text{ Vs}^{-1}$  of the lipid coated Pt/Hg electrode in PBS pH 7.4. By changing the pH of the PBS, the charge on the lipid head group changes. This induces a change in orientation of the lipid layer and this was reflected on the RCV scans. The change in the capacitance current peaks may be attributed to the change in lipid orientation occurring on the Pt/Hg.

The effects of cholesterol, stigmasterol and ergosterol on the physical properties of DOPC layer have also been investigated. The results show that the interaction between DOPC and sterols are complex and depend on the details of structure and functional groups present on the sterols. Changes to lipid permeability are reflected by the changes in capacitance current peaks. A more conclusive interpretation of lipid behaviour will need further experiments using different phospholipids with different types of acyl chains.

## REFERENCES

- [1] Voet D. Voet, JG. *Biochemistry ACS*: **1990** Washington, DC, USA.
- [2] Simon J. Attwood Y, Leonenko Z. *Int. J. Mol. Sci.* **2013** 14: pp3514-3539.
- [3] Sabitha V. *J Pharm Bioallied Sci.* **2011** 3(1): pp4–14
- [4] Nelson A. *Analytica Chimica Acta*, **1987** 194: pp139-149
- [5] Mohamadi S, Tate DJ Vakurov A, Nelson A, *Anal Chimica Acta* 2014 813: pp83–89.
- [6] Miller IR, Grahame DC *Journal of Colloid Science*, **1961** 6(1): p23.
- [7] Vakurov A. *ACS Nano*, **2014** 4: pp3242–3250
- [8] Nelson A. *Journal of Electroanalytical Chemistry*, **2007** 601: pp. 83–93.
- [9] Chen S, Abrufia HD *Langmuir* **1994**,10: pp3343-3349,
- [10] Bizzotto D, Nelson A *Langmuir* **1998** 14(21): pp6269-6273
- [11] Whitehouse C. O'Flanagan, R, Nelson, A. *Langmuir* **2004**, 20: pp136–144.
- [12] Leermakers, FAM, Nelson AJ. *Electroanal. Chem.* **1990**, 278: pp53–72.
- [13] Kycia AH, Wang J, Merrill R. *Langmuir*. **2011**, 27: pp10867–10877.
- [14] Zhou, Y, Raphael RM *Biophys J.* **2007** 92(7): pp2451–2462.
- [15] Seddon JM. Kaye RD, Marsh, D. *Biochim. Biophys. Acta.* **1983** 734: pp347–352.
- [16] Lindblom. *Biochemistry* **2002** 41: pp11512–11515.
- [17] Gennis RB. *Biomembrane Molecular Structure and Function.* **1989** C. R. Cantor, editor. Springer-Verlag, New York.
- [18] Petrache, HI, Zemb T, Belloni L. *Proc. Natl. Acad. Sci. USA.* **2006** 103:pp7982–7987.
- [19] Zhou Y, Raphael RM. *Biophysical Journal.* **2007**. 92: pp2451–2462.
- [20] Orädd G, Shahedi V. *Biochimica et Biophysica Acta (BBA) -Biomembranes* **2009** 1788(9): pp1762-1771
- [21] Presti FT, Pace RJ, Chan SI, *Biochemistry.* **1982** 10(21): p3831.
- [22] Urbina JA, Pekerar S. *Biochimica et Biophysica Acta* **1995** 1238: pp163
- [23] Seddon JM. *Biochim. Biophys. Acta* **1990**, 1031:pp1
- [24] Roy H, Dare K, Ibba M, *Mol Microbiol*, **2009**, 71(3): pp547-550.
- [25] de Kroon A, Timmermans JW, Killian JA. *Chem. Phys. Lipids.* **1990** 54: pp33–42.

# CHAPTER 5

## THE MODES OF ACTION OF LONG CHAIN

### ALKYL COMPOUNDS

#### 5.1 INTRODUCTION

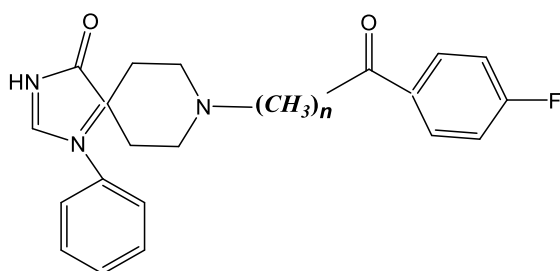
Compound interactions with the monolayer are affected by the nature of functional groups present, either enhancing or diminishing effects of the parent/backbone compound. The effects of compound chain length on its interaction with lipid membranes are well documented [1].

Increasing a compound's chain length can make a significant difference on its interaction with lipid membrane. Indeed the extent of chain length of a compound can either enhance or hinder the compound's interaction with the lipid sensor element. In this way, the effects of chain length deserve attention in this study. In this respect, three classes of compounds have been studied; (i) novel bispyridinium compounds, (ii) spiperone and its derivatives with increasing alkyl chain length and (iii) ionic liquids. These investigations included assessing the effects of increasing chain length for each compound-lipid interaction and in the case of spiperone, assessing compound-

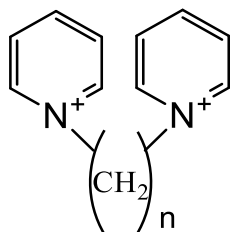


lipid interaction of similar analogues related to spiperone. The ionic liquid study was conducted in collaboration with Massimiliano Galluzzi from the Dipartimento di Fisica, Università degli Studi di Milano, Italy.

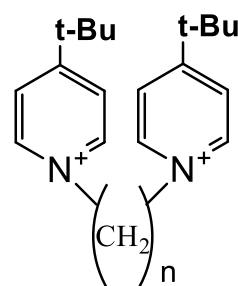
(a)



(b)



(c)



(d)

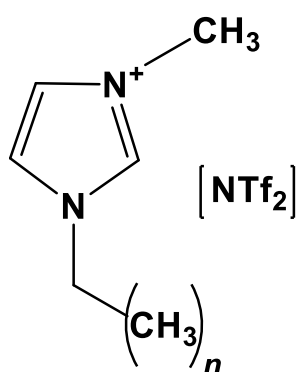


Figure 5.1: Molecular structures of a) spiperone, b) bis(pyridinium) and c) bis(4-tert-butylpyridinium), d) 1-butyl-3-methylimidazolium bis(trifluoromethylsulfonyl)imide

### 5.1.2 N-ALKYL SPIPERONE DERIVATIVES

Siperone is derived from a class of compounds known as butyrophenones which is used in the manufacture of antipsychotics. Siperone is a typical antipsychotic. References on the mechanism of action of siperone are few and require further investigation. However studies have proven that siperone has high affinity for dopamine and serotonin receptors [2] making siperone a lead for novel compound studies for illnesses such as dementia and schizophrenia. It is also discovered recently that siperone stimulates the release of  $\text{Ca}^{2+}$  by activating a phospholipase c pathway. It is thought that it does this by interaction with surface protein receptors leading to the possible alteration of the cellular membrane. It means that siperone or its analogues could be used to treat conditions such as cystic fibrosis. Cystic fibrosis (CF) is a genetic disorder caused by mutations to the genes that produce the cystic fibrosis transmembrane conductance regulator (CFTR).

This condition mostly affects the lungs but can influence the pancreas, liver and intestine. It is commonly associated with respiratory diseases which are also the main cause of morbidity. In healthy cells, CFTR acts as a chloride channel and regulates sodium, chloride and bicarbonate transport across the airway epithelial cells. When this channel does not function, it causes a reduction in  $\text{Cl}^-$  secretion and an increase in  $\text{Na}^+$  adsorption [3]. This leads to a net increase in water absorption. The volume of the liquid that sits on the airway surface is reduced and the mucus in the airways becomes more viscous. This in turn is perfect conditions for harbouring bacteria. It is common that sufferers of CF become infected with *Staphylococcus aureus*, *Hemophilus influenza* and *Pseudomonas aeruginosa*, all of these requiring intense antibiotic therapies.  $\text{Ca}^{2+}$ -activated  $\text{Cl}^-$  channels (CaCCs) are present in the airway surface epithelia [4]. Increases in cytosolic  $\text{Ca}^{2+}$  activate the epithelial CaCCs, which provides an alternative  $\text{Cl}^-$  secretory pathway in CF. And as mentioned earlier, siperone is able to activate CaCCs and thus be a treatment option for CF.

Other studies have found that related compounds could also stimulate the coupled phospholipase C-dependent pathway but assays need to be conducted to determine the more potent form of analogue [5]. Results obtained from these studies would help determine structural features that would improve compounds' (such as spiperone's) selectivity to their end target. The MFE is thus used to assay, screen and investigate spiperone analogues. To my knowledge, there has only been one other screening assay conducted with spiperone [6].

### 5.1.3 BIS PYRIDINIUM COMPOUNDS

Pyridinium is the cationic conjugate acid of pyridine. It is formed from the electrophilic reaction on nitrogen [7]. The lone electron pair on the nitrogen atom of pyridine is not delocalised and hence can be easily protonated. Compounds with pyridinium inclusion are known to hydrogen-bond to the phosphate moiety of lipid layers such as DMPC bilayers [8]. Pyridinium compounds are highly ubiquitous in nature with medicinal applications and are used as organic bases in chemical reactions and with industrial uses in analytical and physical chemistry. The pyridinium ion forms the basis of pharmaceuticals with trade names: Nexium, Plavix, Avandia, Concerta, Cingulair, Aricept. These compounds have different modes of action which demonstrates the universality of the pyridinium moiety. Its inclusion in medicinal compounds has been found to improve the activity of certain compounds including antimicrobials [9]. Furthermore, bis(pyridinium) salts in particular containing different alkyl chain lengths and various organic counterions are being used similar to ionic liquids as a non-volatile alternative to electrolyte solution. It is known as good candidate in the context of "green" chemistry.

#### 5.1.4 IONIC LIQUIDS

Ionic liquids (IL) are materials that are solely composed of anions and cations. They are a promising class of new material for prospective technological and chemical applications. They have fascinating properties that make them an interest for chemists especially in their emergence in “green” chemistry [10, 11]. Ionic liquids lack measurable vapour pressure which characterizes them as green solvents and therefore a wide range of chemical reactions can be performed in them. Due to their distinctive properties, ionic liquids are attracting increasing attention in many fields including organic chemistry, electrochemistry, catalysis and engineering. Ionic liquids are used as solvents to facilitate chemical transformations such as that of vegetable oil into new products. Recently ILs have been used in sensor development in particular as sensing materials for organic vapours [12].

The miscibility of ionic liquids with water or organic solvents depends on the side chain lengths and on the cation and the choice of anion. Previous work carried out on ionic liquids interacting with lipid monolayer has characterized phospholipid defects created by 'room temperature ionic liquids' [13, 14]. However, the number of studies conducted that explain the interaction of ionic liquids with lipids are too few.

## 5.2 MATERIALS AND METHODS

All the compounds were purchased from Sigma Aldrich, each with purity grade greater than 98.0%, apart from the byspiridinium compounds which were supplied by the Ministry of Defence- Defence science and technology laboratory (MoD-Dstl). For hydrophobic ILs, a methanol(50%)-water(50%) solvent was employed to prepare IL sample solutions at  $0.1 \text{ mol dm}^{-3}$  concentration. For the spiperone compounds, an initial stock sample solution was prepared with methanol. For all the other test compounds, a stock solution was prepared in Milli-Q water ( $18.2 \text{ M}\Omega$ ). Working solutions of all test compounds were obtained by mixing the sample solution with standard electrolyte solution (PBS or  $0.1 \text{ mol dm}^{-3}$  KCl) to obtain the desired concentration. The electrochemical technique was conducted as previously described in Chapter 2 with the exception of the ionic liquid study where the potential excursion is altered from -0.4 to -1.2 V to -0.4V to -1.8V which provides an RCV profile of DOPC on Hg with 5 voltammetric peaks instead of 2. This is in order to see if ionic liquids will affect the adsorption process of DOPC which occurs at higher negative potentials. RCV of DOPC layers in the presence of methanol were conducted to clarify the controls. The effect of methanol on the RCV plot of the DOPC coated Pt/Hg is insignificant.

## 5.3 RESULTS AND DISCUSSION

### 5.3.1 SPIPERONE

Spiperone was investigated having different n-alkyl lengths of C<sub>0</sub>, C<sub>2</sub>, C<sub>3</sub>, C<sub>4</sub>, and C<sub>6</sub>. Results are shown in Figures 5.2 a) to f).

The RCV scans present the effects on capacitance current peaks. There is a strong decrease in height of both peaks with respect to the control; but more predominantly the first peak. There is also a positive shift of potentials and eventually with increasing chain lengths, a flattening of peaks. The increase in capacitance between -0.4V and -0.8V is an indication that there is penetration into the layer. Note Figure 5.2 e) in particular showing the increase in capacitance in this range. However, upon removal of the test compound from the assay solution to which the lipid monolayer sensor element is exposed, the capacitance current peaks recover to varying degrees showing the original lipid monolayer structure is restored. The recovery is shown in Figure 5.2 f). This indicates that the spiperone essentially adsorbs on the DOPC layer surface. Furthermore, it can be assumed that the recovery of the lipid layer structure is related to the amount of spiperone removed. However, the extent of recovery of the lipid sensor element depends on the chain length of the spiperone which interacts with the lipid. The spiperone with C<sub>6</sub> chain number is only partially removed from the lipid sensor element whereas the spiperone with C<sub>0</sub> is completely removed from the sensor element.

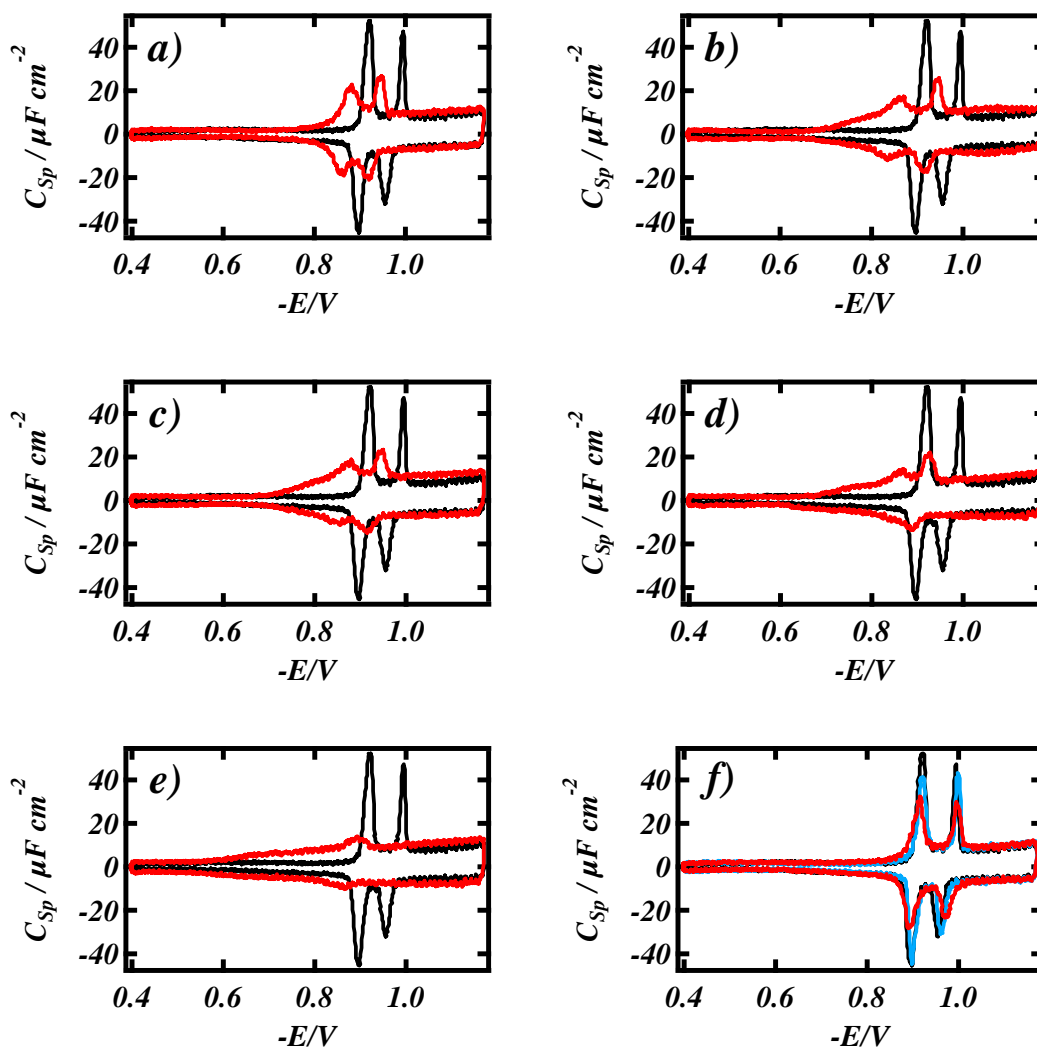


Figure 5.2: RCVs recorded at  $40 \text{ Vs}^{-1}$  of a DOPC coated Pt/Hg electrode in PBS at pH 7.4 (black line) in the presence of  $0.25 \text{ mmol dm}^{-3}$  spiperone with the following alkyl chain lengths (a)  $\text{C}_0$ , (b)  $\text{C}_2$ , (c)  $\text{C}_3$ , (d)  $\text{C}_4$  and (e)  $\text{C}_6$ . (f) Current capacitance peaks recovering after testing with  $0.25 \text{ mmol dm}^{-3}$   $\text{C}_0$  spiperone (blue line) and after testing with  $0.25 \text{ mmol dm}^{-3}$   $\text{C}_6$  spiperone (red line).

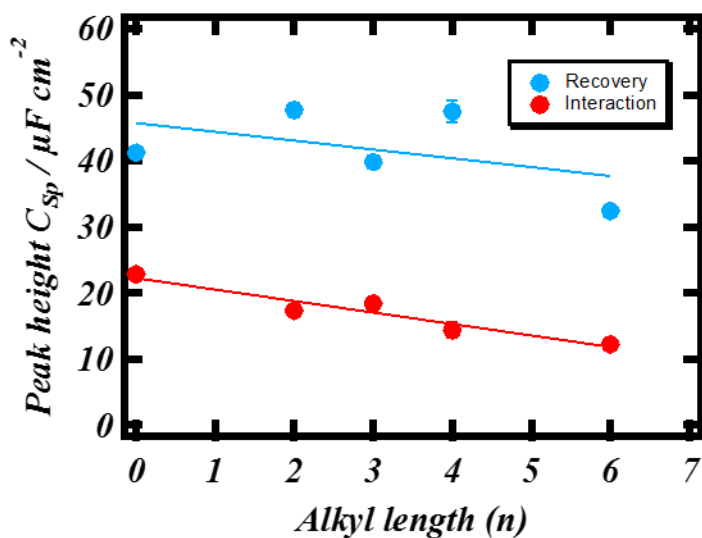
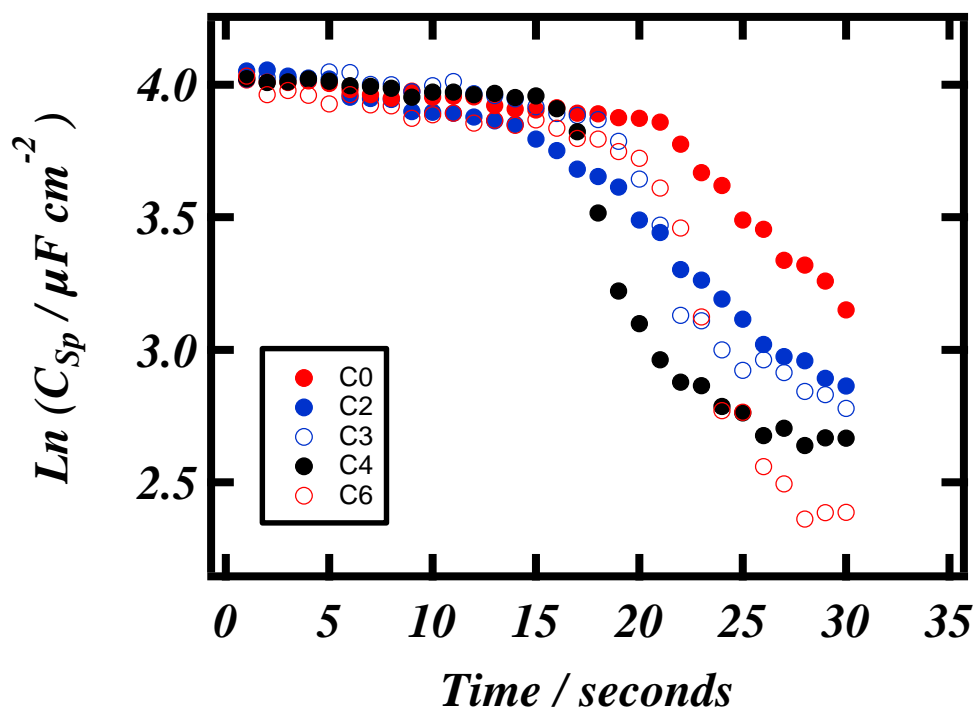


Figure 5.3: Graph showing the effect of increasing alkyl chain length of spiperone on the first capacitance current peak height (red line) and extent of recovery of the capacitance current peak height (blue line). The value of R is -0.9835 showing a strong negative correlation. The values are presented in Table 5.1.

Alkyl length (n)	$C_{SP}$ peak height
0	22.84
2	17.37
3	18.44
4	14.39
6	12.25

Table 5.1: Alkyl lengths (n) of spiperone and their capacitance current peak height ( $\mu F cm^{-2}$ ).





**Figure 5.4: Exposure time (30 seconds) on the effect of spiperones with varying alkyl chain on DOPC monolayer first capacitance current peaks.**

Figure 5.4 shows the effect of varying alkyl chain lengths at a given concentration ( $0.25 \text{ mmol dm}^{-3}$ ) on the time dependence of the spiperone-lipid monolayer interaction. Lipid interaction increases slowly over time until around 15 - 20 seconds, where there is a sudden pronounced increase in membrane interaction (represented by the reduction in peak height). This slowly plateaus off representing complete saturation. The extent of interaction is also increased with increasing chain length in order of  $C_0$ ,  $C_2$ ,  $C_3$ ,  $C_4$ ,  $C_6$ . Findings clearly show that increasing chain length enhances phospholipid monolayer interaction. Time dependent testing is used in aquatic toxicology tests (bioassays) to provide qualitative and quantitative data on the deleterious effects on organisms from a toxicant. These tests assess the potential for damage from a toxicants' exposure to an aquatic environment and provide a database that can be used to assess the risk associated for a specific toxicant. Commonly, tests

include acute toxicity tests that can last 24–96 hours whereas longer chronic tests of up to 7 days can also be conducted [15].

### 5.3.2 BISPYRIDINIUM COMPOUNDS

Interactions of bis(pyridinium) and bis(4-tert-butylpyridinium) compounds with DOPC coated microfabricated Pt/Hg electrodes in flow cell are demonstrated here. The results are recorded RCV. The measurements were made in real time with 1 minute per compound interaction. The testing process involved investigating the interaction of the compound as  $20 \mu\text{mol dm}^{-3}$  concentration with the DOPC layer and examining the effect of the compound on the RCV response.

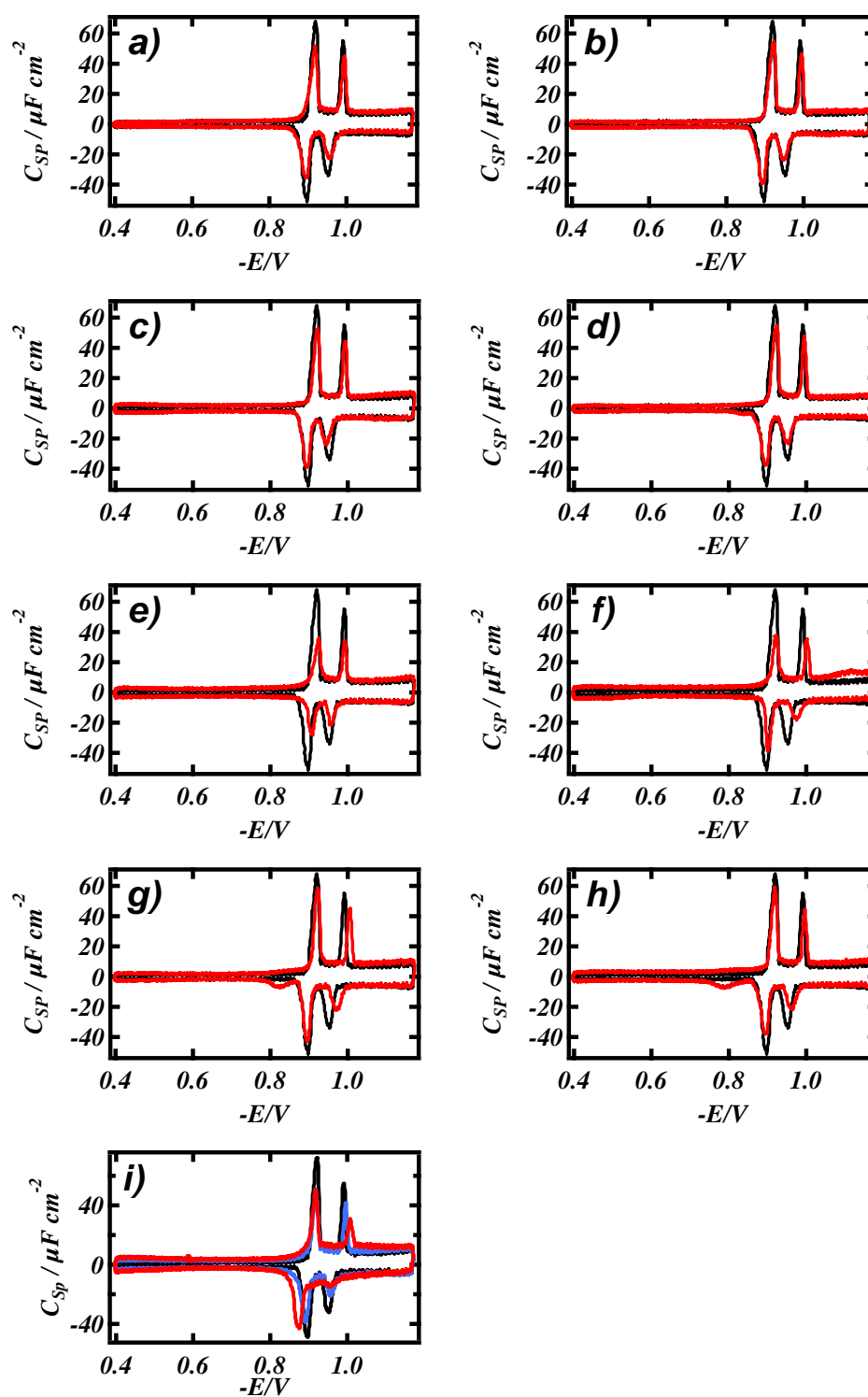


Figure 5.5: RCVs recorded at 40 Vs<sup>-1</sup> of a DOPC coated Pt/Hg electrode in PBS at pH 7.4 (black line) in the presence of 20  $\mu\text{mol dm}^{-3}$  bis(4-tert-butylpyridinium) compounds (red line) a) MB408, b) MB442, c) MB444, d) MB505, e) MB775, f) MB520, g) MB778, h) MB779 and i) 20  $\mu\text{mol dm}^{-3}$  (red line) and 50  $\mu\text{mol dm}^{-3}$  (blue line) MB777.

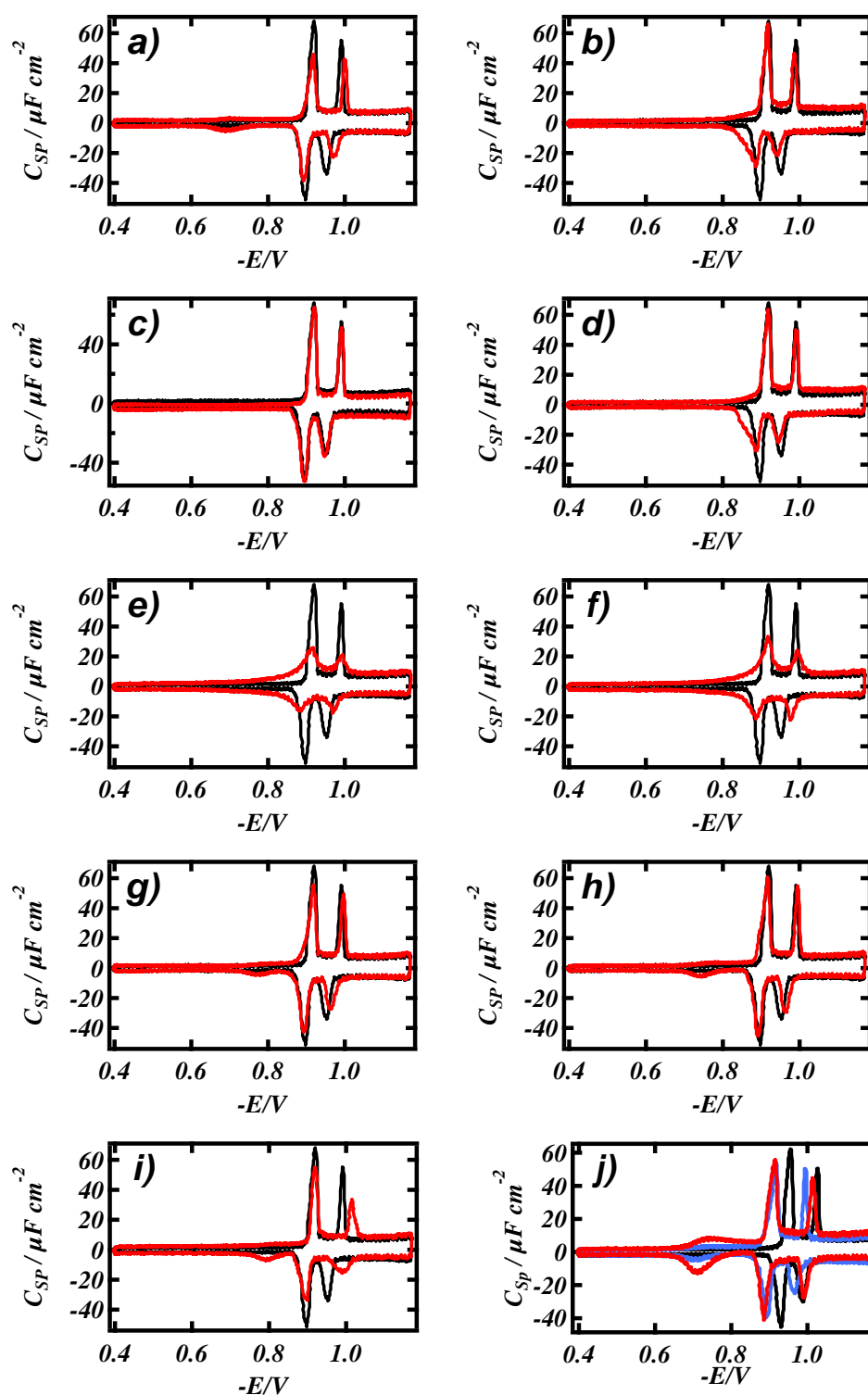
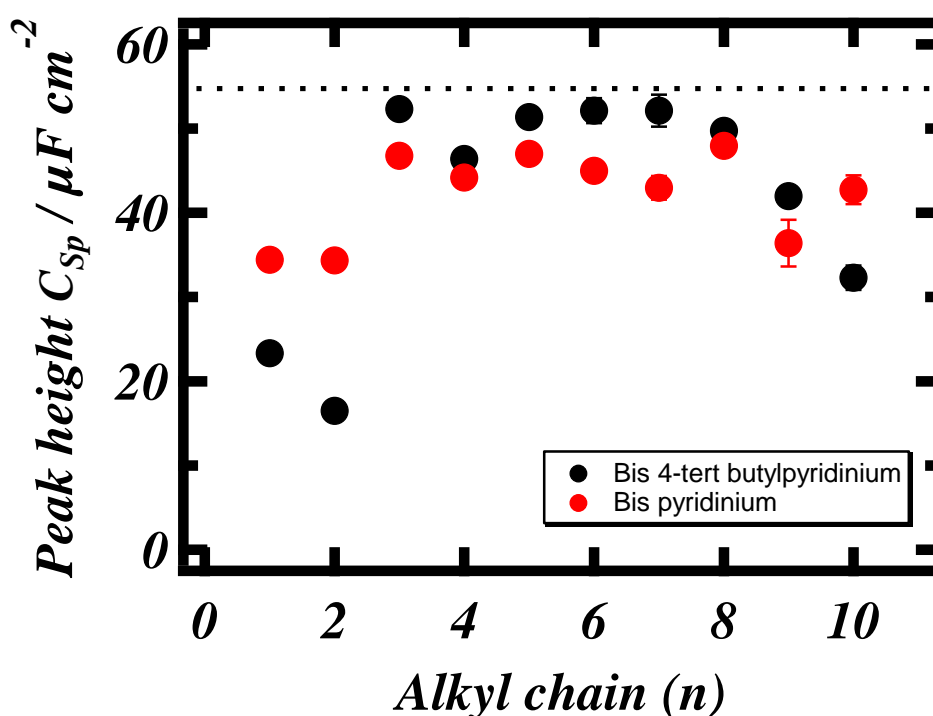


Figure 5.6: RCVs recorded at  $40 \text{ Vs}^{-1}$  of a DOPC coated Pt/Hg electrode in PBS at pH 7.4 (black line) in the presence of  $20 \mu\text{mol dm}^{-3}$  bis(4-tert-butylpyridinium) compounds (red line) a) MB582, b) MB781, c) MB782, d) MB327, e) MB583, f) MB780, g) MB783, h) MB784, i) MB786 and j)  $20 \mu\text{mol dm}^{-3}$  (red line) and  $50 \mu\text{mol dm}^{-3}$  (blue line) MB785.

Out of the bis(4-tert-butyl) substituted and unsubstituted bispyridinium compounds investigated where the connecting methyl chain extends from 1 to 10 carbons, the bispyridinium compounds with 1 and 2 carbon linking chain show the strongest interaction with the phospholipid monolayer. A longer carbon linking chain weakens the activity of the compound with the layer but the compound's activity increases gradually when the carbon linking chain extends to 9 and 10 carbons.



**Figure 5.7: Graph of capacitance current peak height of Bis 4-tert butyl and Bis pyridinium compounds on DOPC coated Hg electrode in PBS at pH 7.4 vs. n-alkyl chain length.**

Figure 5.7 represents peak height suppression in response to compound interaction. The extent and type of interaction depends on the chain length but only to a certain extent. For both group of compounds, monolayer affinity increases when up to 2 methyl groups in the chain are present. After this, membrane affinity decreases until a critical number of carbon linkers in chain are present which facilitates membrane interaction. It should also be noted that the presence of 4-tert-butyl increases

membrane affinity when 1 and 2 methyl groups are also present. Furthermore on observing the RCV scans, a “hump” on the baseline is apparent between -0.6V and -0.8V forms, the extent and presence of which is dependent on the functional groups present. When 4-tert-butyl is present, the hump occurs when 6 or more methyl groups are also present, whereas on absence of 4-tert-butyl, the hump first occurs when 8 or more methyl chain groups are present. These results serve to emphasize the effect of compound structure on the nature of and sensitivity to their interaction with the DOPC coated electrode. The lipophilicity of the compounds increases with increasing chain length however the extent of interaction does not depend on this property but is related to an optimum chain length.

The degree of interaction seems to decrease with increase in chain length, however there is an optimum chain length when the degree of interaction is maximum. These results match another result published [16] on the anti-malarial properties of the bispyridinium salts but with different conclusions. In this case the analogues of bispyridinium vary slightly in structure from the bispyridinium observed in this study however there is a differential effect on their anti-malarial properties when increasing alkyl chain length. The anti-malarial properties of these salts were compared against cytotoxicity induced, FM3A EC50 (nM). The highest toxicity occurred at the lowest chain length, however with increasing chain length, the cytotoxic properties decrease but increase again at higher chain lengths.

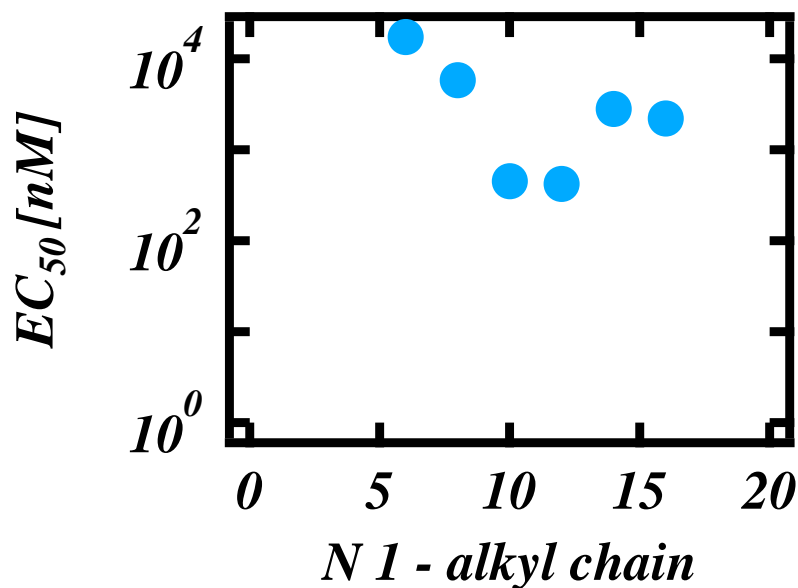


Figure 5.8: Effect of N1-alkyl chain lengths against anti-malarial toxicity [16].

Alkyl length ( <i>n</i> )	EC FM3A EC50 (nM)
6	17,300
8	5800
10	450
12	420
14	2800
16	2200

Table 5.2: Antimalarial toxicity for compounds' alkyl length listed [16].

### 5.3.3 IONIC LIQUIDS

Ionic liquid (IL) interaction studies were performed on Pt/Hg MFE system independently and under my supervision by a visiting phd student, Massimiliano Galluzzi from the Dipartimento di Fisica and CIMaNa, Univeristy of Milano on visit to the University of Leeds. Massimiliano Galluzzi's work with the screening tool produced

the same constant, reproducible results for this independent study. His study established the reliability of the technology.

Here we report the study carried out of the interaction of different ILs with varying alkyl chain lengths of the cation form. Analysis of the structural changes induced by different ILs on lipid monolayers is conducted in the presence of electric fields. The ILs have shown to induce structural changes on interaction with phospholipid layers.

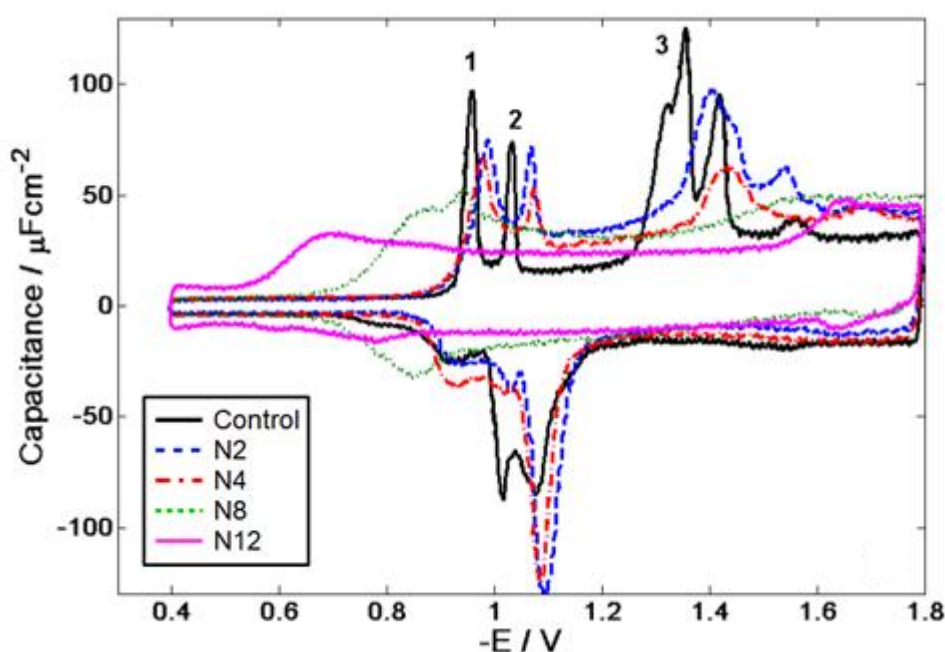


**Figure 5.9:** RCVs recorded at  $40 \text{ Vs}^{-1}$  of a DOPC coated Pt/Hg electrode in PBS at pH 7.4 (black line) with potential excursions from  $-0.4\text{V}$  to  $-1.8\text{V}$  in the presence of  $0.1 \mu\text{mol dm}^{-3}$   $[\text{C}_n\text{MIM}][\text{NTf}_2]$  with n2 (blue dashed line), n4 (red dash-dotted line), n8 (green dotted line), and n12 (pink line). The numbers 1 – 3 represent the DOPC transition phases (Chapter 4).

The effect of the chain length  $[\text{C}_n\text{MIM}][\text{NTf}_2]$  with  $n=2,4,8,12$  is used, highlighting the effect of extending the chain length. The numbers 1 – 3 represent the phases that lipid undergo upon inducing potential. Peak 1 represents the movement of ions, peak 2 represents the potential induced nucleation and growth process, following on from



peak 3 is the process undergoing desorption/bilayer formation [13] (Chapter 4). The interaction with DOPC is stronger if the chain is increased to 8 and 12 carbon atoms, as demonstrated in Figure 5.9 by the increase in the monolayer capacitance and an enhanced suppression/alteration of the capacitance peak current values. Compounds with long hydrocarbon chain structure are more lipophilic. It can be seen that the capacitance increases with an increase in chain length. This suggests that there is a breach in monolayer integrity. The increase in chain length of hydrocarbon chains allows for closer proximity of ILs through hydrophobic attractive forces. There are recent studies conducted on the toxicity character of ILs in aqueous environment. One such is the standard ecotoxicological bioassay (ISO 11348), which correlates the reduction of luminescence in cultures of *Vibrio fischeri* with toxicity represented as EC50 values. Detection limits for the ionic liquids were conducted. From our data, a linear correlation was found of logarithmic values of LoD with toxicity values log EC50 for *Vibrio fischeri*; Figure 5.10 a) and octanol/water partition coefficient log K<sub>ow</sub>; Figure 5.10 b). Table 5.3 lists the values.

Ionic liquid	Log K <sub>ow</sub> <sup>(a)</sup>	LoD (log μmol dm <sup>-3</sup> )	EC50 (log μmol dm <sup>-3</sup> ) <sup>(b)</sup>
[BMIM][Cl]	-2,4	4,69	3,47
[BMIM][BF <sub>4</sub> ]	-2,5	3,88	3,54
[EMIM][NTf <sub>2</sub> ]	-1,01	4,43	3,3
[BMIM][NTf <sub>2</sub> ]	-0,77	2,92	2,46
[OMIM][NTf <sub>2</sub> ]	0,92	0,78	0
[C12MIM][NTf <sub>2</sub> ]	/	-1,73	-1,2

**Table 5.3: Parameters for the ionic liquids used in this study. (a) Ecotoxicol. Environ. Saf. 2004, 58: pp396–40. (b) Green Chem. 2011, 13: pp1507–1516.**

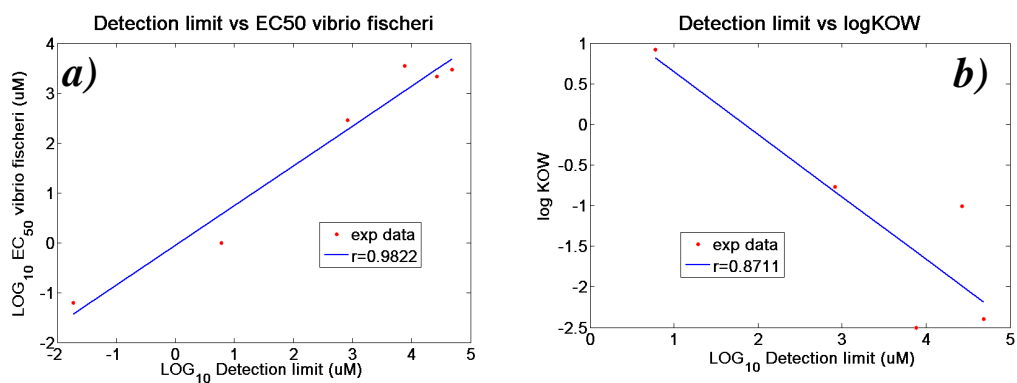


**Figure 5.10: Correlations of a) toxicity values of EC<sub>50</sub> for *Vibrio fischeri* and b) log K<sub>ow</sub> all vs. LoD at DOPC coated Hg electrode in PBS at pH 7.4.**

## 5.4 SUMMARY

It has been shown that compounds exhibit chain length dependent lipid layer perturbation effects however these perturbation trends vary. The degree of interaction is dependent on the nature of the functional group and the length of the alkyl chain. These results indicate that there are optimum chain lengths for compounds that correspond to their interaction efficiency but also evidence of size dependent membrane interaction ability and their selectivity functional groups

Some compounds exhibit increased activity with increasing chain length whereas others show that increasing chain length instigates a hindrance to interaction. For example, increasing chain length and thus hydrophobicity of spiperone encourages stronger interaction. Hydrophobicity is a consequence of the increased alkyl chain and not necessarily the cause for the increased interaction. The indirect relationship between hydrophobicity and interaction are referred to again in Chapter 6. The results from the bispyridinium compounds do not follow a similar pattern to spiperone which indicates that there are other contributions to lipid interaction besides hydrophobicity. Pyridine has a  $pK_a = 5.19$  and therefore is charged at neutral pH. Previous studies have shown that the pyridine functional group in bispyridinium compounds promote interaction with lipid layers by means of hydrogen bonding. [17] Pyridinium is also a small cationic molecule which can easily access the headgroup region of lipid monolayer. Increasing the alkyl chain length increases the molecule size conceivably reducing accessibility to the lipid headgroup region. Spiperone is uncharged. Their interaction will therefore depend on their size and functional groups present. In this case, the interaction with the lipid and the degree to which the species perturbs the layer increases with increasing alkyl chain length [18].

**REFERENCE**

- [1] Roche Y, Peretti P, Bernard S *Biochimica et Biophysica Acta* **2006** 1758(4): pp468-478.
- [2] Mach RH. *J. Med. Chem.* **1992** (35):pp423-430.
- [3] Boucher RC, Tarran R, Donaldson S. *Semin Respir Crit Care Med* **2007** 28(3):pp295-302.
- [4] Anderson MP, Welsh MJ. *Proc Natl Acad Sci* **1991** 88(14): pp6003–6007.
- [5] Joo NS, Wine JJ, Cuthbert AW. *Am J Physiol Lung Cell Mol Physiol* **2009** 296(5):pp811-824.
- [6] Liang L. *Am J Physiol Cell Physiol* **2008** 296 (1):pp131–41
- [7] Eicher T, Hauptmann S. *The Chemistry of Heterocycles* **1995**, p272, New York.
- [8] Hendersen. *Biophysical Journal* **1994** 67: pp238-249.
- [9] Carlsson S, Kontturi AK, Kontturi, K. *Eur. J. Pharm. Sci.* **2006**, 29:pp451–459.
- [10] Earle MJ, Seddon KR. *Pure and Applied Chemistry.* **2000** 7:pp1391–1398
- [11] Yang Z, Wubin P *Enzyme and Microbial Technology* **2005**. 37(1):pp19–28
- [12] Daguinet, Dyson C P. *J Organometallics* **2004** 23:pp6080.
- [13] Galluzzi M, Zhang S, Mohamadi, S, Vakurov A, Nelson A. *Langmuir* **2013** 29: pp6573.
- [14] Yurn C, Warmack RJ, Barnes CE, Dai S, *Anal. Chem.* **2002** 74:pp2172.
- [15] Rand, GM, Petrocelli SR. *Fundamentals of aquatic toxicology: Methods and applications.* **1985** Washington: Hemisphere Publishing.
- [16] Fujimoto K, Morisaki D. *Bioorganic & Medicinal Chemistry Letters* **2006** (16): pp2758–2760.
- [17] Nakano Y et al. *Colloid and Polymer Science* **1987**, 265: pp139-147.
- [18] Hansch C, Verma RP, Kurup A et al. *Bioorganic and Medicinal Chemistry Letters* **2005** 15: pp2149-2157.

# CHAPTER 6

## INTERACTION STUDIES I

### 6.1 INTRODUCTION

Through observing the capacitance current peaks in the voltammograms, alterations in the peak configuration can be detected when chemical compounds interact with the layers. A compound's biomembrane activity is manifested by characteristic changes in capacitance current – voltage plots which represent modifications to the phospholipid layer conformation [1]. The present study reports results of a performance evaluation of this sensing system which screens compounds which are known to be biomembrane active. The classes of compounds investigated are environmental toxins and/or or have biological and clinical activities. The responses are characterised for each class of compound.

The detection limits are estimated and quoted as the minimum concentration of compound in water to elicit a response and these detection limits are related to compound molecular structure and the known biological effect of each compound. The work includes the following compound classes: steroids, polycyclic aromatic hydrocarbons (PAH), tricyclic depressants (TCA) and tricyclic phenothiazines. Previous work looking at similar groups of compounds was carried out some time ago

[2-4]. Those studies used the system of phospholipid layers supported on a Hg drop electrode and selective interactions between classes of compounds and the phospholipid layers were reported. However the fragility of the electrode and the length of time required to conduct the assays precluded the use of the system as a working sensor. The present *on-line* high throughput system enables a large number of compounds to be screened. This developed analytical technology offers a significant noteworthy improvement, on the original concept and later developments [1, 5]. Employing a suitable configuration of flow systems and electrodes, the device is shown to have the capability to screen in high throughput mode the biomembrane activity of pharmaceuticals and pollutants in water. The paper reports on the relation between the compounds' limit of detection (LoD) as screened in water, their physical and structural properties and their biological activity. Figure 6.1 shows the structures of representative compounds screened in this work.

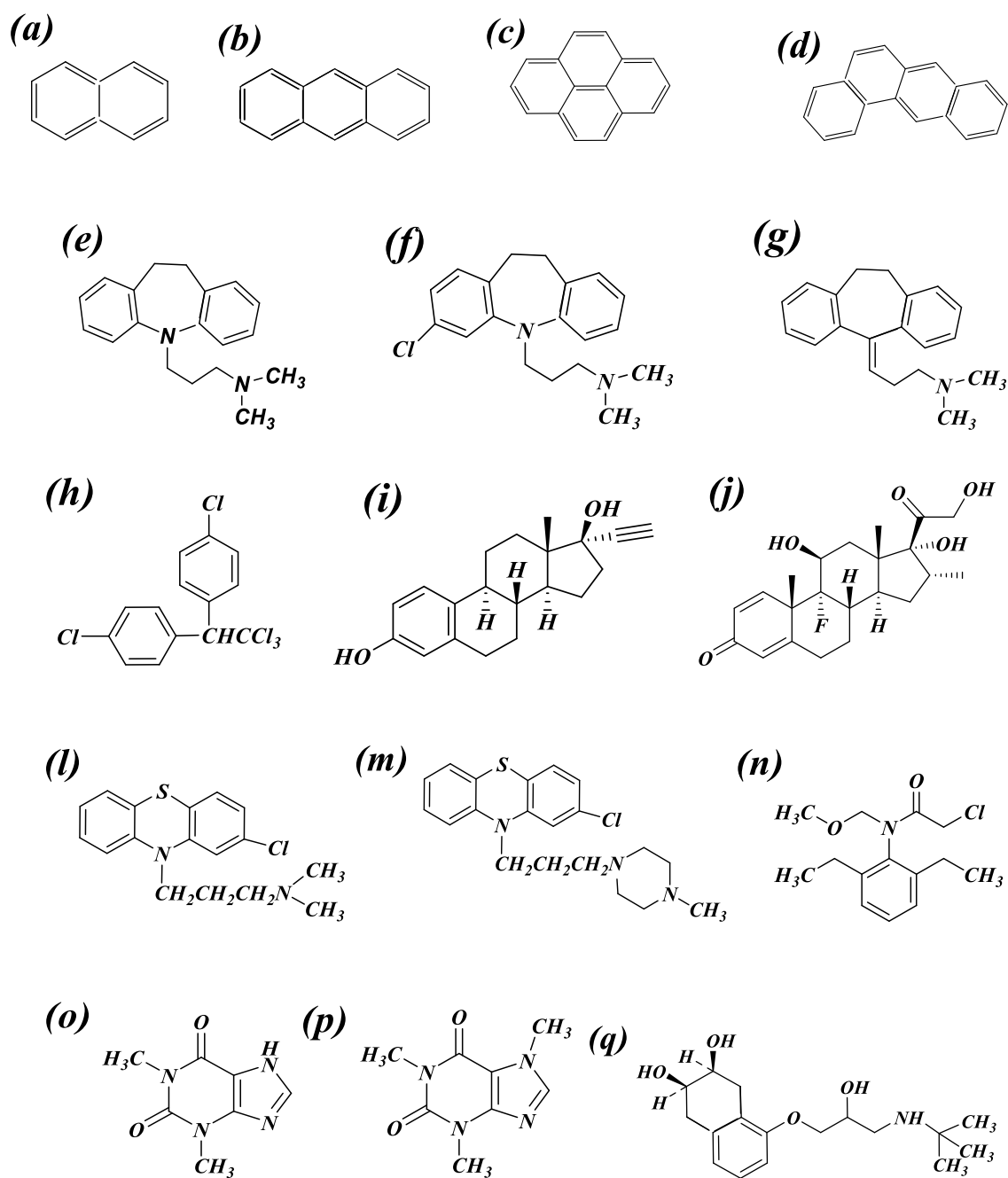


**Figure 6.1: Molecular structures of (a) naphthalene, (b) anthracene, (c) pyrene, (d) benzanthracene, (e) imipramine, (f) clomipramine, (g) amitriptyline, (h) 1,1,1-trichloro-2,2-di(4-chlorophenyl)ethane (DDT), (i) ethinyl estradiol, (j) dexamethasone, (k) phenothiazine, (l) chlorpromazine, (m) prochlorperazine, (n) alachlor, (o) theophylline, (p) caffeine and (q) nadolol.**

## 6.2 MATERIALS AND METHODS

The test compounds of 99% or greater purity were purchased from commercial suppliers, and were used as received. The phospholipid employed for coating electrodes was 1, 2-dioleoyl-sn-glycero-3-phosphocholine (DOPC) (Avanti Polar Lipids Alabaster, AL) and was >99% pure. All other reagents were of analytical grade and purchased from Sigma-Aldrich. Stock solutions were made up as follows. The polycyclic aromatic hydrocarbons (naphthalene, anthracene, pyrene and benzanthracene), the steroids (dexamethasone and ethinyl estradiol), 1,1,1-trichloro-2,2-di(4-chlorophenyl)ethane (DDT), phenothiazine, prochlorperazine and chlorpromazine were dissolved in acetone and the tricyclic anti-depressants (TCAs): imipramine, clomipramine and amitriptyline, were dissolved in Milli-Q water (18.2M $\Omega$ ). Concentrations of test compounds were prepared by adding small aliquots of the working solutions to PBS to provide concentrations for testing. The DOPC dispersion for electrode coating was prepared by gently shaking DOPC with PBS to give 0.2 mg cm<sup>-3</sup> dispersion.

For the assay, the fabricated Pt/Hg electrode was contained in a flow cell. A constant flow of PBS was passed over the electrode with a flow rate of 5-10 cm<sup>3</sup> min<sup>-1</sup> maintained by a peristaltic pump. Capacitance current vs potential profiles were monitored using RCV at scan rate 40Vs<sup>-1</sup>. Interactions of compounds with the DOPC monolayer were monitored by RCV while cycling the electrode potential from -0.4V to -1.2V for 2 minutes during compound exposure. The electrochemical methods are explained in Chapter 2.



### 6.3 RESULTS AND DISCUSSION

Figure 6.2 displays the results of the changes to the RCV plots from the interaction of DOPC coated Pt/Hg with representative compounds. The compounds interact with the DOPC coated electrode to varying degrees as shown by their effect on the capacitance current peaks in the RCV plot. These capacitance current peaks are representative of the reorientation/adsorption/desorption processes of the DOPC layers in response to potential change. [6-8] It is observed that each class of compound interaction effects a "fingerprint" visual profile on the RCV plot which manifests itself as an alteration in the shape, height and position of the capacitance current peaks. It can be seen that (i) pyrene elicits a negative potential shift and suppression of the capacitance current peaks (Figure 6.2 (a)), (ii) dexamethasone causes a positive potential shift of the capacitance current peaks (Figure 6.2 (b)) and, (iii) clomipramine, DDT and prochlorperazine implement a suppression of the capacitance current peaks (Figures 6.2 (c), (d) and (f)).

It is significant that the interaction of the tricyclic phenothiazine (Figure 6.1) with the DOPC layer effects a shift of the RCV capacitance current peaks to negative potentials concurrent with a peak depression (Figure 6.2 (e)). On the other hand, the effect of a side chain attached to the phenothiazine nitrogen atom in prochlorperazine (Figure 6.1) greatly increases the sensitivity of DOPC to the interaction and alters the response of the RCV plot to the interaction in that the capacitance current peaks are depressed with minimal shift (Figure 6.2 (f)). This only serves to emphasize the effect of compound structure on the nature of and sensitivity to their interaction with the DOPC coated electrode.

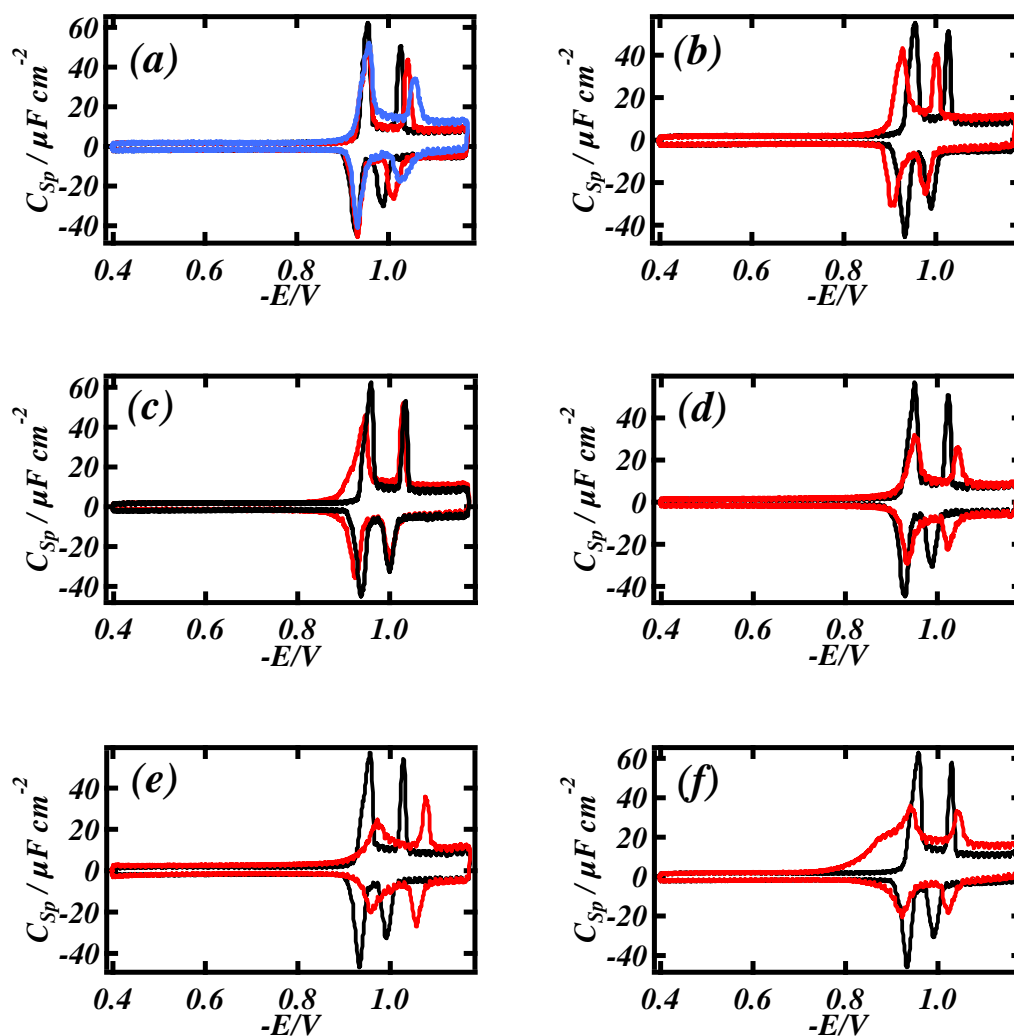


**Figure 6.2:** RCVs recorded at  $40 \text{ Vs}^{-1}$  of a DOPC coated Pt/Hg electrode (black line) in the presence of (a)  $0.0005 \mu\text{mol dm}^{-3}$  (red line) and  $0.002 \mu\text{mol dm}^{-3}$  (blue line) pyrene, (b)  $3 \mu\text{mol dm}^{-3}$  dexamethasone (red line), (c)  $0.3 \mu\text{mol dm}^{-3}$  clomipramine (red line), (d)  $0.3 \mu\text{mol dm}^{-3}$  DDT (red line), (e)  $5 \mu\text{mol dm}^{-3}$  phenothiazine (red line) and (f)  $0.3 \mu\text{mol dm}^{-3}$  prochlorperazine (red line), in PBS at pH 7.4.

It can be hypothesised that the planar PAH compounds and near planar tricyclic phenothiazine interleave between the DOPC molecules and primarily influence the energetics and hence the potential of the phase transitions. On the other hand, the side chain substituted phenothiazine molecules adsorb on top of the DOPC layer

interfering with the phospholipid mobility and depressing the capacitance current peaks. Such an effect is seen when SiO<sub>2</sub> nanoparticles are visibly adsorbed on DOPC coated Hg electrodes [9]. In order to obtain a more quantitative estimate of the effect of each compound on the DOPC layer, detection limits (LoD) for each compound in PBS were estimated (LoD referred to in more detail in Chapter 2). Examples of this procedure applied to the effect of the PAH-DOPC interaction on the capacitance current peak of the RCV are shown in Figure 6.3.

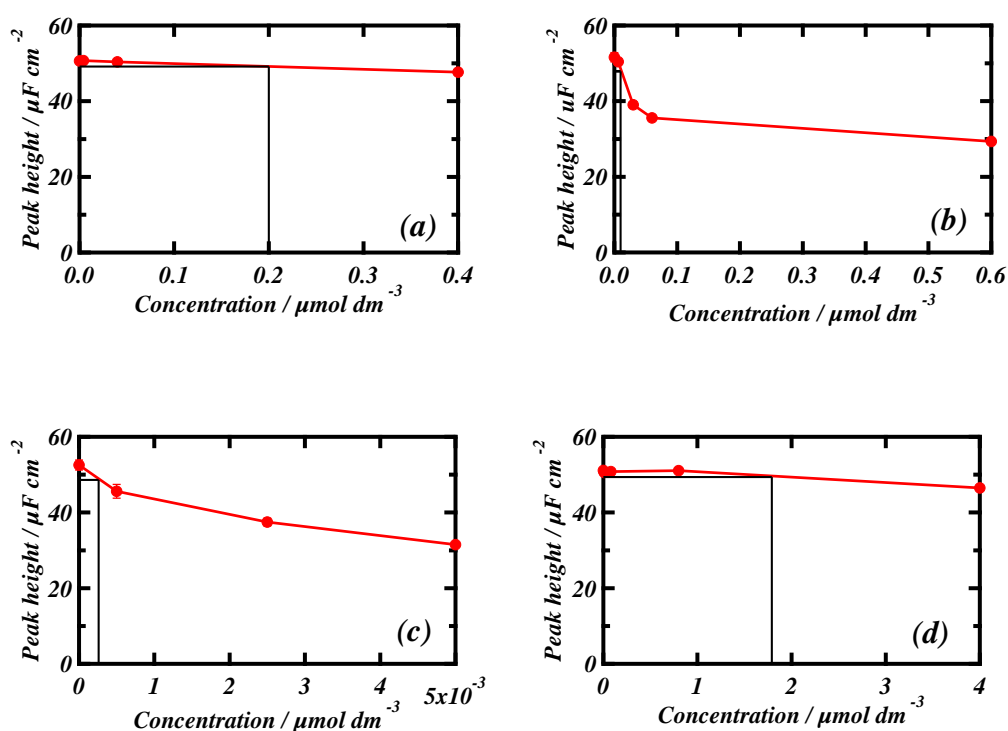


**Figure 6.3: Method for LoD determination by estimating concentration corresponding to three times standard deviation (SD) of DOPC control capacitance current peak height on the capacitance current peak height versus concentration curve for, (a) benzantracene, (b) anthracene, (c) pyrene and (d) naphthalene interaction with DOPC coated Hg in PBS at pH 7.4.**

A list of LoDs estimated for the compounds studied together with their respective log octanol-water partition coefficients ( $\log K_{\text{OW}}$ ) is given in Table 6.1. The  $\log K_{\text{OW}}$  has previously been used [10] as a convenient measure of the hydrophobicity of a

compound and as a predictor of the compound's biological activity and bioavailability. The log  $K_{ow}$  values for compounds were obtained from the PubChem Compound database [11].

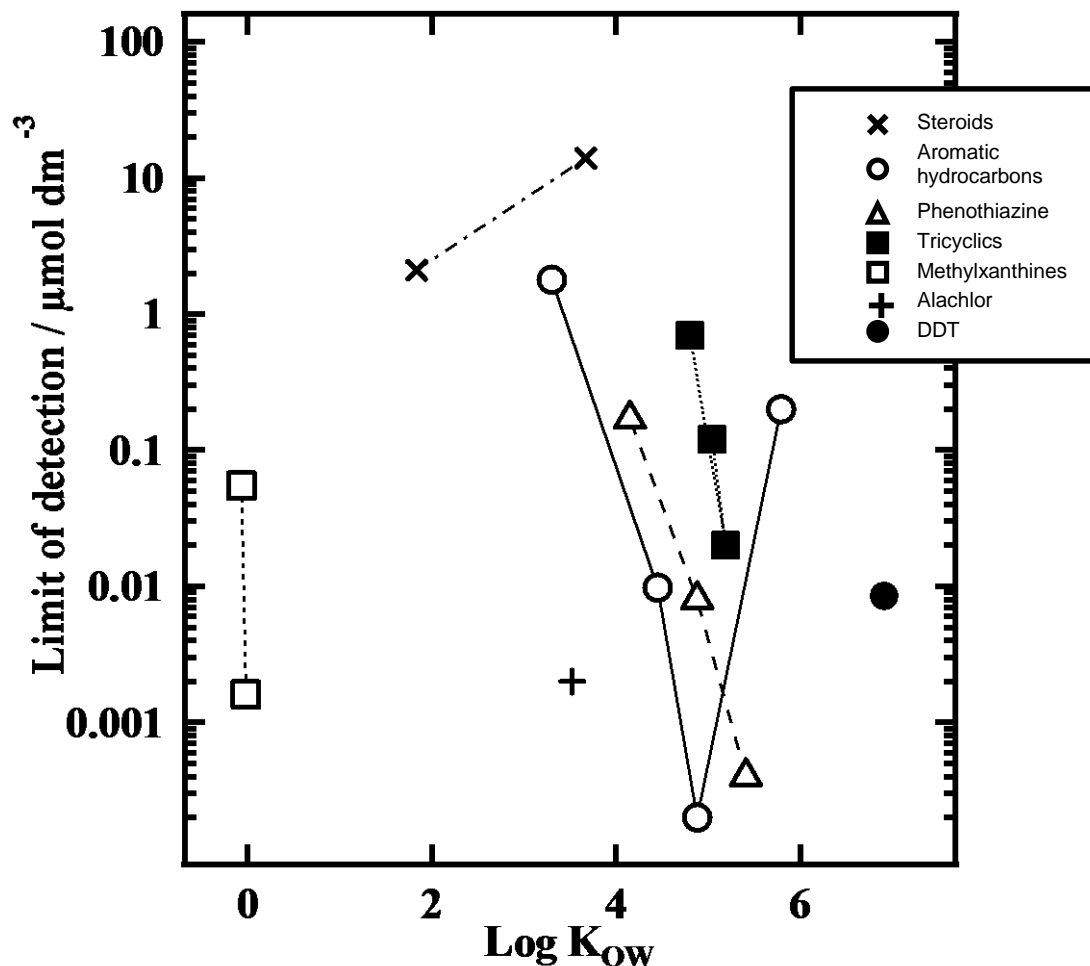


Figure 6.4: Scatter plot of compounds' LoD at DOPC coated Hg electrode in PBS at pH 7.4 vs their respective log octanol - water partition coefficient (log  $K_{ow}$ ) for following compounds and classes of compounds: DDT (filled circle), polycyclic aromatic hydrocarbons (open circle), tricyclic phenothiazines (open triangle), tricyclic antidepressants (filled squares), methylxanthines (open squares), alachlor (plus sign) and steroids (diagonal cross signs). Symbols representing compounds belonging to same class are connected by line for clarity.

Figure 6.4 displays a scatter diagram of the LoD (log scale) vs log  $K_{OW}$  value of the compounds which show trends relating to the structure of compounds contained within compound classes. A compound class is defined as those compounds of homologous or related structure as depicted in Figure 6.1. The scatter in the diagram shows that the log  $K_{OW}$  of a compound is not a reliable indicator of the compound's ability to interact with phospholipid monolayers but is only an approximate guide to the extent of interaction of a series of compounds in the same class. For example, alachlor and theophylline from different compound classes have different log  $K_{OW}$  values (3.52 and -0.04 respectively) but similar LoD values. On the other hand within one compound class there is generally but not always a regular inverse relationship between the compound's log LoD and its log  $K_{OW}$ .

The interactions of the phenothiazine derived antipsychotics and the TCAs with the DOPC monolayer show that the presence and nature of the substituent side-chain alters the compound's LoD value considerably. Note that the unsubstituted tricyclic phenothiazine log LoD-log  $K_{OW}$  relationship falls near to that of the PAH group on the diagram since phenothiazine has a structure related to that of the PAH (see Figure 6.1), whereas the substituted phenothiazines show an increasing departure therefrom. Where the LoD value inversely correlates with the log  $K_{OW}$  within a compound class, the relationship is indirect. This is because in one class of compounds the increase in aromaticity or side chain length leads to an increase of the hydrophobicity of the molecule. Indeed structural properties such as aromaticity and the nature of side chain and substituents are the molecular features which directly determine the extent of interaction. It is noted that the relationship between the log LoD and log  $K_{OW}$  is inversely linear for naphthalene, anthracene and pyrene but the log LoD-log  $K_{OW}$  relationship for benzanthracene is an outlier to this. The trend of interaction for naphthalene, anthracene and pyrene can be related to the increase in the number of aromatic rings whereas the decreased interaction of the four-

membered benzanthracene may be explained by its markedly decreased solubility of  $0.014 \text{ mg dm}^{-3}$  in water compared to the water solubilities of naphthalene, anthracene and pyrene which are 31.7, 0.073 and  $0.135 \text{ mg dm}^{-3}$  respectively [12]. It can be intimated that the very low solubility of benzanthracene in water limits its transfer from the aqueous phase to the DOPC although further experiments will need to be done to establish this. In a way this can also be seen as a molecular cut-off where the molecular shape of benzanthracene (see Figure 6.1) determines its decreased interaction despite its increased  $\log K_{ow}$ . Such an effect has been well documented for the anomalous relation between the potency of anaesthetics and their  $\log K_{ow}$  values. [13]

Compound	Log K <sub>ow</sub> <sup>(i)</sup>	LoD/ $\mu\text{mol dm}^{-3}$
Naphthalene	3.3	1.79
Anthracene	4.45	0.0098
Pyrene	4.88	0.0002
Benzantracene	5.79	0.2
Imipramine	4.8	0.7
Clomipramine	5.19	0.02
Amitryptilline	5.04	0.12
DDT	6.91	0.0085
Ethinyl Estradiol	3.67	14
Dexamethasone	1.83	2.1
Phenothiazine	4.15	0.17
Chlorpromazine	5.41	0.0004
Prochlorperazine	4.88	0.008
Caffeine	-0.07	0.055
Theophylline	-0.02	0.002
Alachlor	3.52	0.002

**Table 6.1: Log K<sub>ow</sub> values of compounds and their LoDs using sensing device.**

**(i) Values from PubChem Compound database.**

## 6.4 SUMMARY

This chapter presented the successful configuration of Pt/Hg electrode to selectively screen organic compounds in water.

Classes of compounds of related structure and shape interact with DOPC coated Pt/Hg with a distinct response specific to each class.

Within each compound class, the extent of interaction is correlated with, (a) aromaticity and molecular shape of the PAH; (b) side chain composition of tricyclic phenothiazines and TCAs; (c) presence of substituents on tricyclic phenothiazines and TCAs and; (d) Substitution on steroid skeleton. Any relation between the extent of interaction and the compound log  $K_{OW}$  is indirect.

Interaction studies are continued in Chapter 7.



## REFERENCES

- [1] Coldrick Z, Penezic A, Nelson A. *J Appl Electrochem*, **2011**, 41: pp939–949.
- [2] Nelson A. *Analytica Chimica Acta*, **1987**, 194: pp139–149
- [3] Nelson, A. Auffret N, Readman J. *Analytica Chimica Acta*, **1988**, 207: pp47–57
- [4] Nelson A, Auffret N, Borlakoglu J. *Biochemica et Biophysica Acta*, **1990**, 1021: pp205–216.
- [5] Coldrick Z, Steenson, P, Millner P, Nelson A. *Electrochimica Acta*, **2009**, 54: pp4954–4962.
- [6] Brukhno AV Akinshina A, Coldrick Z, Auer S. *Soft Matter*, **2011**, 7: pp1006–1017.
- [7] Nelson A, Leermakers FAM. *J. Electroanal. Chem.* **1990**, 218: pp73–83.
- [8] Nelson A. *Journal of Electroanalytical Chemistry*, **2007**, 601: pp83–93.
- [9] Vakurov A, Brydson R, Nelson A. *Langmuir*, **2012**, 28: pp1246–1255.
- [10] Mackay D. *Environ. Sci. Technol.* **1982**, 16: pp274–278.
- [11] <http://www.ncbi.nlm.nih.gov/pccompound>
- [12] Lua GN, Danga Z, Taob XQ, *QSAR Comb. Sci.*, **2008**, 27: pp618 – 626.
- [13] Luglia AK, Yostb CS, Kindler CH. *Eur J Anaesthesiol.* **2009**, 26: pp807–820.

# CHAPTER 7

## INTERACTION STUDIES II

### 7.1 INTRODUCTION

The interplay between many molecular compounds with biological membranes remains poorly understood. These relationships are of critical importance when attempting to understand, predict or modify the pharmacokinetics and bioavailability of compounds. This chapter aims to understand the parameters that promote or hinder monolayer interaction. Specific compound interactions have been investigated. The compounds are not necessarily related to each other, however, they each possess functional groups that have a propensity to affect the lipid monolayer in some way.

The behaviour of some drug compounds correlates well with log  $K_{ow}$  values. As a rule, hydrophobic compounds have a greater affinity for lipid membranes than hydrophilic compounds [1]. However, there are many more exceptions to this when considering specific active processes [2].

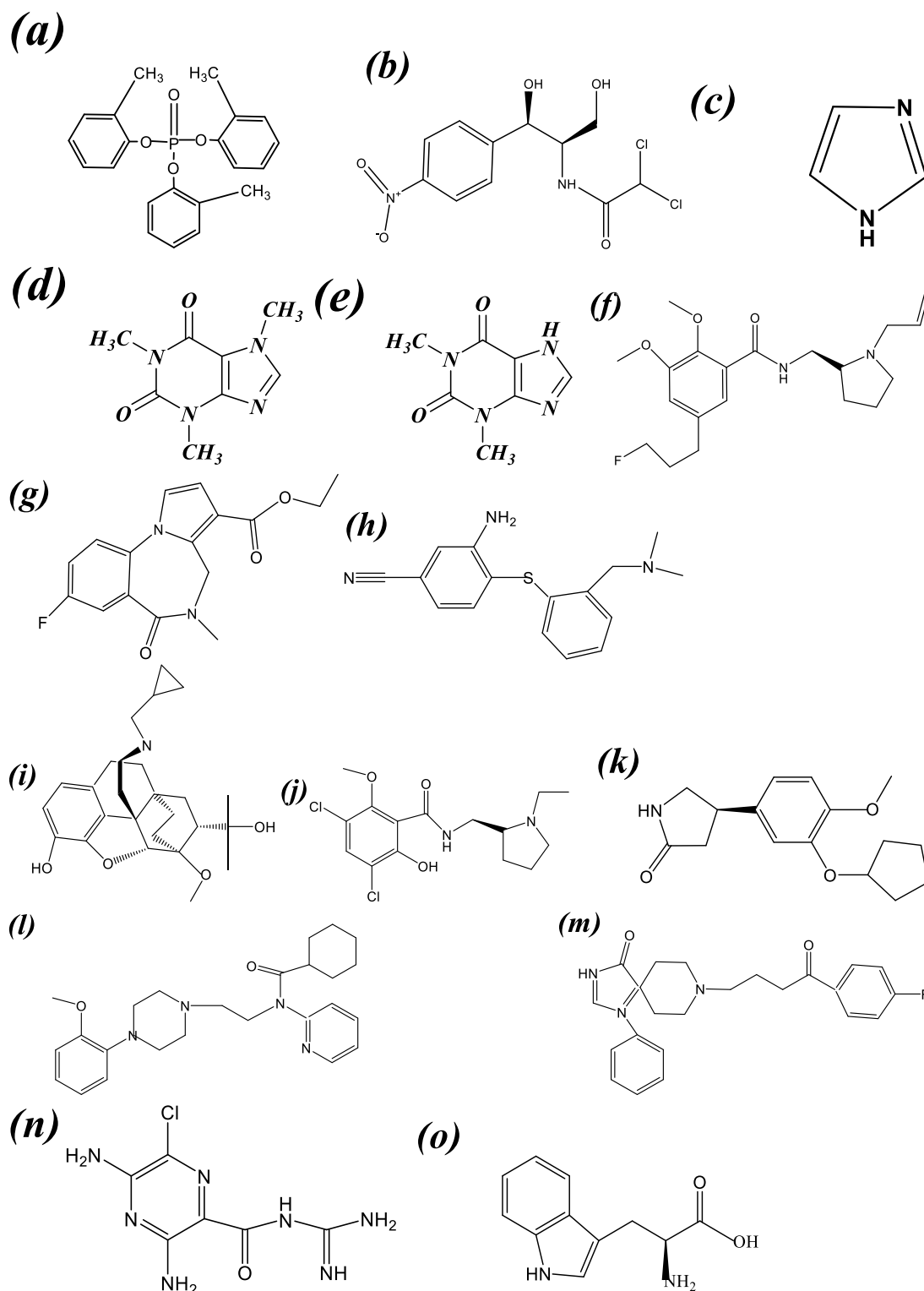


**Figure 7.1: Molecular structures a) tricresyl phosphate, b) chloramphenicol c) imidazole, d) caffeine e) theophylline f) fallypride g) flumazenil, h) DASB i) diprenorphine j) raclopride k) rolipram l) WAY m) spiperone n) amiloride o) tryptophan**

### 7.1.1 TRICRESYL PHOSPHATE

Tricresyl phosphate (TcP) is an organophosphate compound. It has diverse applications; it is used as a plasticizer in varnishes, an additive in gasoline, and an anti-wear additive in lubricants [3]. TcP is also added to jet engine oil to prevent wearing down of the engine. The aircraft cabin ventilation releases air directly from the engine. Worn or defective engine seals can result in the release of engine oil into the cabin air supply and as a result, there could be some bleed of TcP into cabin air. Adverse health effects are hypothesized to be due to exposure to tricresyl phosphate mixed esters referred to as aerotoxic syndrome [4]. However, it is still unproven if the toxicity is associated directly with contamination in the cabin air. The developed MFE sensor can be used to test for exposure to TcP. The type of association that TcP has with the lipid monolayer can be exploited as a sensing event.

### 7.1.2 CHLORAMPHENICOL

Chloramphenicol is well documented for its toxicity profile. Studies have suggested that the reason for its toxicity could be related to its nitro reduction properties and the subsequent production of nitric oxide [5]. As shown in Figure 7.1, chloramphenicol contains a nitrobenzene ring, an amide bond, and an alcohol group. The nitrobenzene is relevant because it leads, on reduction, to the formation of aromatic amines which are potentially carcinogenic. The nitro group can be reduced to a hydroxylamine that lead to methaemoglobinemia in babies in the 1950s (grey baby syndrome) [6, 7]. Other side effects of chloramphenicol include anaemia and bone marrow suppression [8].

The mechanisms of these side effects are uncertain as there are wide individual variations in its metabolism and elimination [9]. It is effective against a wide range of bacteria but due to its safety concerns it is not used readily. Currently, its most prevalent use is in eye drop formulation for the treatment of conjunctivitis. As it is in a

very low concentration in eye drops, the toxicity risk in this formulation is lower. However, there are some risks still present even in this use [10]. Aromatic amines can also be metabolised to carcinogens through oxidation or reduction. When the nitrogen – oxygen bond is broken, the nitrogen attains a positive charge with 2 unshared electrons. Due to this, the compound becomes very reactive. It could then interact with a rich source of electrons such as DNA. This could be the route to carcinogenesis however it has not been ascertained. Drugs that metabolise to toxic amines fail clinical trials. The MFE screening system can thus be applied to detect for toxic amines.

### 7.1.3 SPIPERONE AND ANALOGUES

Siperone is a dopaminergic receptive compound that also has high binding affinity to various serotonin (5-HT) receptors. Siperone has been used in radioligand binding studies for identifying particular types of 5-HT receptors [11]. Siperone is also classed as an antipsychotic. Siperone has been previously discussed in Chapter 5.

In this Chapter, compounds with similar binding sites as siperone (namely dopamine and serotonin receptors) are investigated to determine how functional groups affect their affinity to a biological target. They all share similar binding sites but have different modes of action. These compounds are briefly introduced.

Flumazenil is a GABA receptor antagonist with various clinical uses, however one of its important use is to counteract the over dosage of benzodiazepine or to reverse effects of benzodiazepine when used in surgery. Fallypride has a high affinity for dopamine receptors as an antagonist and currently has no main clinical uses. Diprenorphine is an opioid receptor antagonist and can be used to reverse the effects of those opioids with incredibly high binding affinity. It is only used to treat over dosage of opioids which cannot be treated with the conventional naloxone. 3-amino-4-[2-[(di(nethyl)amino)methyl]phenyl]sulfanylbenzonitrile or DASB binds to 5-HT

transporters but also has affinity for blood brain barriers. DASB has not been extensively studied. Raclopride is a dopamine antagonist and used to determine the degree of dopamine binding to dopamine receptor via positron emission tomography. Rolipram is a selective phosphodiesterase-4 inhibitor. It has been studied for possible antidepressant and antipsychotic effects. Animal studies have shown an improved long term memory, increased wakefulness and neuroprotection upon administration of Rolipram. WAY (systemic name *N-tert-butyl-3-(4-(2-methoxyphenyl)-piperazin-1-yl)-2-phenylpropanamide*) is selective for both 5-HT, specifically 5-HT<sub>1A</sub> (as an antagonist) and dopamine (as an agonist). This compound has particular antagonist activity for 5-HT<sub>1A</sub> leading to a heightened effect of opioids which can be fatal, since it is the 5-HT<sub>1A</sub> agonists that reduce opioid induced respiratory depression.

Serotonin or 5-HT is a neurotransmitter. Serotonin has various functions, well known and over popularised for its cognitive effects. Many antidepressants aim to release or increase serotonin in the prefrontal cortex to improve mood. However, serotonin is not just related to cognitive functions, it is in fact much more ubiquitous; being found in plants, fungi and even in seeds [12]. The main classes of drugs that target the 5-HT system include antidepressants, antipsychotics, recreational drugs, antiemetics and antimigraine drugs.

The compounds fallypride, flumazenil, DASB, diprenorphine, raclopride, rolipram, WAY and spiperone were provided by Chemistry department, Imperial College, London. The work conducted was also part of a screening validation service for Imperial College, Chemistry; Dr. Oscar Ces.

#### 7.1.4 METHYLXANTHINES

Imidazole, is a component of methylxanthines. It has the molecular formula  $C_3H_4N_2$  (Figure 7.1 c)). Imidazole is a highly polar compound, as evidenced by the calculated

dipole of 3.61D [13]. The compound is classified as aromatic due to the presence of a sextet of  $\pi$ -electrons, consisting of a pair of electrons from the protonated nitrogen atom and one from each of the remaining four atoms of the ring. It is a major component in the molecular structure of theophylline and caffeine. The main difference between caffeine and theophylline is that caffeine has a  $\text{CH}_3$  on the nitrogen group on the imidazole moiety (R3) and theophylline has a hydrogen on R3. Caffeine and theophylline are classed as adenosine receptor antagonists. They differ to each other by potency and selectivity. Theophylline in particular is primarily adapted for treatment of COPD [14].

## 7.2 MATERIALS AND METHODS

The test compounds of 99% or greater purity were purchased from commercial suppliers, and were used as received. The phospholipid employed for coating electrodes was 1, 2-dioleoyl-sn-glycero-3-phosphocholine (DOPC) (Avanti Polar Lipids Alabaster, AL) and was >99% pure. All other reagents were of analytical grade and purchased from Sigma-Aldrich. Concentrations of test compounds were prepared by adding small aliquots of the working solutions to PBS to provide concentrations for testing. The DOPC dispersion for electrode coating was prepared by gently shaking DOPC with PBS to give  $0.2 \text{ mg cm}^{-3}$  dispersion. The electrochemical methods are repeated as per Chapter 2. Interactions of compounds with the DOPC monolayer were monitored by RCV while cycling the electrode potential from -0.4 to -1.2 V for 60 seconds during compound exposure.

## 7.3 RESULTS AND DISCUSSIONS

### 7.3.1 TRICRESYL PHOSPHATE

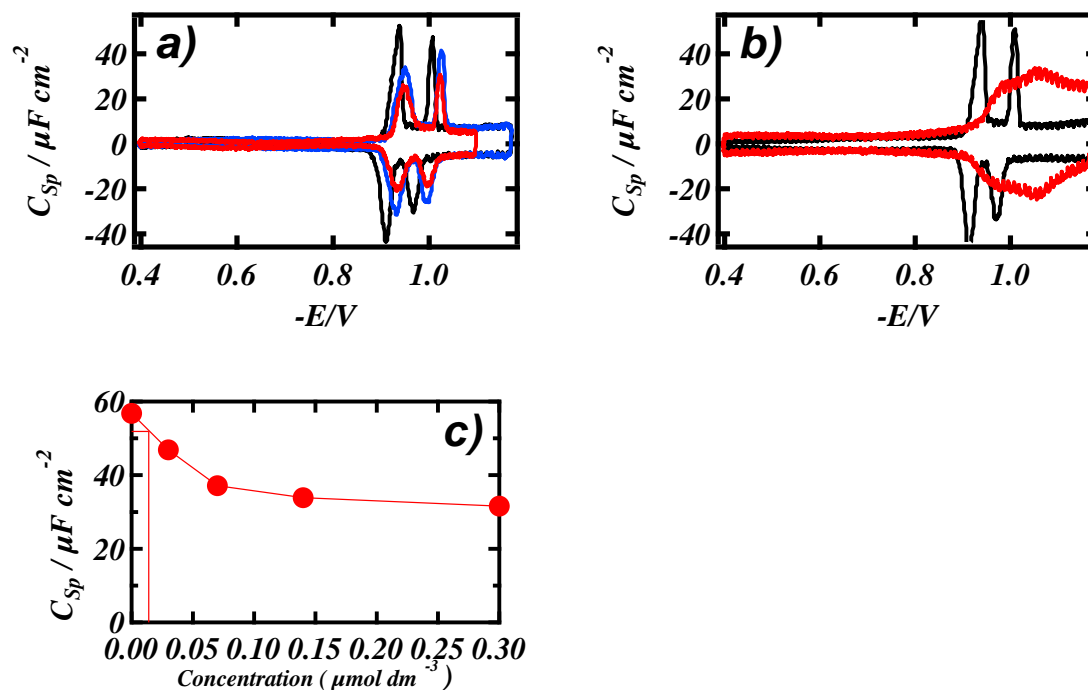


Figure 7.2: RCVs recorded at  $40 \text{ Vs}^{-1}$  of a DOPC coated Pt/Hg electrode in PBS at pH 7.4 (black line) in the presence of a)  $0.003 \mu\text{mol dm}^{-3}$  (red line) and  $0.14 \text{ nmol dm}^{-3}$  (blue line) TcP and b)  $0.05 \mu\text{mol dm}^{-3}$  (red line) TcP. d) LoD determination by estimating concentration corresponding to three times SD of DOPC control capacitance current peak height on capacitance current peak height versus concentration curve for TcP interaction with DOPC coated Hg in PBS at pH 7.4 (error bars within the markers).

Figures 7.2 a) and b) show a distinct profile for TcP. The first capacitance current peak decreases more markedly than the second peak and there is a potential shift to more negative values. Concentration influences the extent of peak suppression and peak shift; at higher concentrations, there is a broadening of the peaks along with a



decrease in peak height. This intense interaction is immediate following sample injection (Figure 7.2b)). This is indicative of a disruption in the DOPC layer structure. An increase in the capacitance is also noticeable in the potential region -0.4V to -1V. TcP has one of the lowest calculated LoD in the interaction studies as shown in Figure 7.2 c) at  $0.014 \text{ nmol dm}^{-3}$ .

### 7.3.2 CHLORAMPHENICOL

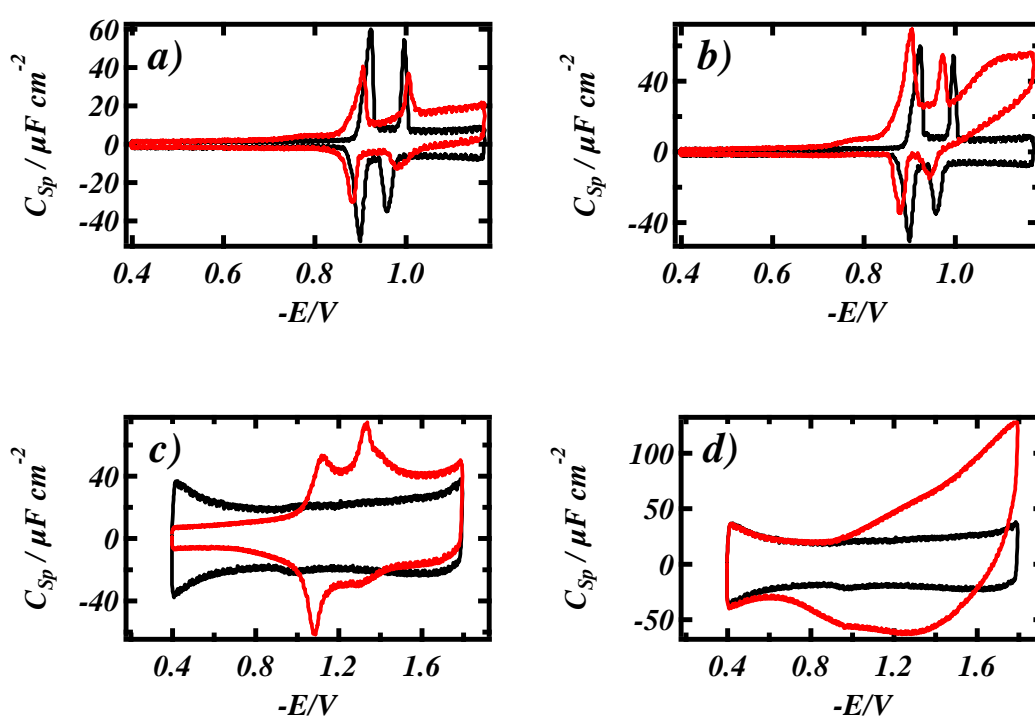


Figure 7.3: RCVs recorded at  $40 \text{ Vs}^{-1}$  of a DOPC coated Pt/Hg electrode in PBS at pH 7.4 (black line) in the presence of a)  $3 \times 10^{-4} \mu mol dm^{-3}$  chloramphenicol (red line) and b)  $6 \times 10^{-4} \mu mol dm^{-3}$  chloramphenicol (red line). c) RCV recorded of uncoated Pt/Hg electrode (black line) at  $40 \text{ Vs}^{-1}$  in PBS at pH 7.4 in the presence of  $3 \times 10^{-4} \mu mol dm^{-3}$  chloramphenicol (red line) and d) RCVs recorded at  $40 \text{ Vs}^{-1}$  in PBS at pH 7.4 of uncoated Pt/Hg electrode (black line) and uncoated Pt/Hg electrode post chloramphenicol studies (red line).

RCV scans (Figure 7.3) show the increase in capacitance current which appears due to the reduction process. The reduction is initiated at potentials more negative than -0.8V. At the negative potentials, the redox processes result in production of reactive ions and species that can subsequently reduce at the electrode surface thus having an effect on the stability of the lipid monolayer. In addition, chloramphenicol is able to deposit onto the mercury surface and form individual capacitance peaks; Figure 7.3 c). This can be attributed to chloramphenicol's amphiphilic properties. However, the peaks are neither uniform nor reproducible. It was difficult to re-establish the mercury layer after exposure; Figure 7.3 d).

### 7.3.3 METHYLXANTHINES

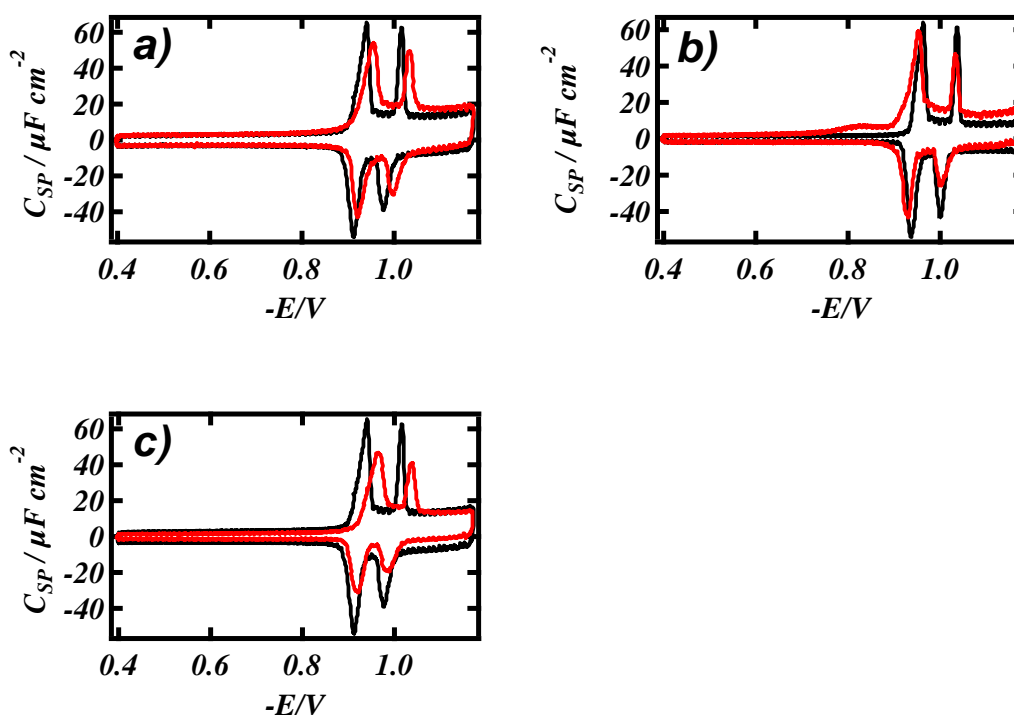


Figure 7.4: RCVs recorded at  $40 \text{ Vs}^{-1}$  of a DOPC coated Pt/Hg electrode in PBS at pH 7.4 (black line) in the presence of (a)  $10 \mu\text{mol dm}^{-3}$  imidazole (red line) b)  $10 \mu\text{mol dm}^{-3}$  theophylline (red line) and c)  $10 \mu\text{mol dm}^{-3}$  caffeine (red line).

As can be seen in Figure 7.4, theophylline has a distinct effect compared to the other compounds in the same class. The change in the capacitance current profile in the potential region of -0.7V and -0.9V could represent theophylline penetrating the DOPC layer.

#### **7.3.4 SPIPERONE AND ANALOGUES**

RCV results of spiperone and compounds that also share similar target receptors are shown in Figure 7.5.

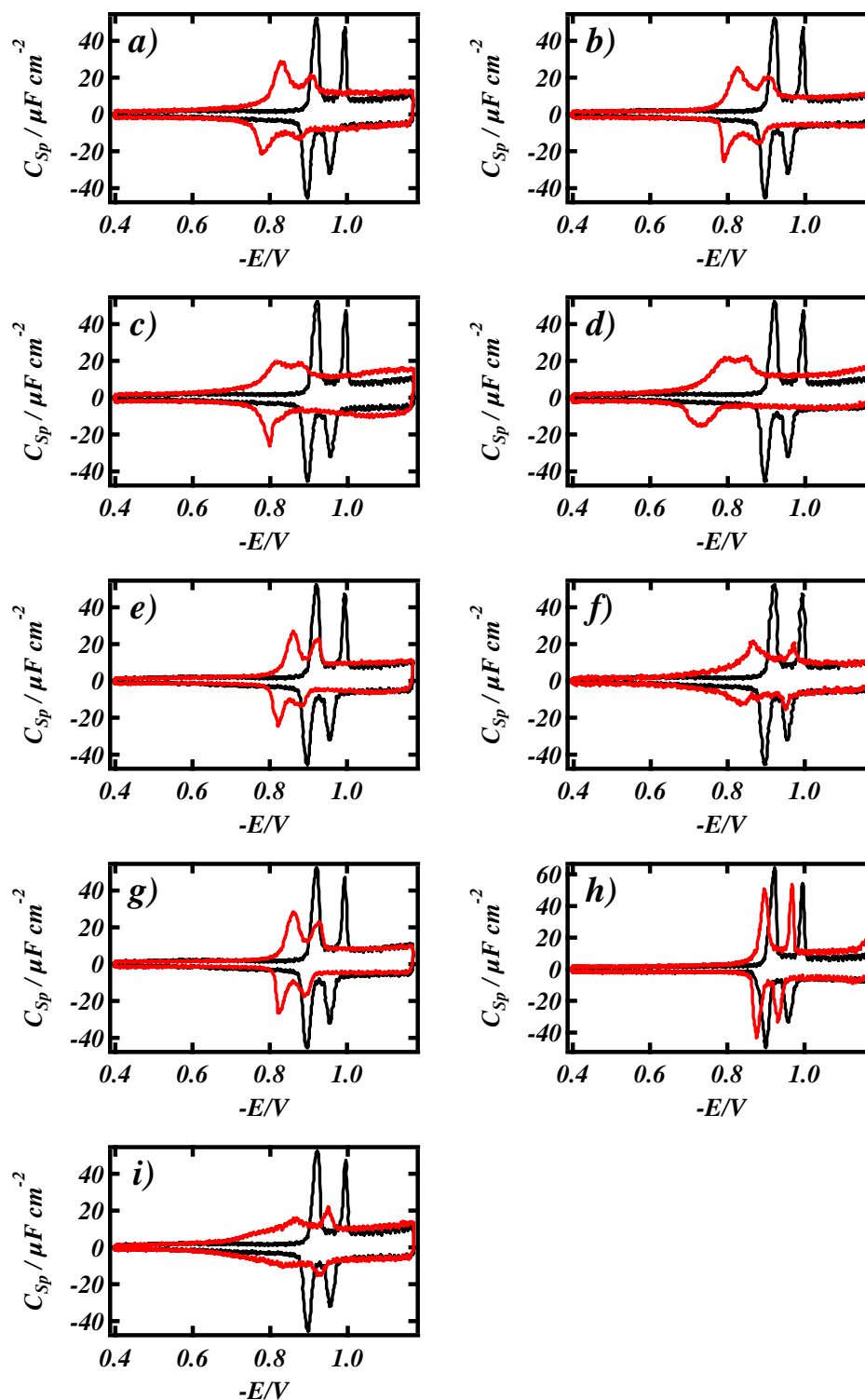


Figure 7.5: RCVs recorded at  $40 \text{ Vs}^{-1}$  of a DOPC coated Pt/Hg electrode in PBS at pH 7.4 (black line) in the presence of  $0.25 \text{ mmol dm}^{-3}$  (red line) a) fallypride, b) flumazenil, c) DASB, d) diprenorphine, e) raclopride, f) WAY, g) rolipram h) serotonin and i) spiperone

The RCV results show the effect on capacitance / potential peaks. The capacitance current peak potential shifts to more positive values accompanied by a decrease in the capacitance current peak height. The extent of these changes depends on the compound being used.

## 7.4 NEGATIVE CONTROL

In order to validate the responses to positive interactions of biomembrane active pharmaceutical compounds with the phospholipid layer, RCV scans of DOPC layers in the presence of relatively biomembrane inactive compounds have been carried out. The purpose of this procedure was to identify any analytical flaws and to help distinguish between significant and insignificant responses. Tryptophan is a non-toxic compound and not known to be biomembrane active. [15] In other studies, it was found that the compound amiloride also has insignificant interaction with lipid membranes. Amiloride is used as a diuretic [16]; and its activity is manifest in the blocking of sodium channels in the distal convoluted tubules of the kidney with no known effect on the phospholipid component.

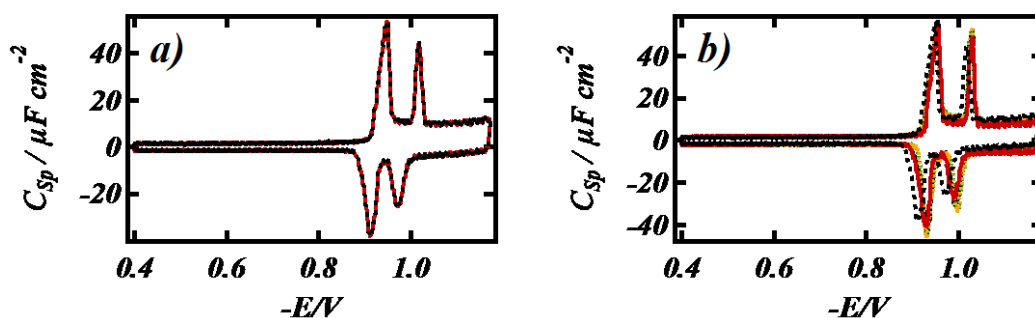


Figure 7.6: RCVs recorded at  $40 \text{ Vs}^{-1}$  of a DOPC coated Pt/Hg electrode in PBS at pH 7.4 (black line) in the presence of a) amiloride with increasing concentrations from  $0.005$  to  $5 \mu\text{mol dm}^{-3}$  and b) l-tryptophan with increasing concentrations from  $0.005$  to  $5 \mu\text{mol dm}^{-3}$ .

The effect of amiloride and l-tryptophan on the RCV plot of the DOPC coated Pt/Hg electrode is insignificant (Figure 7.6).

## 7.5 SUMMARY

The compounds studied in this Chapter all show varying degrees of affinity with phospholipid monolayers. These interactions cause responses to the capacitance current peaks in RCVs recorded at the DOPC Pt/Hg MFE and can be measured readily. Conclusions are summarised in the points below.

1. The capacitance current increases in the presence of a nitro group on the interacting compound. The capacitance current increase is also dependent on concentration. This is due to redox processes occurring at electrode surface. RCV results produced characteristics indicative of a diffusion-controlled electrode process.
2. Classes of compounds of related structure and shape interact with DOPC coated Pt/Hg with a distinct response specific to that compound.
3. Within each compound class, the extent of interaction is correlated with functional groups present.
4. Compounds that target the same biological receptor have been studied. Their interactions on DOPC coated Pt/Hg vary extensively as revealed by RCV. Structural properties such as aromaticity and the nature of side chain and substituents are the molecular features which directly determine the extent of interaction. This emphasizes further the effect of compound structure on the nature of and sensitivity to their interaction with the DOPC coated electrode.

## REFERENCES

- [1] Bowe CL. *Pharmacology* **1997**, 94: pp12218–12223.
- [2] Rosso L, Gee AD, Gould IR. *J. Comput. Chem.* **2008**, 29: pp2397–2405.
- [3] Svara J, Weferling N, Hofmann T. *Phosphorus Compounds, Organic.* **2006**  
Ullmann's Encyclopedia of Industrial Chemistry.
- [4] Liyasova M, *Toxicol Appl Pharmacol.* **2011**, 256(3): pp337–347
- [5] Holt DE, Bajoria R. *Hum Exp Toxicol.* **1999** 18(2):pp111-8.
- [6] Lietman PS. *Clinics in Pharmacology* **1979**; 6:pp151–62.
- [7] Laferriere CI, Marks MI. *Pediatr Infect Dis.* **1982** (4):pp257-64.
- [8] Paul R. McCurdy, M.D. *Journal of Am. Medical Association* **1961**  
176(7):pp588-593
- [9] Laferriere CI, Marks MI *Pediatr Infect Dis* **1985** (1):pp367-72.
- [10] Lancaster T, Stewart AM, Jick H. *British Medical Journal* **1998**. 316 (7132):  
p667.
- [11] Peroutka SJ, Snyder SH. *Mol Pharmacol*, **1979**; 16:pp687-699
- [12] Kang K, Park S. *Appl. Microbiol. Biotechnol* **2009**. 83 (1): 2pp7-34.
- [13] Jie JL. *Heterocyclic Chemistry in Drug Discovery*, **2013** p333 Wiley
- [14] Giovanni P, Mojgan B, Tabrizi A *Chem. Rev.* **2008**, 108: pp238–263
- [15] Caeser CE, Esborner EK, Lincoln P, Norden B. *Biochemistry* **2006**  
45(24):pp7682-92.
- [16] The British National Formulary [B.N.F.] March **2014**. Edited by The Joint  
Formulary Committee.



# CHAPTER 8

## POLYCYCLIC AROMATIC HYDROCARBONS

### 8.1 INTRODUCTION

Over the years, there has been increasing concern about the potential risk of hydrocarbons in the environment, in particular polycyclic aromatic hydrocarbons (PAHs) [1]. Furthermore, there has been increasing interest because more than 20% of the carbon in the universe may be associated with PAH and they are also thought to be the possible starting material for the earliest form of life. It was not till 2004 that reports on a study on the Red Rectangle nebula found signatures representing the presence of anthracene and pyrene; there have been no other complex structures found in space till then [2]. In June 2013, the detection of PAHs in the upper atmosphere of Titan, which is the largest moon of Saturn, has been reported [3].

PAHs are organic compounds composed of fused aromatic rings. They are found naturally in the environment such as in fossil fuels, through volcanic activity or they can have an anthropogenic source such as from industrial and domestic wastewaters, from incomplete combustion of organic matter and from engines and incinerators. Most PAHs, such as anthracene are used to make dyes, plastics and smoke screens [4]. They can also be used as pesticides and thus have the propensity to leak into

water systems. There are various health risks associated with the exposure of PAH. They range from minor skin irritation to carcinogenicity [5-8]. PAHs are ubiquitous; they are present as trace contaminants in air, water and soil [9] and thus have a high probability of exposure to almost all species of organisms, making them a necessity to study.

The PAHs are grouped in terms of their molecular weight; low molecular weight (LMW) i.e., those containing two- and three-rings with molecular weight up to 178 g/mol and higher molecular weights (HMW) i.e. those containing four-and higher rings with molecular weights greater than 202 g/mol. Quantifying the detection limits of the sensor element to them is a powerful method of providing an index to exposure levels. PAHs cause an irreversible change to the DOPC sensing element even when the introduced PAH is removed from the surrounding aqueous media. Interestingly, it is well known that PAHs are bio accumulative and persistent. [10]

Detection of PAHs is conventionally carried out using gas chromatography coupled to a mass spectrometer or GC-MS. This is normally employed for environmental contaminant identification. GC and MS are individual tests in their own right but often their individual results are unreliable hence both methods interfaced together are used for analysis of sample. This is not compatible for high throughput sampling. In addition, both GS and MS are expensive and time consuming techniques [11]. GC-MS requires many factors to be considered before testing commences. These include establishing retention times, quantification of ions and the choice of carrier gas that does not react with the sample.

Results published by Nelson et al showed that the interaction between aromatic compounds with the phospholipid monolayers on the Hg surface may be monitored by observing changes in the capacitance profile over a potential range [12-13]. The resulting potential-capacitance plots revealed specific profiles for the aromatic

compounds from which information about the chemical properties of the interactants could be derived.

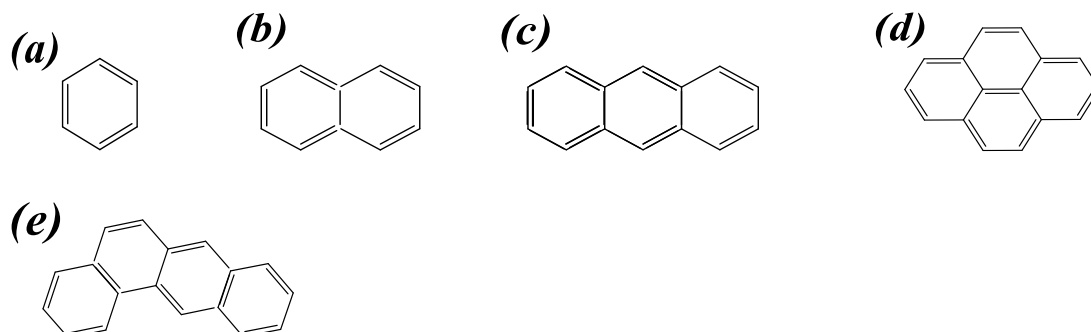


**Figure 8.1: Molecular structures of compounds (a) benzene, (b) naphthalene, (c) anthracene, (d) pyrene (e) benzanthracene**

This work continues the assessment of the PAHs using a more robust and efficient system, thus increasing reproducibility, robustness and reliability. The compounds studied were benzene, naphthalene, anthracene, pyrene and benzanthracene. Figure 8.1 shows the chemical structures. They are composed of fused aromatic rings. Benzene represents the unit building block of PAH and is used in this study.

Currently, the most general method of analysing bioaccumulation of toxins is through the use of marine animals [14-15]. These assays come with disadvantages. Some marine species are less sensitive to certain contaminants, rendering the bioassay less valid. On the other hand, some marine species are more sensitive to certain contaminants than others, making the measurements less precise. As a result, the search for relevant organisms becomes time consuming. Other complications include the apparatus used for the study of the organisms. In static conditions, the organisms can deplete resources and thus suffer adverse effects. As well, when they metabolise, substances are released such as carbon dioxide. When these accumulate in the static system, they become toxic to the organism itself. There is a general lack of control over the organisms own physiological condition [16-17]. The phospholipid coated Hg

on MFE system provides the novel approach to investigating the putative bioactivity of these pollutants through its application as a biomembrane model. The system provides many advantages. It does not show resistance to any compound and interacts objectively, naturally and selectively depending on the compound assayed. Fresh PBS is continuously being pumped over the sensor-element, thus decreasing the loss of toxic compounds to degradation, adsorption, and volatilization. Lipids are found in all organisms. The phospholipid membrane is the route that most toxins and compounds will take to enter the host. The MFE system readily accommodates differences in samples from different sites. This is presented in Chapter 11 where analysis of samples from tap water, almost static surface water and constantly moving underground water will be discussed. There will be two objectives in this Chapter, firstly to assess the performance of the MFE in detecting these compounds and second, to understand what molecular factors lead to their differences in interaction with phospholipids.

## 8.2 MATERIALS AND METHODS

The apparatus, materials and methods for preparing the monolayers and monitoring the electrical properties of the film have been described [18]. The standard MFE system set up for RCV scan is used as before. The test compounds of 99% or greater purity were purchased from commercial suppliers, and were used as received. The phospholipid employed for coating electrodes was 1, 2-dioleoyl-sn-glycero-3-phosphocholine (DOPC) (Avanti Polar Lipids Alabaster, AL) and was >99% pure. Stock solutions were made for the test compounds, benzene, naphthalene, anthracene, pyrene and benzanthracene, were dissolved in acetone. The electrolyte used throughout the experiments was PBS. Concentrations of test compounds were prepared by adding small aliquots of the working solutions to PBS to provide concentrations for testing. The potential shift and height of capacitance current peaks were measured as these are sensitive to PAH penetration [19].

## 8.3 RESULTS

Figure 8.2 shows RCV scans corresponding to each PAH-DOPC interaction. It can be seen that the PAHs all elicit a negative potential shift and suppression of the capacitance current peaks, predominantly of the second peak; this is a specific occurrence in the presence of aromatics. It is significant that the interaction of 3 to 4 ringed PAHs of planar arrangement namely anthracene and pyrene with the DOPC layer effects a significant shift of the second RCV capacitance current peaks to negative potentials concurrent with a peak depression. On the other hand, the effect of decreasing ring numbers, or introducing a non planar configuration greatly decreases the sensitivity of DOPC monolayers to the interaction with PAH and alters the response of the RCV plot to the interaction in that the capacitance current peaks have minimal shift .

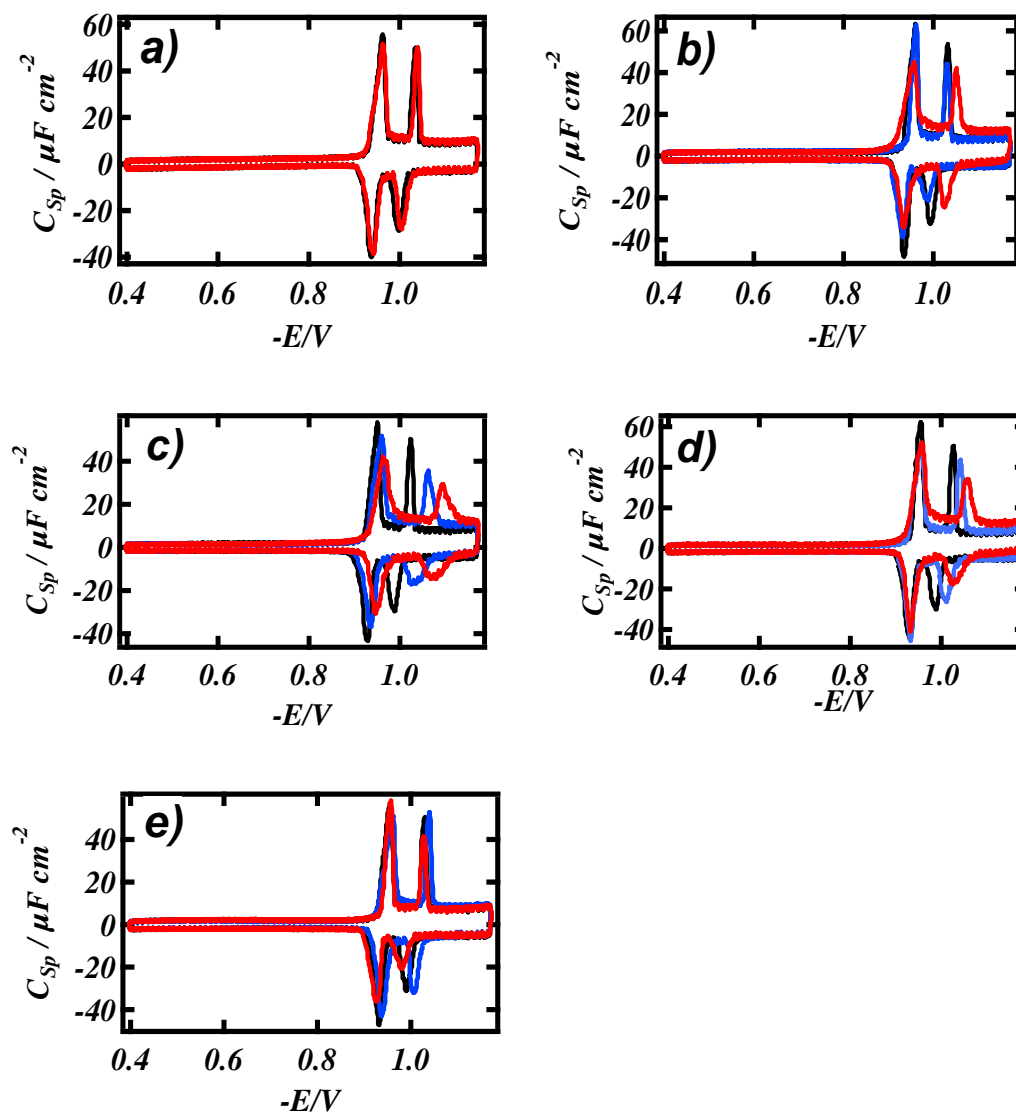


Figure 8.2: RCVs recorded at  $40 \text{ Vs}^{-1}$  of a DOPC coated Pt/Hg electrode in PBS at pH 7.4 (black line) in the presence of a)  $8 \mu\text{mol dm}^{-3}$  benzene (red line), b)  $0.8 \mu\text{mol dm}^{-3}$  (blue line) and  $8 \mu\text{mol dm}^{-3}$  (red line) naphthalene, c)  $0.06 \mu\text{mol dm}^{-3}$  (blue line) and  $0.6 \mu\text{mol dm}^{-3}$  (red line) anthracene, d)  $0.0005 \mu\text{mol dm}^{-3}$  (blue line) and  $0.002 \mu\text{mol dm}^{-3}$  (red line) pyrene and e)  $0.8 \mu\text{mol dm}^{-3}$  (blue line) and  $8 \mu\text{mol dm}^{-3}$  (red line) benzantracene.

Increasing the concentration of the compounds gives rise to higher responses following PAH-DOPC interaction. Concentration influences the extent of peak suppression and peak shift. The extent of the peak shift following compound

interaction with the DOPC layer is shown in Figure 8.3. This serves to emphasize the effect of compound structure on the nature of and sensitivity to their interaction with the DOPC coated electrode.

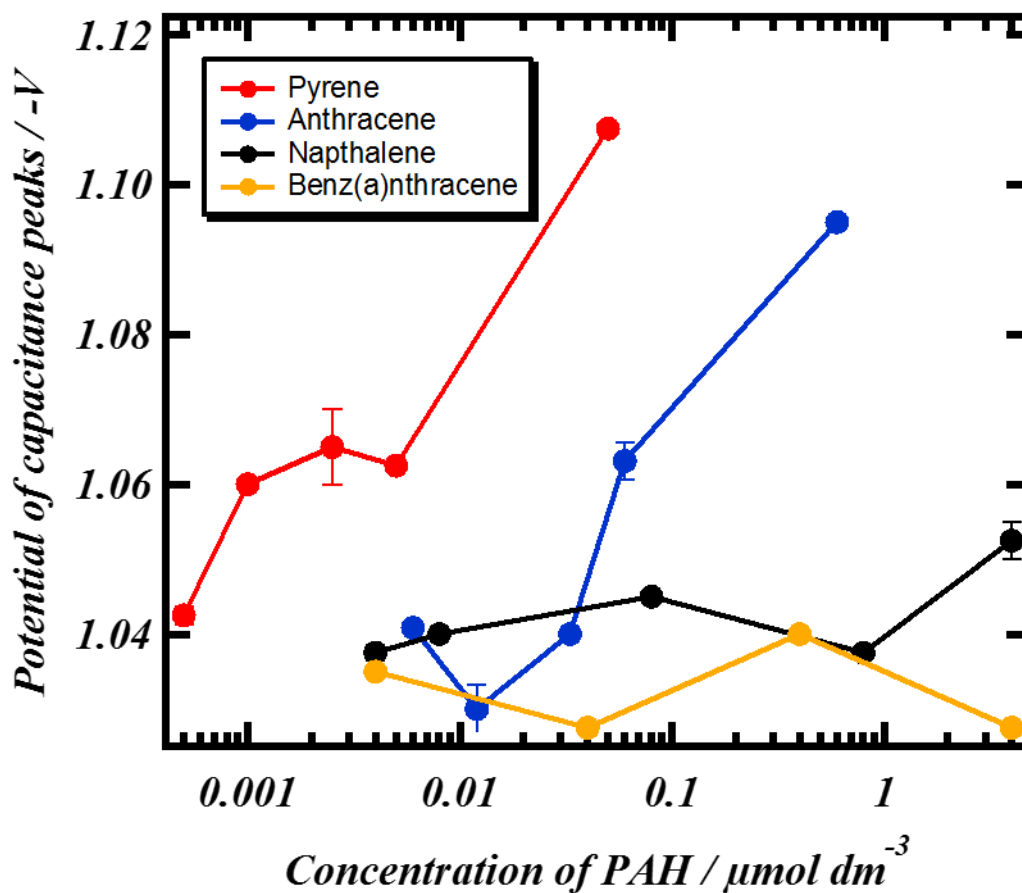
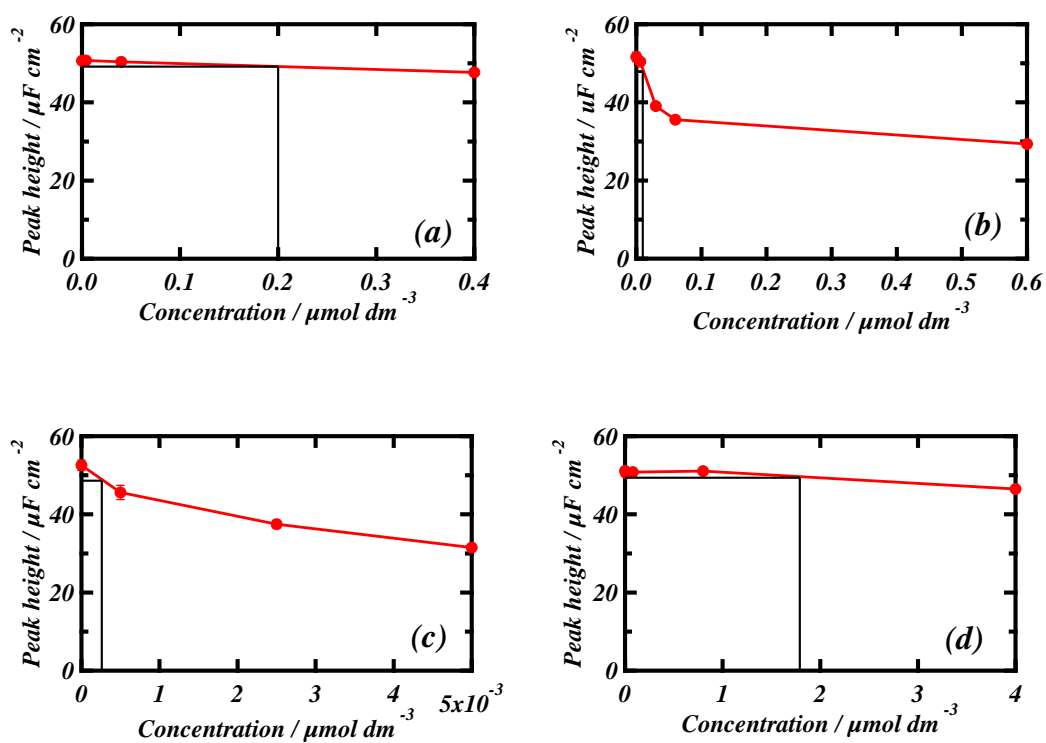


Figure 8.3: Plot showing the effect of PAH compounds on the potential (-V) of the second capacitance current peak vs. concentration ( $\mu\text{mol dm}^{-3}$ ). Potential values were obtained from the RCV experiments ( $-0.4\text{V}$  to  $-1.2\text{V}$  at  $40\text{V}\cdot\text{s}^{-1}$  in PBS at pH 7.4).

Compound	Log $K_{OW}^{(i)}$	No. of rings	LoD/ $\mu\text{mol dm}^{-3}$
Benzene	2.13	1	40
Naphthalene	3.3	2	1.79
Anthracene	4.45	3	0.0098
Pyrene	4.88	4	0.0002
Benzanthracene	5.79	4	0.2

**Table 8.1:** Log  $K_{OW}$  values of compounds, their number of aromatic ring and their calculated LoDs. (i) Values from PubChem Compound database.



**Figure 8.4:** LoD determination by estimating concentration corresponding to three times SD of DOPC control capacitance current peak height on capacitance current peak height versus concentration curve for, (a) benzanthracene, (b) anthracene, (c) pyrene and (d) naphthalene interaction with DOPC coated Hg in PBS at pH 7.4.



The most sensitive compound was pyrene which has the lowest limit of detection (LoD) of  $0.2 \text{ nmol dm}^{-3}$ . A list of LoDs estimated for the PAHs studied together with their respective log octanol-water partition coefficients ( $\log K_{ow}$ ) is given in Table 8.1.

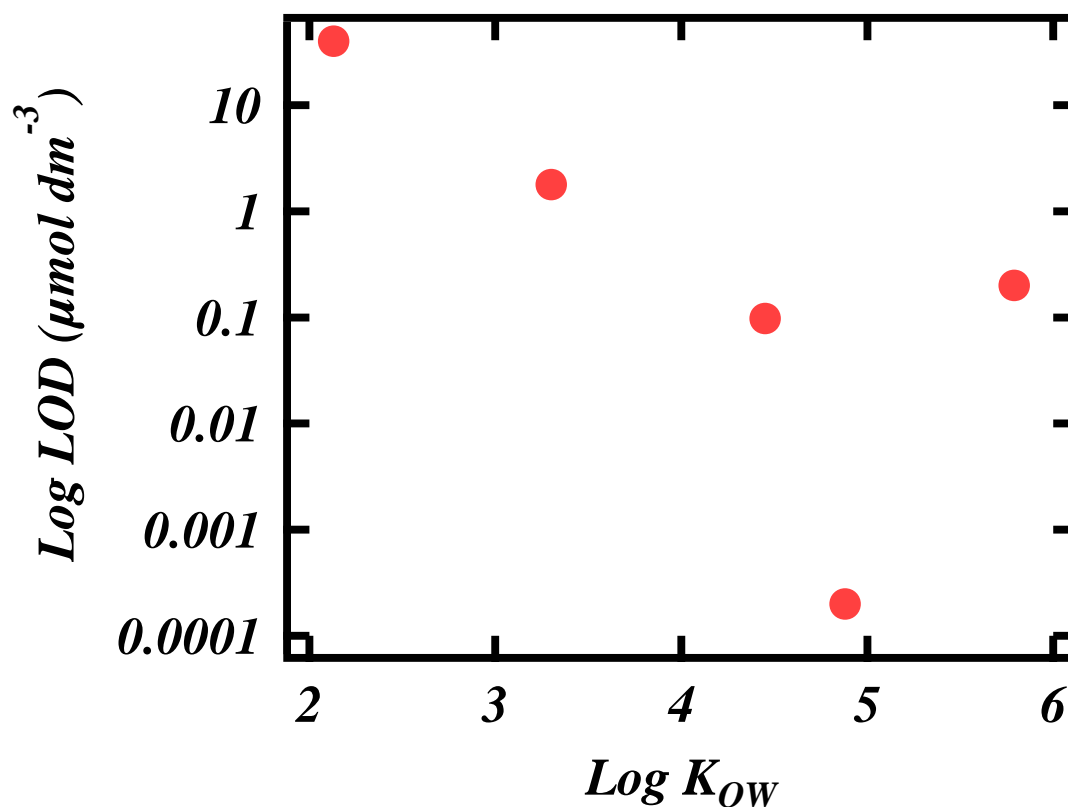


Figure 8.5: Scatter plot of PAH compounds' log LoD at DOPC coated Pt/Hg in PBS at pH 7.4 for benzene, naphthalene, anthracene, pyrene and benzanthracene vs. their respective log octanol - water partition coefficient ( $\log K_{ow}$ ).

## 8.4 DISCUSSION

The relationship between the log LoD and log  $K_{OW}$  is inversely linear for benzene, naphthalene, anthracene and pyrene with benzanthracene as an outlier as shown in Figure 8.5. The trend of interaction for naphthalene, anthracene and pyrene can be related to the increase in the number of aromatic rings whereas the decreased interaction of the four-membered benzanthracene may be explained by its markedly decreased solubility of  $0.014 \text{ mg dm}^{-3}$  in water compared to the water solubilities of naphthalene, anthracene and pyrene which are 31.7, 0.073 and  $0.135 \text{ mg dm}^{-3}$  respectively [20]. It can be intimated that the very low solubility of benzanthracene in water limits its transfer from the aqueous phase to the DOPC although further experiments will need to be done to establish this. In a way this can also be seen as a molecular cut-off where the molecular shape of benzanthracene (see Figure 8.1) determines its decreased interaction despite its increased log  $K_{OW}$ . Such an effect has been well documented for the anomalous relation between the potency of anaesthetics and their log  $K_{OW}$  values [21].

In general, the characteristics that appear to be important for interaction are aromaticity, hydrophobicity and stereochemistry [13]. One advantageous factor is their planarity that allows penetration of lipid monolayer with ease, causing a shift of capacitance peaks. This ease is further noted due to rapidity of interaction. The other factor that compliments their interaction ability is the hydrophobicity (log  $K_{OW}$ ). Anthracene and pyrene have Log  $K_{OW}$  4.45 and 4.88 respectively. These compounds show pronounced membrane activity and have high sensitivity showing that aromaticity plays an important role in the interactions. On the other hand, benzanthracene with a higher log  $K_{OW}$  of 5.79 has a markedly smaller and almost insignificant effect on the lipid monolayer due to its decreased water solubility and irregular molecular shape as discussed above.

The potential shifts of the second capacitance peaks are specific to PAH penetration. This is contributed by the presence of aromatic rings, the high Log  $K_{OW}$  water solubility values and  $\pi$ -electron interactions. This is proven when there is an increase in potential shift using the same concentration of compound with a different number of aromatic rings. The potential of zero charge (PZC) is a fundamental characteristic of the interface of an electrode and the surrounding analyte. The shift of PZC due to adsorption of an organic compound on an electrode interface can be explained by the Esin-Markov effect. The magnitude of the shift is usually linear with the logarithm of electrolyte activity, and the slope of the linear plot is the Esin-Markov coefficient for the condition of surface charge density  $\sigma_M = 0$ . When compounds or ion species are specifically adsorbed and the electrode is being held at the PZC,  $\sigma_M$  changes. Since the electrode is more polarizable than the solution, to regain the condition  $\sigma_M = 0$ , the potential must be shifted to a more negative value. The extent and direction of PZC is useful information that dictates the nature of the adsorbed compound. In general, specific adsorption of anions causes a shift of the PZC towards negative potential. A more negative potential is required to compensate with solution charge. On the other hand, cations cause a shift to positive. It is known the presence of  $\pi$  bond interactions or existence of permanent dipoles cause a greater shift in the PZC [22].

The importance of the presence of the aromatic ring as opposed to hydrophobicity for compound interaction with DOPC monolayers has a generality with pharmaceutical manufacture; the inclusion of an aromatic ring in a compound seems to encourage interaction of an otherwise simple compound with the monolayer. Biologically active painkillers such as paracetamol, ibuprofen and aspirin all contain a benzene ring [23].

## 8.5 SUMMARY

Several important outcomes can be made from this study.

The interaction of PAH compounds in water with DOPC monolayers has an effect on the RCV of these layers on MFE. The capacitance current peaks respond selectively to the interaction of the DOPC monolayer with these compounds which is recorded as a potential shift and reduction of the capacitance current peak height. This has enabled a selective detection of PAHs to be achieved in water.

The extent of penetration vary for different compounds. The characteristic response of the PAHs depends on their number of aromatic rings and orientation of the rings; planar aromatic molecules cause a negative shift of the capacitance current peaks.

The rates of penetration depend to some extent on the water solubility of the PAH. Water solubility enhances the rate of transfer of the PAH from the hydrophilic to the hydrophobic region of the lipid monolayer.

The shift of PZC due to adsorption of an organic compound on an electrode interface can be explained by the Esin-Markov effect.

The findings in this Chapter have stimulated studies on the applications of the lipid-coated electrode to the assay of PAH in natural waters. These results are reported in Chapter 11.

## REFERENCES

- [1] Laffon. *Food and Chemical Toxicology* **2006** 44(10): pp1714–1723.
- [2] Mulas, G Mallocci, G Joblin, C. Toublanc, D. *Astronomy and Astrophysics*, **2006** 446 (2): p537.
- [3] L´opez-Puertas M, Dinelli BM. *The Astrophysical Journal* **2013**, 770 (132) pp8.
- [4] Eickhoff CV, He S, Law FCP. *Environ. Toxicol. Chem.* **2003**, 22(1): pp 50-58.
- [5] Moore. *Environ. Sci. Technol.* **1989** 16: pp31-38.
- [6] Meador. *Mar Ecol Prog Ser* **1995** 123: pp107-124.
- [7] Baars BJ. *Toxicology letters* **2002** 128: pp55-68.
- [8] Laffon. *Mutation Research/Genetic Toxicology and Environmental Mutagenesis* **2006** 20(6): pp1013-1018.
- [9] Pigini I. *Wiley Inter Sci.* **2006** 20 (6): pp1013-1018.
- [10] Meador JP, Stein JE, Reichert WL, Varanasi U. *Rev Environ Contam Toxicol* **1995** 143: pp79-165.
- [11] Reddy CM, Quinn JG. *Marine Pollution Bulletin*, **1999** 38(2) pp:126-135.
- [12] Nelson A. Auffret, N. Readman J. *J. Analytica Chimica Acta* **1988**. 207:pp47–57.
- [13] Nelson A. *Anal. Chim. Acta*, **1987** (194): p139.
- [14] Tietge JE, *Journal of Environmental Indicators*, **2010** 5: pp69-88.
- [15] Tietge JE, Mount DR, Gulley DD. *Environ Toxicol Chem.* **1994** 16: pp2002-2008
- [16] Greene, JC, Bartels CL, Warren-Hicks WJ. B.R. *Protocols for Short-term Toxicity Screening of Hazardous Waste Sites.* **1989** pp3-88.
- [17] Environmental Research Laboratory, Office of Research and Development, U.S. Environmental Protection Agency, Corvallis, American Society for Testing and Materials (ASTM). **1992**. Standard Guide for Conducting Sediment Toxicity Tests with Freshwater Invertebrates.

- [18] Mohamadi S, Tate DJ Vakurov A, Nelson A, *Anal Chimica Acta* **2014** 813: pp83–89.
- [19] Nelson A. Benton A, *J. Electroanal. Chem.* **1986** 202: pp253.
- [20] Lua GN. Danga Z. Taob XQ. Yanga C. *QSAR Comb. Sci.* **2008**, 27: pp 618 – 626.
- [21] Luglia AK. Yostb CS. Kindlerc CH. *Eur J Anaesthesiol.* **2009**, 26: pp807–820.
- [22] Arcade SD, Gildea EE *Electrosorption*. On. Plenum Press. **1967** New York, p87.
- [23] Rainsford KD. *Aspirin and Related Drugs* CRC press **2004**, London.

# CHAPTER 9

## STEROIDS

### 9.1 INTRODUCTION

In Chapter 4, a range of steroids were studied whilst they were incorporated into the layer as part of the monolayer structure, whereas in this Chapter, a range of steroids are studied as an analyte interacting with the lipid monolayer. This Chapter reports the interaction of steroid compounds with DOPC monolayer using RCV electrochemical technique providing further insight into the relation between the compounds' limit of detection (LoD), their structural properties and their biological activity.

Steroids are a class of compounds with a gonane backbone and are essential to life. Steroids have many broad physiological functions including roles in growth and carbohydrate metabolism [1]. Their applications in medicine and pharmaceuticals are also extensive and include anti-inflammatory properties and are used as anti-tumour agents. Conversely glucocorticoids, including dexamethasone have also been found to encourage hippocampal neuronal cell death [2, 3]. The molecular interactions of the steroids; dexamethasone, ethinyl estradiol, stigmaterol, ergosterol and cholesterol with DOPC monolayers on microfabricated Pt/Hg electrodes in an *on-line* high throughput flow system are studied by recording capacitance current peak

changes in RCV. The chemical structures of these compounds are shown in Figure 9.1. They were chosen due to their wide therapeutic use or emphasis to study due to their properties.

Ethinyl estradiol and dexamethasone are semisynthetic steroids. Ethinyl estradiol is a derivative of 17 $\beta$  estradiol; a major endogenous estrogen in humans as well as being used in combined oral contraceptives; one of the main uses of this compound. Dexamethasone is a synthetic corticosteroid. It has anti-inflammatory properties and has a wide use in medicine namely in glucocorticoid resistance therapy and cancer therapy; to counteract the side effect of some antitumor medication.

Another class of steroids are the sterols which are a subgroup of steroids that occur naturally in plants, animal and fungi. Amongst the sterols, ergosterol, stigmasterol and cholesterol were selected for this study. A notable feature of these sterols is the presence of a hydroxyl group at the 3<sup>rd</sup> carbon (C3) position of the typical A-ring of the steroid system. Ergosterol differs structurally from cholesterol in that ergosterol has two more double bonds (at C7 and C22) and an additional 24 $\beta$ -methyl group. Stigmasterol has a core structure identical to that of cholesterol and a side chain structure at C17 similar to that of ergosterol (including a double bond at C22 and a 24 $\beta$ -ethyl group). Ergosterols are the major component of cell membranes found in lower eukaryotes such as protozoa, yeast and fungi. Cholesterol is the most abundant of the sterols, and is the major component of membranes found in higher eukaryotes. It has extensive roles and is essential for all animal life, including as a precursor in biosynthesis of bile acids and vitamin D. Stigmasterol is a plant sterol; also known as a phytosterol. It is found in soya beans, numerous types of vegetables and medicinal herbs.

It is well documented that cholesterol is able to intercalate between lipid molecules, decreasing their permeability and increasing their rigidity by integrating into any free



spaces in the lipid membrane. [4] [5] [6]. Since sterols/steroids are so essential to life, to study them is imperative.

Steroid hormones initially need to penetrate through the cell membrane prior to interacting with target receptors. Whether the membrane permeation process takes place by passive diffusion, by the help of mediators or by some other mechanism(s) is not clear [7].

Dipole moments have also been addressed in this Chapter as a significant parameter promoting steroid interaction with the DOPC layer. Studies on biological activities of other steroid compounds have been explained as instigated through their dipole moments [8].

Dipole moment,  $\mu$  (unit expressed as debye units (D) ) is a measure of molecular polarity. It is the product of distance,  $r$  (the distance expressed in meters (m) ), between magnitudes of charges  $Q$  (expressed in Coulomb (C) ) and represented by the equation

$$\mu = Q \times r \quad (9.1)$$

with the units of

$$\mu \text{ as } C_m \quad (9.2)$$

Non-polar molecules do not possess a dipole moment. The dipole moment is a tool to predict the polarity of a molecule and subsequently its shape:

If  $\mu = 0$ , the bond or molecule is non-polar

If  $\mu > 0$ , the bond or molecule is polar.

Dipole moments provide information about the charge separation in a molecule. The larger the difference in electronegativities of bonded atoms, the larger the dipole moment. Configurational properties can be determined using dipole moment.

Since ions and polar molecule have positive and negative charges, we can use Coulomb's law to evaluate the force between them

$$F = k_e \cdot q_1 q_2 / r^2 \quad (9.3)$$

where  $q_1$  and  $q_2$  are the charges on atoms,  $k_e$  is the electrostatic constant or coulombs constant ( $k_e = 8.9875517873681764 \times 10^9 \text{ N}\cdot\text{m}^2/\text{C}^2 \text{ (m/F)}$ ) and  $r^2$  is the distance between two separated charges.

Dipole potential is an important electrostatic property of biological membranes. Steroids, such as cholesterol are known to influence the dipole potential (as well as other physical properties) of membranes. This could be due to a direct influence of cholesterol's own dipole moment or through cholesterol's condensing ability such that it influences the biological membrane organisation. It is currently thought that a combination of both dipole moment and condensing effect influences the interaction of steroids with biological membranes [9].

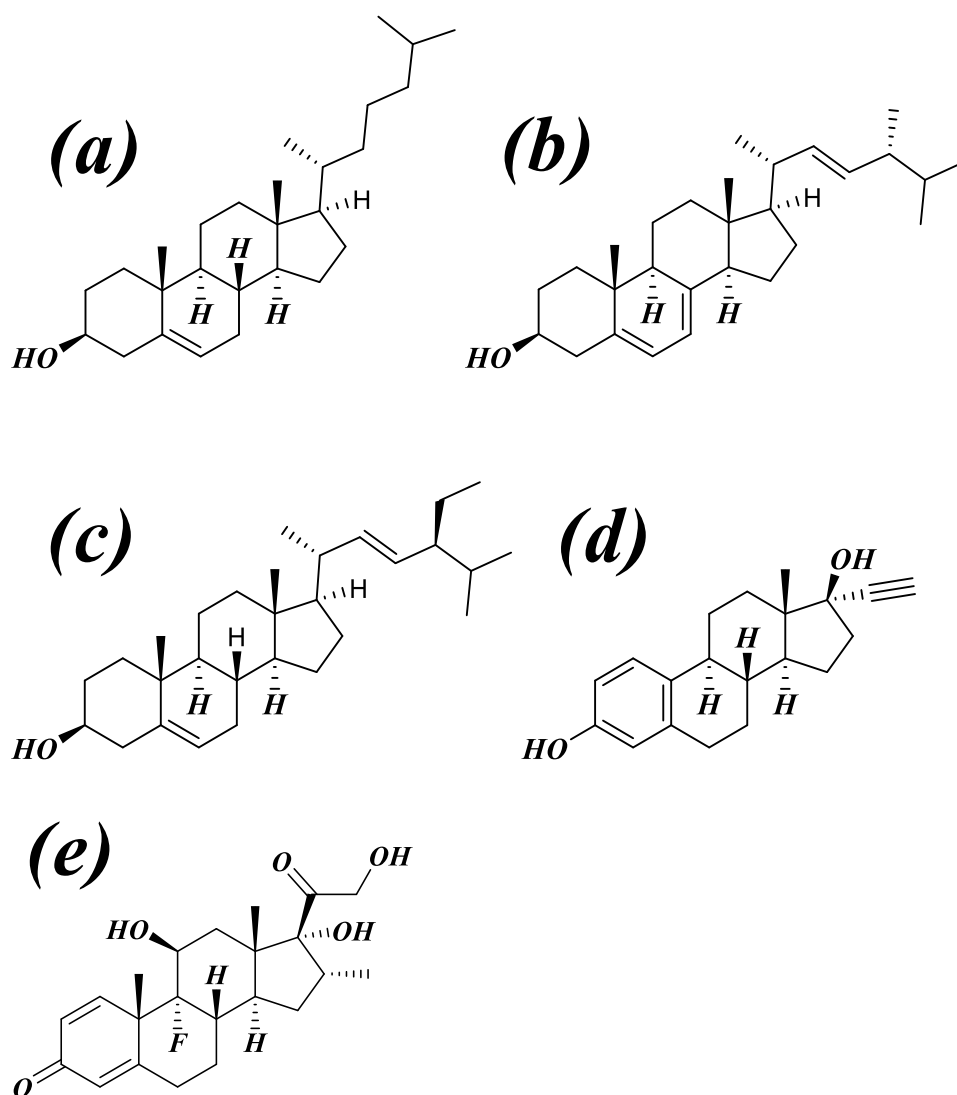


Figure 9.1: Molecular structures of a) cholesterol, b) ergosterol, c) stigmasterol, d) ethinyl estradiol, e) dexamethasone.

## 9.2 MATERIALS AND METHODS

The test compounds of 99% or greater purity were purchased from commercial suppliers, and were used as received. The phospholipid employed for coating electrodes was 1, 2-dioleoyl-sn-glycero-3-phosphocholine (DOPC) (Avanti Polar Lipids Alabaster, AL) and was >99% pure. All other reagents were of analytical grade and purchased from Sigma-Aldrich. The steroids dexamethasone, ethinyl estradiol,

cholesterol, stigmasterol and ergosterol were dissolved in acetone. Concentrations of test compounds were prepared by adding small aliquots of the working solutions to PBS to provide concentrations for testing. The DOPC dispersion for electrode coating was prepared by gently shaking DOPC with PBS to give  $0.2 \text{ mg cm}^{-3}$  dispersion. RCV of DOPC layers in the presence of acetone were conducted to clarify the controls. The effect of acetone on the RCV plot of the DOPC coated Pt/Hg is insignificant. Electrochemical methods were conducted as described in Chapter 2.

## 9.3 RESULTS AND DISCUSSION

### 9.3.1 STEROID – DOPC INTERACTION STUDY

Interaction of steroids with the DOPC monolayer elicits a positive potential shift of the capacitance current peaks. There is a slight but insignificant decrease in the capacitance current peak height however the peaks remain sharp. (Figure 9.2 a) to e)). The largest capacitance current peak potential shift is instigated by dexamethasone-DOPC interaction. The degree of potential shift is also concentration dependent. In addition, the interactions were reversible once the steroid was removed from the flow cell under constant PBS flow. However, the recovery for peak height was dependent on the concentration used and the steroid in question. If the steroid has a particularly high perturbation effect or is in a high enough concentration, it will cause an incomplete recovery of the capacitance current peaks. Figure 9.2 f) displays full recovery of the current peaks after  $3 \mu\text{mol dm}^{-3}$  dexamethasone was removed from the flow cell that is under constant buffer flow over the DOPC coated Pt/Hg electrode. These results show a specific fingerprint to each steroid-DOPC interaction in the system.

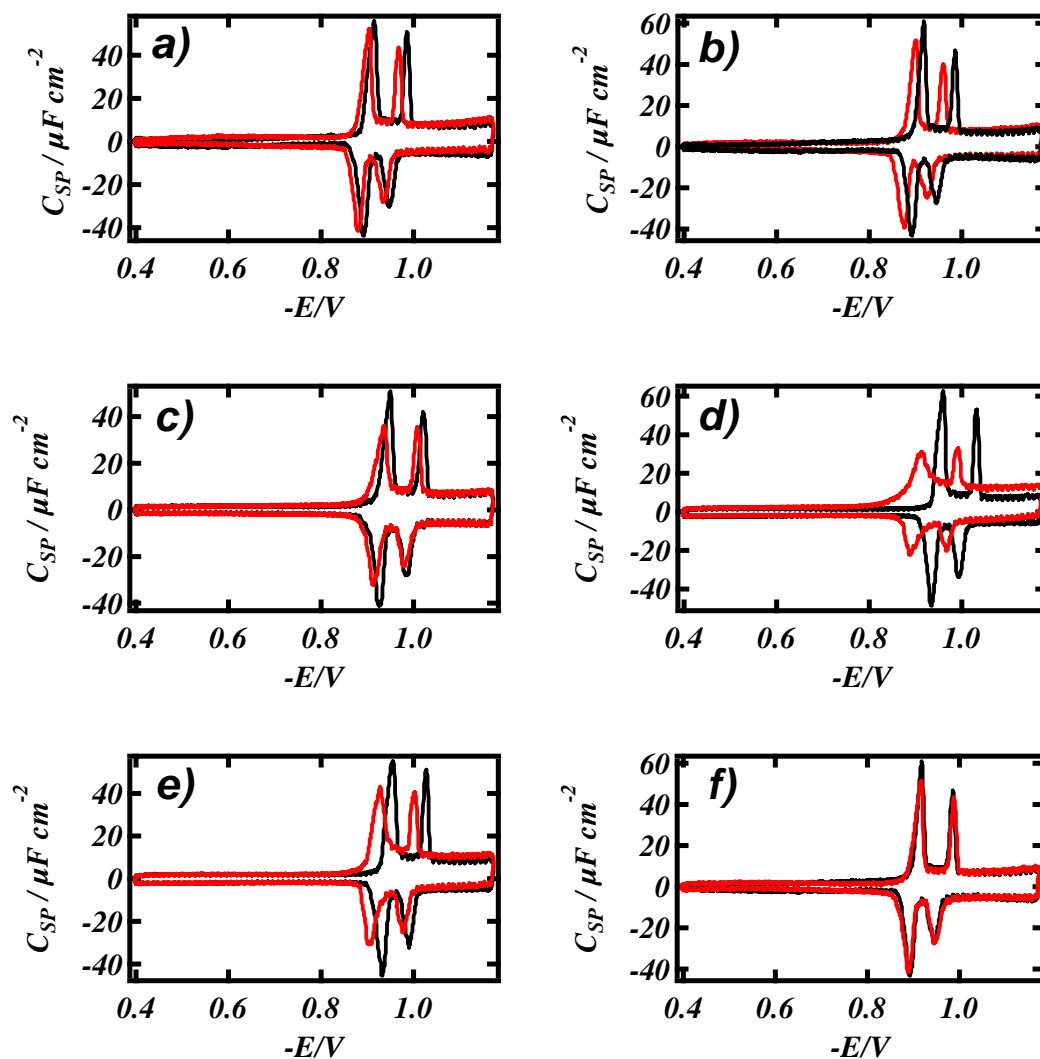


**Figure 9.2:** RCVs recorded at  $40 \text{ Vs}^{-1}$  of a DOPC coated Pt/Hg electrode (black line) in the presence of (red lines) a)  $6 \mu\text{mol dm}^{-3}$  cholesterol, b)  $6 \mu\text{mol dm}^{-3}$  stigmasterol, c)  $3 \mu\text{mol dm}^{-3}$  ergosterol, d)  $30 \mu\text{mol dm}^{-3}$  ethinyl estradiol and (e)  $3 \mu\text{mol dm}^{-3}$  dexamethasone. f) shows the recovery of capacitance current peaks post  $3 \mu\text{mol dm}^{-3}$  dexamethasone interaction.

The detection limits for each steroid was estimated (Figure 9.3). The changes in potential of the capacitance current peak on the RCV is used for the LoD estimation since it is significantly affected by the steroid-DOPC interaction. The LoD values are displayed in Table 9.2. From the LoD results, the extent of interaction of the steroids

is found to be in the order cholesterol < ergosterol < stigmasterol < ethinyl estradiol < dexamethasone.

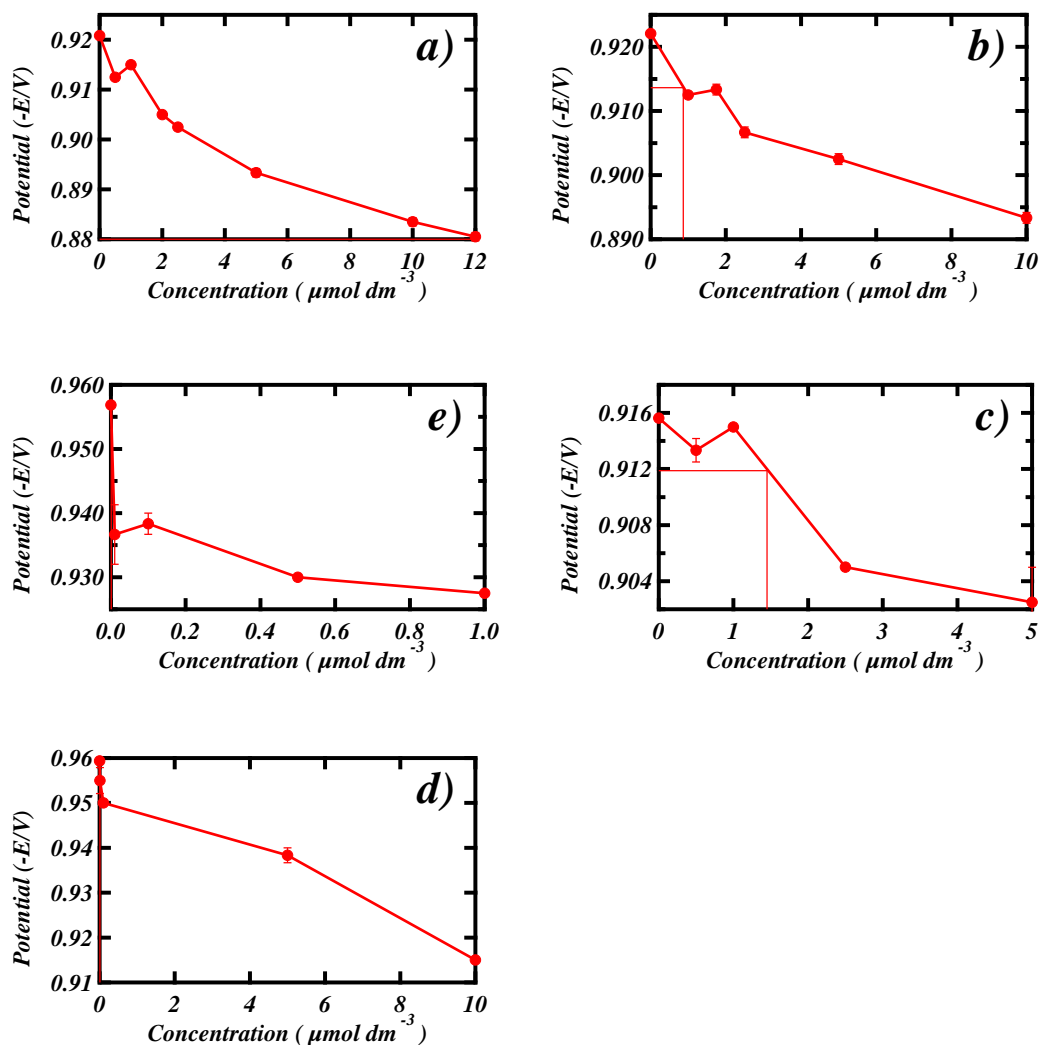


**Figure 9.3: LoD determination by estimating concentration corresponding to three times standard deviation (SD) of DOPC control capacitance current peak potential versus concentration curve for a) cholesterol, b) stigmasterol, c) ergosterol d) ethinyl estradiol and e) dexamethasone interaction with DOPC coated Hg in PBS at pH 7.4.**

### 9.3.2 POTENTIAL SHIFT VS. CONCENTRATION

The interaction of the steroids with DOPC monolayers is concentration dependent as well as compound dependent (Figure 9.4). The capacitance current peak potential's dependence on steroid interaction show that the capacitance peaks relating to phase transitions form at more positive potentials; indicating that overall the membrane is more positive.

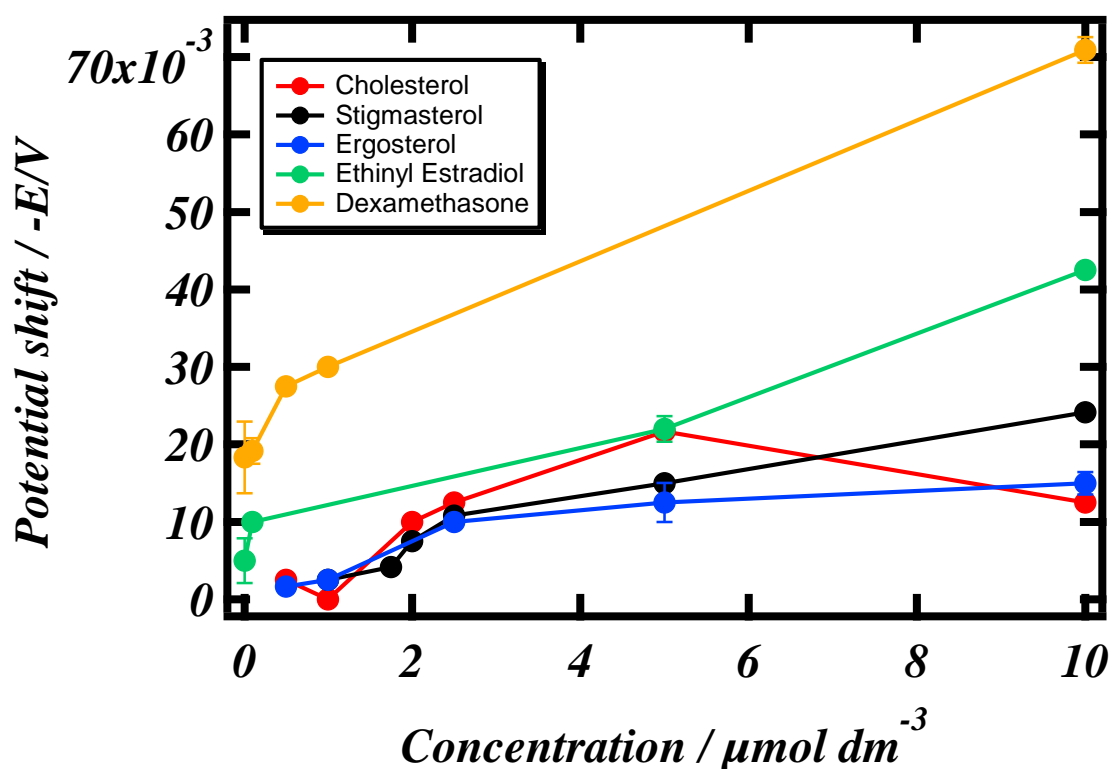


Figure 9.4: Plot showing capacitance current potential ( $-E/V$ ) vs. concentration ( $\mu\text{mol dm}^{-3}$ ) of the steroid compounds cholesterol (red line), stigmasterol (black line), ergosterol (blue line), ethinyl estradiol (green line) and dexamethasone (yellow line). Potential values were obtained from RCV experiments ( $-0.4\text{V}$  to  $-1.2\text{V}$  at  $40\text{V}\cdot\text{s}^{-1}$  in PBS at pH 7.4).



### 9.3.3 DIPOLE MOMENT

Previous studies have shown that cholesterol influences the surface potential of biomembranes, through increasing the membrane dipole potential [8]. Dipole moments are important in the interactions which occur between molecules. It is described as the attraction of the uncharged, partial positive end of a first polar molecule, commonly designated as  $\delta^+$ , to the uncharged, partial negative end of a second polar molecule, commonly designated as  $\delta^-$ . Dipole interactions can occur between the electropositive head group of DOPC, for example the choline head group, of phosphatidylcholine and an electronegative atom commonly associated in steroids for example, a heteroatom, such as oxygen.

Steroid interaction studies have been conducted with monomolecular films of insoluble lipid molecules on water using Langmuir trough [10] and L- $\alpha$ -dipalmitoylphosphatidylcholine (DPPC) in a monolayer and in a bilayer [11]. Results from these previous studies show that interaction between the phospholipids and steroids would be dependent on the number of functional group present. Factors such as the side chains and the existence of a double bond in the side chain of the steroid ring were found to be the influencing features to lipid interaction. The presence of substituents can significantly affect the polarity of the steroid compounds. The presence of hydroxyl group increases polarity, whereas the position of double or triple bonds and chain lengths decreases polarity but increases polarisability to varying degrees [12]. The effect of steroid polar/apolar regions influencing interaction has been favourably shown in other studies [13, 14].

Compound	Dipole moment ( $\mu$ )	Potential shift (-V)
Cholesterol	1.87	0.009861
Stigmasterol	2.487	0.010694
Ergosterol	1.48	0.008333
Ethinyl estradiol	4.8	0.019792
Dexamethasone	3.828	0.02375

**Table 9.1: Dipole moments ( $\mu$ ) of steroids and average potential shifts (-V) of concentrations ranging from 0.5 to 10  $\mu\text{mol dm}^{-3}$**

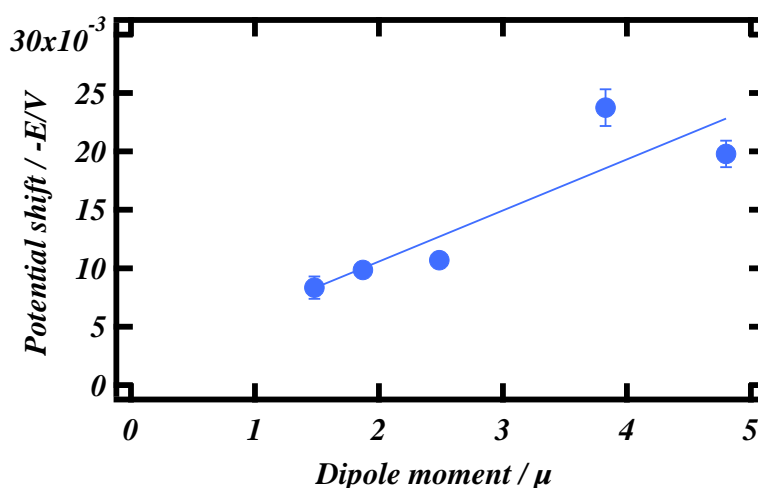


**Figure 9.5: Plot showing the relationship of potential shift (-E/V) and dipole moment ( $\mu$ ) of steroids. The values are listed in Table 9.1.**

A correlation is found between dipole moments,  $\mu$  ( $\mu$ ) values [15-17] of steroids vs. the effect on peak potential shift. Table 9.1 lists these values. A positive linear correlation was observed between these parameters with a correlation coefficient  $r^2 = 0.7864$  (Figure 9.5). These results suggest that membrane dipole potential could be a sensitive determinant of lipid-steroid interactions.

Compound	Dipole moment ( $\mu$ ) [15-17]	LoD ( $\mu\text{mol dm}^{-3}$ )
Cholesterol	1.87	12
Stigmasterol	2.487	0.8
Ergosterol	1.48	1.4
Ethinyl estradiol	4.8	0.007
Dexamethasone	3.828	0.0011

**Table 9.2: Dipole moment values of the steroid compounds and their LoDs.**

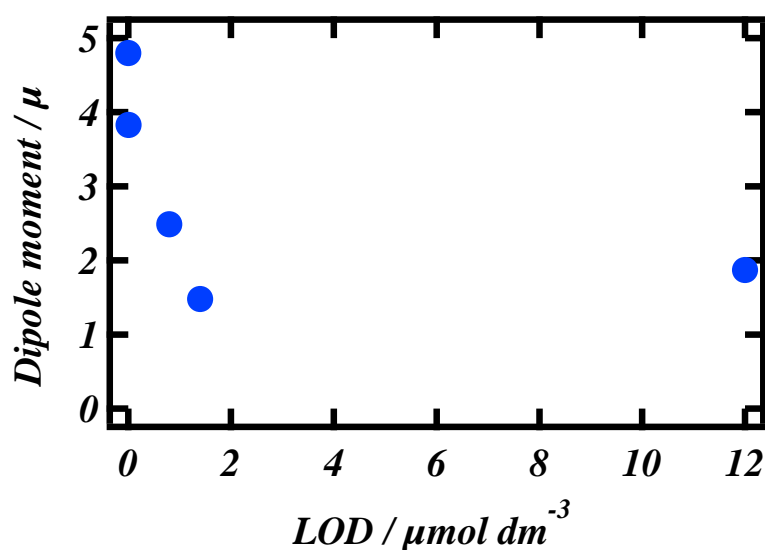


**Figure 9.6: Plot of dipole moment ( $\mu$ ) vs. limit of detection (LoD) at DOPC coated Pt/Hg in PBS at pH 7.4 for steroid compounds.**

A further relationship is found between steroid compounds' dipole moments vs their LoD values. Plots of the dipole moments of the steroid compounds vs. their LoDs in Figure 9.6 show a correlation. The  $\mu$  and LoD values are listed in Table 9.2. The negative correlation shows that dipole moment may be partly responsible for the activity at the level of the phospholipid membrane. However, the dipole moment-LoD relationship for cholesterol is an outlier to this. The larger dipole moments of dexamethasone and ethinyl estradiol greatly increase their sensitivity to DOPC interaction.

## 9.4 SUMMARY

There have been studies to attempt the recognition of steroid molecules using synthetic receptors or other sensor systems [18, 19]. With the DOPC coated Pt/Hg electrode MFE system, the interaction and exclusive sensing of steroids in solution have been shown. This system is not limited to steroids; it has been a great sensing tool for many compounds.

The steroids interact with the DOPC coated electrode to varying degrees as shown by their effect on the capacitance current peaks in the RCV plot, even though structural differences between them are subtle.

From the RCV plots, the capacitance current peak height and potential shifts are recoverable when the steroid is removed from the DOPC environment. This suggests that the steroids can integrate into the lipid monolayer to an extent but not fully which is also indicative of a surface active compound. Studies have shown that steroids are surface active even though their biological effects are produced with receptors [20]. This gives an important insight to the hypothesis that some steroids adsorb at platelet surfaces and are able to alter the surface properties but also that the alterations are temporary.

The ability of the steroids to integrate into the lipid monolayer indicates that they can form specific complexes with the phospholipid. It is also possible that the steroids are able to change surface charge on lipid membrane. This has important implications as changing surface charge on a membrane can greatly affect cellular activities. For example, alteration in the potential of the membrane has been shown to influence the activity of integral membrane proteins such as  $\text{Na}^+/\text{K}^+$ -ATPase [21] and the ion channel gramicidin [22] as well as the activity of ionic drug compounds that would normally interact with the lipids.

It is well known that one of the important functions of cholesterol is its barrier properties for phospholipids. Cholesterol is known to reduce permeability of biomembranes due to its condensing and packing effect. However, any defects due to bad packing can cause the membrane to be more permeable to ions. Other sterols can cause the same effect. The condensing effect of sterols has been referred to in more detail in Chapter 4.

**REFERENCES**

- [1] Voet. D , Voet JG. *Biochemistry* **2004** Wiley, new York 3<sup>rd</sup> edition
- [2] Goericke SL, Engelhorn T. *J Cereb Blood Flow Metab* **2010** 30(4): pp801–807
- [3] Sapolsky RM, Pulsinelli WA *Science* **1985** 229: pp1397–1400
- [4] Hanukoglu I. *J Steroid Biochem Mol Biol* **1992** 43 (8): pp779–804
- [5] Corvera E. Mouritsen OG. Singer MA, Zuckermann MJ. *Biochimica et Biophysica Acta* **1992**. (1107): pp261-270.
- [6] Needham D, Nunn RS. *Biophysical Journal*. **1990** 58: pp997-1009.
- [7] Farach-Carson MC, Davis PJ. *J Pharmacol Exp Ther*. **2003** 307(3): pp839-45.
- [8] Dittrich F, Repke KRH, *Experientia Supplementum* **1976** 23: pp249-254.
- [9] Starke-Peterkovic, T, Turner N, Clarke RJ. *Biochemistry* **2006** 47: pp7090–7096.
- [10] Gershfeld NL, Muramatsu M *The Journal of General Physiology* **1971** 58: pp 650-666
- [11] Yamauchi H, *Langmuir* **1993**,9: pp300-304
- [12] Starke-Peterkovic T, Turner N, Vitha MF. *Biophys J*. **2006**; 90(11): pp4060–4070
- [13] Orsi M, Essex JW, *Soft matter*, **2010**, 6: pp3797 – 3808
- [14] Bernsdorff C., Winter R. J. *Phys. Chem. B*. **2003** 107: pp10658–10664.
- [15] Haldar S, Kanaparthi RK, Samantha A. *Biophys J* **2012** 102(7): pp1561-1569
- [16] Lewis DFV, Loannides C, Parke DV, *Journal of Steroid Biochemistry and Molecular Biology* **2000** 74(4): pp179-185
- [17] Lewis FV. Ogg. MS, Goldfarb PS, Gibson GG. *Journal of steroid biochemistry and molecular biology* **2002** 82: pp195-199
- [18] Higler, P. Timmerman,W. Verboom, DN. *J. Org. Chem*. **1996**, 61: pp5920-5931.
- [19] Paleos CM, Tsiourvas D. *Advance Matter*. **1997**, 9: pp695-710

- 
- [20] Rebolj K, Maček P, Sepčič K *Biochimica et Biophysica Acta* **2006** 1758: pp1662–1670.
- [21] Starke-Peterkovic T, Turner N., Clarke R.J. *Am. J. Physiol. Regul. Integr. Comp. Physiol.* 2005 288: pp663–670.
- [22] Duffin RL, Garrett MP, Busath DD. *Langmuir*. 2003 19:pp1439–1442.

# CHAPTER 10

## TRICYCLIC ANTIDEPRESSANTS AND PHENOTHIAZINES

### 10.1 INTRODUCTION

Tricyclic antidepressants also known as TCAs and tricyclic phenothiazines, are widely used for the treatment of affective disorders. Affective disorder is a collective term for a range of mood disorders, the main types being depression, bipolar disorder, and anxiety disorder. Each of these types have subtypes which vary in severity and also vary per individual. Neurotransmitters play a major role in affecting mood. If the neurotransmitters are imbalanced in anyway an affective disorder can result. Causes of neurotransmitter imbalance and hence affective disorders are actively being studied. To date, there is no known single cause for affective disorders and there are various pathways to which the neurotransmitters can become impaired. However, it is generally accepted that the reasons can be due to several factors. These are genetic defects, traumatic environmental influences and/or induced by the use of drugs/alcohol. A person may be more predisposed to affective disorders if they had a combination of these factors.

At a molecular level, undoubtedly, any defect in gene expression will result in faulty expression of proteins integrated in neurotransmitter functions. Studies on neurotransmitters often show opposing results [1, 2]. This is partly due to the behavioural methods chosen but also due to the many individual variations and



predispositions mentioned making it complicated to generalise results. Symptoms of affective disorder manifest in different ways for different people. Current treatments available often take several weeks to work, can sometimes be ineffective which results in delay in treatment and have a host of side effects. Clearly there is a need for a successful treatment. There are many neurotransmitters under investigation in the hopes of targeting and curing affective disorders. The neurotransmitters most prevalently studied and known to have an effect are serotonin and dopamine. It should be noted that treatment is often targeted at both these neurotransmitters.

### **10.1.1 NEUROTRANSMITTERS: BRIEF INTRODUCTION TO 5-HT AND DOPAMINE**

#### **10.1.1.1 SEROTONIN (5-HT) AND 5-HT RECEPTOR**

Serotonin is biosynthesised via a biochemical conversion process. Tryptophan, a building block to proteins, combines with tryptophan hydroxylase to form, 5-hydroxytryptamine (5-HT) otherwise known as serotonin. Serotonin is not only a neurotransmitter, it also has roles in the cardiovascular system, muscles and various elements in the endocrine system, thus any pharmaceutical compound targeting serotonin has implications manifested in side effects. Considerable evidence has ensued in the last two decades to support the hypothesis that alterations in serotonergic neuronal function in the central nervous system occur in patients with major depression [3]. Serotonin (5-HT) receptors are classified into 7 types, 5-HT<sub>1</sub>, 5-HT<sub>2</sub>, 5-HT<sub>3</sub>, 5-HT<sub>4</sub>, 5-HT<sub>5</sub>, 5-HT<sub>6</sub> and 5-HT<sub>7</sub>. Each type can have further subtypes, classified by a letter. These receptors are coupled to G proteins except 5-HT<sub>3</sub> receptors which are channels. The distribution of 5-HT receptors are not localised to a specific area within the body.

A correlation has been found between the 5-HT affinity  $K_i$  of the tricyclic compounds drugs with their LoDs determined in this work.  $K_i$  represents the concentration of compound that could occupy 50% of receptive space (where no radioligand is present) and is an absolute value. It has been hypothesised that various antipsychotic drugs have affinity for various types of 5-HT in particular 5-HT<sub>2</sub> [4]. Other studies have concluded that effective antipsychotics have multiple target sites [5]. Phenothiazines for example have affinity to dopamine receptors which are discussed in the next section; however their clinical effect is enhanced by simultaneous binding to 5-HT. Empirical data show that phenothiazines have greater affinity to dopamine and 5-HT receptors than the other tricyclics studied. In fact phenothiazines are predominantly dopaminergic but they do have affinity towards 5-HT as well. One definite functional group that enhances affinity to 5-HT<sub>2</sub> is the presence of an aromatic ring [6].

#### **10.1.1.2 DOPAMINE AND DOPAMINE RECEPTOR**

Dopamine is biosynthesised by the conversion of amino acid L-tyrosine to L-3,4-dihydroxyphenylalanine (L-DOPA) with catalysis by tyrosine hydroxylase. L-DOPA is a precursor to dopamine. Dopamine is known for its reward, motivation, addiction behaviour and the regulation of motor control [7]. Patients with depression often exhibit reduced motivation, anhedonia and lethargy. The physiological conditions underlying reduced dopamine signalling could result from either diminished dopamine release from presynaptic neurons or impaired signal [7]. Interestingly, motor defects of Parkinson's disease can be alleviated with levodopa [8]. Studies have shown that antipsychotic drugs may show their clinical influence by affinity to more than one target receptor, one being dopamine D<sub>2</sub> receptor. It is known that there is increased potentiation of neurotransmission in the mesolimbic dopamine system. This neural system plays a role in motivation and reward related behaviour which is moderated in

patients with depression. Therefore, antidepressant drug compounds target dopamine receptors and in particular the receptor subtype D2 has been found to be the most clinically significant. There are other D subtypes; however their role in anti-depression targeting is inconclusive. Studies have shown that there are unique differences between antipsychotic drugs for their degree of affinity to receptors [9]. The tricyclic antidepressants and phenothiazines that have been studied in this chapter are surface active and amphiphilic. Surface active drugs bind to the biomembrane surface causing disruption while they are solubilised in this state. Hydrophobic interactions have a contribution to the binding affinity to the dopamine receptor, however steric interactions plays a key selectivity role in binding [9].

### **10.1.2 TRICYCLIC ANTIDEPRESSANTS AND PHENOTHIAZINES**

The TCAs are amphiphilic; they bear an ionic (zwitterionic, anionic or cationic) or non-ionic polar head group and a hydrophobic portion. In light of the properties and applications of tricyclic antidepressants and phenothiazines, the AGNP-TDM panel of experts has emphasized the importance of therapeutic drug monitoring [10]. Furthermore, there is still uncertainty about the mechanism by which tricyclics and most common antidepressants work. An example is that of chlorpromazine. In 1952 chlorpromazine was the first of the modern antipsychotic drugs to be released and has been the subject of countless research studies over the years [11]. Chlorpromazine is extensively metabolized in the body and some of the metabolites remain pharmacologically active for some time. Understanding how these compounds work has improved, due to better technology. In spite of this, much is still to be understood about the mechanisms of their membrane permeability since studies are often not comprehensive or conclusive. This is partly due to the pharmacokinetic variability that these compounds possess making it difficult to understand their mechanism of action and response. These compounds may undergo different

associations and their site of action in the organism is frequently the plasma membrane. Even if their target is intracellular, the interaction with the membrane barrier plays a fundamental role although the compounds are already known to bind to biological membranes.

Previous studies have acknowledged that TCAs can interact with cell membranes, [12] or have proven that TCAs can induce lipidosis [13] and even further studies over the years have attributed the side effects of the TCAs to changes they cause to lipid physical state and integrity [14-19]. Due to their clinical importance, analytical methods have been developed to monitor these compounds. The analytical methods commonly employed for monitoring are chromatography (GC, HPLC) and mass spectrometry. However, these methods are laborious and time consuming.

In this chapter, a new assay method has been employed using a fabricated MFE within flow system and RCV as an interrogative technique; which has highlighted its excellent reproducibility and characterised the effects of 6 tricyclic compounds. A complimentary technique; fluorescence spectrophotometry has also been used.

These technologies will be discussed further. The results suggest that, the structural changes in the biomembrane-like sensor elements caused by interaction with these tricyclic drugs depend on the chemical structure of these drugs. This study focuses at the molecular level, to establish the primary interaction that these compounds have with the biomembrane which is the primary barrier to most of these compounds into the organism. The structural integrity of lipids also determines the biological functions of the biomembrane entities such as enzymes and receptors [20, 21]. It is possible that while the antidepressant drugs are targeting a receptor, a proportion interacts with the membrane and perturbs the membrane and thus cause disruption to membrane linked moieties. This could be the cause of side/toxic effects. Figure 10.1

shows how closely related receptor proteins are linked to cell membranes. Any perturbation of cell membrane could affect the functioning of linked proteins.

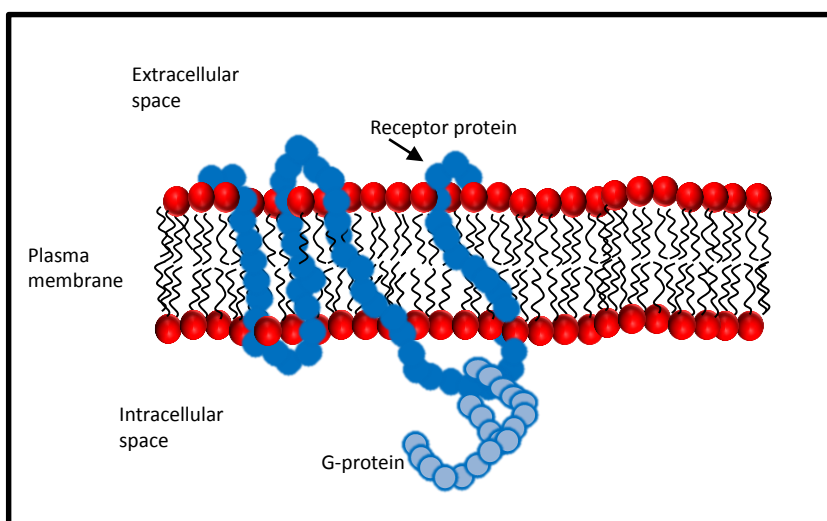


**Figure 10.1: Molecular structure of plasma membrane with integrated G-coupled protein.**

Drug compounds should be able to reach their target. If too hydrophobic, it will be unable to pass through the blood brain barrier (BBB) and if too hydrophilic then higher concentrations are required to promote biomembrane penetration. The difference in biological and biomembrane activity between the compounds can be attributed to differences in steric properties and size due to their functional groups. Using the empirical data in this study, we are able to obtain information about the parameters and functional groups behind drug selectivity and improved binding properties. The work is beneficial to finding lead compounds from a range of novel pharmaceutical agents.

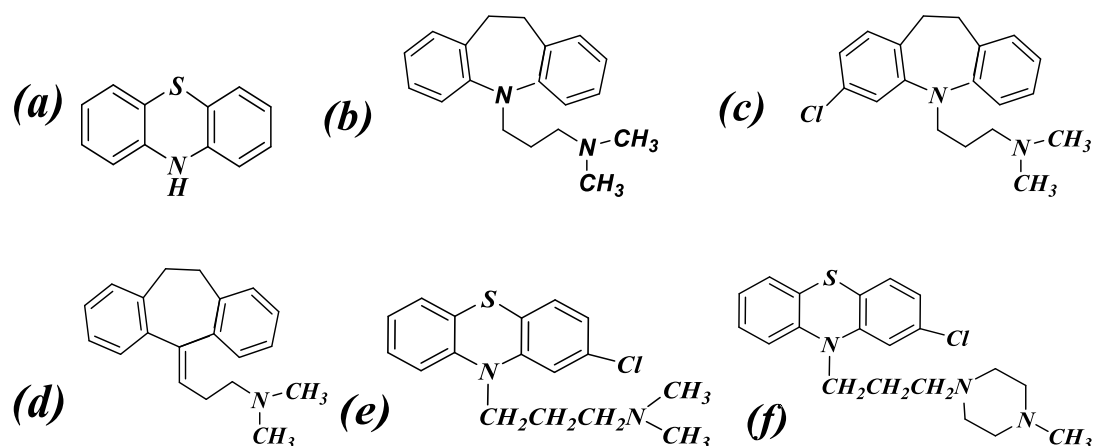


**Figure 10.2: Molecular structures of tricyclic antidepressants and tricyclic phenothiazines. a) phenothiazine, b) imipramine, c) clomipramine, d) amitryptilline, e) chlorpromazine f) prochlorperazine.**

### 10.1.3 FLUORESCENCE SPECTROSCOPY

Fluorescence spectroscopy is one of the most widely used techniques due to its intrinsic selectivity and sensitivity. The compounds being studied will have a natural low energy state or ground electronic state ( $S_0$ ) as well as higher excited energy states ( $S_1$ ). In both of these energy states are various vibrational states.

Experiments involve using a beam of ultraviolet light that excites the aromatic part of the test compound capable of fluorescence. The  $\pi$  electrons of the aromatic system absorb the light and then step from the ground electronic state  $S_0$  to the excited electronic state  $S_1$ . Collisions with other molecules in the vicinity of the test compound causes loss of vibrational energy which eventually leads to the compound dropping to one of the vibrational levels of  $S_0$  again whilst emitting light in the process. This light emitted results in fluorescence. Thus, measurements are made of the intensity of emitted energy of a compound after it is exposed to an excited light source. The compounds used in this study such as imipramine have natural fluorescence.

In these measurements, a quencher is used at varying concentrations. Quenching is the process that decreases fluorescence intensity. Common chemical quenchers are iodide ions and acrylamide [22]. In the absence of a quencher, the excited compound emits light when returning to  $S_0$ . When a quencher is present, the excited compound can return to  $S_0$  by transferring its energy to the quencher without the emission of light. Changes in fluorescence intensity can be used to determine any binding of test compounds with DOPC vesicles.

In the current experiment, potassium iodide, KI is used as the quencher. Iodide ( $I^-$ ) does not penetrate the hydrophobic region of the bilayer which is suitable in this study as it will not interfere with lipid interaction.

## **10.2 MATERIALS AND METHODS**

The test compounds of 99% or greater purity were purchased from Sigma Aldrich, and were used as received. The phospholipid employed for coating electrodes was 1, 2-dioleoyl-sn-glycero-3-phosphocholine (DOPC) (Avanti Polar Lipids Alabaster, AL) and was >99% pure.

### **10.2.1 ASSAY EXPERIMENT**

For the assay, RCV was conducted as described in Chapter 2. The electrolyte used throughout the experiments was PBS at pH 7.4. Stock solutions were made up as follows. Phenothiazine, prochlorperazine and chlorpromazine were dissolved in acetone and the tricyclic anti-depressants (TCAs): imipramine, clomipramine and amitriptyline, were dissolved in Milli-Q water (18.2M $\Omega$ ). Concentrations of test compounds were prepared by adding small aliquots of the working solutions to PBS to provide concentrations for testing. PBS with no compound addition was the control

electrolyte. The DOPC dispersion for electrode coating was prepared by gently shaking DOPC with PBS to give  $0.2 \text{ mg cm}^{-3}$  dispersion.

### 10.2.2 FLUORESCENCE SPECTROSCOPY

For the fluorescence study, the required solutions are prepared as follows:

A primary DOPC stock solution of  $10 \text{ mg/ml}$  ( $20 \text{ mL}$ ) is prepared by dissolving DOPC in  $0.1 \text{ mol dm}^{-3}$  KCl with added  $0.001 \text{ M}$  phosphate buffer. Giant unilamellar vesicles containing  $4.2 \%$  ethanol and  $0.2 \text{ mg cm}^{-3}$  DOPC are prepared by diluting calculated amount of DOPC stock solution in a measuring flask containing calculated amount of ethanol followed by the addition of  $0.1 \text{ mol dm}^{-3}$  KCl (containing  $0.01 \text{ mol dm}^{-3}$  phosphate buffer) gently along the wall of flask with constant swirling. The buffer must be added gradually and along the side of container.

A primary stock solution of KI ( $8.0 \text{ mol dm}^{-3}$   $20 \text{ ml}$ ) is prepared in  $0.2 \text{ mmol dm}^{-3}$  sodium thiosulphate in ( $18.2 \text{ M}\Omega$ ) MilliQ water. Sodium thiosulphate is used as an oxidant to prevent the oxidation of iodide to iodine. Secondary stock solutions of  $2 \text{ mL}$  of KI are prepared by dilution from  $8 \text{ M}$  KI again using  $0.2 \text{ mmol dm}^{-3}$  sodium thiosulphate in ( $18.2 \text{ M}\Omega$ ) MilliQ water.

The experimental procedure is as follows:

The fluorescence quenching experiments of the drug were performed in the presence of vesicles using the quencher potassium iodide.

- [1] Excitation wavelengths of the compounds are obtained from determined literature values. Excitation wavelength of  $310 \text{ nm}$  and emission wavelength of  $415 \text{ nm}$  was used.



- [2] Fluorescence spectra of 3 mL of DOPC vesicles with added 0.15 mL buffer (to compare the dilution to that of quencher addition) at specific excitation wavelengths (for each compound) are recorded as blanks.
- [3] 3ml of the test compound is then added to the primary DOPC vesicle stock solution. The final concentration of the test compound was calculated.
- [4] Fluorescence spectra of 3 mL of DOPC vesicles containing test compound with added 0.15 mL buffer at specific excitation wavelengths (for each compound) are recorded in the absence of quencher.
- [5] Aliquots of concentrated solutions of 0.15ml KI were added directly to the drug/vesicle solution contained in the fluorescence cuvette and the fluorescence intensities were monitored; data were analyzed by Stern–Volmer plots

This is then repeated for all the concentrations of KI secondary stock solutions prepared and for all the test compounds [23].

Maximum fluorescence intensities were measured from the fluorescence spectra and  $F^0/F^0 - F$  is calculated where  $F^0$  is the maximum fluorescence intensity of compound in vesicles in the absence of KI and  $F$  is the maximum fluorescence intensity of compound in vesicles in the presence of KI at that particular concentration,  $[Q]$  is the concentration of quencher, and  $(1/f_a K)$  is the slope.  $F^0/F^0 - F$  is plotted versus concentration of the KI according to the modified Stern-Volmer equation. The percentage of the accessible (quenched) and inaccessible (not quenched) compounds were calculated. The Stern-Volmer quenching constants are calculated from slope  $(1/f_a K)$  of the plots.

$$F^0/F^0 - F = \frac{1}{f_a K [Q]} + 1/f_a \quad (10.1)$$

Plotting the Stern-Volmer plot allows the estimation of the slope which indicates the accessibility of the test compound to the quencher,  $K_I$  [24]. Changes in the slope are as a result of substrate binding. A linear Stern-Volmer plot also indicates that the test compounds behave similarly. On the other hand curved Stern-Volmer plots suggest that there may be two different classes of compounds present.

## 10.3 RESULTS AND DISCUSSION

### 10.3.1 RCV SCANS

RCV scans have shown that the TCA and tricyclic phenothiazine interactions with lipid are reversible. The reversibility was dependent on the concentration of the compound used and the particular compound in question. Once the compounds have desorbed from the lipid; the lipid monolayer reverts to its original configuration. These results indicate that the compounds interact by associating with the surface of lipid monolayer.

Figure 10.3 displays the results of the RCV plots from the interaction of DOPC coated MFE with the tricyclic compounds. An excellent reproducibility of the peaks was achieved in the presence of the tricyclics. The interaction of the tricyclic phenothiazine (Figure 10.2) with the DOPC layer effects a shift of the RCV capacitance current peaks to negative potentials concurrent with a peak depression (Figure 10.3 f)). On the other hand, the effect of a side chain attached to the phenothiazine nitrogen atom in prochlorperazine (Figure 10.2) greatly increases the sensitivity of DOPC to the interaction and alters the response of the RCV plot to the interaction in that the capacitance current peaks are depressed with minimal shift (Figure 10.3 f)). The interactions of the phenothiazine derived antipsychotics and the TCAs with the DOPC monolayer show that the presence and nature of the substituent side-chain alters the

compound's LoD value considerably. The determination and significance of LoD was explained in Chapter 2.

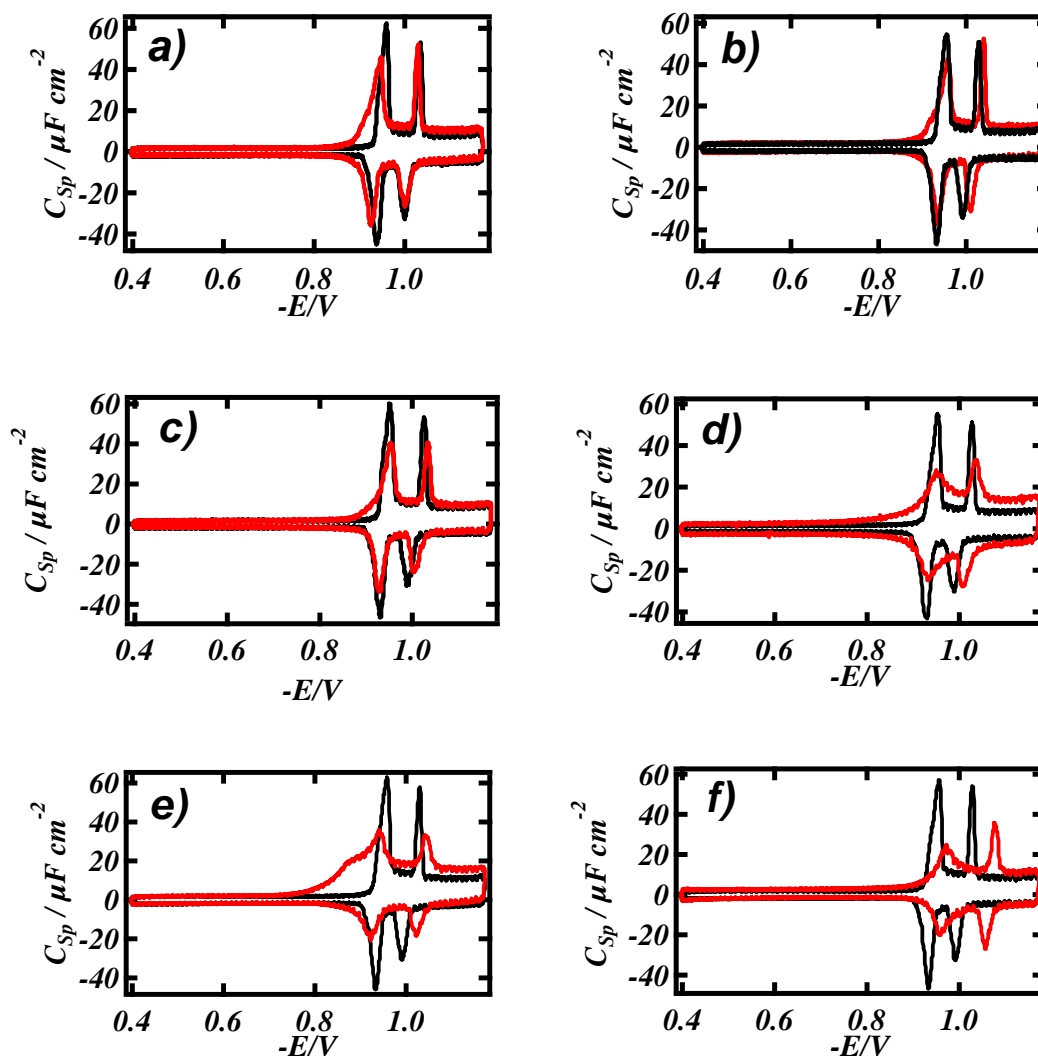


**Figure 10.3:** RCVs recorded at  $40 \text{ Vs}^{-1}$  of a DOPC coated Pt/Hg electrode (black line) in the presence of a)  $0.3 \mu\text{mol dm}^{-3}$  clomipramine, b)  $0.3 \mu\text{mol dm}^{-3}$  imipramine, c)  $0.3 \mu\text{mol dm}^{-3}$  amitryptilline, d)  $0.3 \mu\text{mol dm}^{-3}$  prochlorperazine e)  $0.3 \mu\text{mol dm}^{-3}$  chlorpromazine, and f)  $5 \mu\text{mol dm}^{-3}$  phenothiazine (red line) in PBS at pH 7.4.

Plots of the therapeutic activity of the drug pharmaceutical compounds vs. the detection limit values for the tricyclic phenothiazines and antidepressants in Figure 10.4 show a correlation. Uncertainty is introduced by a range of literature values for

the therapeutic “normal” concentration [25-31] of the pharmaceutical compound but the positive correlation shows that activity at the level of the phospholipid membrane maybe partly responsible for the compounds' respective therapeutic activity.

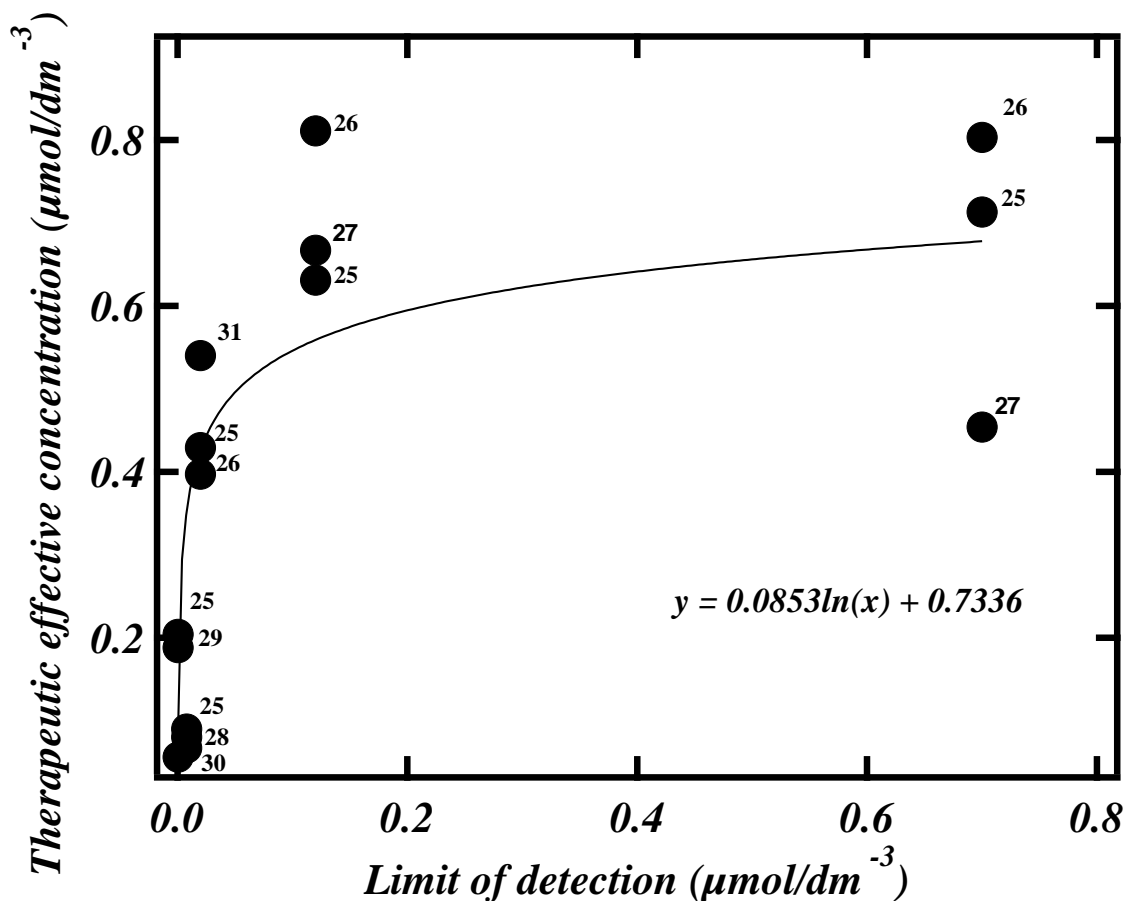


Figure 10.4: Plot of therapeutic effective concentrations (TEC) from sources as referenced on diagram vs. limit of detection (LoD) at DOPC coated Pt/Hg in PBS at pH 7.4 for tricyclic phenothiazines and antidepressants. Best fit line for plot and equation therefore shown on diagram.

### 10.3.2 EFFECTS OF VARYING pH

The interactions of the TCAs imipramine and clomipramine with DOPC with varying pH have been investigated. The pH ranges are from 2 to 12. For each of the compounds and pH ranges, three concentrations were used;  $0.3 \mu\text{mol dm}^{-3}$ ,  $6 \mu\text{mol}$

$\text{dm}^{-3}$  and  $15 \mu\text{mol dm}^{-3}$ . These are represented as scatter plots in Figures 10.5 a) and b).

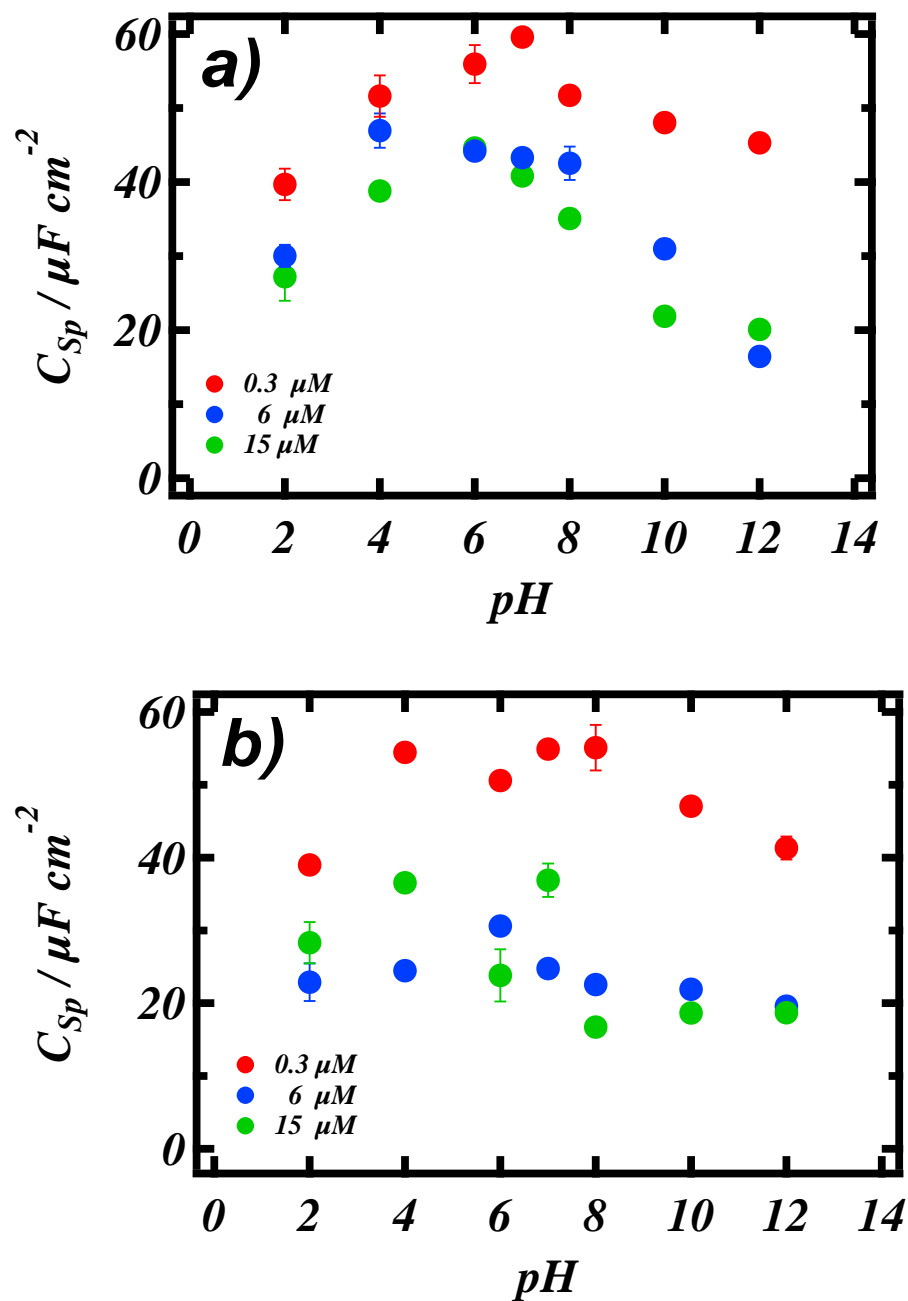


Figure 10.5: Plot of the first capacitance current peaks ( $\mu\text{F cm}^{-2}$ ) vs. pH for the interaction of a) imipramine with DOPC coated Pt/Hg electrode in PBS with concentrations 0.3, 6 and 15  $\mu\text{mol dm}^{-3}$  as shown in the legend inset and b) clomipramine with DOPC coated Pt/Hg electrode in PBS with concentrations 0.3, 6 and 15  $\mu\text{mol dm}^{-3}$  as shown in the legend inset.

Changes in pH strongly influence the interaction of TCAs with DOPC monolayers. At the pH of 7.4 representing physiological conditions, the TCA molecules in solution carry a positive charge ( $pK_{NH^{3+}} = 9.2 - 9.4$ ). It is possible that the interaction is due to attractive forces to the polar head groups of DOPC thereby allowing the TCA to gain close proximity to the monolayer.

At lower pH, the DOPC control in itself is not stable. Therefore the TCAs are able to interact more readily with an already unstable monolayer.

At higher pH, the compounds are neutralised as they both have  $pK_{as}$  of about 9.2 to 9.4. Being neutral at higher pH values, the hydrophobic moieties dominate the interaction. From the results, the interaction is more severe at higher pH as indicated by the reduction in capacitance current peak height.

In addition, the results also show TCA concentration dependency on the interaction with varying pH.

### 10.3.3 BINDING AFFINITY TO RECEPTORS

When a novel drug compound is synthesised, the drugs' properties are evaluated carefully with series of tests commencing with *in vitro* tests all the way to sophisticated *in vivo* testing. The constant  $K_i$  is evaluated by an *in vitro* drug tests similar to LoD and results have shown that the absolute values obtained when calculating LoD has a correlation with the absolute values of  $K_i$ .

When the  $K_i$  values for dopamine binding affinity for five TCA compounds are compared with their LoD, a positive correlation is found (Figure 10.6). Table 10.1 presents these values. Imipramine has the lowest affinity. Imipramine is the smallest ligand out of the five tricyclic compounds being compared. The dopamine receptors

are shallow and therefore larger ligands are able to fit deeper which might be influencing the binding affinity to membranes.

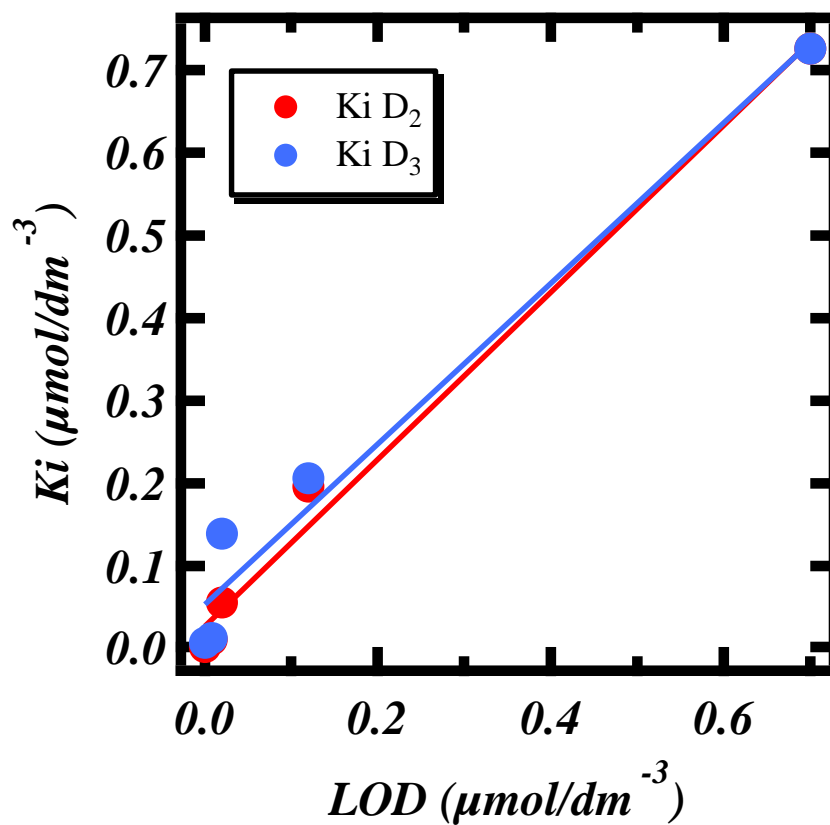


Figure 10.6: Binding affinities ( $K_i$ )<sup>(i)</sup> for TCAs and tricyclic phenothiazines with dopamine receptors D2 and D3 vs. their LoD at DOPC coated Pt/Hg in PBS at pH 7.4. The values are listed in Table 10.1.

Compounds	LoD ( $\mu\text{mol dm}^{-3}$ )	K <sub>i</sub> D2 <sup>(i)</sup>	K <sub>i</sub> D3 <sup>(i)</sup>
Clomipramine	0.02	0.056	0.139
Imipramine	0.7	0.726	0.726
Amitryptilline	0.12	0.196	0.206
Chlopromazine	0.0004	0.002	0.0069
Prochlorperazine	0.008	0.011	0.013

**Table 10.1: Representing listed compounds with their calculated LoD and K<sub>i</sub> values<sup>(i)</sup> for dopamine receptors, D2 and D3. (i) These values were verified by comparison with log D (7.4) values from the ChemSpider database (<http://www.chemspider.com>).**

There is also some correlation between the compounds' LoD and their binding with 5-HT<sub>2</sub> which is represented by their K<sub>i</sub> values. 8 compounds were tested and their respective LoD calculated. This was compared to their K<sub>i</sub> values. All these compounds have affinity for 5-HT<sub>2</sub>. This is illustrated in Figure 10.7. These compounds can have multiple binding sites, but dopamine and 5-HT receptors are their most prevalent target for the treatment of affective disorders and so the binding affinities for these were chosen. Table 10.2 presents the values.



Compound	LoD ( $\mu\text{mol dm}^{-3}$ )	$K_i$ of 5-HT <sub>2</sub> <sup>(i)</sup>
Spiperone	0.0002	0.0053
Chlorpromazine	0.0004	0.00331
Prochlorperazine	0.008	0.078
Clomipramine	0.02	0.0083
Amitryptilline	0.12	0.015
Imipramine	0.7	0.094
Phenothiazine	4.15	2.236
Serotonin	851	0.93

Table 10.2: List of compounds with their calculated LoD using sensing device and  $K_i$  values for 5-HT<sup>(i)</sup>. (i) These values were verified by comparison with log D (7.4) values from the ChemSpider database (<http://www.chemspider.com>).

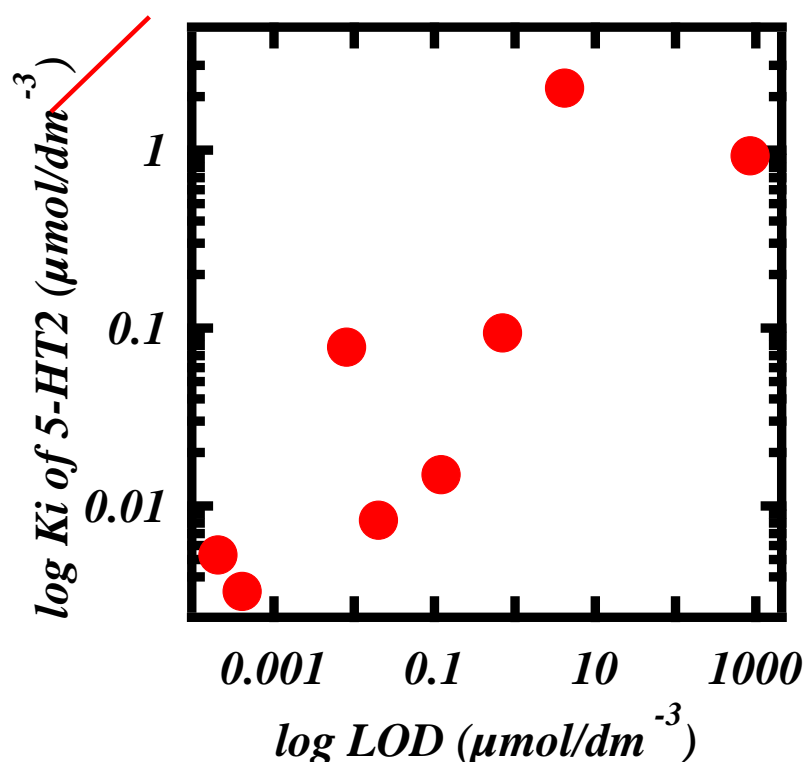
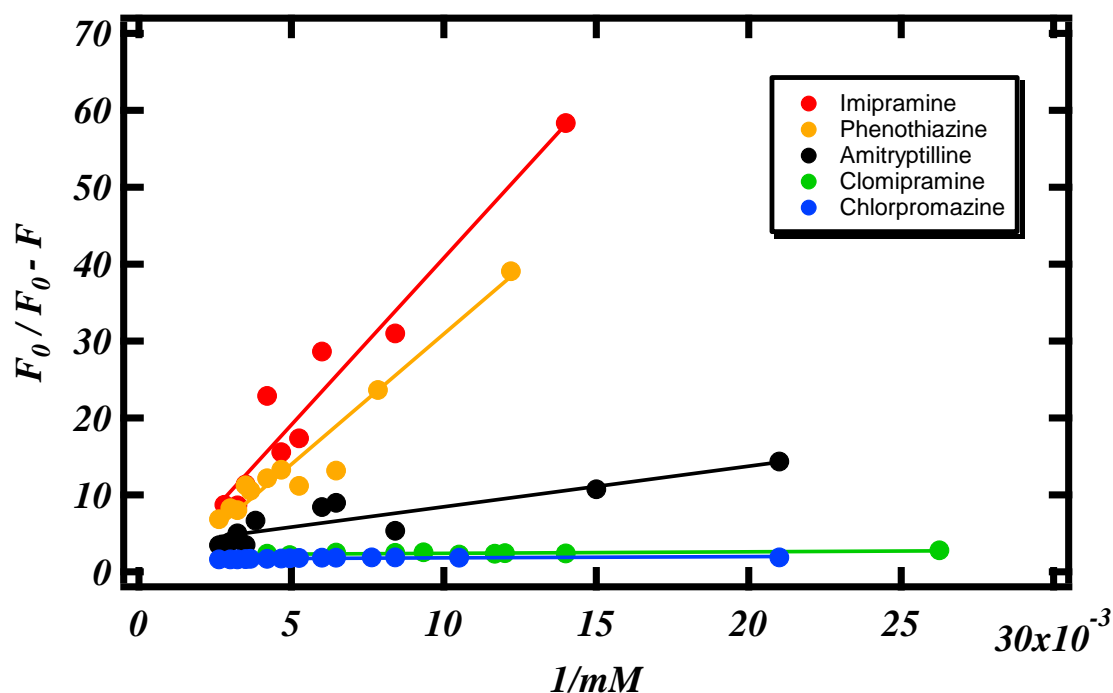


Figure 10.7: Plot of log of the binding affinity,  $K_i$  to the receptor 5-HT vs. LoD at DOPC coated Hg electrode in PBS at pH 7.4 for the compounds listed in Table 10.2.

The aromatic ring is clearly important in promoting hydrophobic interaction and a second aromatic ring increases interaction. Other studies have shown that the presence of the ring and the geometric relationship plays a part in enhanced affinity. The high binding affinities are also attributed to the configuration of the aromatic rings and presence of functional groups. Serotonin has the highest LoD value (Figure 10.7); one aromatic ring is not sufficient to promote significant binding. The other compounds tested possess two aromatic rings and their binding to 5-HT is enhanced which corresponds to their lower LoD values (Figure 10.7).

The results show that the LoD correlates well with binding affinity to these receptors. This is mainly because the compounds' functional groups provide the selectivity to membranes and this is detected by the electrochemical data. It does not however show selectivity for particular binding sites. Biologically active compounds undergo a variety of associations in order to reach their target source. However, they all encounter the plasma membrane barrier, even if their target is intracellular. The first interaction with the membrane is a fundamental process which is the rationale of focus on in these studies.

## 10.3.4 FLUORESCENCE SPECTROSCOPY



**Figure 10.8: Stern–Volmer plots for KI induced fluorescence quenching of TCAs and tricyclic phenothiazines (listed and colour coded in legend inset) with DOPC vesicles in PBS at pH 7.4.**

It can be determined by the slope and height of the Stern-Volmer plots that imipramine interacts most efficiently with KI (quenching efficiency per unit concentration) whereas the interaction is weak in the case of clomipramine and chlorpromazine (Figure 10.8). All the plots are linear indicating similarity in this class of compound in the way they interact with the vesicles.

The y-intercept determines the amount that is quenched by KI outside the vesicles. Consequently, we can calculate the % of compounds that has penetrated into vesicles. There is a correlation when comparing % of compound penetration vs. their LoD values obtained using the electrochemical model (Figure 10.9).

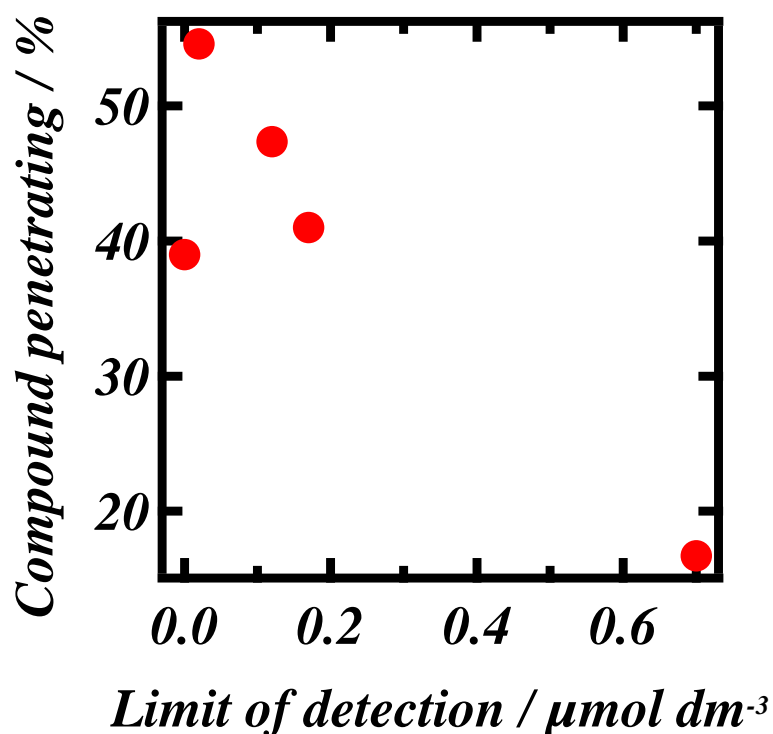


Figure 10.9: Scatter plot to show % of TCA and tricyclic phenothiazines compounds that have penetrated into DOPC vesicles vs. their respective LoD at DOPC coated Pt/Hg. These values are listed in Table 10.4.

Compounds	LOD	%vesicle penetrated
Imipramine	0.7	16.70%
Clomipramine	0.02	55.47%
Amitryptilline	0.12	47.36%
Phenothiazine	0.17	41%
Chlorpromazine	0.0004	41.91%

Table 10.3: List of compounds with their respective LoD values (using sensing device) and % of DOPC vesicle penetration (calculated using Stern-Volmer plots).

The differences in the behaviour of vesicle penetration reside in the specific compounds' structure. Amitriptyline has a carbon atom on the aromatic structure and

imipramine has nitrogen. With amitriptyline, the carbon atom that is present on the aromatic structure promotes more affinity towards the lipid tail region.

The nitrogen atom restricts rotational movement of imipramine [32]. Imipramine is least penetrating of the vesicles; it is quenched to the highest extent as indicated by the fluorescence intensity in the Stern-Volmer plot. This further verifies that imipramine remains adsorbed on or near the vesicle surface. This is commensurate with other studies which have shown that imipramine is repelled by the positive charges on polar lipid regions and remains on the lipid vesicle surface [33]. Imipramine has a high LoD; indicating that it has a low affinity for the lipid monolayer compared to the other tricyclic compounds studied here.

Clomipramine and chlorpromazine on the other hand exhibit the lowest quenching. This does not immediately indicate that these compounds can penetrate through the vesicles in a similar way. Calculations on % penetrated show that clomipramine penetrates through vesicles at a higher extent than chlorpromazine (Figure 10.9). This could indicate that chlorpromazine has a binding point somewhere within lipid membrane without completely penetrating through, the location of which could not be entirely on the surface as it would be quenched more thoroughly like imipramine. Other studies have certainly shown that chlorpromazine has additional binding sites in the inner part of liposome bilayers [33, 34]. The results with imipramine and chlorpromazine are consistent with previous studies [33].

## 10.4 SUMMARY

Fluorescence spectroscopy and electrochemical methods have been used to study the interaction of the tricyclic drugs with DOPC coated Pt/Hg electrode. The TCA and tricyclic phenothiazines all show affinity for the DOPC layer and DOPC vesicles but to various extents. The differences in their affinity can be explained by their distinct functional moieties. Several conclusions can be made from these findings.

Firstly, the compounds' differences can be explained on the basis of the variations in their chemical structure. The high binding affinity to lipid monolayer exhibited by compounds such as clomipramine could be due to the greater polarisability of the aromatic groups which enhance interaction. Inclusion of larger molecules such as chlorine tend to be more polarisable making the induced-dipole forces stronger thus promoting a stronger interaction with the lipid layer. The inclusion of chlorine in clomipramine could account for their higher binding affinity to the DOPC coated Hg layer.

Second, the ability of the tricyclic compounds to partition to an extent into the membrane is an important factor in their mode of action. The ability of a drug to partition into the membrane is effective for lipid membrane disordering compared to the drugs which bind near or on the membrane surface. Lipid disordering leads to changes in the membrane fluidity which can affect the functioning of membrane bound proteins. Therefore, understanding compound induced changes to lipid integrity would be useful in designing new drugs with better efficacy and fewer side effects. Studies have shown that amitriptyline can cause disorders to the membrane lipid bilayer, but at the same time amitriptyline is also an effective inhibitor of the Na<sup>+</sup>-K<sup>+</sup>-ATPase activity in the synaptosomes [32]. It can be hypothesised that membrane disordering can directly affect lipid-protein interactions and thereby indirectly affecting protein functions such as ion fluxes and natural ligand-receptor binding.

Lastly, DOPC coated microfabricated Pt/Hg electrode installed within a flow cell has been successfully configured to selectively screen the tricyclic compounds in water. Pharmaceutical pollutants can still remain active when released into the environment, and therefore, may cause a detrimental effect to aquatic organisms. Many compounds can cause chronic contamination that can effect an organism continuously over their lifecycle [35]. Consequently, it is important to be able to screen pharmaceutical compounds as potential toxicants once they are released into the environment.

## REFERENCES

- [1] Tye KM. *Nature* **2012** 493: pp537-541.
- [2] Chaudhury D, *Nature* **2012** 493: pp532–536.
- [3] Owens MJ, Nemeroff CB. *Clin Chem* **1994** 40(2):pp288-95.
- [4] Westkaemper RB, Glennon RA *Current Topics in Medicinal Chemistry* **2002** 2: pp575-598.
- [5] Lummis SCR, Baker J. *Neuropharmacology*, **1997** 415: pp.665–670.
- [6] Kim D. *The Journal of Neuroscience* **1999** 19(14): pp6213-6224.
- [7] Boadie W. Dunlop MD. Charles B. Nemeroff, MD. *Arch Gen Psychiatry*. **2007** 64(3): pp327-337.
- [8] Marras C, Lang A. *Neurol.* **2008** 70: pp1996-2003.
- [9] Sidhu A. *Neuroscience Letters* **2003** 3:pp189–192.
- [10] Baumann P, Hiemke C, Ulrich S, Eckermann G. *Pharmacopsychiatry* **2004**, 37: pp243–265.
- [11] Ban TA. *Neuropsychiatr Dis Treat.* **2007**. 3(4): pp495–500
- [12] Yeung PK, Hubbard JW, Korchinski ED *European J Clin Pharmacol* **1993** 45: pp563-569.
- [13] Xia Z, Ying G, Hansson AL, *Progress in Neurobiology* **2000** 60: pp501-502.
- [14] Lee B, Sur BJ. *Progress in Neuro-Psychopharmacology and Biological Psychiatry* **1986** 10: pp599–610.
- [15] Fišar Z. *Gen. Physiol. Biophys.* **2005** 24: pp161—180.
- [16] Sengupta N , Datta SC, Sengupta D, *Psychiatry research*, **1980** 3: pp337–344.
- [17] Rybakowski JK, Lehmann W *Neuropsychobiology*, **1994** 30(1): pp11–14.
- [18] Hibbeln J, Salem N. *The American Journal of Clinical Nutrition*, **1995** 62: pp1-9.
- [19] Frasure-Smith N, Lesperance F, Julien P *Biological psychiatry*, **2004**.



- [20] Salesse R, Garnier J, Leterrier F, Devilloose D, Vire J. *Biochemistry* **1982** 21: pp1581–1586.
- [21] Vigh L, Maresca B, Harwood JL. *Trends Biochem Sci* **1998**; 23: pp369–374.
- [22] Phillips SR, Wilson LJ, Borkman RF. *Curr Eye Res.* **1986** 5(8): pp611-9.
- [23] Moscho A. *Proc Natl Acad Sci U S A.* **1996** 93: pp11443-11447
- [24] Yan Q, Sharom. *Membrane transporters, methods and protocols.* Chapter 8 **2003** Humana press Inc. NJ.
- [25] Schulz M, Schmoldt A. *Pharmazie* **2003**, 58: pp447–474.
- [26] Donabedian R, Hodsdon M, Malkus H. *Clin Chem*, **2005**, pp1-13.
- [27] Tedeschi E, Winek C. *Winek's Toxicology; Forensic Medicine*, **2001**, 3, chapter 72.
- [28] Tanaka E, Nakamura T, Terada M. *Journal of chromatography* **2007**, 854: pp116-120.
- [29] Ellenbroek BA. *Pharmacology & therapeutics* **1993** 57: pp1-78.
- [30] Baselt RC, Cravey RH. *Journal of analytical toxicology* **1977** 1: pp81-103.
- [31] Linder M W, Keck Jr. PE. *Clinical Chemistry* **1998** 44: pp1073–1084.
- [32] Sangannahall BG. *Life Sciences* **2000**, 68: pp81–90.
- [33] Romer J, Marcel H. *Biochemical Pharmacology*, **1979** 28: pp799-805.
- [34] Di Francesco C, Bickel MH, *Chemico-Biological Interactions*, **1977** (3): pp335-346.
- [35] Péry ARR, Gust M. *Chemosphere*, **2008** 73(3): pp300–304.

# **CHAPTER 11**

## **APPLICATION OF FLOW CELL SYSTEM AS BIOSENSOR**

### **11.1 INTRODUCTION**

A sensor can be defined as a device which measures a physical and/or chemical quantity and transmits the response signal to a suitable measuring or control instrument. Conventional sensors include thermometers, pH electrodes and oxygen sensors. The more sophisticated concept of a biosensor was introduced over three decades ago in an attempt to mimic the very effective physical/chemical sensing mechanisms of living organisms. For example, human senses of smell and taste are a far more effective chemical sensing system than any current man-made technology. If these biological mechanisms could be replicated artificially on a commercial scale, then highly functional sensing systems could be designed. Such sensing systems are termed biosensors [1]. A biosensor consists of (a) a biological sensing element which can be a membrane, enzyme, antibody, nucleic acid, ion channel and (b) a transducer which transforms the signal from the sensing element to an electronic measurable event. Many biosensing concepts have been developed, but few are available

commercially. The reason for this is that, despite their great scientific interest, most of them cannot yet be deployed as rugged, useable devices. This is unfortunate since devising robust nano-based biosensing systems would offer tremendous scientific and commercial benefit for environmental and health screening systems which go beyond the capabilities of conventional sensing technology. In fact since the majority of working environmental sensors employ heavy metal ion *on-line* detection systems [2] there is a shortage of devices for routine screening of both air and water for the presence of toxic organic agents. To exemplify this, the Water Industry in Europe still uses classical UV absorption to measure levels of dissolved organic material in water and non-specific lengthy bioassays with organisms for example *Vibrio fischeri* to measure toxicity [3,4].

In this Chapter, environmental applications of the sensing system are examined. Tests on tap water and screening of toxins and pharmaceuticals as well as selected compound mixtures have been carried out. Some work was also conducted in collaboration with a water company with laboratories based in Cardiff (Modern Water PLC). This collaboration provided further evidence that the sensing system has applications to the environment. A list of environmentally impacting compounds were tested. Other milestones include the use of raw waters (sea/fresh) as an analytical matrix. The results are discussed in this Chapter and a full report in the form of performance evaluation was sent to Modern Water.

The MFE system can be used to the screen hazardous substances in the water supply. The measurements are carried out in real time which means that potentially toxic compounds are detected rapidly. This will contribute greatly to environment safety and health. Indeed, the identification of ecological risks and environmental toxins are a forefront of investigation. The current status of art with toxicity testing is that assays are primarily animal based such as fish, invertebrates, plants, algae and bacterial.

The most common species used in toxicity assays is *Vibrio fischeri*. It has worldwide use in determining toxicities of substances from most matrices including wastewater [5]. This technique has disadvantages including long incubation times, limited measurable parameters e.g. mortality and lack of reproducibility between consecutive assays due to the individual differences among organisms in the same species. In some cases, more space and apparatus is required to accommodate treatment or incubation of organisms before testing thus introducing additional complications. The use of a biomimetic systems such as the one described in this thesis enables the composition of the sensor element to be controlled allowing flexibility in meeting analytical requirements. The system as a whole can be miniaturized, takes up less space and produces less wastage thus improving sustainability in analysis.

There is increasing emphasis into non animal toxicity testing. Since 2007, the Environmental Protection Agency, the National Institutes of Health, the National Toxicology Program, and the US Food and Drug Administration are cooperating to develop new technologies to modernize chemical testing [6].

This Chapter addresses the aforementioned issue by describing an *on-line* high throughput toxicity sensing system for use in environmental and pharmaceutical screening. The device employs a membrane-like sensor element. Membrane systems as a class of biosensor have previously been applied, [7-9] but have proved to be fragile, complex and of high cost, making them unsuitable for environmental applications. The present Chapter characterises the performance of a membrane-based sensing device developed over the last decade that is unique, since it uses a highly tenacious mercury (Hg) layer bound strongly to a platinum (Pt) contact. A phospholipid monolayer is deposited on these Hg electrodes which act as the membrane-like sensing element. The principle of the technique is that the monolayer is selectively damaged by biomembrane-active compounds in the sample. This damage is detected electrochemically as an alteration in the nanoscale forces of self

assembly within the layer manifest as an alteration in the characteristics of two voltage induced phase transitions [10]. The reason for the applicability of the Hg supported phospholipid layer compared to other supported membrane techniques is that liquid Hg [11] is entirely compatible with the relatively temperature insensitive fluid phospholipid [12-14] and allows for the formation of defect-free, self-sealing membranes. This unique property enables any disrupting events, such as those caused by biomembrane active nanoparticles [15] or organic compounds [16], to be measured. The Hg-phospholipid system has been miniaturised by fabricating Hg coated Pt microelectrodes on a silicon wafer.[10,17] This has alleviated health concerns over the use of Hg due to the binding of Hg to the Pt and the minute amount of Hg used, enabling the device to be deployed within a flow system.

### **11.1.1 FINGERPRINT SCREENING**

In relation to their use as sensing elements, phospholipid layers are known to have interesting properties when exposed to applied potentials. This enables electrochemical methods to be an effective way of investigating their structure and properties [18]. Phospholipid behaviour in response to potential changes has been studied extensively on Hg electrodes [19-21]. Monolayers of DOPC undergo two potential induced phase transitions characterised by two sharp capacitance current peaks respectively. These peaks correspond to the ingress of electrolyte into the layer and the re-organisation of the layer to form bilayer patches [19-21]. Through observing the capacitance current peaks in the voltammograms, alterations in the peak configuration can be detected when chemical compounds interact with the layers. A compound's biomembrane activity is manifested by characteristic changes in capacitance current – voltage plots which represent modifications to the phospholipid layer conformation. The classes of compounds investigated are environmental toxins

and/or or have biological and clinical activities. The responses are characterised for each class of compound.

### **11.1.2 MATRIX EFFECT AND FRESHWATER/CAVE WATER SAMPLING**

In order to assess the performance of the sensing device in a "real life" scenario, its operation has been tested in the presence of humic acid and in tap water as an applicable matrix. Subsequent assessments were conducted on the feasibility of the sensing device on more than one compound in the system. Humic acid was employed as a potential interferent since it is commonly present in soils, surface water, sewage, and marine and lake sediments [22]. Humic substances consist of heterogeneous mixtures of molecules which arise from the degradation of plant and animal residues occurring in water [23].

The concentrations of humic acid used in these experiments matched characteristic humic acid concentrations in drinking water [24]. Pyrene was used because it has been reported to have a high affinity for humic acids [25] as well as binding to the lipid monolayers as shown in our studies. An extension to the real life scenario is made with the testing of fresh water and cave water [26]. Identifying a potential contaminant in the environment means further attention can be provided to that particular site.

### **11.1.3 MIXTURES**

It is more difficult to screen a mixture of toxins / chemical compounds than to screen a single compound on its own because each compound displays their own effect and compounds / toxins can compete to enhance or reduce each others' effects. Nonetheless, this is an important parameter to address. In real life scenarios, common toxins can occur as mixtures. They include cigarette smoke, industrial waste and

gasoline. The results presented in this section highlights the progress of the MFE system in its ability to screen more than one compound.

## 11.2 MATERIALS AND METHODS

The test compounds of 99% or greater purity were purchased from Sigma Aldrich, and were used as received. The phospholipid employed for coating electrodes was 1, 2-dioleoyl-sn-glycero-3-phosphocholine (DOPC) (Avanti Polar Lipids Alabaster, AL) and was >99% pure. The byspiridinium compounds are supplied by the Ministry of Defence- Defence Science and Technology Laboratory (MoD-Dstl). The freshwater samples were sourced from two locations in Leck Fell, Lancashire, UK. Samples of surface water over Notts 2 Pot was collected and samples of water flowing through passages of Notts 2 Pot underground were also collected. Both these samples have various organic and inorganic interferents that are not specified such as major ions and humic acid. All other reagents were of analytical grade and purchased from Sigma Aldrich.

Stock solutions were made up as follows. The polycyclic aromatic hydrocarbons (pyrene and anthracene), prochlorperazine and DDT were dissolved in acetone. Concentrations of test compounds were prepared by adding small aliquots of the working solutions to PBS to provide concentrations for testing. The DOPC dispersion for electrode coating was prepared by gently shaking DOPC with PBS to give 0.2 mg cm<sup>-3</sup> dispersion. The electrochemical methods conducted are as described in Chapter 2.

### 11.2.1 MATRIX EFFECTS AND CAVE WATER SAMPLING

Matrix effect studies were conducted by studying the influence of humic acid on the electrochemical response of DOPC coated electrodes. Concentrations of humic acid

were prepared from  $0.5 \text{ mg dm}^{-3}$  to  $3 \text{ mg dm}^{-3}$  in PBS solution. The concentrations were then tested on the DOPC coated Pt/Hg when introduced into the flow cell and monitored by the RCV scan. Following this,  $0.5 \text{ } \mu\text{g dm}^{-3}$  pyrene added to a solution of  $3 \text{ mg dm}^{-3}$  humic acid in PBS was tested for its effect on the DOPC coated electrode. Tap water experiments were carried out under open circuit conditions. To conduct these studies, a sample of tap water was introduced via continuous flow over the DOPC coated Pt/Hg having disconnected the cell from the potentiostat prior to exposure. Following exposure, the cell was reconnected and PBS re-introduced to the flow cell to monitor the DOPC layer in a conducting medium. The experiment was then repeated with  $0.5 \mu\text{g dm}^{-3}$  pyrene in tap water.

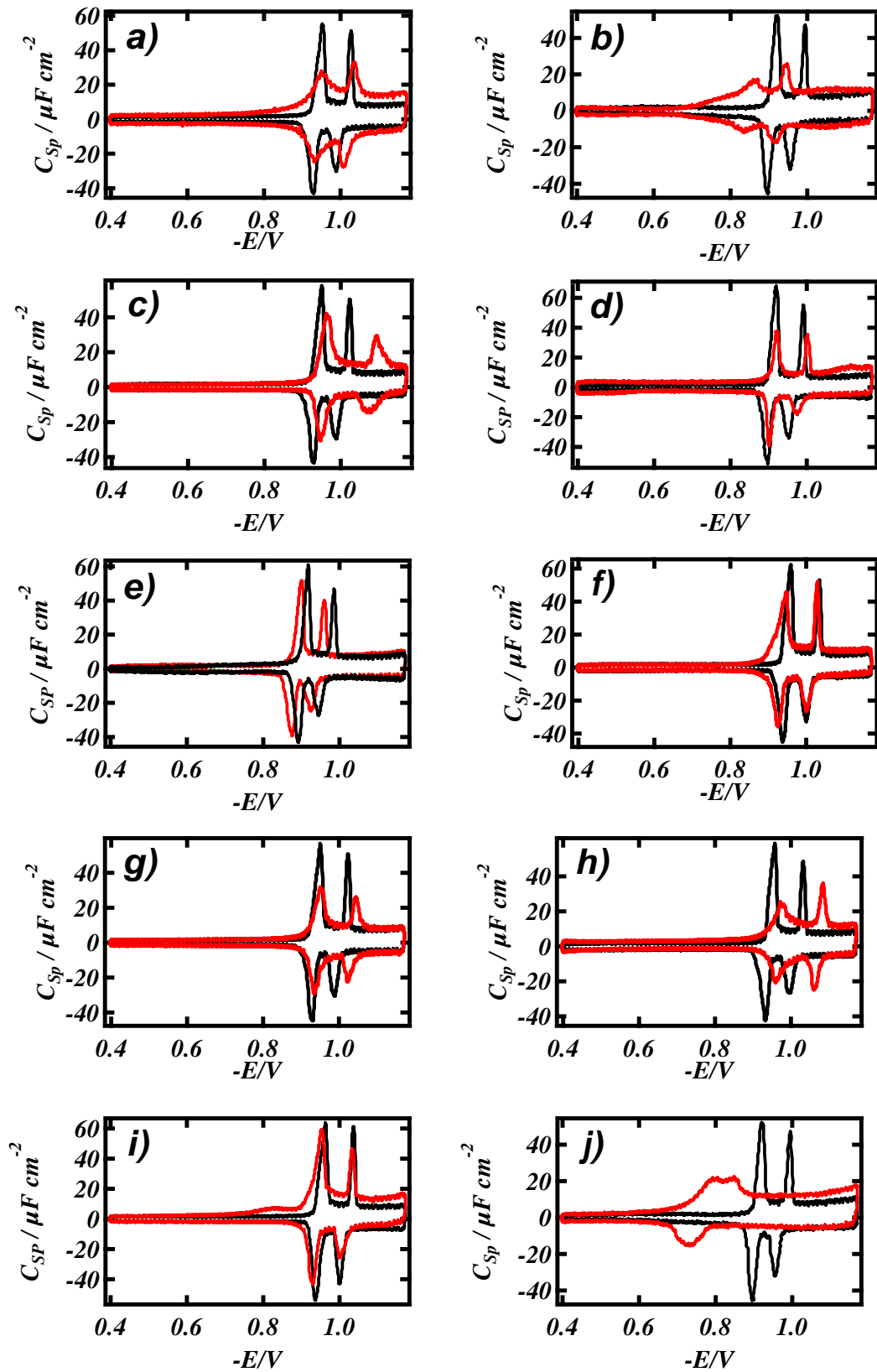
Natural cave water samples were first tested on the DOPC coated Pt/Hg and monitored by the RCV scan to assess for any significant changes. Following this,  $0.5 \text{ } \mu\text{g dm}^{-3}$  pyrene added to a sample of water was tested for its effect on the DOPC coated electrode. The results evaluate the screening/detection ability for potential environmental toxins.



## 11.3 RESULTS AND DISCUSSIONS

### 11.3.1 FINGERPRINT DATABASE

Figure 11.1 displays the results of the changes to the RCV plots from the interaction of DOPC coated Pt/Hg with representative compounds. The compounds interact with the DOPC coated electrode to varying degrees as shown by their effect on the capacitance current peaks in the RCV plot. These capacitance current peaks are representative of the reorientation/adsorption/desorption processes of the DOPC layers in response to potential change [19, 21]. It is observed that each class of compound interaction effects a "fingerprint" visual profile on the RCV plot which manifests itself as an alteration in the shape, height and position of the capacitance current peaks (Figure 11.1).



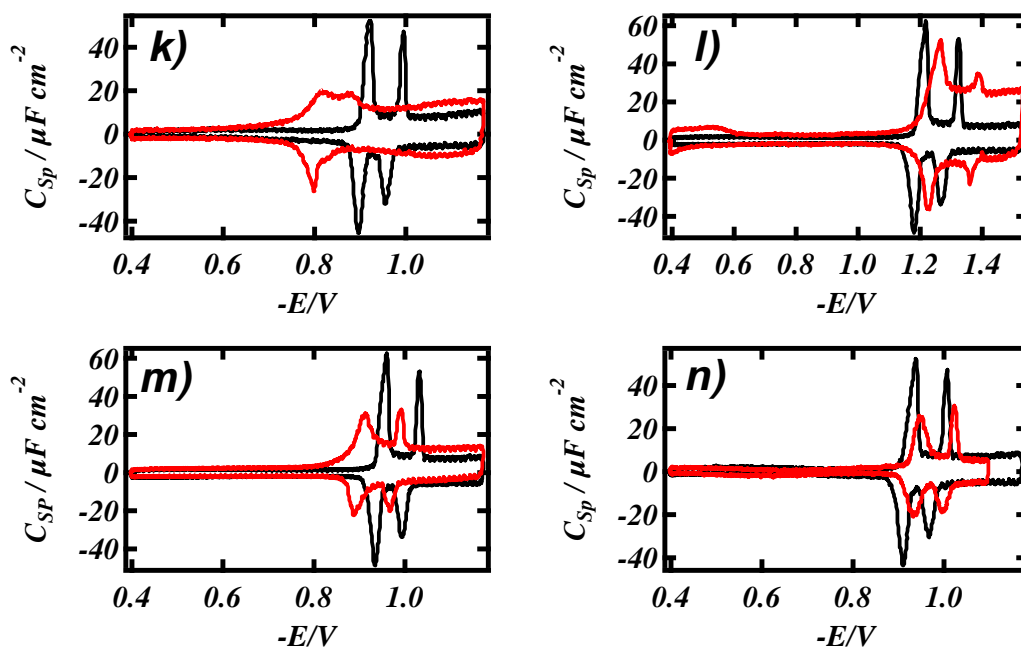


**Figure 11.1:** RCVs recorded at  $40 \text{ Vs}^{-1}$  of a DOPC coated Pt/Hg electrode in PBS at pH 7.4 (black line) in the presence of compounds a) to n) (red line). The RCV scans can be used a “fingerprint” database for compounds. a)  $10 \mu\text{mol dm}^{-3}$  chlorpromazine, b)  $0.25 \text{ mmol dm}^{-3}$   $\text{C}_2$  spiperone, c)  $1 \mu\text{mol dm}^{-3}$  anthracene, d)  $20 \mu\text{mol dm}^{-3}$  MB520, e)  $1 \mu\text{mol dm}^{-3}$  stigmasterol, f)  $1 \mu\text{mol dm}^{-3}$  clomipramine, g)  $0.25 \mu\text{mol dm}^{-3}$  DDT, h)  $5 \mu\text{mol dm}^{-3}$  phenothiazine, i)  $10 \text{ mmol dm}^{-3}$  theophylline, j)  $0.25 \text{ mmol dm}^{-3}$  diprenorphine, k)  $0.25 \text{ mmol dm}^{-3}$  DASB, l)  $10 \mu\text{mol dm}^{-3}$  BMIM Br, m)  $10 \mu\text{mol dm}^{-3}$  ethinyl estradiol and n)  $0.003 \mu\text{mol dm}^{-3}$  TcP.

### 11.3.2 MATRIX EFFECTS

A  $3 \text{ mg dm}^{-3}$  solution of humic acid in PBS was passed over the DOPC coated Pt/Hg electrode. An insignificant suppression of the capacitance current peak is observed shown in Figure 11.2 a). Following this a  $0.5 \mu\text{g dm}^{-3}$  pyrene added to  $3 \text{ mg dm}^{-3}$  humic acid in PBS was passed over the DOPC coated Pt/Hg electrode. A characteristic response of the DOPC to the pyrene is observed (see Figure 11.2 b)) of Figure 8.2 d). The system was then applied to the assay of pyrene in tap water.

The effect of tap water on the RCV plot of the DOPC coated Pt/Hg is insignificant (see Figure 11.2 c)). Subsequently  $0.5 \mu\text{g dm}^{-3}$  pyrene in tap water was passed over the DOPC coated Pt/Hg electrode. Figure 11.2 d) shows that the response of DOPC in the tap water matrix has not altered compared to the response in unspiked and humic acid spiked MilliQ water. The shift of peaks is significantly greater with humic acid and pyrene in PBS (Figure 11.2 b)) than tap water spiked with pyrene (Figure 11.2 d)). A possible reason for this is that the humic acid as surfactant associates with the apolar pyrene in solution and facilitates the transfer of pyrene across the solution/ DOPC layer interface.

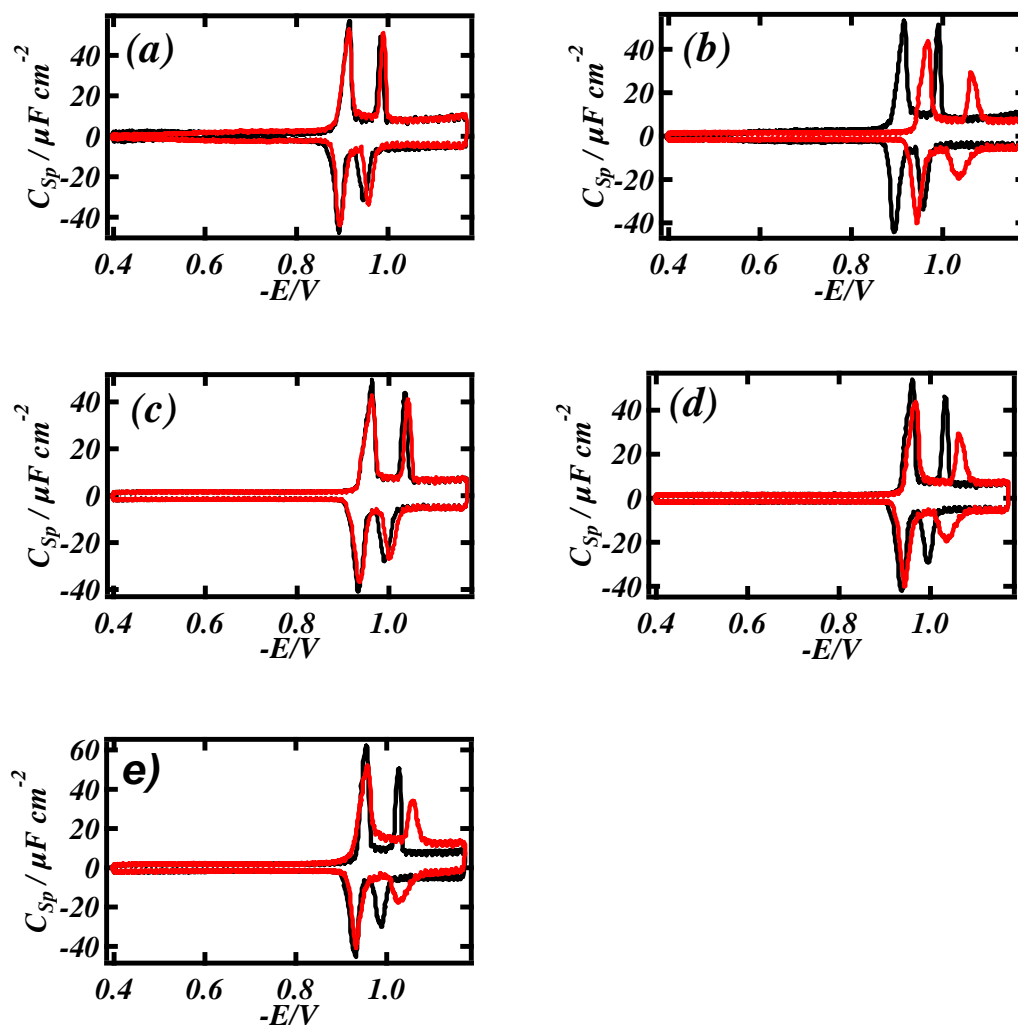


Figure 11.2: RCV scans at  $40 \text{ Vs}^{-1}$  of DOPC coated Pt/Hg electrode (black line) in the presence of (a)  $3 \text{ mg dm}^{-3}$  solution of humic acid in PBS at pH 7.4, (b)  $3 \text{ mg dm}^{-3}$  solution of humic acid in PBS at pH 7.4 with  $0.002 \text{ } \mu\text{mol dm}^{-3}$  pyrene, (c) tap water, (d) tap water spiked with  $0.002 \text{ } \mu\text{mol dm}^{-3}$  pyrene and (e) PBS at pH 7.4 with  $0.002 \text{ } \mu\text{mol dm}^{-3}$  pyrene.

### 11.3.3 NATURAL WATER

Natural surface and cave water samples were passed over the DOPC coated Pt/Hg electrode. An insignificant suppression of the capacitance current peak is observed when surface running water has been introduced (Figure 11.3 a)). On the other hand,

a much greater effect is observed when water that has percolated underground is introduced to DOPC (Figure 11.3 b)). The capacitance current peak suppression is significantly greater with natural water and pyrene (Figure 11.3 c)) than PBS with pyrene (Figure 8.2 d)) or tap water and pyrene (Figure 11.2 d)). The presence of any multiple of organic constituents in the freshwater samples could be facilitating the interaction of pyrene with DOPC monolayer.

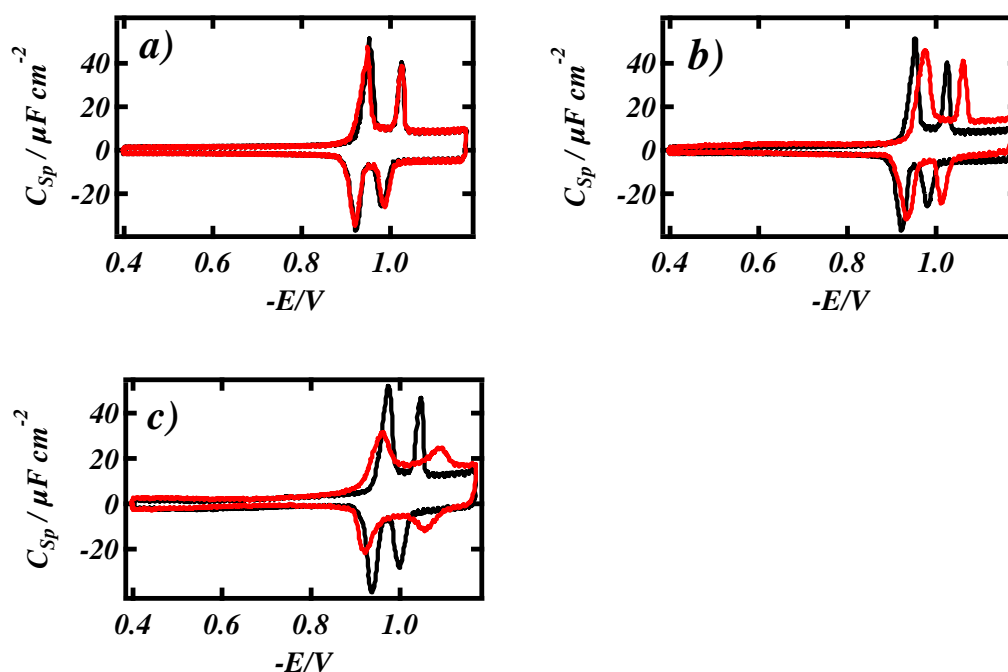


Figure 11.3: RCV scans at  $40 \text{ V s}^{-1}$  of DOPC coated Pt/Hg electrode in PBS at pH 7.4 (black line) in the presence of a) surface running water (red line), b) water sample from cave (red line) and c) surface running water spiked with  $0.002 \mu\text{mol dm}^{-3}$  pyrene (red line).

#### 11.3.4 COMPOUND MIXTURES

Mixtures containing two compounds were passed over the DOPC coated Pt/Hg electrode. The mixtures of compounds addressed are pyrene and prochlorperazine, DDT and pyrene, anthracene and prochlorperazine and MB779 and pyrene. These

combinations were chosen due to their individual distinct profiles that distinguishes each of them independently. They also have different pharmacological actions when interacting with lipid monolayer.

#### 11.3.4.1 PYRENE AND PROCHLORPERAZINE

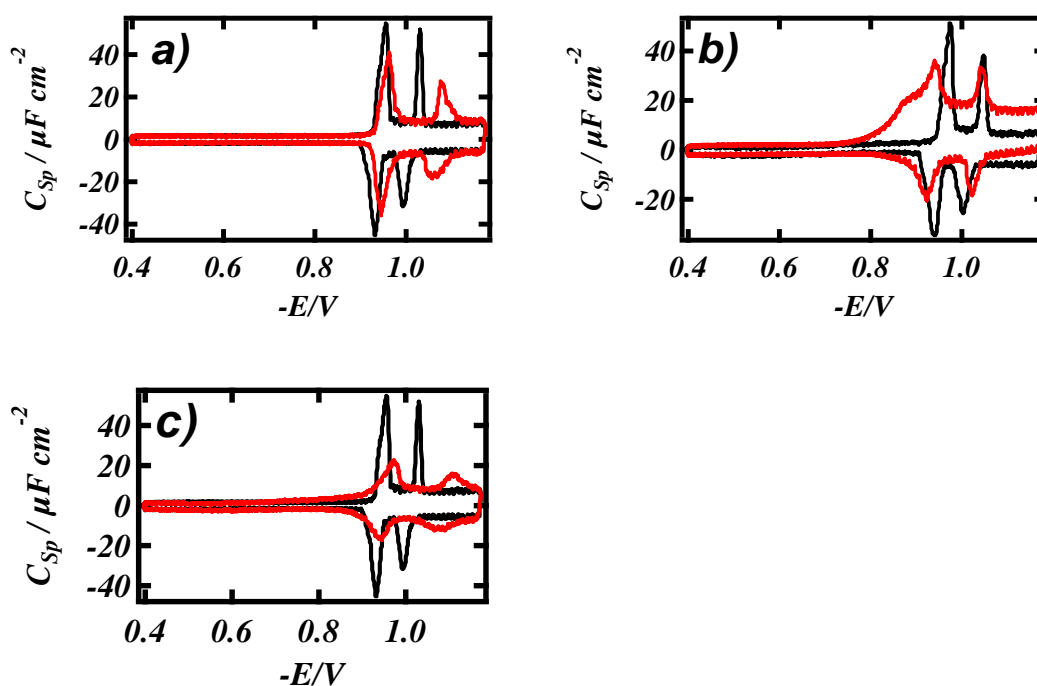


Figure 11.4: RCV scans at  $40 \text{ V s}^{-1}$  of DOPC coated Pt/Hg electrode in PBS at pH 7.4 (black line) in the presence of a)  $0.0025 \mu\text{mol dm}^{-3}$  pyrene, b)  $0.26 \mu\text{mol dm}^{-3}$  prochlorperazine, c)  $0.0025 \mu\text{mol dm}^{-3}$  pyrene and  $1.3 \mu\text{mol dm}^{-3}$  prochlorperazine (red line).

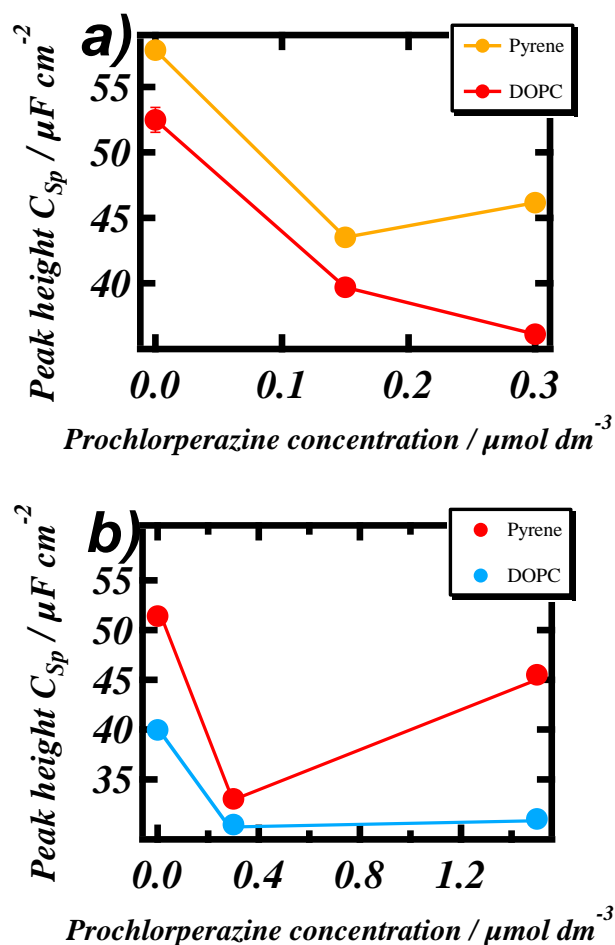
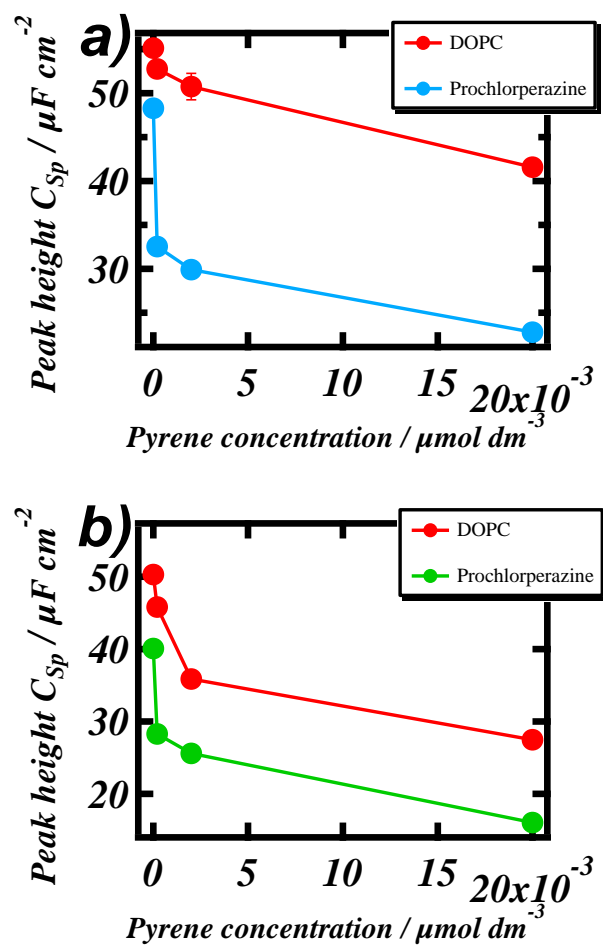


Figure 11.5: Plot showing the effect on capacitance current peak heights vs. increasing concentrations of prochlorperazine with a)  $0.2 \text{ mg cm}^{-3}$  dispersion of DOPC coated Pt/Hg electrode in PBS at pH 7.4 (red line) and in a mixture with  $0.025 \text{ } \mu\text{mol dm}^{-3}$  pyrene (yellow line) affecting the first capacitance current peak height, b)  $0.2 \text{ mg cm}^{-3}$  dispersion of DOPC coated Pt/Hg electrode in PBS at pH 7.4 (blue line) and in a mixture with  $0.025 \text{ } \mu\text{mol dm}^{-3}$  pyrene (red line) affecting the second current capacitance peak height.





**Figure 11.6:** Plot showing the effect on capacitance current peak heights vs. increasing concentration of pyrene with a)  $0.2 \text{ mg cm}^{-3}$  dispersion of DOPC coated Pt/Hg electrode in PBS at pH 7.4 (red line) and in a mixture with  $1.3 \text{ } \mu\text{mol dm}^{-3}$  prochlorperazine (blue line) affecting the first capacitance current peak height and b)  $0.2 \text{ mg cm}^{-3}$  dispersion of DOPC (red line) and in a mixture with  $1.3 \text{ } \mu\text{mol dm}^{-3}$  prochlorperazine (green line) effecting the second capacitance current peak height.

Figure 11.5 shows when the sensor element is exposed to varying concentrations of prochlorperazine with a constant pyrene concentration in solution, the effect of prochlorperazine on the lipid monolayer is decreased. Figures 11.5 a) to b). This is depicted by the increase in LoD compared to prochlorperazine on its own.  $0.08 \text{ } \mu\text{mol dm}^{-3}$  compared to  $0.008 \text{ } \mu\text{mol dm}^{-3}$  (Figure 11.7 a)).

In contrast, when the concentration of pyrene is varied with a constant prochlorperazine concentration in solution, the effect of pyrene to the lipid monolayer is enhanced (Figures 11.6 a) and b)) The surface active compound, prochlorperazine, increases the sensitivity of the aromatic compound, pyrene depicted by the decrease in LoD compared to pyrene on its own.  $0.00006 \mu\text{mol dm}^{-3}$  compared to  $0.0002 \mu\text{mol dm}^{-3}$  (Figure 11.7 b)).

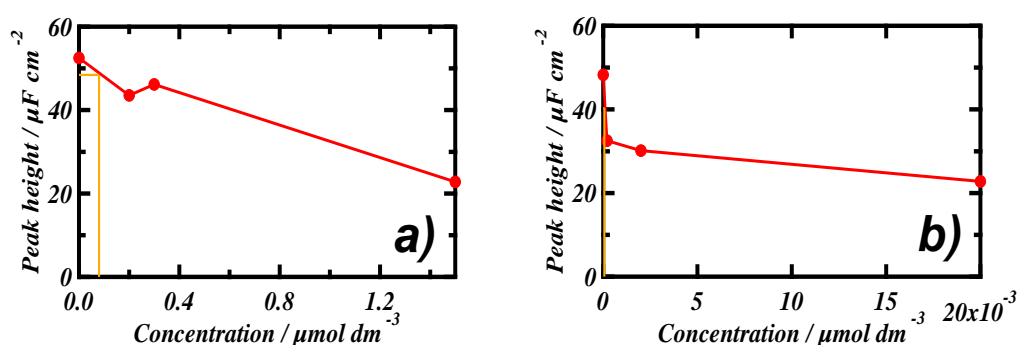


**Figure 11.7: LoD determination by estimating the concentration corresponding to three times SD of DOPC control capacitance current peak height on capacitance current peak height versus concentration curve for a) prochlorperazine when in a mixture with  $0.025 \mu\text{mol dm}^{-3}$  pyrene in PBS at pH 7.4 and b) pyrene when in a mixture with  $1.3 \mu\text{mol dm}^{-3}$  prochlorperazine PBS at pH 7.4. Error bars confined within the markers.**

These results show very clearly that pyrene 'protects' the lipid monolayer from interaction with prochlorperazine and that prochlorperazine enhances pyrene interaction with the lipid monolayer. The penetration of the monolayer by pyrene lowers the affinity of the lipid monolayer for prochlorperazine. On the other hand prochlorperazine as a surfactant [27] solubilises pyrene and facilitates its increased availability to the lipid monolayer.

### 11.3.4.2 DDT AND PYRENE

When DDT is combined in a mixture with pyrene, the penetration of the monolayer by DDT increases the affinity of the lipid monolayer for pyrene (Figure 11.8 c)) compared to pyrene on its own (Figure 11.8 b)). In addition, there is a significant shift of the first and second RCV capacitance current peaks to negative potentials concurrent with a peak depression. This could be due to increased proximity of electrons to electrode surface affecting the PZC (Chapter 8).

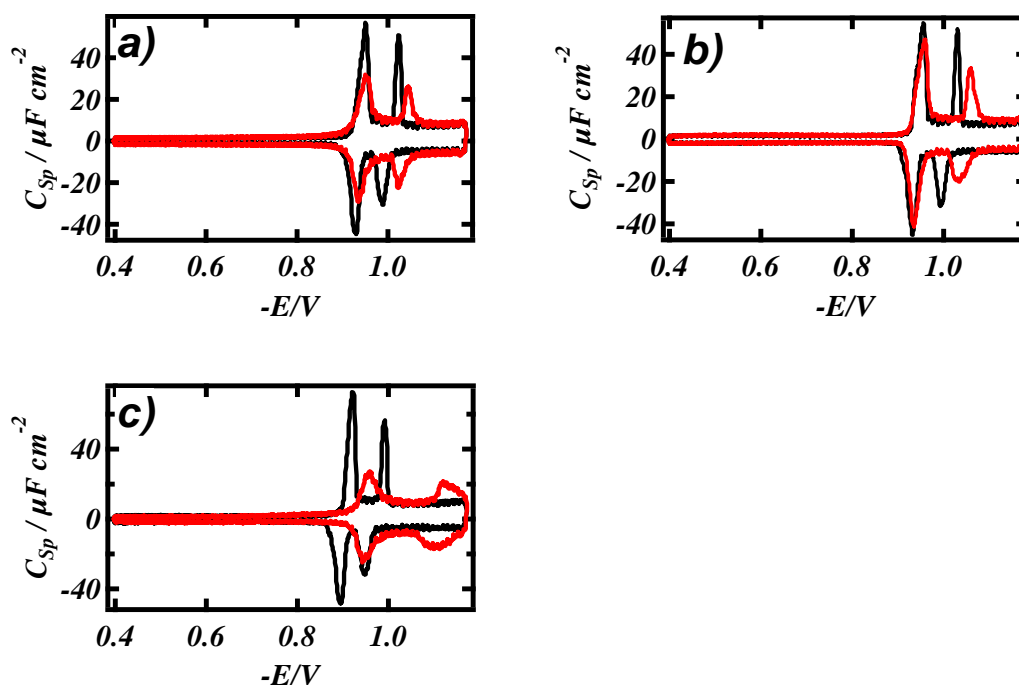


**Figure 11.8:** RCV scans at  $40 \text{ V s}^{-1}$  of DOPC coated Pt/Hg electrode in PBS at pH 7.4 (black line) in the presence of a)  $0.3 \mu\text{mol dm}^{-3}$  DDT (red line), b)  $0.0025 \mu\text{mol dm}^{-3}$  pyrene (red line) and c)  $0.00125 \mu\text{mol dm}^{-3}$  pyrene and  $0.002 \mu\text{mol dm}^{-3}$  DDT (red line).

## 11.3.4.3 ANTHRACENE AND PROCHLORPERAZINE

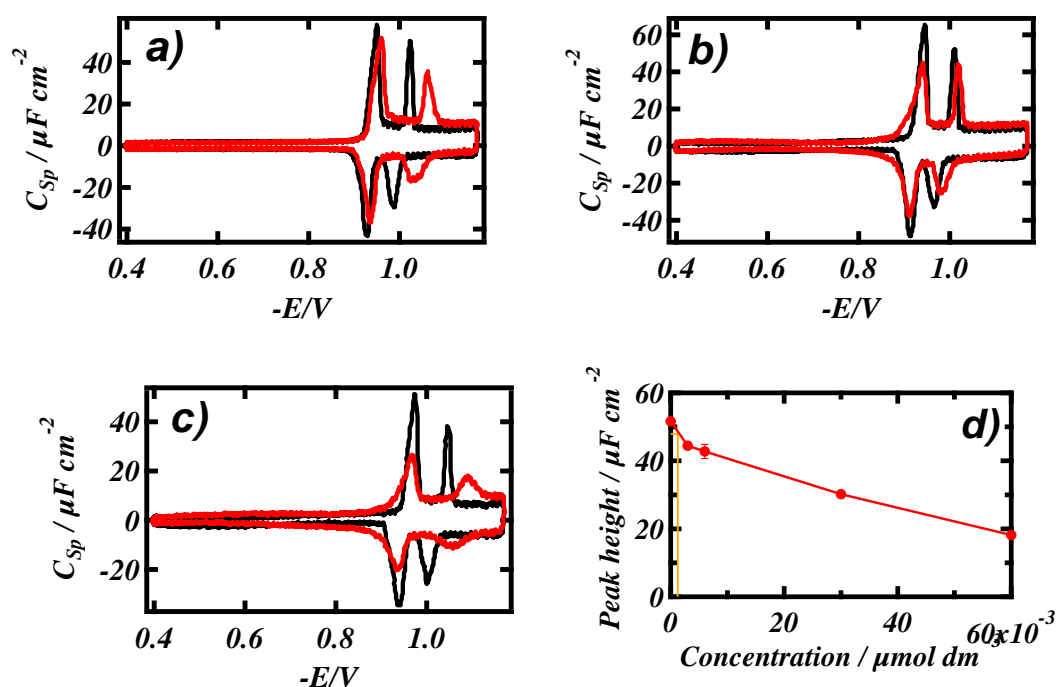


Figure 11.9: RCV scans at  $40 V s^{-1}$  of DOPC coated Pt/Hg electrode in PBS at pH 7.4 (black line) in the presence of a)  $0.03 \mu mol dm^{-3}$  anthracene (red line), b)  $0.003 \mu mol dm^{-3}$  anthracene in a mixture with  $0.26 \mu mol dm^{-3}$  prochlorperazine (red line) and c)  $0.06 \mu mol dm^{-3}$  anthracene in a mixture with  $0.26 \mu mol dm^{-3}$  prochlorperazine (red line). d) LoD determination of DOPC control capacitance current peak height on capacitance current peak height versus concentration curve for anthracene in a mixture with of  $0.3 \mu mol dm^{-3}$  prochlorperazine in PBS at pH 7.4.

The presence of prochlorperazine enhances anthracene's sensitivity to the lipid monolayer, which can be seen by the increasing shift of the peak potential to more negative values on the RCV scan. The distinct RCV characteristic of prochlorperazine however is not easily visible. Figure 11.4 b) shows the full potential of prochlorperazine on lipid monolayer. A greater concentration of prochlorperazine is needed to promote a minute effect. It seems that the presence of prochlorperazine

decreases the barrier for anthracene to incorporate into its binding position whereas anthracene destroys the binding points of the surface active prochlorperazine by causing disruption to the integrity of the lipid monolayer, and thus the surface.

When the concentration of anthracene is varied with a constant prochlorperazine concentration in solution, the effect of anthracene to the lipid monolayer is enhanced (Figures 11.9 b) and c)) The surface active compound, prochlorperazine, increases the sensitivity of the aromatic compound, anthracene depicted by the decrease in LoD compared to anthracene on its own.  $0.0098 \mu\text{mol dm}^{-3}$  compared to  $0.00125 \mu\text{mol dm}^{-3}$  (Figure 11.9 d)).

#### **11.3.4.4 MB779 AND PYRENE**

When concentration of pyrene was combined in a mixture with MB779, both compounds' distinct characteristic responses can be seen (Figure 11.10 c)). MB779 is one of a group of novel bispyridinium compounds and has positively charged aromatic polyatomic ions. The positive charge could account for the slight shift to more positive potentials.

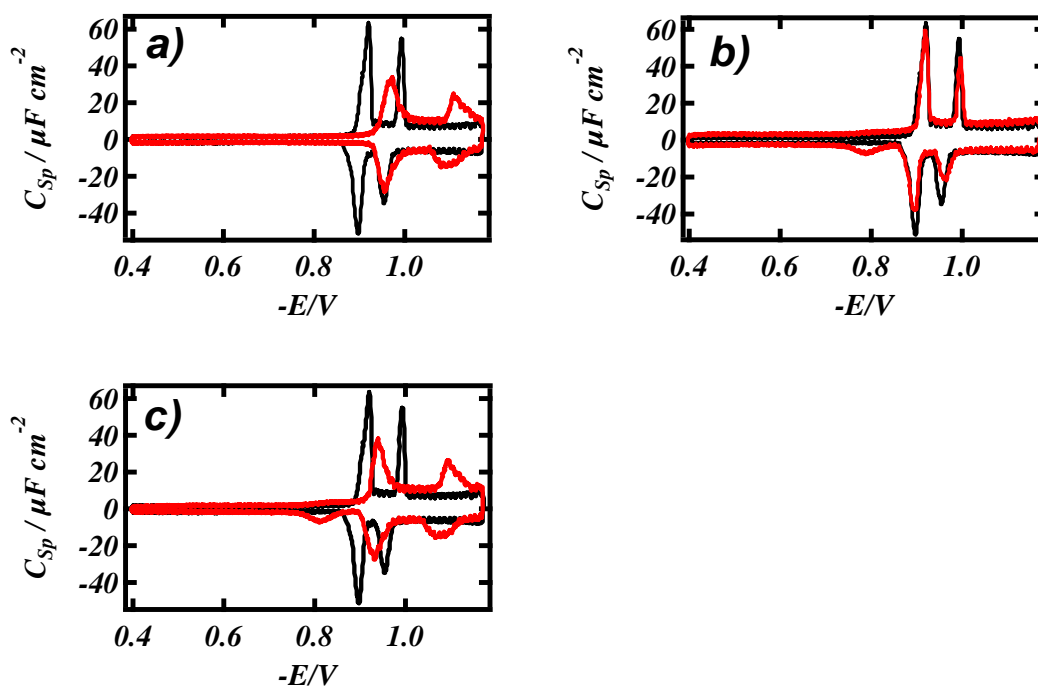


Figure 11.10: RCV scans at  $40 \text{ V s}^{-1}$  of DOPC coated Pt/Hg electrode in PBS at pH 7.4 (black line) in the presence of a)  $0.05 \text{ } \mu\text{mol dm}^{-3}$  pyrene (red line), b)  $20 \text{ } \mu\text{mol dm}^{-3}$  MB779 (red line) and c)  $20 \text{ } \mu\text{mol dm}^{-3}$  MB779 and  $0.05 \text{ } \mu\text{mol dm}^{-3}$  pyrene (red line).

## 11.5 SUMMARY

These results show several possibilities for applications of lipid coated electrodes. In the preceding chapters, the selective properties and response characteristics of compound interaction have been described showing applications for structure-activity relationships (SAR), toxicological profiling and screening. To conclude the analytical applications of the current work;

- The DOPC coated microfabricated Pt/Hg electrode installed within a flow cell has been successfully configured to selectively screen organic compounds in water. The data enables detection limits representing the lowest concentration of compound in water which significantly interacts with the DOPC layer to be calculated.
- The sensing assay has been successfully tested in the presence of humic acid as a potential interferent and in a tap water matrix. The system can screen compounds in the presence of humic acid ( $3 \text{ mg dm}^{-3}$ ) and in a tap water matrix.
- The RCV scans from tap water testing showed little difference to the capacitance peaks. When the samples were spiked with a known compound, its characteristic change in capacitance profile was observed making it credible for use in *real life* testing.
- Results have shown that compound activity at the level of the phospholipid membrane maybe partly responsible for the compounds' respective therapeutic activity. The results from electrochemical responses may be directly linked to the efficacy of compounds to cross biological membranes.
- These results show several possibilities for applications of lipid coated electrodes. A potential use of compound mixture studies is the ability to create database for *in vivo* pharmaceutical SAR. This can provide information

about structural attributes of pharmaceutical compounds, toxicological effects and drug – drug interactions since these interactions occur when a drug interacts, or interferes, with another drug. This can alter the way one or both of the drugs act in the body and could potentially cause unforeseen side effects. The drugs involved can be prescription medications, over-the-counter medicines and even vitamins and herbal products. Some common interactions are combining aspirin with anti-coagulants like coumarin that can cause excessive bleeding. Certain antacids may prevent many medications, like antibiotics, anti-coagulants and heart medications from being absorbed through the intestinal epithelial membrane as they should. This may cause the medication to be less effective or not work at all.



## REFERENCES

- [1] Setzu S, Monduzzi M, Mula G, Salis A. *Biosensors - Emerging Materials and Applications*; **2011**.
- [2] Zhou ZA, Macknight E. *Sensors and Actuators*. **2008**, 134: pp18–24.
- [3] Marugán J, Bru D, Pablos C, Catalá M. *Journal of Hazardous Materials*. **2012** 117(122): pp213 – 24.
- [4] Froehner K, Backhaus T, Grimme LH. *Chemosphere*, **2000**, 4: pp821-8
- [5] Ghosh, *Anaerobic Treatment of Agricultural Residues and Wastewater Application of High-Rate Reactors* **1996**
- [6] U.S. Environmental Protection Agency. *Tools for Integrated Approaches to Testing and Assessment*. **2010**. Available:  
<http://www.epa.gov/pesticides/science/testing-assessment.html>
- [7] Kochev V, Karabaliev M. *Bulg. J. Phys.* **2001**, 28 : pp153-167.
- [8] Odashima K, Sugawara M, Umezawa Y. *Trends in Analytical Chemistry*. **1991**, 10: pp207–215.
- [9] Lipkowski J. *Phys. Chem*, **2010**, 12: pp13874-13887.
- [10] Coldrick Z, Penezic A, Gasparovic B, Steenson P, Merrifield J, Nelson A. *J Appl Electrochem*, **2011**, 41: pp939–949.
- [11] Economou A, Fieldenb PR. *Analyst*, **2003**, 128: pp205–212.
- [12] Bizzotto D, Nelson A. *Langmuir*, **1998**, 21: pp6269-6273.
- [13] Nelson A, *Current Opinion in Colloid & Interface Science*, **2010**, 15: pp455–466.
- [14] Chen S, Abruna HD. *Langmuir*, **1994**, 10: pp3343-3349.
- [15] Ormategui N, Zhang S, Loinaz I, Brydson R, Nelson A, Vakurov A. *Bioelectrochemistry*, **2012**. 87: pp211-219.
- [16] Protopapa E, Ringstad L, Aggelia A, Nelson A. *Electrochimica Acta* **2010**, 55: pp3368-3375.

- [17] Coldrick Z, Steenson P, Millner P, Davies M, Nelson A. *Electrochimica Acta*, **2009**, 54: pp4954–4962.
- [18] Vakurov A, Brydson R, Nelson A. *Langmuir*, **2012**, 28: pp1246–1255.
- [19] Brukhno AV, Akinshina A, Coldrick Z. *Soft Matter*, **2011**, 7: pp1006-1017.
- [20] Nelson A, Leermakers, FAM. *J. Electroanal. Chem.* **1990**, 218: pp73-83.
- [21] Nelson A. *Journal of Electroanalytical Chemistry*, **2007**, 601: pp83–93.
- [22] Duan J, Wang J, Grahan N, Wilson F. *Desalination*, **2002**, 151: pp53-66.
- [23] Baigorri R, Fuentes M, Gonzalez-Gaitano G. *Journal of Physical Chemistry*, **2007** 111(35): pp10577–10582.
- [24] Moore DRJ. Ambient Water Quality Criteria for Organic Carbon in British Columbia **1998**
- [25] Landrum PF, Nihart SR, Eadle BJ, Gardner WS, *Environ. Sci. Technol.*, 1984 18: pp187
- [26] Peachey RI. 'Cave Science on Leck Fell', *Descent*, reproduced by permission of Wild Places Publishing. **2013** 232: pp10
- [27] Sears DF, Brandes KK. *Agents and Actions*, **1969**, (2): pp28-35

# CHAPTER 12

## CONCLUDING REMARKS

Interactions of biological compounds with biomembranes are complex. They can represent the main site of action for the drug or only a preliminary step that leads up to a toxic or therapeutic activity. By understanding how compounds initially interact with an exposed membrane model, rather than trying to pursue their activity in a very complex cellular model such as cell cultures, a framework of step by step processes can be made.

In the course of this thesis, a system capable of monitoring low levels of biomembrane active compounds dispersed in an electrolyte flow was achieved. Electrochemical techniques using RCV and an optimised flow cell with phospholipid coated Pt/Hg on MFE allowed for studies to take place in areas of pharmaceuticals and toxin screening. DOPC is used primarily as the model phospholipid in these experiments. RCV scans of the DOPC coated Hg are very reproducible and accord with a defect-free and stable layer which remains stable for at least 30 minutes.

Drug effectiveness is traditionally measured by determining their partition coefficients, which is an estimate of the amount of drug that will partition through a lipid membrane into the biological system. Partition coefficients are usually estimated for drugs by using two-phase solvent systems such as octanol-water. Lipid on Pt/Hg as can be a better and more informative alternative to the traditional methods.

Using DOPC on Pt/Hg, cellular interactions and processes can be easily detected and different parameters distinguished and quantified due to the sensitivity of the MFE screening system. The affinity of compounds for biomembranes can be determined by calculating their LoD which can be referred back to in Chapter 2. Sensitivity to concentrations as low as  $\text{nmol dm}^{-3}$  has been detected. This sensitive and selective method offers the opportunity for simultaneous screening and quantification of membrane active compounds thus enabling a “fingerprint” data to be produced from a vast class of compounds. The development and subsequent optimisation of the flow cell enabled the local environment of the electrodes to be monitored and cleaned over much shorter time-scales when compared with the same device in a static cell.

Biomembrane active compounds can have various effects on the lipid coated Hg electrode. These effects can be identifiable with RCV scans. A compound's lipid layer activity is manifested by characteristic changes in capacitance current – voltage plots which represent modifications to the phospholipid layer conformation. It is observed that each class of compound interaction affects a visual profile on the RCV plot which manifests itself as an alteration in the shape, height and position of the capacitance current peaks

The interactions of the various compounds with the DOPC layer show that the presence and nature of the substituent side-chain can significantly alter the compound's sensitivity and affinity towards the DOPC layer. Side chain substitutions can greatly increase or decrease membrane interactions. This has been observed with the side chain substituted phenothiazine molecules, prochlorperazine and chlorpromazine where interaction with DOPC coated Hg significantly increased (Chapter 6). Other examples are the inclusion of chlorine in clomipramine compared to its absence in imipramine making clomipramine more membrane active (Chapters 6 and 10) and increasing alkyl chain length can increase the activity of some compounds whereas it can instigate a hindrance to interaction with other compounds

(Chapter 5). Where the LoD value inversely correlates with the log  $K_{OW}$  within a compound class, the relationship is indirect. This is because in one class of compounds the increase in aromaticity or side chain length leads to an increase of the hydrophobicity of the molecule. Structural properties such as aromaticity and the nature of side chain and substituents are the molecular features which directly determine the extent of interaction.

The performance of the MFE sensing device has been successfully assessed in a "real life" scenario; its operation has been tested in the presence of humic acid and subsequently in tap water and natural waters as an applicable matrix (Chapter 11). After establishing new capacitance current peak controls, pyrene was used to spike the water samples as a means of assessing whether the MFE device is able to identify a potential toxicant in the environment and water supply. The characteristic response commonly associated with pyrene of the DOPC was observed in all the matrix studies but the shift in peaks appeared significantly greater in the presence of humic acid in PBS and even more so with natural water samples. A reason for this is that humic acid as a surfactant associates with the apolar pyrene in solution and facilitates the transfer of pyrene across the solution/ DOPC layer interface. This would also occur if there are naturally high concentrations of humic acid or other surfactants present in the surface water sample.

### **COLLABORATIVE WORK**

Following successful characterization and analysis of various compounds with MFE, collaborative work was possible with various industries and universities.

Ionic liquid study was conducted in collaboration with Massimiliano Galluzzi from the Dipartimento di Fisica, Università degli Studi di Milano, Italy (Chapter 5).

Work was conducted in collaboration with a water company with laboratories based in Cardiff (Modern Water PLC). This collaboration provided further evidence that the sensing system has applications to the environment. A full report in the form of performance evaluation was sent to Modern Water.

Work was conducted in collaboration with a high tech consultancy company (Platform Kinetics) specialising in technology and instrumentation. This collaboration is for the purpose of configuring and adapting the flow cell device further. Parameters for assay in the form of a brief report were sent to Microfluidics. (Appendix A).

Electrochemical studies were conducted as a screening validation service for Imperial College, Chemistry; Dr. Oscar Ces (included in Chapter 7).

Work was conducted for a technology company specialising in the manufacture of gas sensors, detectors and alarms (Analox Ltd.). The work was conducted on the compound TcP to determine the lowest level of detection possible as well as to provide analysis of TcP-lipid behaviour.

Work was conducted for Ministry of Defence- Defence science and technology laboratory (MoD-Dstl) on the bispyridinium compounds (included in Chapter 5).

## **DIRECTIONS FOR FUTURE RESEARCH**

The device can be adjusted for applications in atmospheric sensing so that it becomes possible to detect air-borne contaminants.

This high throughput screening device can be improved further. Miniaturisation of analytical systems has become an important area in research. Advantages of these miniaturised systems include a reduction in manufacturing costs, ease of transport, and minimal space requirements in the laboratory. Progressive future work can be done by miniaturising the system.

Enzyme-based biosensors are used in the pharmaceutical industry in the search for new antibiotics and cancer therapeutic drugs, among others. The DOPC layer on Pt/Hg can become more specialised by the inclusion of functionalized membrane bound proteins and receptors (Figure 12.1). The required enzyme or ligand specific proteins such as enzymes, antibodies or receptors directly on DOPC layer coated on Pt/Hg, or can be immobilised onto the DOPC coated Hg layer. The monolayer integrity with immobilised enzyme can then be simply monitored in real time using RCV scans and producing new peak controls. The effect of target substrates for the enzymes can then be measured using RCV. Using such adaptations can broaden the use of the high throughput system to include marine studies, several applications in the field of biotechnology, antibiotic production, sensors and in drug lead selection such as pharmaceutical profiling.

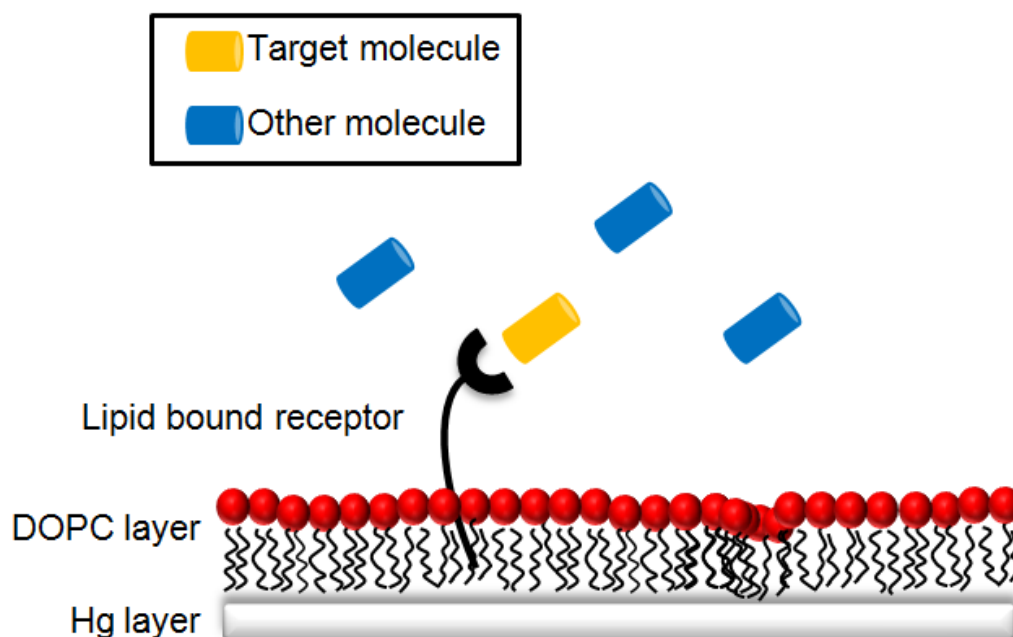


**Figure 12.1: Illustration of membrane bound target receptors on Pt/Hg for future developments and research.**

**ACHIEVEMENTS**

The work described in this thesis has contributed towards the 'Early Career Scientist' award following my presentation at the In Vitro Toxicology Society meeting.

The work conducted on TcP led to a Technology Strategy Board (TSB) grant with MicroLab devices, Analox Ltd and Pall.



# **APPENDIX A**

## **MFE FLOW CELL: PARAMETERS FOR**

### **ASSAY**

## MFE flow cell. Parameters for assay

<p><b>Principal of MFE flow cell.</b></p>	<p>The DOPC coated microfabricated Pt/Hg electrode installed within a flow cell has been successfully configured to screen the type and concentration of organic compounds in water. The data enables detection limits which represent the lowest concentration of compound in water which statistically interacts with the DOPC layer to be calculated from the data.</p> <p>It is an <i>on-line</i> high throughput system.</p>
<p><b>Set up.</b></p>	<p>The MFE is contained in a closed flow cell. A constant flow of pH 7.4 PBS is passed over the electrode by a peristaltic pump.</p> <p>The flow cell is connected to a research potentiostat interfaced to a Powerlab signal generator and controlled by Scope software. Standardized capacitance/voltage plots are produced when various electric potentials are applied. Thus, a profile can be obtained which is non-linear and dependent on the applied voltage.</p> <p>The monolayers undergo two pronounced phase transitions characterized by two capacitance current peaks. The peaks correspond to the redistribution of charges or polar molecules with the monolayer interface.</p>
<p><b>How is the data produced?</b></p>	<div style="text-align: center;"> </div> <p>The figure (a) displays the results of the changes to the RCV plots from the interaction of DOPC with the example compound pyrene in two concentrations. The compounds interact with the DOPC coated electrode can be seen by their</p>

	<p>effect on the capacitance current peaks in the RCV plot. These capacitance current peaks are representative of the reorientation/adsorption/desorption processes of the DOPC layers in response to potential change.</p> <p>It is observed that each class of compound interaction effects a “fingerprint” visual profile on the RCV plot which manifests itself as an alteration in the shape, height and position of the capacitance current peaks.</p>
<p><b>Advantages of MFE assay.</b></p>	<p>The system can be applied to the screening of putative hazardous substances and pharmaceuticals allowing for early detection thereof in the water supply.</p> <p>The measurements are made in real time which means that potentially. Toxic compounds are detected rapidly within &lt;10 min per assay. This technology will contribute greatly to environment safety and health.</p> <p>The present on-line high throughput system enables a large number of compounds to be screened. This is due to the three way solenoid valve which allows one component to be introduced into the flow cell at one time. This advantageous feature of the system allows for controlled introduction of control PBS, lipid dispersion and then the test compound. This also means that re-depositing lipid and introducing another test compound can be done as easily as a switch of the valve.</p> <p>“Fingerprint” data has applications in toxicity sensing in environment as a large database of distinct fingerprints can be used to determine a potentially toxic contaminant in water supply. Tap water studies contaminated with a contaminant has been successfully tested.</p> <p>There is reduction of wastage due to minute quantities of solution being used. Easy to use software with plenty of parameters for case studies.</p> <p>A robust system. After first use, the MFE itself can be left and stored in the designated flow cell</p>

	at room temperature and has a shelf life of up to 4 months.
<b>What results can be obtained using MFE assay?</b>	Permeability, membrane damage, membrane recovery, surface activity, rate of interaction, extent of interaction, bioavailability, determining structural activity relationships, toxicity screening.
<b>What is the recommended compound concentration?</b>	This is dependent on the potency of the compound (which is based on the functional groups present that promote membrane interaction). The assay has however detected compounds as low as 0.014nM and start concentrations can range from 0.01 to 1µM. Higher concentrations are also acceptable however in the case of persistent samples, please refer to issues below.
<b>Any issues on using this assay.</b>	<p><b>MEMORY EFFECT</b> To avoid memory effect from persistent samples, dilute piranha solution; a hot solution of sulfuric acid and 30% hydrogen peroxide at a ratio of 3:1 and dilution ratio of 1:100 is passed over the electrode for a few seconds while repetitive cycling at -0.4V to -3.00V.</p> <p><b>PHYSICAL SURFACE DAMAGE</b> Any electrode that is excessively damaged by organics, mishandling or applying inappropriate potentials needs further treatment. Removing the MFE from the flow cell, any solid contamination can be removed by carefully rubbing some acetone over the electrode while avoiding the mercury. Depending on severity of damage, the MFE may need replacement and re-deposition of the Hg.</p>
<b>Can this assay be used in natural waters?</b>	This assay has successfully operated with tap water. The device can effectively screen potentially toxic compounds in natural waters.
<b>Is it possible to use different pH environments?</b>	pH of flow cell can be manipulated to study this influence on the test compounds' permeability which is important in determining bioavailability. This also allows estimation of compound permeability in pH ranges that reflect / mimic physiological pHs.

<p><b>What is limit of detection?</b></p>	<p>The detection limits are quoted as the minimum concentration of compound in water to elicit a response and these detection limits are related to compound molecular structure and the known biological effect of each compound. This parameter has key applications in bioavailability and thus important in novel compounds studies and pharmaceuticals.</p>
<p><b>What is bioavailability?</b></p>	<p>Bioavailability is a measurement of the rate and extent to which a drug reaches the systemic circulation. The MFE assay can measure this.</p> <p>Compounds can be tested on the time taken to interact with monolayer by simply changing setting on the Scope software. Magnitude of interaction can be measured as the effect the compound has on the RCV scan. Studies have shown that the magnitude of interaction is structurally related as well as concentration dependent. Changing functional groups can remarkably enhance interaction.</p> <p>Bioavailability studies benefit in the development and usefulness of novel compounds. Early clinical studies will provide an understanding of the compound's pharmacokinetics and bioavailability, thereby contributing towards decisions around the feasibility of the novel compound.</p>
<p><b>How does MFE assay compare with PAMPA</b></p>	<p>PAMPA has an overnight incubation period whereas MFE assay requires no incubation period.</p> <p>They also check cell layer intact using TEER measures. TEER is used to measure integrity of the monolayer after interaction of compound. This technique involves use of Lucifer yellow, a membrane marker incorporated with the test compound. In MFE assay we use the presence and integrity of peaks shown to discuss if the compound has affected the monolayer and also how. MFE assay is faster in determining monolayer integrity simply by monitoring the real time RCV scans when lipid is deposited onto the electrode. This takes seconds to determine</p>

	<p>and does not require any additional marker or component.</p> <p>PAMPA also aims to mimic cell layers for permeability studies but it does not study recovery or damage as MFE assay does.</p>
<p><b>How does MFE assay compare with MDCK permeability assays?</b></p>	<p>MDCK assays are used to identify drug efflux from a particular type of transporter protein. This makes this assay too specific and exclusive. Our system can also be adapted to specific proteins that can be adsorbed onto monolayer.</p> <p>MDCK assays take at least 4 days to set with a further 60 minutes for the actual monolayer monitoring in presence of test compound. MFE assays set up and including testing of compounds with results can take less than 20 minutes.</p>
<p><b>How does MFE assay compare with octanol/water partition coefficient?</b></p>	<p>Octanol is structurally very different to phospholipid layers and so cannot model interactions well.</p> <p>MFE assay can show permeability and interaction of hydrophobic and hydrophilic compounds.</p> <p>Generically, structural properties such as aromaticity, nature of side chain and substituents are the main factors which determine the extent of interaction. Hydrophobicity alone cannot determine extent of interaction.</p>